# waterloopkundig laboratorium
# delft hydraulics laboratory

## Beach and dune erosion during storm surges

P. Vellinga

# Beach and dune erosion during storm surges

Thesis approved by the Delft University of Technology

P. Vellinga

## Abstract

**Beach and Dune Erosion during Storm Surges**

The process of coastal dune erosion was investigated by scale model reproduction of storm surge conditions and beach profile changes. The relation between the process in the field and the process in a scale model was theoretically derived. This (scale) relation was verified in the laboratory by a series of small scale and large scale model tests. The dune erosion to be expected in nature under (extreme) storm surge conditions was determined by conversion of the model results using the scale relations.
During the tests detailed measurements were taken of the wave height, the flow velocity, the sediment concentration and the beach profile changes. On the basis of the laboratory investigations a computer model was developed for the prediction of dune erosion as a function of the coastal profile before the storm surge, the grain size of the dune sand, the waterlevel and the wave conditions during the storm surge. The model was verified by an extensive series of field data like the erosion data of the storm surge of 1953.

The model is applied by the Public Works Department of The Netherlands (Rijkswaterstaat) to check the safety of the existing dunes as a primary sea defence system, and to determine the required reinforcements. The model is not directly applicable for strongly curving coastlines and other situations with a large longshore transport gradient.

## Acknowledgements

The research project described in this thesis is a follow up of the dune erosion experiments started by Jan van de Graaff. His initiative and critical interest during the studies have been decisive for the present results.

The high quality of the data obtained throughout the extensive series of tests is fully due to the effort and the dedication of all my colleagues involved during the tests and the elaboration of data at the Delft Hydraulics Laboratory.

Especially acknowledged are Riemer Reinalda and Huib de Vriend for their comments and stimulating support during the writing of this thesis.

# CONTENTS

CONTENTS (continued)

References

List of Symbols

List of Tables

List of Figures

BEACH AND DUNE EROSION DURING STORM SURGES

## 1. Introduction

### 1.1 General

During storm surges the sea level rises considerably above normal high water level. As a result the storm driven waves reach the front of the dunes and erosion occurs. The eroded sand is moved in offshore direction and settles on the beach, see Figure 1. This way a new beach profile is developed at a more elevated level. In fact the process of dune erosion can be considered as an extreme case of the continuous adjustment of the coastal profile to the ever changing hydraulic and meteorological conditions.

Most of the inhabitants of The Netherlands live below mean sea level. The population and the goods are only protected from the sea by a narrow stretch of sandy beaches and dunes. Due to long term erosion the row of dunes is thinning down. Many parts are becoming critical with respect to the vital rôle of the dunes as a primary sea defence system. Reinforcement works are necessary to prevent a breakthrough during storm surges. This situation calls for a detailed knowledge of the dune erosion phenomenon.
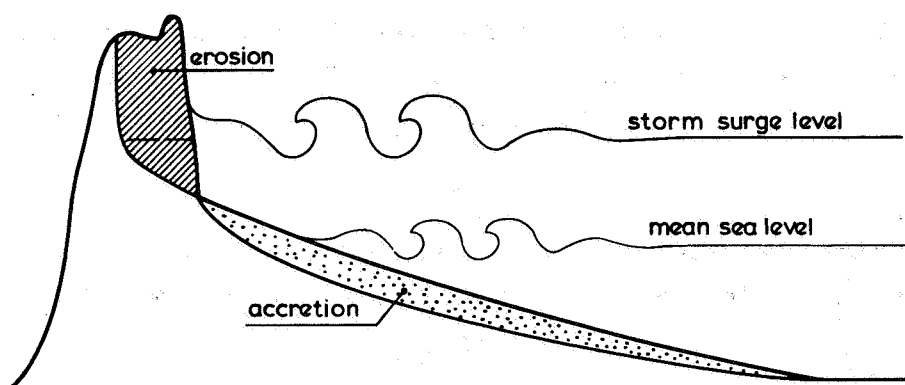


**Figure 1** Dune erosion during a storm surge

The question how wide the dunes should be to withstand an extreme storm surge can also be put as "how much dune erosion will occur under extreme storm surge conditions". Edelman (1968) was the first to present a method for the prediction of dune erosion. His method was improved in 1972 by Van de Graaff (1977), who defined an erosion profile on the basis of field observations. Due to lack of data the prediction methods were based on a number of rather speculative assumptions. Further research was required to develop a reliable model for the prediction of dune erosion during extreme storm surges.

With this aim a comprehensive programme for field data collection has been carried out by the Ministry of Transport and Public Works (Rijkswaterstaat), and extensive laboratory experiments have been carried out at the Delft Hydraulics Laboratory.

The results of the investigations can be summarized in three points:

1) Development and verification of scale relations for the laboratory reproduction of dune erosion during storm surges.
2) Development and verification of a computer model for the prediction of dune erosion during storm surges.
3) A better understanding of the process of dune erosion, in terms of wave conditions, flow field, sediment concentrations and profile changes.

The set up and the results of the research programme are described in this thesis.

## 1.2 Summary and conclusions

### Theoretical scale relations

Dune erosion is a complicated process. A physical-mathematical approach to the problem is not feasible as the physical descriptions of sediment transport in the breaking waves zone are insufficiently developed. Experimental laboratory research is required. However, the scale relations for space and time of the process are not known.

Therefore a set of theoretical scale relations has been developed on the basis of a dimensional analysis of the sediment transport process. The relations are indicated below.

$$n_H = n_L = n_d = n_T^2 \qquad \text{(Froude scale for hydraulic conditions)} \qquad (1)$$

$$n_l/n_d = (n_d/ n_w^2)^{0.25} \qquad \text{(model distortion)} \qquad (2)$$

$$n_t = (n_d)^{0.5} \qquad \text{(morphological time scale)} \qquad (3)$$

in which

n  is indicating the ratio of the prototype value over the model value of the index parameter

H  is wave height

L  is wave length

d  is water depth

T  is wave period

l  is length

w  is the fall velocity of the sediment

t  is time

The analysis of the sediment transport process in dimensional terms and the development of the theoretical scale relations are described in Chapter 3.

**Small scale tests**

The theoretical scale relations were verified by means of a series of small scale tests with three different depth scale factors ($n_d$ = 84; 47 and 26) and four different grain sizes ($D_{50}$ = 225 µm, 150 µm, 130 µm and 95 µm). The principle of the scale series is shown in Figure 2. Twenty four tests were carried out for an idealized coastal profile and for idealized storm surge conditions.



X  model result
O  model result converted to prototype
● final prototype result
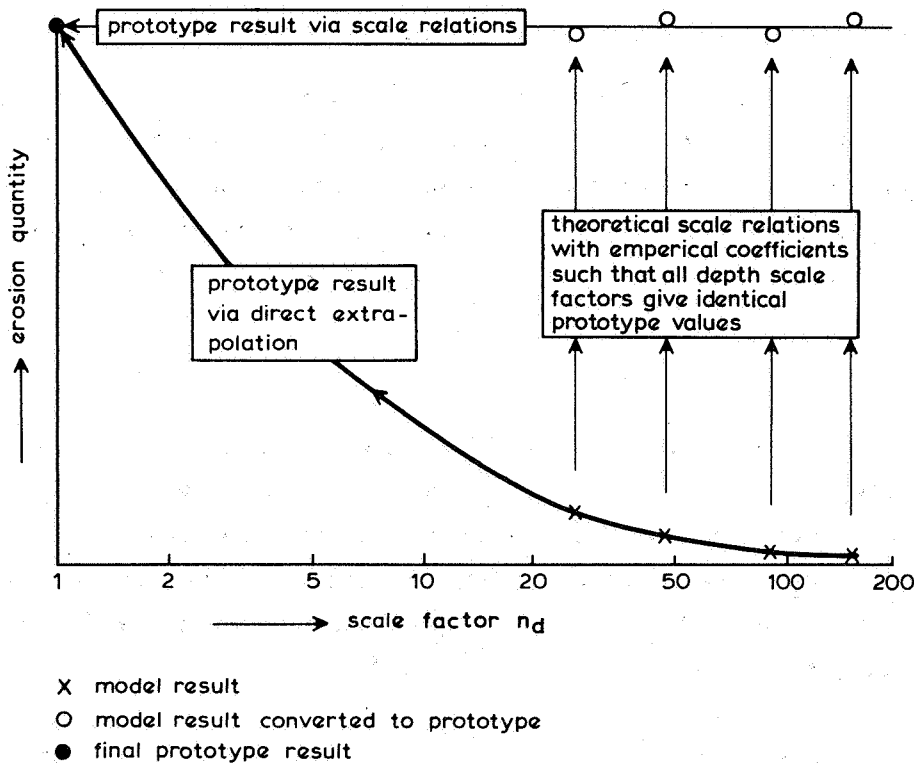
**Figure 2**  Principle of a scale series

The basic form of the theoretical scale relations and the validity of the use of the dimensionless fall velocity parameter H/Tw was confirmed by the test results. Tests with equal H/Tw value show a geometrically similar profile development (H is significant wave height, T is wave period, peak of spectrum and w is fall velocity of the sediment).

The values of the exponents in the theoretical scale relations, see (2) and (3) were determined by correlation analysis of erosion profiles, erosion rates and erosion quantities. The following set of scale relations was found:

$$n_H = n_L = n_T^2 = n_d \qquad \text{(Froude scale for hydraulic conditions)} \qquad (1)$$

$$n_l/n_d = (n_d/n_w^2)^{0.28} \qquad \text{(model distortion)} \qquad (4)$$

$$n_t = (n_d)^{0.5} \qquad \text{(morphological time scale)} \qquad (5)$$

The values for the exponents as found from the experiments are identical to the values as derived on a theoretical basis except for of the exponent in the distortion relation, $\alpha$. The experiments indicate that $\alpha = 0.28$, whereas theory indicates that $\alpha = 0.25$. The difference is very small. For practical use it is recommended to apply the empirical value $\alpha = 0.28$ as this value has been found by a thorough elaboration of the test results. The theoretical value, $\alpha = 0.25$ is more elegant when the dimensions are considered. For further theoretical analysis it may be better to apply the value $\alpha = 0.25$.

The two-dimensional model tests were carried out in a wave flume. Additional model tests were also conducted in a three-dimensional basin and the results of these tests confirm that a two-dimensional reproduction of dune erosion is fully acceptable for relatively straight beaches. The results of the small scale tests and the verification of the theoretical scale relations are described in Chapter 4.

**Large scale model tests**

Although a value for dune erosion in the field can now be found by up-scaling of the model data, there is a considerable scatter in the thus predicted values. Further it is not certain that the scale relations are valid outside the range tested so far ($n_d = 84$ up to $n_d = 26$). Therefore, experiments were carried out at a larger scale with the aim of confirming the scale relations over a broader range and producing more accurate results.

The idealized beach and dune profile was tested using a scale factor $n_d = 5$ i.e. under model conditions with a significant wave height $H_s = 1.5$ m, a grainsize $D_{50} = 225$ $\mu$m, and a waterdepth of 5.0 m, see Figure 3. An additional correlation analysis was carried out on the data obtained in both the large scale and the small scale tests and this confirmed the scale relations and the values of the exponents given earlier. Confidence has been further increased by an additional two large scale tests including a reproduction of the field data of the 1953 storm surge. The experimental set-up and the results of the large scale tests are described in Chapter 5.
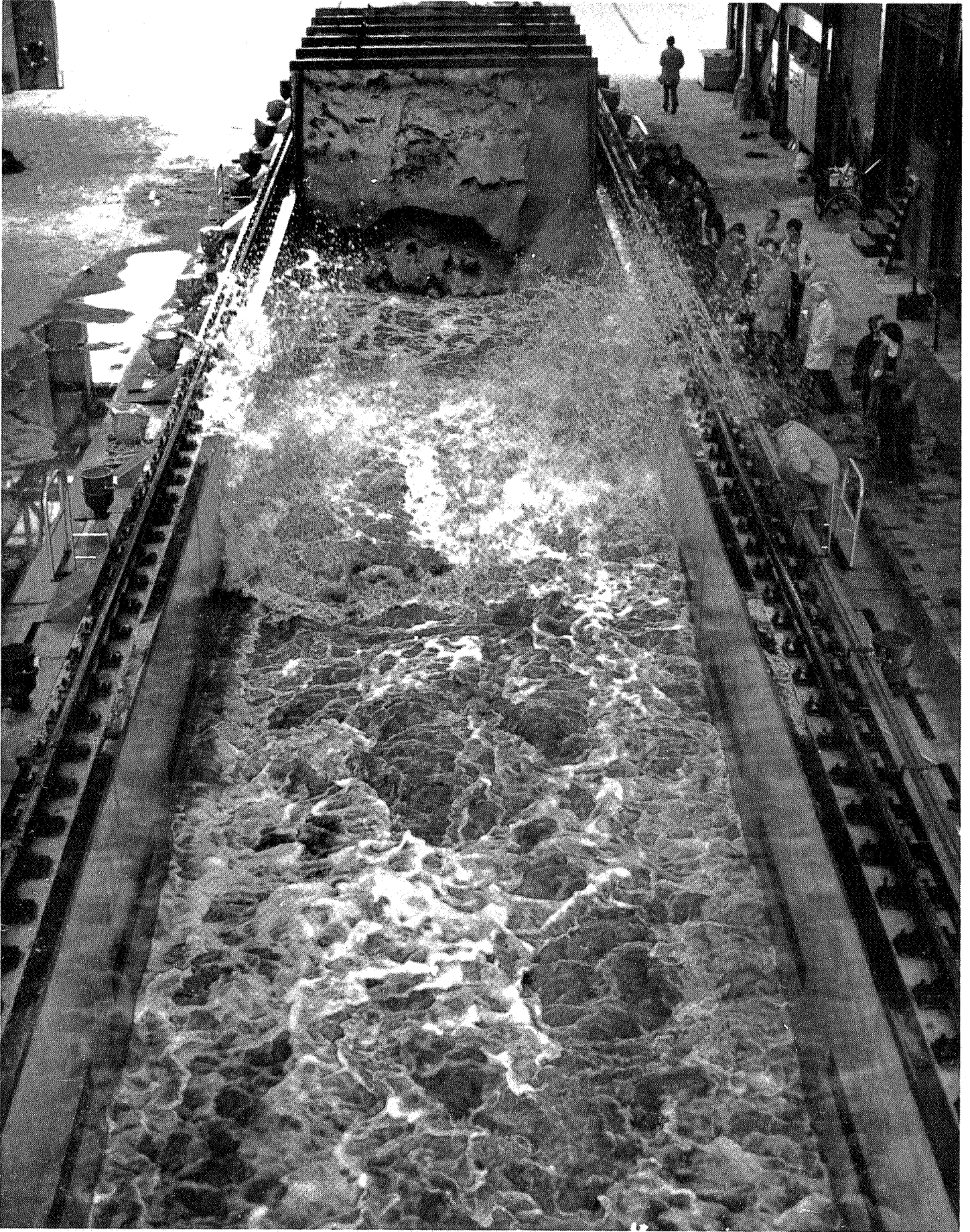
**Figure 3a** Large scale test in the Deltaflume
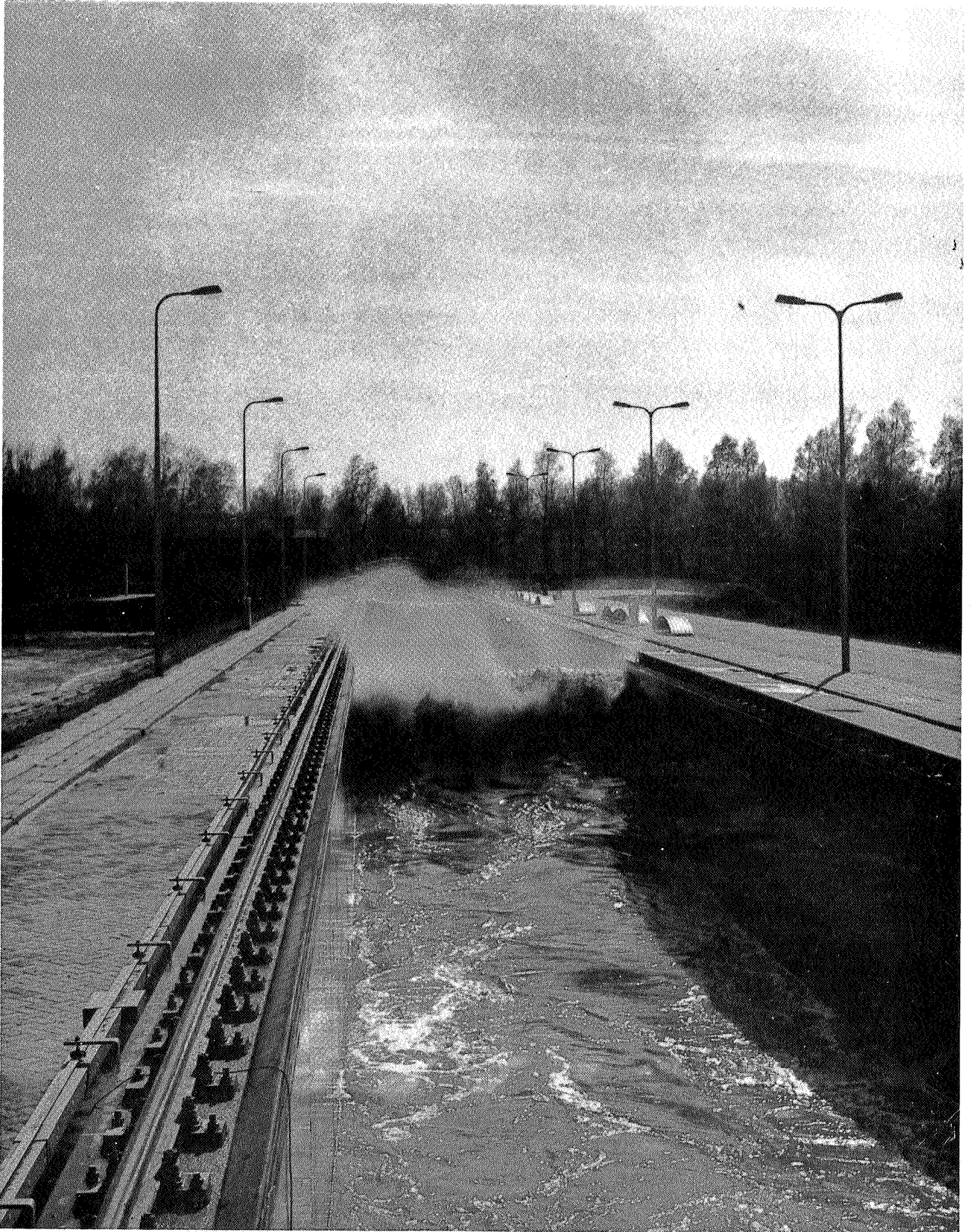
**Figure 3b** Large scale test in the Deltaflume

## Development and verification of a dune erosion prediction model

The test results have enabled the development of a dune erosion prediction model. The model is based on the observation that a typical erosion profile develops during storm surges. This profile can be represented as a function of storm surge level, wave height and the settling velocity of the eroded sand, see Figure 4.

Additional tests verified the prediction model for a wide range of conditions including variations in storm surge level, wave height, wave period, wave-spectrum form and initial profile (bars, troughs and dune height).



erosion profile to be shifted in landward direction
until erosion-sedimentation is balanced. Erosion profile:
$(7.6/H_{0s})\, y = 0.47 \left[ (7.6/H_{0s})^{1.28} (w/0.0268)^{0.56} x + 18 \right]^{0.5} - 2.00$

seaward limit $x = 250\,(H_{0s}/7.6)^{1.28}(0.0268/w)^{0.56}$ ; $y = 5.72\,(H_{0s}/7.6)$
x, y and $H_{0s}$ in m; w in m/s
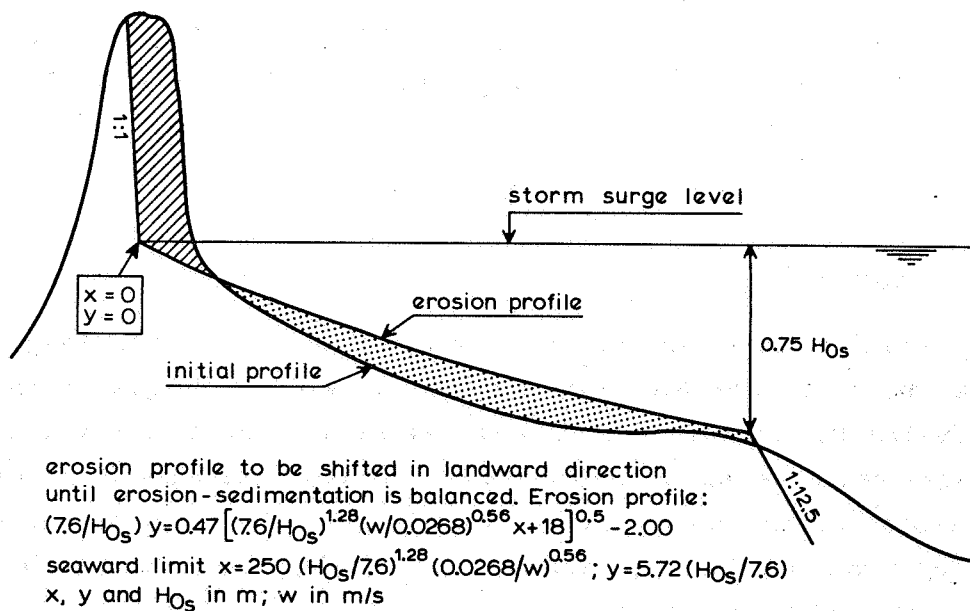
**Figure 4** Principle of the dune erosion prediction model

The prediction model was also verified for field data. Hindcast computations were carried out for 58 coastal profiles for the storm surge of 1976 that caused a mean erosion of 30 m³/m' with extremes up to 80 m³/m'. Moreover the prediction model was verified for the storm surge of 1953 that caused a mean erosion quantity of about 100 m³/m. Sargent and Birkemeier (1985) demonstrated that the application of the model is also justified for United States East Coast and Gulf Coast storm conditions.

The computer model is presently applied to predict the safety of the coastal dunes in The Netherlands and to design the required reinforcements.

The experimentally derived erosion profile can also be used for more general purposes. The profile is in accordance with beach profiles described by Bruun (1954) for coasts that suffer a long term erosion. Further elaboration has shown that the effect of the grain size as described by the scale relations continues to hold even for coarser material such as gravel. A general description has been derived tentatively for the erosion profiles of sandy beaches, gravel beaches and rock beaches. This general profile may be helpful in the design of beach fills.

Finally it should be noted that the dune erosion prediction model is only applicable in situations with relatively straight homogeneous coastlines, i.e. where a two-dimensional idealization of the dune erosion process is possible. Further research is required to enable the prediction of dune erosion where there is a large longshore transport gradient, such as along strongly curved shorelines, and in the direct vicinity of an inlet or a non-erodible discontinuity in the sandy shoreline.

The development and the verification of the dune erosion prediction model are described in Chapter 6.

**The process of dune erosion**

During the tests detailed measurements were carried out. The wave height attenuation across the surf zone has been measured at various stages of the erosion process. During the process the velocity field and the sediment concentrations were measured at several depths and at various distances from the dune front. The results of the measurements indicate that the transport process is dominated by transport in suspension. On the basis of the data it has been hypothesized that (Vellinga, 1982):

1) the offshore transport process is controlled by the sediment concentrations as generated by the breaking waves
2) the sediment is carried in offshore direction by the vertical circulation (return flow below the level of the wave troughs)
3) the rate of offshore transport is equal to the product of the time averaged sediment concentration and the time averaged vertical circulation.

This hypothesis has been verified by comparing the beach profile changes with the product of the time-averaged velocity field and the time averaged sediment concentrations as measured during the tests. The agreement is surprisingly good in view of the simplified reproduction of the process in mathematical terms.

A tentative model for time dependent sediment transport and beach and dune profile changes has been developed. Although the results are encouraging, it

is clear that a considerable research effort is still required for the development of a time dependent dune erosion model that is reliable both in a qualitative and a quantitative sense.

During the period of the research described above, the possibility of the scale-model and numerical-model simulation of dune erosion and cross-shore transport was being investigated elsewhere as well. The final part of this thesis describes the simultaneous work of Hughes (1983), Hallermeier (1985), Kriebel and Dean (1985) and Stive and Battjes (1984).

Finally the results of the present investigations are evaluated, the future possibilities and problems regarding the modelling of coastal erosion during storm surges are discussed and recommendations for further research are given.

## 2. Background

### 2.1 The coastal morphological system

**Long-term developments**

The formation and deformation of sandy beaches and dunes have played a major role in the development of The Netherlands in its present geomorphological form. The development of beach ridges and barrier islands started about 6000 years ago when the sea level rise stagnated after continuously rising by 40 m since the beginning of the Holoceen era, see Figures 5 and 6 (Fairbridge 1961, Jelgersma 1961, Veenstra 1968 and Veenstra 1976). From this time there has been a sequence of barrier island formation and deformation characterized by erosion on the exposed sea side and sedimentation in the sheltered area of tidal flats. The process is illustrated in Figure 7 (Van Straaten, 1975). This process has been affected by human activities for the last 1000 years. Dikes were built to protect low lying areas from flooding during storm surges and shallow inlets were closed. As time went on the coast line was more and more controlled by human activities.
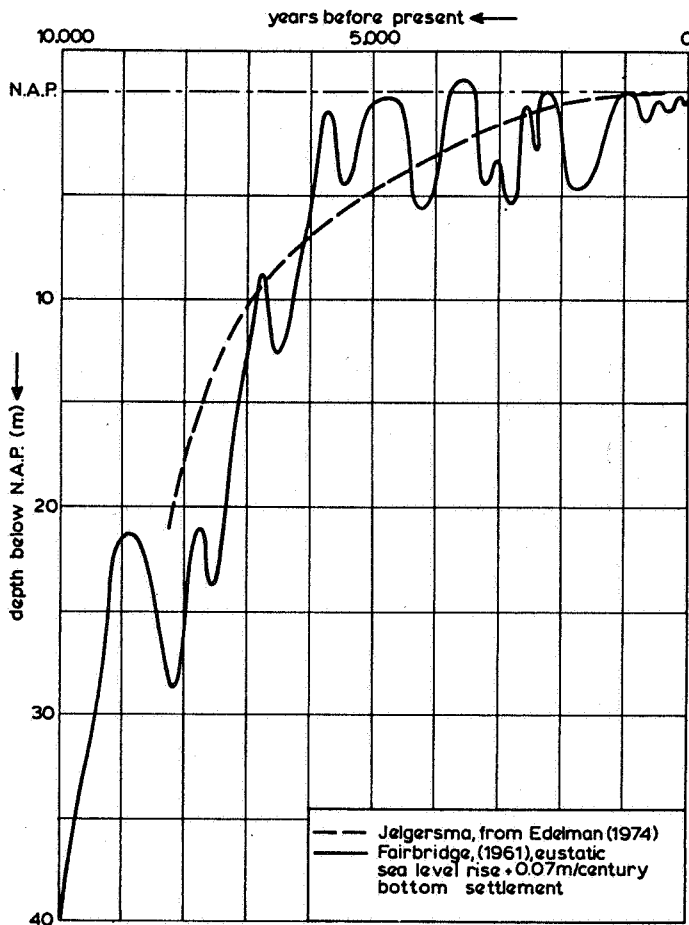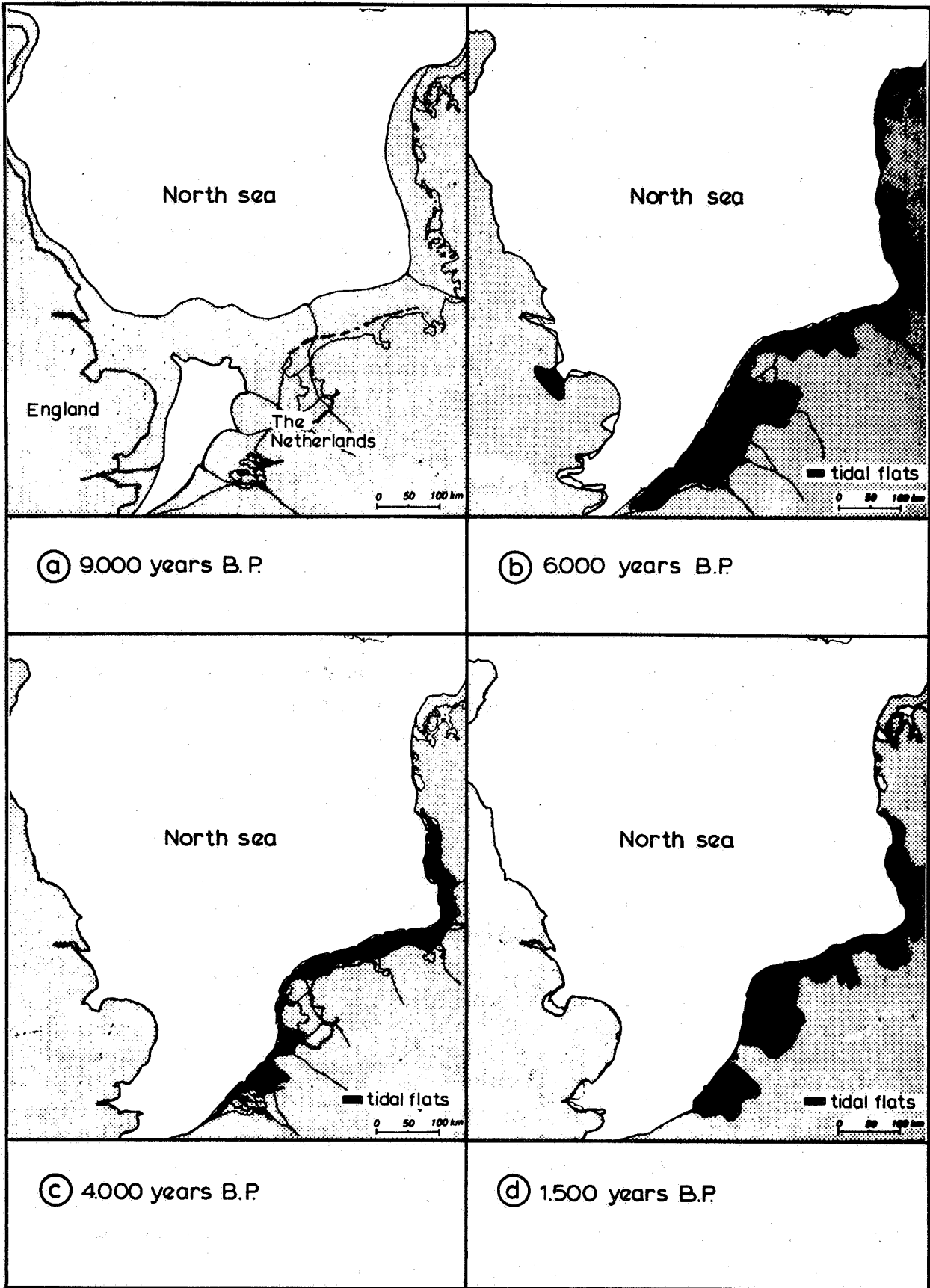


**Figure 5** Relative sea level rise in The Netherlands

**Figure 6** Geological development stages of the North Sea coast
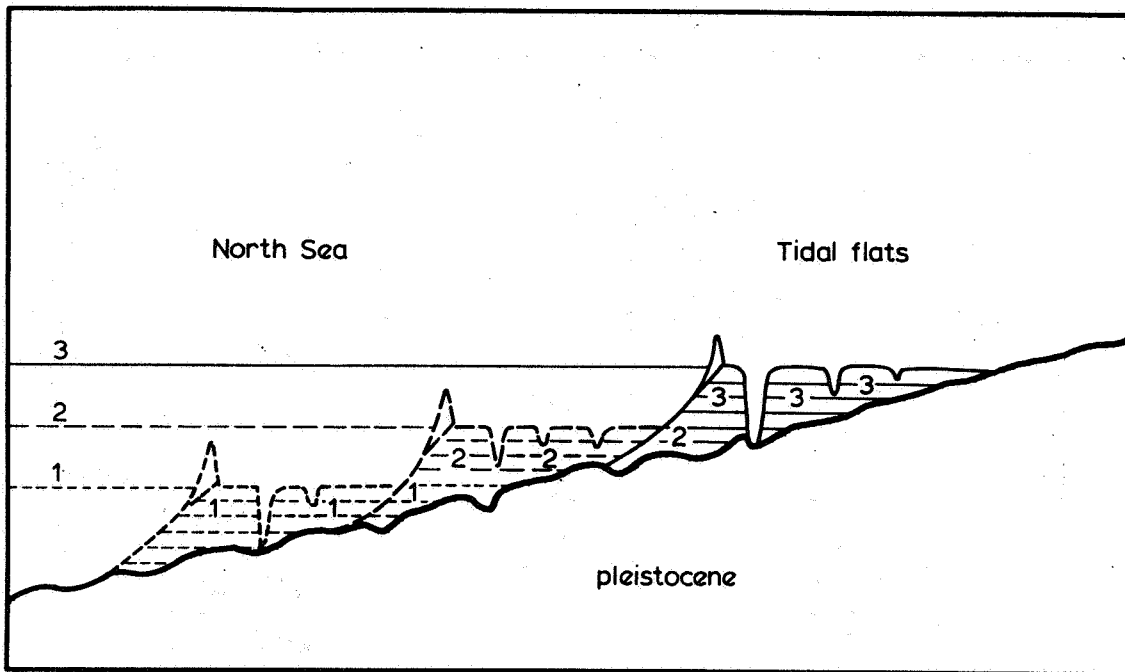
**Figure 7** Transgression

However, the morphological system is still of a dynamic nature. In the north of The Netherlands the system is dominated by the sedimentation of the Wadden-zee. The sediment accumulation in this sheltered area is estimated at 10 million $m^3$ per year of sand and about the same amount of mud (Delft Hydraulics Laboratory, 1979). The sand originates from the bed of the North Sea and from the shores of the barier islands. The total shore line erosion of the barrier islands and of the northern part of North-Holland is in the order of two million $m^3$/year (Roelse, 1985; Rijkswaterstaat and Delft Hydraulics Laboratory, 1986). So the major part of the sand must come from the surrounding sea bed.

The middle part of the shoreline of the Netherlands is fairly stable. Edelman (1961) found that this part has been accreting at a rate of 0.5 m/year in the period from 1850 to 1950, see Figure 8. However, the shoreline data from 1950 up to 1980 indicate that the accretion process has stagnated (Kohsiek, 1986).

In the southern part of the Netherlands the morphological developments are more complicated. The effects of the closing of some major branches of the Rhine and Meuse estuary are dominating the natural developments. The originally east-west system of tidal currents and corresponding bars and gullies is changing into a mainly north-south system (Kohsiek, 1987). As a result the headlands are eroding and the areas in front of the closure dams are shoaling. At the same time the outer delta is deepening and the inner delta is shoaling (Kohsiek, 1987).
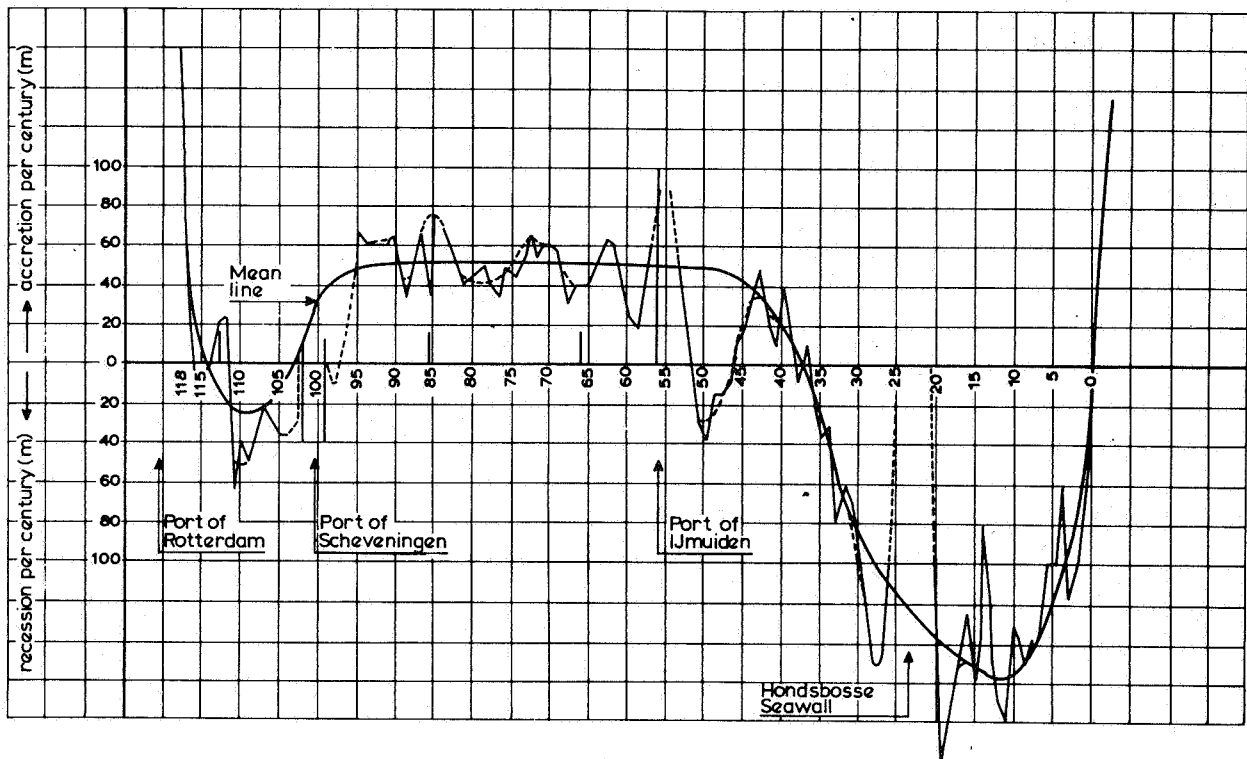
**Figure 8** Erosion and accretion between Rotterdam and Den Helder, according to Edelman (1961)

The eroding parts of the Netherlands shoreline are indicated in Figure 9. The present rate of erosion of the beach profiles is about 4 million $m^3$/year over a shore line length of 300 km (Roelse, 1985; Rijkswaterstaat and Delft Hydraulics Laboratory, 1986). This gives an average shoreline retreat of 1 m/year; the extremes are in the order of 10 m up to 40 m per year. The processes described above are continuous. The shoreline changes are the result of the adjustment of the sea bottom and shoreline contours to the long term hydraulic, meteorological and geological conditions.

**Short term fluctuations**

Beside the long-term development of the shoreline, short-term fluctuations can be observed. Such fluctuations are the result of the continuously changing hydraulic and meteorological conditions. The sediment transports involved are mainly perpendicular to the shore. The fluctuations in the position of the shoreline contours are much larger than the long term average changes. Under conditions with wind from the land and swell type waves a relatively wide beach is formed with a berm with a relatively steep slope at the waterline. During winds from the sea and especially during storms a more evenly sloping beach is developed. Changes from one condition to the other are associated with a change in the position of the beach contours in the order of 10 metres or more in a day.
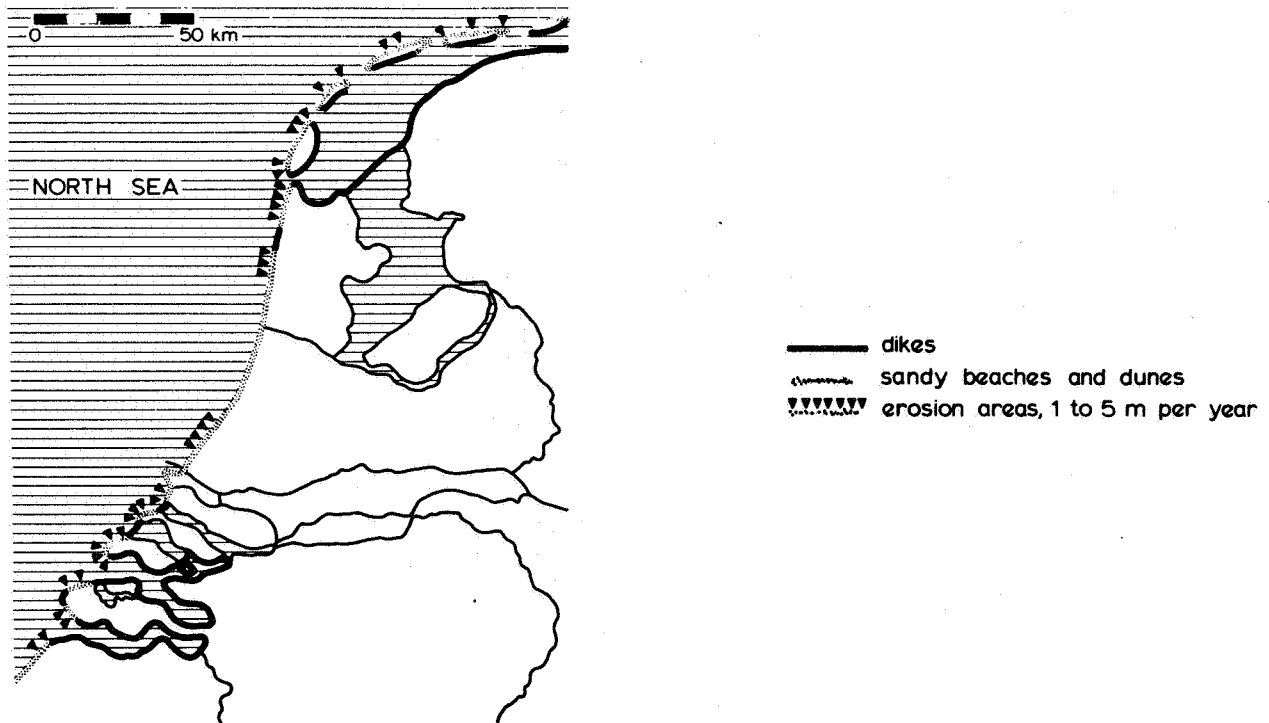
**Figure 9** Erosional areas along the North Sea coast of The Netherlands (Vellinga, 1978)

Dune erosion during a storm surge is an extreme case of the continuous adjustment of the beach profile to the hydraulic and meteorological conditions. During the passage of a low pressure field accross the North Sea in a south easterly direction strong winds are generated initially from S.W. and shifting to N.W. direction. Together with the tidal effect such storms cause a sea level rise of several metres. The significant wave height under storm surge conditions is 5 to 8 m. Because of the rise in sea level the waves reach the front of the dunes. The wave energy is dissipated over a very short distance as the dunes and the beach just in front of it are relatively steep. Consequently relatively high waves break in relatively shallow water. The breaking waves "hit" the bottom and large quantities of sediment are stirred up. The larger part of the suspended sediment settles further seaward in a less turbulent environment. This way the dunes are eroded and the beach is elevated. As a result the slope of the beach becomes more gentle, the wave energy is dissipated over a larger distance and consequently the offshore transport decreases. This process would continue until a new equilibrium beach profile is formed corresponding to the storm surge sea level. However, beach profile changes are slower than the changes in hydraulic and meteorological conditions and such an equilibrium condition is not usually reached during a single storm surge.

## Longterm - shortterm interaction

For beaches that are relatively stable the dune erosion phenomenon can be considered as a temporary redistribution of the sand in the coastal profile. Even after extreme storm surges the major part of the eroded sand will return to the upper beach and within a few years the dunes will be restored by the combined action of waves, winds and vegetation.

Things are different for beaches that suffer a continuous erosion due to large scale morphological developments. The erosion of the coastal profile below mean high waterlevel is a continuous process which causes the beach to become relatively steep. During a storm surge an erosion profile is formed independant of the initial profile as will be illustrated later on. Thus steep beaches are associated with relatively large dune erosion. After the storm surge a large part of the sand eroded from the dunes is transported in longshore direction. Only part of it will return to the upper beach and the dunes. Thus dunes on eroding beaches suffer more severely and more frequently than those on stable beaches. This is evidenced by field observations. For eroding beaches the dune erosion phenomenon must be considered as a discontinuous feeding of the under-nourished beach in front of it.

## 2.2 Dunes as a primary sea defence structure
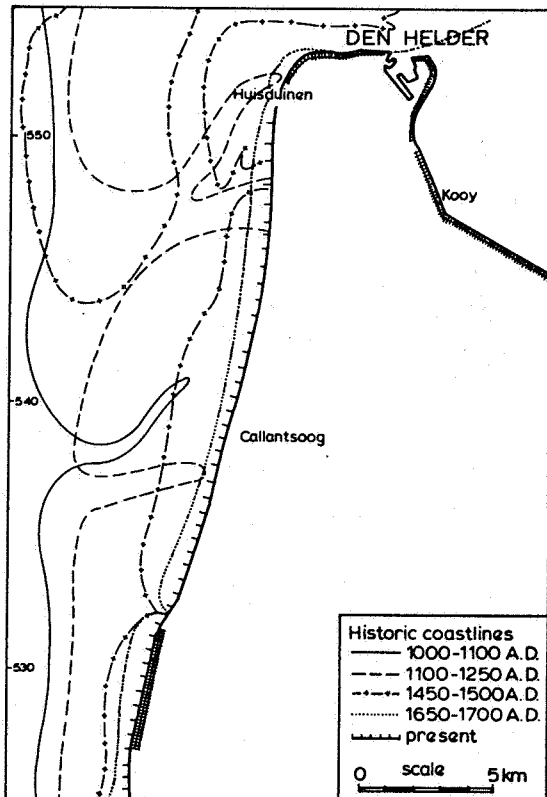


Over the years many seawalls, groynes and dune foot revetments have been built to reduce the rate of shoreline erosion. One example is the Hondsbosse Seawall constructed in the 16th century and reconstructed one kilometre further inland in the 19th century (Schoorl, 1982). A reconstruction of the historic coastlines is shown in Figure 10. Another example is the erosion between Rotterdam and The Hague, shown Figure 11. Groynes were constructed in the first half of the 19th century and extended landwards in the 20th century (van der Kolff, 1985). At present the shoreline has more or less stabilized, although beach nourishments are carried out incidentally to maintain the beach (see Figure 14).

**Figure 10** Coastal erosion since the 11th century near Den Helder
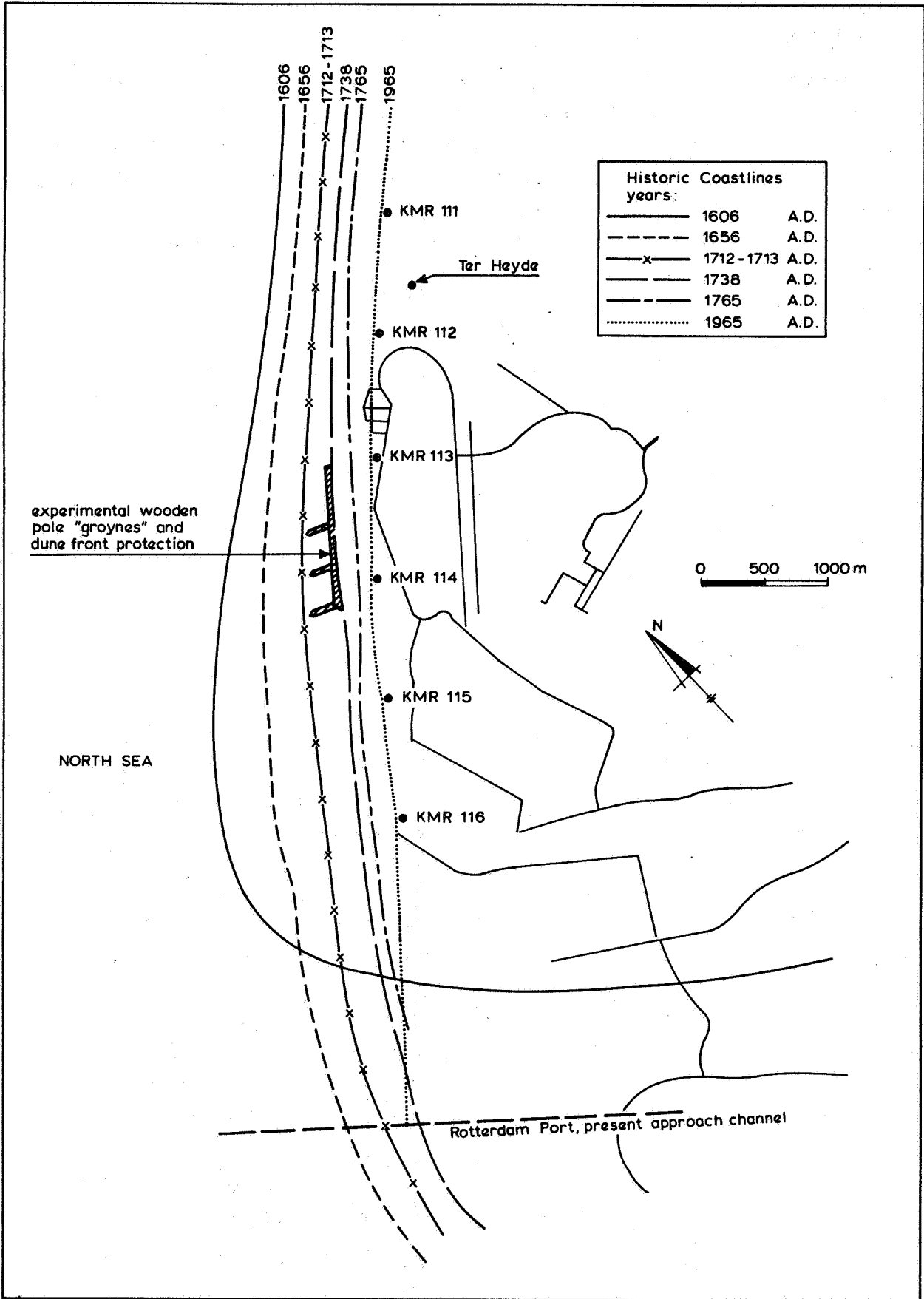
**Figure 11** Coastal erosion between Rotterdam and The Hague since the 16th century

The locations and the types of coastal protection along the shores of The Netherlands are shown in Figure 12 and 13. During the last decades it has been noticed that the construction of solid beach protection works is not always the best solution from a technical nor from an economical point of view (Rijkswaterstaat and Delft Hydraulics Laboratory, 1986).

In most cases nowadays a flexible solution to the long term erosion problem is beach nourishment by natural sand. Since 1952 some 27 million $m^3$ of sand has been put on The Netherlands' beaches. The locations and the quantities are shown in Figure 14. The total erosion of the beaches along the North Sea shore of The Netherlands is in the order of 4 million $m^3$ per year. The beach nourishment during the last 34 years amounts to 0.8 million $m^3$/year (Roelse, 1985). As a result of the deficit an increasing number of coastal sections are becoming critical with respect to the reliability of the dunes as primary sea defence structure.
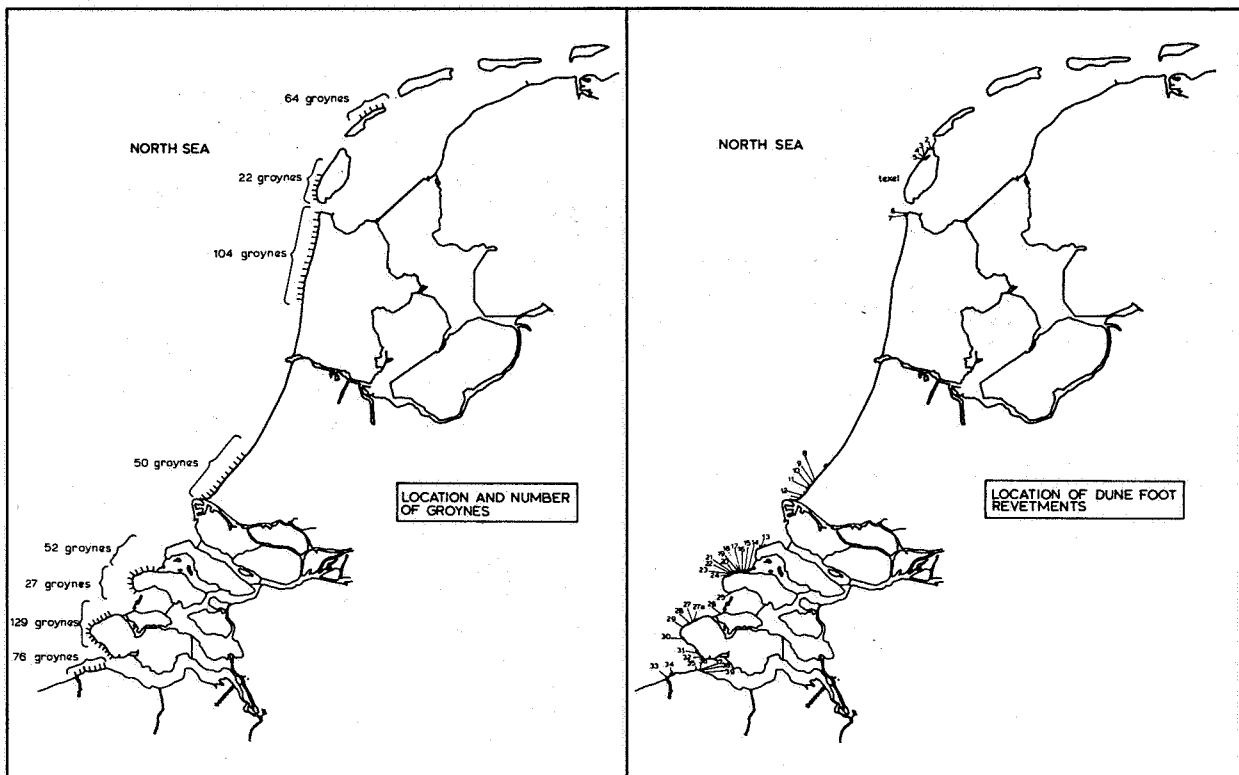


**Figure 12**  Coastal protection, locations and types

storm surge level

basalt blocks

mean high water

mean low water

osier cover

fascine mattress

groyne

storm surge level m.s.l.+ 5.35 m

dune

m.s.l.+2.35

1:3.5

wooden piles

beach

basalt blocks (0.30m/0.40)

bed of bricks

clay layer

m.s.l. 1.20

DUNE FOOT REVETMENT

wooden piles

11.5 m
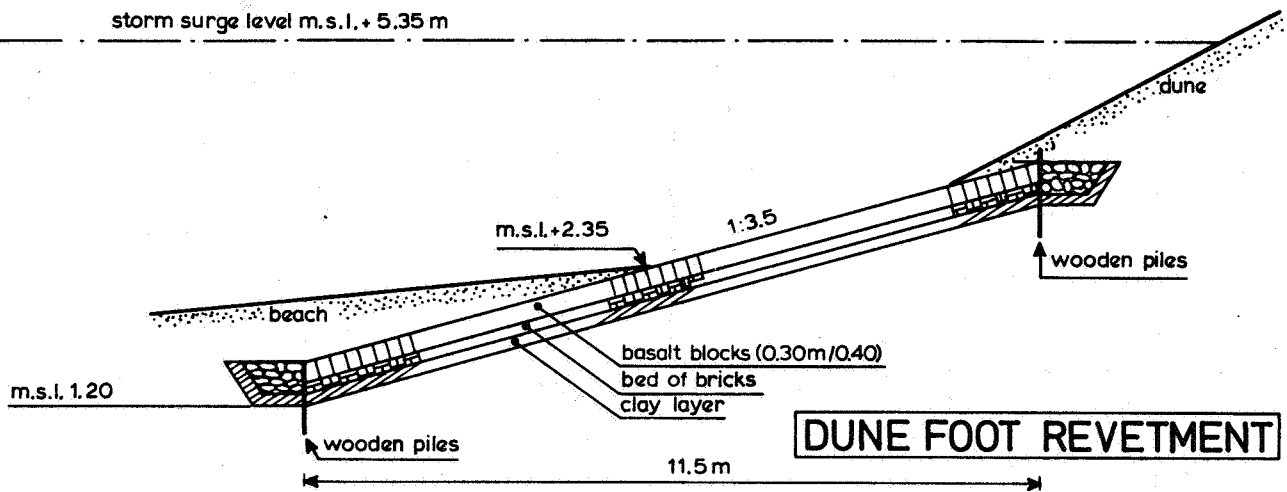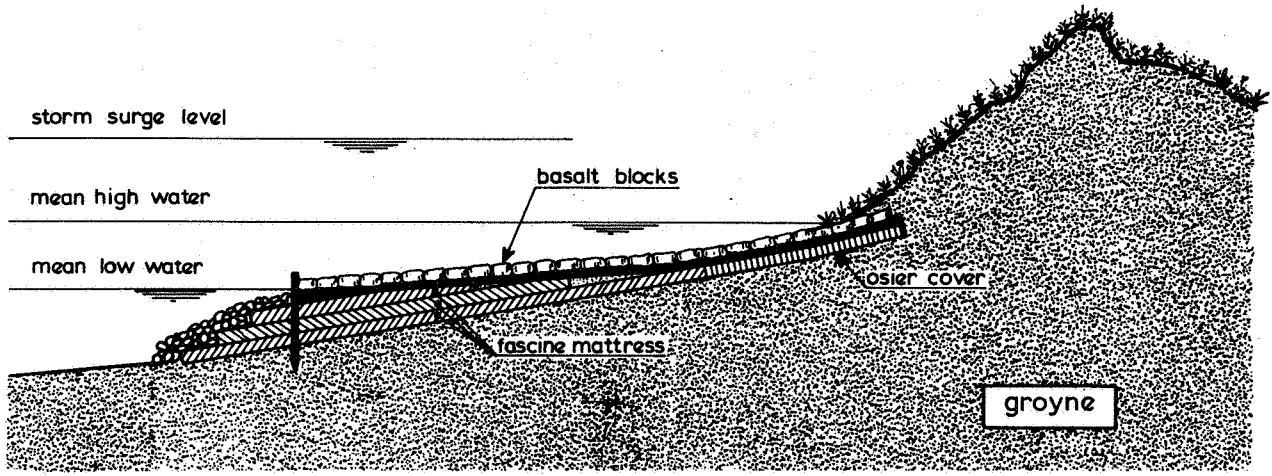
**Figure 13** Coastal protection, types
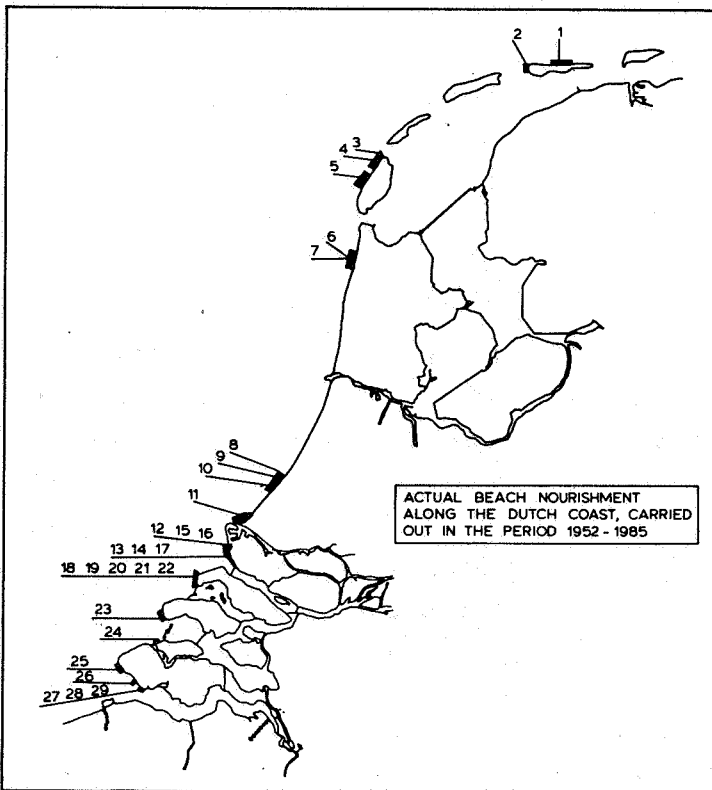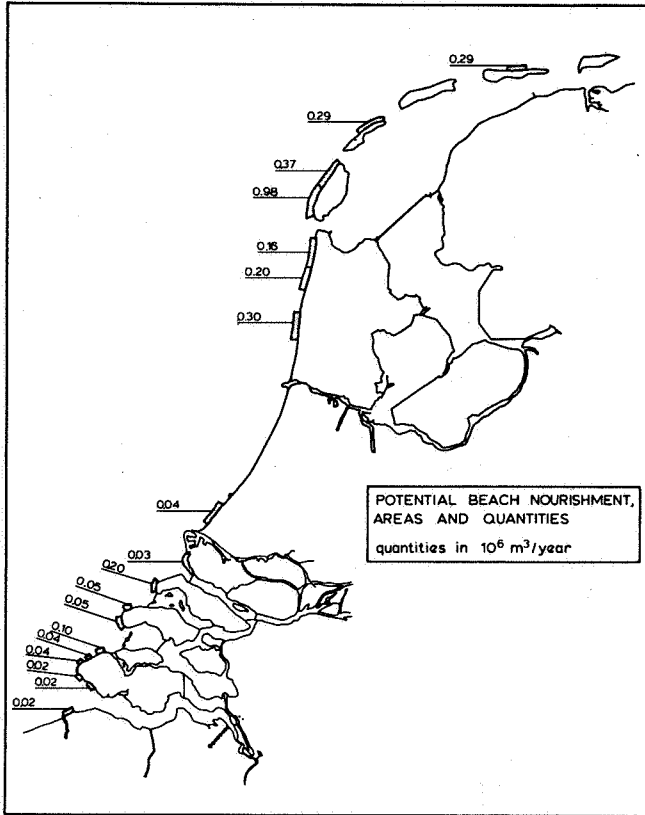
| Actual beach nourishment 1952-1985 | | |
|---|---|---|
| Number | Volume m$^3$ | Year |
| 1 | 2,200,000 | 1980 |
| 2 | 310,000 | 1979 |
| 3 | 3,050,000 | 1979 |
| 4 | 2,800,000 | 1985 |
| 5 | 3,000,000 | 1985 |
| 6 | 350,000 | 1976-1977 |
| 7 | 470,000 | 1979-1980 |
| 8 | 45,000 | 1969 |
| 9 | 70,000 | 1975 |
| 10 | 330,000 | 1985 |
| 11 | 870,000 | 1977-1978 |
| 12 | 150,000 | 1979-1980 |
| 13 | 110,000 | 1974 |
| 14 | 150,000 | 1974 |
| 15 | 1,100,000 | 1977 |
| 16 | 3,200,000 | 1985 |
| 17 | 440,000 | 1983 |
| 18 | 400,000 | 1969-1970 |
| 19 | 610,000 | 1971 |
| 20 | 3,640,000 | 1973-1974 |
| 21 | 1,270,000 | 1977 |
| 22 | 860,000 | 1984-1985 |
| 23 | 112,000 | 1975 |
| 24 | 210,000 | 1973 |
| 25 | 100,000 | 1985 |
| 26 | 775,000 | 1952-1959 |
| 27 | 50,000 | 1952 |
| 28 | 32,000 | 1966 |
| 29 | 45,000 | 1975 |

Total = 26,749,000 m$^3$ in 34 years

**Figure 14**  Potential and actual beach nourishment
(Roelse, 1985)
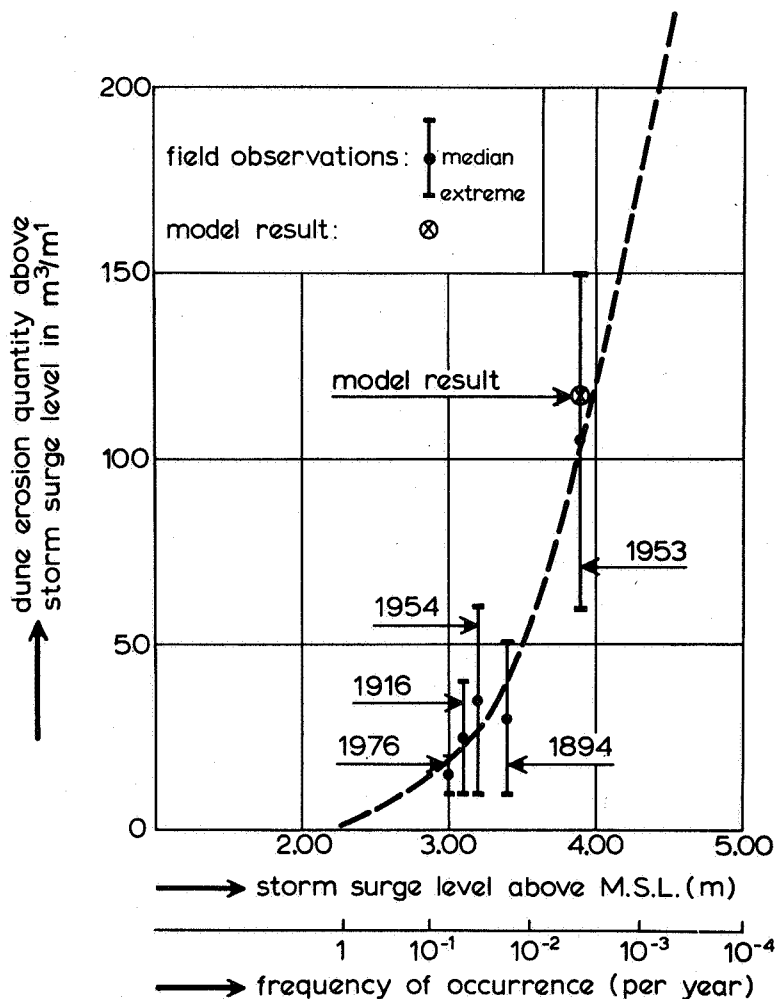
**Figure 15** Dune erosion in Delfland since 1894

## 2.3 Dune erosion prediction

A first estimate of the erosion to be expected during extreme storm surges can be found from field observations. A reasonably reliable set of data is available for the coastal stretch of Delfland, see Figure 15. The highest sea level was recorded in 1953 at a height of 3.9 m above mean sea level. This level has a frequency of exceedance of 1/300 per year. The erosion of the dunes during this storm surge was derived from recorded dune foot recessions. The dune foot receded by an average of 30 m. This corresponds to an erosion quantity above storm surge level of about 100 m³/m' (cubic metre per running metre along the beach).

By law the primary sea defence system should be able to withstand a storm surge with a peak level that has a frequency of exceedance of 1:10,000 per year. A rough extrapolation of the field data of Delfland, shown in Figure 15, shows that a sea level of 5.25 m above mean sea level, having a frequency of exceedance of 1/10,000 per year is associated with an erosion quantity in the order

of 300 m³/m' up to 600 m³/m' depending on the type of extrapolation. For Delfland with a dune height of about 10 m above mean sea level this corresponds with a dune front recession ranging from 60 to 120 m. In the actual situation the dunes at Terheyde in Delfland are about 70 m wide. A similar situation is found in North-Holland at Callantsoog. In the southern part, on Walcheren and Schouwen, coastal stretches can be found with dunes less than 50 m wide, partially protected with revetments. This situation makes it urgent to have a thorough understanding of the dune erosion phenomenon and to have a reliable safety criterion for the dunes as a primary sea defence system.

Thus the requirement for the dune erosion research project can be summarized as follows:

1) The coastal dunes are of vital importance as a primary sea defence structure for the major part of The Netherlands.
2) The knowledge about the process of dune erosion during storm surges is insufficient to define the minimum required dimensions of the dunes.
3) The long term shoreline erosion is creating an increasing number of critical situations along the coast calling for technically safe and economically feasible solutions.

The above shows that knowledge about dune erosion during storm surges is of vital interest for The Netherlands. In other parts of the world there is generally no such risk of inundation and the effects of dune erosion are restricted to a marginal loss of land and eventually the loss of properties situated on the dunes. However, there is a growing international interest in coastal and dune erosion because of increasing capital investment in recreation facilities at the sea front and an anticipated accelerated sea level rise.

Studies of dune erosion outside The Netherlands before 1980 are mainly of a qualitative character, see viz. Leatherman, 1979. After 1980, simultaneously with the present studies, quantitative studies have been carried out by Hughes (1983), and Kriebel and Dean (1985). The results of these studies are discussed in Chapter 7.

Edelman (1968) in The Netherlands was the first to develop a quantitative method for the prediction of dune erosion. The method is based on the assumption that during a storm surge a normal beach slope will develop but at a higher level than before. Edelman applied a straight beach slope of 1:50 in his computations. In 1972 this method was improved by Van de Graaff (1977), who defined a realistic concave erosion profile. The form of this profile was

derived from field measurements directly after the 1953-storm surge in the northern part of North-Holland. Van de Graaff assumed that this beach profile can be considered as typical of the profiles that will develop during storm surges. He also assumed that the profile will develop up to a waterdepth of 1.28 $H_{bs}$ below the peak level of the storm surge, in which $H_{bs}$ is the wave height at initial breaking of a wave with significant deep water wave height $H_{0s}$.

Van der Meulen and Gourlay (1968) were the first to investigate the process of dune erosion in small scale movable bed models. The tests were mainly carried out in a basin with monochromatic waves. The tests provided qualitative answers for the question how dune erosion is influenced by: dune height, initial beach profile, wave height, wave period, wave reflection, sea level (variation) and grain size characteristics. Lateron, Hulsbergen (1974) found that such tests must have suffered from the effect of secondary waves. From a series of tests he found that, for conditions with monochromatic waves generated by a flap type wave board, the beach profile development is strongly related to the distance between the wave board and the shoreline. Hulsbergen clearly demonstrated that this relation is explained by the presence of secondary waves. Earlier Fontanet (1961) had shown that these secondary waves are a by-product of monochromatic waves generated by a flap type wave generator. Additional experimental research at Delft Hydraulics Laboratory demonstrated that the effects of secondary waves in a random wave field on the development of the bottom profile are one to two orders of magnitude smaller than under conditions with monochromatic waves (Delft Hydraulics Laboratory, 1981).

## 2.4 Research programme

In 1974 a series of dune erosion tests was carried out with random waves by Van de Graaff (1977). An idealized coastal profile and idealized storm surge conditions were reproduced in a wind wave flume with depth scale factors $n_d$ = 150; 84; 47 and 26. Two different grain sizes were tested, $D_{50}$ = 150 µm and $D_{50}$ = 225 µm. It was anticipated that the model should be distorted for an adequate reproduction. Therefore various length scale factors were applied for the reproduction of the initital profile. Scale relations were developed on the basis of a correlation analysis of erosion quantities and erosion profiles. A prototype value was found by application of the best fit scale relations.

The approach of studying the process of dune erosion by means of a scale series was considered succesful. However, considerable scale effects were still observed and the gap between $n_d$ = 26 and $n_d$ = 1 was relatively large.

It was concluded that the prototype results derived from the tests were not sufficiently reliable to be the basis of a new dune erosion prediction model. Model tests in the range from $n_d = 26$ to $n_d = 1$ were desired to improve the reliability. However, in 1974 model facilities with random waves larger than the one already used were not available. Given this situation it was recommended to carry out additional small scale tests as there were indications that the scale effects could be decreased by reducing the fall velocity of the bottom material according to the dimensionless fall velocity parameter H/Tw.

Finally the research project has evolved as indicated in Table 1. The experiments were started by Van de Graaff in 1974. The programme after 1975 has been initiated and coordinated by the writer. The tests were carried out by the writer and some of his colleagues at Delft Hydraulics Laboratory, Laboratory De Voorst.

| Research on the erosion of coastal dunes during storm surges with the aim to increase the insight into the phenomenon, and to develop a dune erosion prediction model by which the safety of the existing beaches and dunes as a primary sea defence system can be checked and the required reinforcements can be determined. | |
|---|---|
| 1972 | Provisional model |
| 1974-1975 | Scale series, four scale factors, two grain sizes, two-dimensional |
| 1976-1978 | Scale series, three scale factors, four grain sizes, two-dimensional |
| | Analysis and evaluation of scale relations |
| | Field data analysis of the dune erosion caused by the storm surge of January 3rd 1976. Evaluation of the provisional model |
| 1979-1980 | Verification of two-dimensional approach by means of small-scale tests in a three-dimensional model |
| 1981-1982 | Verification of scale relations by means of large-scale tests |
| | Parametric small-scale model investigations to define the effect of storm surge level, wave height, wave period and the coastal profile on the rate of dune erosion |
| 1982-1983 | Development of a predictive computational model for dune erosion, verification of this model for laboratory and field data |
| 1984-1985 | Analysis of the process of dune erosion in terms of wave conditions, velocity field, sediment concentration and profile changes, with the aim to develop a time dependent computational model |

**Table 1**  Research programme

# 3. Scale relations

## 3.1 Introduction

Which mechanism is controlling the rate of dune erosion? Is it the resistance forces of the dune in terms of soil mechanic properties, or is it the hydraulic transport capacity of the waves? Specialists in soil mechanics and specialists in coastal hydraulics have disputed this matter. (Delft Soil Mechanics Laboratory, 1980). Observations of dune erosion in nature, during moderate storm surges lead to the following concept.

The first series of waves reaching the dune front causes erosion and a consequent lowering of the beach just in front of the dunes. After a number of waves the foot of the dune is eroded to such an extent that the dune front becomes unstable. Then, a slice of sand of between 0.2 and 2.0 m thick (depending on the height and form of the dune) slides down, forming a pile of sand at the foot of the dune. This volume of sand is then gradually eroded by the waves. After some 50 to 100 waves, the pile of sand is cleared away and a new dune front instability occurs. In course of time it takes longer and longer before the pile of sand is removed. The rate of dune erosion decreases with time.

The decrease of the rate of dune erosion with time is likely to be caused by the heightening of the beach and a consequent reduction of the offshore sediment transport capacity. On the basis of the observations and interpretations it is assumed that the erosion of the dunes (the sequence of dune front instability, sliding down of sand, forming of a pile and gradual removal by the waves) is fully controlled by the sediment transport capacity of the breaking waves and that the (soil mechanic) resistance forces are relatively unimportant to the rate and the quantity of dune erosion. During the large scale tests additional measurements have been carried out to asses the influence of soil mechanic properties. The results confirmed the present assumptions (Delft Hydraulics Laboratory 1984 and Delft Soil Mechanics Laboratory 1982).

The physical process of sediment transport in the surf zone is not understood in such detail that it can be described mathematically. Important parameters are the wave conditions, the wave generated velocity field and the sediment characteristics. The scale relations described in literature are generally based on a mixture of theory, assumptions and empirics; see Noda (1972), Le Mehaute (1970), Dalrymple and Thompson (1976) and Gourlay (1980). Actually none of the scale relations proposed by these authors has been verified for conditions with (natural) random waves. The scale relations developed simulta-

neously with the present studies, by Hughes (1983) and by Hallermeier (1985) will be discussed in Chapter 7. As no adequate scale relations were available Van de Graaff (1977) carried out a number of tests in the form of a scale series. By extrapolation of the test results a prototype value was found. In fact this is a black-box method with all its disadvantages. However, the risk involved in the extrapolation has been minimized by a schematization of the test conditions and by a carefully selected extrapolation method. The hydraulic conditions were reproduced on the basis of the Froude law: $n_H = n_L = n_d = n_T^2$. Van de Graaff applied a distortion relation for the conversion of the relatively steep profiles that developed in the models:

$$n_1/n_d = n_d^{\alpha} \tag{6}$$

and a time scale relation for the morphological process to describe the rate of the erosion as a function of the scale factor:

$$n_t = n_d^{\beta} \tag{7}$$

The exponents $\alpha$ and $\beta$ were determined on the basis of a correlation analysis of the dune erosion quantities. Van de Graaff found that $\alpha = 0.28$ and $\beta = 0$ so:

$$n_1/n_d = (n_d)^{0.28} \text{ and} \tag{8}$$

$$n_t = (n_d)^0 = 1 \tag{9}$$

A motivation of the basic form of the scale relations and an evaluation of the final results has not been given by van de Graaff. However, it is considered essential for the present investigations to start with an analysis of the physical processes and the corresponding scale relations. The scale relations for the hydraulic conditions, for the grain size, for the development of equilibrium profiles and for the sediment transport process are discussed in the following paragraphs.

## 3.2 Hydraulic conditions

The water motion in free surface oscillatory waves is mainly determined by gravitational and inertial forces. The ratio of these forces should be preserved in the model for reasons of dynamic similarity. For the present models gravity is the same as in prototype. Consequently, for a proper reproduction, the inertial forces should be the same as in prototype as well. The dynamics of water motion under oscillatory waves can reasonably well be described by linear wave theory:

$$\frac{du}{dt} = \frac{g\pi H}{L} \frac{\cosh\{2\pi(d-y)/L\}}{\cosh 2\pi d/L} \sin (2\pi x/L - 2\pi t/T) \tag{10}$$

$$\frac{dv}{dt} = \frac{-g\pi H}{L} \frac{\sinh\{2\pi(d-y)/L\}}{\cosh 2\pi d/L} \cos (2\pi x/L - 2\pi t/T) \tag{11}$$

in which:

| | | |
|---|---|---|
| x | is the horizontal distance from a reference position | (m) |
| y | is the vertical distance from the time average water level | (m) |
| u and v | are the horizontal and vertical component of the velocity | (m/s) |
| t | is time | (s) |
| d | is water depth | (m) |
| H | is wave height | (m) |
| L | is wave length | (m) |
| T | is wave period | (s) |

The dynamic similarity requirement can be put as

$$n \left(\frac{du}{dt}\right) = n \left(\frac{dv}{dt}\right) = 1 \tag{12}$$

in which n indicates the ratio of the value in prototype over the value in the model. Relation (12) combined with (11) and (10) yields,

$$n(g\pi H/L) = 1 \qquad \text{so} \qquad n_H = n_L \quad \text{and} \tag{13}$$

$$n(2\pi/d-y)/L) = n(2\pi d/L) = 1 \qquad \text{so} \qquad n_d = n_L \quad \text{and} \tag{14}$$

$$n(2\pi x/L) = n (2\pi t/T) = 1 \qquad \text{so} \qquad n_x = n_L \quad \text{and} \tag{15}$$

$$n_t = n_T \tag{16} \tag{18}$$

The parameters L, d and T are not independent in wave motion. Their relation is described by the dispersion relation

$$\left(\frac{2\pi}{T}\right)^2 = \frac{2\pi g}{L} \tanh 2\pi d/L \tag{17}$$

Relation (17) together with relation (14) yields

$$n(L) = n(T^2) = n_d \qquad \text{so} \tag{18}$$

$$n_T = (n_d)^{0.5} \tag{19}$$

Summarizing, the dynamic similarity requirement yields

$$n_H = n_L = n_T^2 = n_t^2 = n_u^2 = n_v^2 = n_d \tag{20}$$

This combination of scale relations (20) is called the Froude scale for wave motion.

To ensure a proper reproduction of the wave field in place and time the respective scale relations should be as follows:

$$n_x = n_L = n_d \text{ and} \tag{21}$$

$$n_t = n_T = (n_d)^{0.5} \tag{22}$$

Experience has shown that when natural sand is applied in small scale models the beach profiles that develop in the model are considerably steeper than in the field. This occurs because the sand grains in the model are proportionately too large and too heavy. Model distortions are applied to get a proper reproduction of the field profiles. In distorted models the length scale factor, $n_l$ (= $n_x$) is unequal to the depth scale factor $n_d$. So relation (21) is violated and the spatial gradient of the acceleration and deceleration forces is not properly modelled. However, according to the linear wave theory accelerations and decelerations are correctly modelled for each individual value of x and t. So, from this point of view a model distortion does not affect the reproduction of the hydraulic conditions. However, for steeper slopes the linear wave theory does not give an adequate description of reality as the type of wave breaking and thus the hydraulic forces are influenced by the slope.

Battjes (1974) has derived a surf similarity parameter for the description of wave breaking characteristics:

$$\xi = \frac{\tan \theta}{\sqrt{H_0/L_0}} \tag{23}$$

in which:

$\xi$     is dimensionless surf similarity parameter     (-)

$\tan \theta$ is the slope of the beach profile     (-)

$H_0$     is the deep water wave height     (m)

$L_0$     is the deep water wave length     (m)

Preservation of this parameter in the model gives

$n(\tan\theta/(H_0/L_0)^{0.5}) = 1$ which can be written as $\qquad(24)$

$n(\tan\theta) = n(H_0/L_0)^{0.5}$ which can be written as $\qquad(25)$

$n_d/n_1 = (n_H)^{0.5}/(n_L)^{0.5}$ $\qquad(26)$

For $n_H = n_d$ this gives

$n_d/n_1 = (n_d)^{0.5}/(n_L)^{0.5}$ yielding $\qquad(27)$

$(n_L)^{0.5} = (n_1/n_d)(n_d)^{0.5} = n_1/(n_d)^{0.5}$, yielding $\qquad(28)$

$n_L = (n_1)^2/n_d$ which can be written as $\qquad(29)$

$n_L = n_1(n_1/n_d)$ $\qquad(30)$

The dispersion relation yields

$n_L = n_T{}^2$, together with (30) this yields $\qquad(31)$

$n_T = (n_d)^{0.5}(n_1/n_d)$ $\qquad(32)$

So if the surf similarity parameter is preserved in distorted models the wave period should not be scaled according to the Froude scale ($n_T = n_d{}^{0.5}$) but according to relation (32).

However, when relation (32) is applied the inertial forces are on a different scale than the gravitational forces. This shows that in a distorted model it is not possible to maintain the geometrical, the kinematical and the dynamical properties of the breaking waves simultaneously. There will always be a scale effect. This effect is a function of the scale factor and it will reduce to zero for depth scale factor $n_d = 1$. As such the effect can be described as an integral part of the scale relations and in principle it does not matter whether the Froude relations or the surf similarity parameter is applied in the present scale series.

However, scaling according to the surf similarity parameter has a major disadvantage. Preservation of this parameter in a distorted model implies that the wave steepness is distorted. A a consequence a large number of waves will break in deeper water. This affects the wave height so that its ratio to waterdepth is not preserved. This ratio is of the utmost importance for the accurate reproduction of the breakerzone. Another inconvenience of the preservation of the surf similarity parameter is the "distorted" time scale (32).

On the basis of these considerations, the Froude scale relation is chosen as a basis for the present scale series.

## 3.3 Grain size

Beach profile changes will only be reproduced correctly when the underlying processes are reproduced correctly. Assuming that the hydraulic conditions are properly scaled, the entrainment of sediment and the settling of sediment should have the proper scale factors. A classical way to derive the scale relations is to describe the ratio of the relevant forces and parameters. Such ratios can be described in terms of dimensionless numbers. The dimensionless numbers should have the same value in model as in prototype.

The three major dimensionless numbers for the interaction of natural water and quartz sand are: the Reynolds number, the densimetric Froude number and the dimensionless fall velocity parameter (Yalin, 1971; Le Mehaute, 1970). The numbers and the corresponding scale relations are elaborated below.

- **The Reynolds number** being the ratio between the inertial forces and the viscosity forces, determines the character of the flow field around a sand grain:

$$Re = v_* D/\nu \tag{33}$$

in which:

$v_*$ is the shear stress velocity $\qquad$ (m/s)
$D$ is grain diameter $\qquad$ (m)
$\nu$ is viscosity $\qquad$ (m$^2$/s)

For the reproduction of a geometrically similar flow field the Reynolds number should have the same value in the model and in prototype, so

$$n(Re) = (n_{v_*} n_D)/n_\nu = 1 \tag{34}$$

The use of natural water in the model gives $n_\nu = 1$. It is assumed that the scale factor for the shear stress velocity is of the same order of magnitude as the scale factor for the orbital velocity so

$$n_{v_*} \approx n_u = n_d^{0.5} \tag{35}$$

Relation (34) with $n_\nu = 1$ together with relation (35) gives

$$n_D = (n_d)^{-0.5} \tag{36}$$

This result indicates that the grain size in a small scale model should be larger than in prototype for a geometrically similar reproduction of the flow field around an individual grain.

- **The densimetric Froude number** being the ratio between pressure forces and gravitational forces characterizes the entrainment of sediment:

$$Fr_* = v_*^2/\Delta gD \qquad (37)$$

in which:

$\Delta$  is the relative density of the sand with respect to water
$$\Delta = (\rho_s - \rho_w)/\rho_w \qquad (-)$$
$v_*$  is the shear stress velocity $\qquad$ (m/s)
$g$  is the gravitational constant $\qquad$ (m/s$^2$)
$D$  is the grain diameter $\qquad$ (m)

For a proper reproduction of the ratio of the forces acting on a grain on the bottom the densimetric Froude number should have the same value in the model as in prototype so

$$n_{Fr_*} = n_{v_*^2}/n_\Delta \, n_g \, n_D = 1 \qquad (38)$$

When in the model the same water and sediment density is applied as in prototype, $n_\Delta$ is equal to 1. Assuming $n_{v_*} \approx n_u$ now leads to

$$n_D = n_d \qquad (39)$$

So, to ensure the same ratio between the relevant forces acting on a sand grain on the bottom, the grain size in the model should be reduced by a factor equal to the depth scale factor.

- **The dimensionless fall velocity parameter** describes the ratio of the orbital velocity, (expressed in terms of wave height and wave period) and the fall velocity:

$$H/Tw \text{ (dimensionless fall velocity parameter)} \qquad (40)$$

in which:

$H$  is wave height $\qquad$ (m)
$T$  is wave period $\qquad$ (s)
$w$  is fall velocity $\qquad$ (m/s)

When the wave conditions are reproduced according to Froude,
the conservation of the dimensionless fall velocity parameter yields

$$n(H/Tw) = n_d/(n_d)^{0.5} \, n_w = 1 \qquad \text{yielding} \qquad (41)$$

$$n_w = (n_d)^{0.5} \qquad (42)$$

- In the Stokes range of fall velocities, $D < \sim 100$ µm
  $(w \sim D^2)$, this yields $n_D = n_d^{0.25}$       (43)

- In the intermediate range, $100$µm $< D < 4000$µm $(w \sim D)$, relation (42)
  yields $n_D = n_d^{0.5}$       (44)

- In the Newton range of fall velocities, $D > 4000$ µm $(w \sim D^{0.5})$
  relation (42) yields $n_D = n_d$       (45)

## Summary dimensionless numbers approach

The results of the dimensionless numbers analysis with respect to grain size are summarized in Table 2. It is clear that contradictory results are found when natural water and sand are considered for the small scale modelling. This would be a reason to apply other materials. However, the investigations of Collins and Chesnut (1975) and Gourlay (1980) and the experience with small scale coastal models at the Delft Hydraulics Laboratory (Reinalda, 1960) have shown that the use of other materials raises more new questions than answering original ones. Therefore natural sediment is still considered the most practical material for small scale modelling. Starting from the idea of a scale series, in principle any grain size scale relation can be chosen. However, the present results are so contradictory that a sensible choice cannot be made. Another way to derive scale relations is to consider equilibrium profile descriptions. This method is elaborated in the next paragraph.

| Reynolds number | Densimetric Froude number | Dimensionless fall velocity number | | |
|---|---|---|---|---|
| $v_* D/\nu$ | $v_*^2/\Delta g D$ | $H/Tw$ | | |
| | | $n_w = n_d^{0.5}$ | $n_w = n_d^{0.5}$ | $n_w = n_d^{0.5}$ |
| | | Stokes-range | Intermediate-range | Newton-range |
| | | $D < 100$µm | $100$µm$< D < 4000$µm | $D > 4000$µm |
| $n_D = n_d^{-0.5}$ | $n_D = n_d$ | $n_D = n_d^{0.25}$ | $n_D = n_d^{0.5}$ | $n_D = n_d$ |

**Table 2** Scale factors for sediment size, dimensionless numbers

## 3.4. Equilibrium profiles

During a storm surge the sea level may rise a few meters. If the elevated sea
level were to last for a long time a new beach profile would develop at this
elevated level. Under normal conditions, with normal water level fluctuations
the shape of the coastal profile is more or less in equilibrium. As dynamic
features like moving bars and throughs can still be observed, the term "dyna-
mic equilibrium" is introduced. For conditions without a major longshore
transport gradient and/or tidal effects, the shape of such a dynamic equili-
brium profile must be related to the wave conditions and the sediment proper-
ties. Hence, for small scale reproduction of beach profile changes the parame-
ters that describe the relation between the hydraulic/sedimentological condi-
tions and the shape of the equilibrium beach profile should be scaled proper-
ly.

A large number of researchers have tried to find a relation between the shape
of the beach profile and the hydraulic/sedimentological conditions. The re-
sults will be reviewed and the corresponding scale relations will be discus-
sed. Distinguished by the main hydraulic parameters, there are four basic
approaches:

1) deep water wave steepness $H_0/L_0$
2) dimensionless fall velocity parameter $H/Tw$
3) ratio of orbital velocity and fall velocity $u/w$
4) wave energy dissipation rate $\partial (Enc)/\partial x$

**Deep water wave steepness**

Johnson (1949) and later on Saville (1957) suggested that the type of beach
profile must be related to the deep water wave steepness:

$$\text{type of beach profile} \sim (H_0/L_0) \tag{46}$$

Hence, for a small scale reproduction of beach profile changes the deep water
wave steepness in the model should have the same value as in the field.

So:

$$\text{if } n(H_0/L_0) = 1 \text{ then } n_1/n_d = 1 \tag{47}$$

However, the findings of Johnson and Saville are mainly based on a series of
tests with monochromatic waves. These tests must have suffered from the effect
of secondary waves and the subsequent typical beach profile developments as
described by Hulsbergen (1974) and Bijker et al (1976). Consequently, relation
(47) should be considered with great caution.

## Dimensionless fall velocity parameter

Wiegel (1964) has demonstrated that the slope of the beach is related to the grain size of the beach sand. Iwagaki and Noda (1963) amongst many others demonstrated that the slope of the beach profile is effected by the wave steepness and by the grain size of the beach sediment. Later on Kemp and Plinston (1968), Noda (1972), Dalrymple and Thompson (1976) and Gourlay (1980) have found on more or less theoretical and empirical grounds that the slope of the beach profile is related to the dimensionless fall velocity parameter H/Tw. Conditions with equal value for H/Tw should yield equal beach slopes. Expressed in terms of scale relations this gives

$$\text{if } n(H/Tw) = 1 \text{ then } n_l = n_d \tag{48}$$

So, undistorted beach profiles are reproduced in a small-scale model when

$$n(H/Tw) = 1 \tag{49}$$

Inserting the scale relations according to Froude yields:

$$\text{if } n_d/(n_d)^{0.5} \, n_w = 1 \quad \text{then} \quad n_l = n_d \tag{50}$$

which can be written as

$$\text{if } n_w = (n_d)^{0.5} \text{ then } n_l = n_d \tag{51}$$

Also this result should be considered with caution as there is no experimental evidence with natural random waves, so far.

## Ratio of orbital velocity and fall velocity

Valembois (1960) has derived scale relations for suspended sediment transport in the surf zone. He suggests that the ratio of fall velocity and water depth over the ratio of the flow velocity and the length perpendicular to the beach should be preserved in the model. Later on Le Mehaute (1970) comes to a similar conclusion. Le Mehaute (1970) states that kinematical similarity is very important in small scale modelling of beach profiles. He suggests that the ratio of orbital velocity over fall velocity should be maintained:

$$n \, (u/w) = 1 \tag{52}$$

Inserting the scale relations according to Froude,

$n_u = n_d^{0.5}$, this yields

$$n_w = n_d^{0.5} \tag{53}$$

Furthermore le Mehaute (1970) states that in case (53) cannot be met the model should be distorted according to

$$n_l/n_d = n_u/n_w \tag{54}$$

Again inserting $n_u = n_d^{0.5}$, this relation yields

$$n_l/ n_d = (n_d/n_w^2)^{0.5} \tag{55}$$

For models with the same grain size as in the prototype this becomes:

$$n_l/ n_d = (n_d)^{0.5} \tag{56}$$

**Wave energy dissipation rate**

Bruun (1954) was the first to relate the form of the beach profile to the distribution of the wave energy dissipation across the surfzone. By assuming an even rate of energy dissipation per unit area across the surf zone he arrived at a simple power curve for the description of the profile:

$$y^{1.5} = px \tag{57}$$

in which
y  is the water depth                          (m)
x  is the distance from the water line        (m)
p  is a dimensional constant                  $(m)^{0.5}$

A similar power curve was derived by Dean (1977). Dean assumed that the wave-beach interaction leads to an equilibrium beach profile such that the incomming wave energy is uniformly dissipated per unit volume of water accross the surf zone. Expressed in terms of energy flux and water depth this gives (Dean, 1977):

$$\frac{\partial E c_g}{y \partial x} = f(D) \tag{58}$$

in which:

E     = wave energy per unit area                    $(J/m^2)$

$c_g$   = wave group velocity                          $(m/s)$

y     = water depth                                  (m)

x     = distance from the water line                 (m)

f(D) = the rate of wave energy dissipation per unit volume of water under equilibrium conditions, as a function of the grain size $(W/m^3)$.


Equation (58) was elaborated as follows (Dean 1977):

$$\frac{\partial Ec_g}{y\partial x} = \frac{\partial\ 1/8\ \rho g\ H^2\ \sqrt{gh}}{y\partial x} = \text{constant} \qquad (59)$$

in which

H  is local wave height in the surf zone             (m)

h  is local water depth in the surf zone             (m)


h = y, (by definition)                                               (60)


H ~ y  (constant breaker index across the surf zone)                 (61)

Substitution of (60) and (61) in (59) yields

$$\frac{\partial y^{2.5}}{y\partial x} = \text{constant} \qquad (62)$$

Integration of (62) yields

$$y^{1.5} = cx \qquad (63)$$

in which

y  is the water depth                                (m)

x  is the distance from the water line               (m)

c  is a constant                                     $(m)^{0.5}$


In Dean's approach the mathematical description of the beach profile is solely determined by the grain size, irrespective of the deep water wave conditions. Only the length of the profile is determined by the wave height. So a small scale model beach and a prototype beach with the same grain size should be described by the same power curve:

$$y_p^{1.5} = c_p\ x_p \qquad \text{(prototype beach profile)} \qquad (64)$$

$$y_m^{1.5} = c_m\ x_m \qquad \text{(model beach profile)} \qquad (65)$$

in which

p-index indicates prototype values and

m-index indicates model values

$$c_p = c_m \qquad (66)$$

according to Dean's theory for conditions with prototype-size sediment in the model.

With the present definitions

$$n_d = y_p/y_m \quad \text{and} \qquad (67)$$
$$n_1 = x_p/x_m. \qquad (68)$$

Elaboration of (64) through (68) yields

$$(n_d)^{1.5} = n_1 \quad \text{which can be written as} \qquad (69)$$

$$n_1/n_d = n_d^{0.5} \qquad (70)$$

## Summary of equilibrium beach profile approach

The results of the analysis of equilibrium beach profile parameterizations as summarized in Table 3 are not very conclusive. If prototype size sand is applied in the model the required distortion ranges from $n_1/n_d = 1$ up to $n_1/n_d = n_d^{0.5}$. In case the sediment fall velocity is reduced by a factor $n_w$, the required distortion ranges from $n_1/n_d = 1$ up to $n_1/n_d = (n_d/n_w^2)^{0.5}$.

| parameter describing equilibrium beach profile | | model distortion |
|---|---|---|
| 1) Deep water wave steepness | $H_0/L_0$ | $n_1/n_d = 1$ |
| 2) Dimensionless fall velocity parameter | $H/Tw$ | for $n_w = n_d^{0.5}$ $n_1/n_d = 1$ |
| 3) Ratio of orbital velocity and fall velocity | $u/w$ | $n_1/n_d = (n_d/n_w^2)^{0.5}$ |
| 4) Wave energy dissipation rate | $\partial \, Enc/\partial x$ | for $n_w = 1$ $n_1/n_d = n_d^{0.5}$ |

**Table 3**  Distortion relation derived from equilibrium profile considerations, summary of results

As described before all the methods summarized in Table 3 show some major shortcomings. Actually the dimensionless fall velocity parameter is most promising. It has a theoretical background that is rather straightforward. However, the applicability of the parameter is rather limited. It only gives the scale factor for sediment for undistorted profiles, whereas for the present tests the relation between grain size, depth scale factor and resulting distortion is required.

Valembois' (1960) and Le Mehaute's (1970) approach indicating that the distortion of a model should be equal to the ratio of the scale factor of orbital velocity and fall velocity seems logical from a kinematic similarity point of view. However, in this approach it is assumed that the orbital velocity is not affected by the distortion of the beach profile. This is questionable since for a given waterdepth in the breakerzone a steeper slope is associated with higher orbital velocities and, more importantly, larger orbital velocity fluctuations due to more concentrated wave breaking. This implies that the profile that eventually develops will probably be more gentle than expected on the basis of the first order kinematic similarity requirement.

The theories of Bruun (1954) and Dean (1977) about the energy dissipation rate as the single important parameter in beach profile development are very interesting because of the physical background. However, a relation between grain size and beach profile has not been given by these authors. Moreover, the elaborations as given by Dean (1977) still raise a number of questions, e.g. concerning the effect of the wave period.

It is concluded that none of the methods evaluated above provides a reliable set of scale relations. For that reason an alternative approach was investigated, as will be described in the next paragraph.

## 3.5 Sediment transport

A fundamental way to derive scale relations is to analyse the sediment transport process and to determine the main dimensions. As stated before this process is rather complex and this is probably why no serious attempt has been perviously made to use this method. In the following the cross-shore sediment transport process is described in an idealized way and the corresponding scale relations are derived.

The sediment transport for two-dimensional conditions, i.e. the transport through a vertical section at a position x can be written as:

$$S_x(t) = \frac{1}{t} \int_0^t \int_0^{\eta(t)} c(z,t) \, u_g(z,t) \, dz \, dt \qquad (71)$$

in which:

| | | |
|---|---|---|
| x | is the horizontal distance from a reference position | (m) |
| z | is the vertical distance from the bottom | (m) |
| t | is time | (s) |
| $S_x(t)$ | is the sediment transport per unit width as a function of time | $(m^2/s)$ |
| $\eta(t)$ | is elevation of the water surface above the bottom as a function of time | (m) |
| $c(z,t)$ | is the sediment concentration as a function of time and position above the bottom | (-) |
| $u_g(z,t)$ | is the horizontal velocity of the sediment grains as a function of time and position above the bottom | (m/s) |

Relation (71) is rather complex to evaluate as it includes the product of two non-stationary dependent variables. Scale relations can only be derived when the formula is strongly simplified. In a first order approach it may be assumed that the variation of the sediment concentration with time is small compared with the time-averaged concentration. This is a reasonable assumption for the surf zone as the sediment transport process will be dominated by sediment in suspension, as will be shown in Chapter 7, and the fall time of the grains in the turbulent environment of the breaking waves is an order of magnitude greater than the wave period. The assumption implies that the contribution of the time-averaged velocity to the sediment transport will be an order of magnitude larger than the contribution of the asymmetry of the wave motion. On this basis relation (71) can be written as

$$S_x = \int_0^{\bar{\eta}} \bar{u}(z) * \bar{c}(z) \, dz \qquad (72)$$

in which

| | | |
|---|---|---|
| $\bar{u}(z)$ | is the time-averaged velocity as a function of the position above the bottom | (m/s) |
| $\bar{c}(z)$ | is the time-averaged sediment concentration as a function of the position above the bottom | (-) |
| $\bar{\eta}$ | is the time-averaged elevation of the water surface | (m) |

The time-averaged velocity field in the surf zone is characterized by a circulation of water in the vertical plane. The velocity field has been measured and described by Miller (1976), by Stive (1980) and by Nadaoka and Kondoh (1982). Above the level of the wave troughs the time-averaged flow is directed

onshore. This flow is compensated by a seaward flow (the undertow) below this level. The resulting sediment transport can be considered as the difference between the transport in two layers, above and below the wave trough level $\bar{\eta}_1$:

$$S_x = \int_o^{\bar{\eta}_1} \bar{u}(z) \; \bar{c}(z) \; dz \; - \int_{\eta_1}^{\bar{\eta}} \bar{u}(z) \; \bar{c}(z) \; dz \qquad (73)$$

Continuity of water volume yields

$$\int_o^{\bar{\eta}_1} \bar{u}(z) \; dz = \int_{\eta_1}^{\bar{\eta}} \bar{u}(z) \; dz = q_{ret} \; [m^3/m's] \qquad (74)$$

in which $q_{ret}$ is the time averaged water flow rate in the vertical plane.

With $c_1$ and $c_2$ denoting the time-averaged and layer-averaged sediment concentrations in the two layers, respectively, relations (73) and (74) yield

$$S_x = q_{ret} \; (c_2 - c_1) \qquad (75)$$

So the scale factor as derived from this first order approach is

$$n(S_x) = n(q_{ret}) \; n(c_2 - c_1) \qquad (76)$$

Assuming the velocity field is reproduced according to Froude,

$n(q_{ret}) = (n_d)^{1.5}$, relation (76) yields
$$n(S_x) = (n_d)^{1.5} \; n(c2 - c1) \qquad (77)$$

For a proper reproduction of the process the scale factor for $c_1$ should be equal to the scale factor for $c_2$. In the present first order approach it is assumed that:

$$n_{c_1} = n_{c_2} = n_c \quad so \qquad (78)$$

$$n \; (c_1 - c_2) = n_c \qquad (79)$$

Now (77) can be written as

$$n(S_x) = n_d^{1.5} \; n_c \qquad (80)$$

## Scale factor for sediment concentration

The sediment concentration under breaking waves has hardly been investigated so far. On the basis of field data, Kana (1979) and Nielsen (1984) conclude that the concentration of sediment is strongly dependent on the type of breaking of the waves. Plunging breakers have a direct effect on the sediment entrainment at the bottom and this type of breaking goes with very intensive mixing. According to Bosman (1982) spilling breakers increase the mixing capacity of the water but contribute little to the total sediment load as there is no extra impact on the bottom.

When an irregular wave field on a sloping bottom is considered it is difficult to asses whether plunging or spilling breaking is predominant. In a first order approach the breaker intensity and hence the turbulence and the related sediment concentrations can be described by the rate of energy dissipation per unit volume of water. This can be illustrated by considering the energy required to keep a certain sediment load in suspension.

Energy is transported to the coast in the form of wave motion. The energy flux in the direction of wave propagation can be described as

$$Ec_g = \frac{1}{8} \rho \, g \, H^2 \, c_g \qquad \text{(W/m)} \qquad (81)$$

in which:

E    is the energy of the wave motion per unit area   $(J/m^2)$
$c_g$   is the group velocity of the wave field   (m/s)
$\rho$    is the density of the water   $(kg/m^3)$
g    is the acceleration due to gravity   $(m/s^2)$
H    is the wave height   (m)

The energy dissipation rate in the surf zone, per unit length ($\Delta x$) and per unit width ($\Delta y$) can be written as

$$\text{Energy dissipation rate} = \frac{\partial E c_g \, \Delta y \, \Delta x}{\partial x} \qquad \text{(W/m}^2) \qquad (82)$$

The sediment entrained by the (breaking) waves is kept in suspension by turbulence. It is reasonable to assume that the degree of turbulence will be related to the rate of energy dissipation. In turn the suspended sediment load will be related to the degree of turbulence and thus to the rate of energy dissipation. On the other hand suspended particles have a certain potential energy. If turbulence were absent, these particles would settle to the bottom. In that case the loss of the potential energy would be

$$\frac{\partial \ mgz}{\partial t} = m \ g \ w \qquad\qquad (W/m^2) \quad (83)$$

in which

m     is the mass of the particles        (kg)

g     is the gravitational constant      $(m/s^2)$

z     is the height above a reference level, say the bottom     (m)

w     is the fall velocity of the particles     (m/s)

The hypothesis that the energy dissipation is related to the energy consumption of the suspended particles, yields

$$mgw \sim \frac{\partial (E \ c_g) \ \Delta y \ \Delta x}{\partial x} \qquad\qquad (W/m^2) \quad (84)$$

The total mass of the particles in suspension can be written in terms of sediment concentration as follows

$$m = c \ \rho_s \ \Delta x \ \Delta y \ d \qquad\qquad (kg) \quad (85)$$

in which

c     is the sediment concentration      $(m^3/m^3)$

$\rho_s$     is the density of the sediment      $(kg/m^3)$

d     is the water depth      (m)

Substitution of (85) and (81) in (84) yields

$$c \ \rho_s \Delta x \ \Delta y \ d \ g \ w \sim \frac{\partial (1/8 \ \rho g \ H^2 \ c_g) \ \Delta x \ \Delta y}{\partial x} \qquad\qquad (86)$$

The scale factor for the sediment concentration can be derived from relation (86). For a situation with natural sand and water ($n_{\rho_s} = n_\rho = 1$) and for the scale relations according to Froude $n_H = n_d = n_c^2$ this yields

$$n_c = n_d^{1.5} \ n_1^{-1} \ n_w^{-1} \qquad\qquad (87)$$

Earlier it was derived on the basis of scale relations for the sediment transport that

$$n(S_x) = n_d^{1.5} \ n_c \qquad\qquad (80)$$

Substitution of (87) in (80) yields

$$n(S_x) = n_d^{1.5} \ n_d^{1.5} \ n_1^{-1} \ n_w^{-1} = n_d^{3} \ n_1^{-1} \ n_w^{-1} \qquad\qquad (88)$$

By definition the scale factor for sediment transport is equal to the scale factor for the rate of change of volume. For two-dimensional conditions this yields

$$n(S_x) = n_A / n_t = (n_d \, n_1)/n_t \qquad (89)$$

in which $n_A$ is the scale factor for area.

Combination of (88) and (89) yields

$$n_d \, n_1 \, n_t^{-1} = n_d^{\ 3} \, n_1^{-1} n_w^{-1} \qquad (90)$$

this can also be written as

$$n_1/n_d = (n_t/n_w)^{0.5} \qquad (91)$$

This result is quite simple. It means that the model distortion $(n_1/n_d)$ is a function of the morphological time scale factor $n_t$ and the fall velocity scale factor $(n_w)$.

When in this relation the morphological time scale factor is chosen equal to the hydraulic time scale factor,

$$n_t = n_d^{\ 0.5} \qquad (92)$$

relation (91) yields

$$n_1/n_d = (n_d^{\ 0.5}/n_w)^{0.5} \qquad (93)$$

which can be written as

$$n_1/n_d = (n_d/n_w^{\ 2})^{0.25} \qquad (94)$$

When the scale factor for the fall velocity is chosen as $n_w = 1$ by applying prototype size sediment, relation (94) can be written as

$$n_1/n_d = n_d^{\ 0.25} \qquad (95)$$

This result is almost identical to the earlier results found empirically by Van de Graaff (1977):

$$n_1/n_d = n_d^{\ 0.28} \qquad (6)$$

By means of equations (87) and (91) the scale factor for sediment concentration can be described in terms of the depth scale factor and the fall velocity scale factor:

$$n_c = n_d^{1.5} \, n_l^{-1} \, n_w^{-1} \tag{87}$$

$$n_l/n_d = (n_t/n_w)^{0.5} \tag{91}$$

Relation (91) can be written as

$$n_l = n_d \, (n_t/n_w)^{0.5} \tag{96}$$

Substitution of (96) in (87) yields

$$n_c = n_d^{0.5} \, n_t^{-0.5} \, n_w^{-0.5} \tag{97}$$

The morphological time scale factor can be chosen to be equal to the hydraulic time scale factor

$$n_t = n_d^{0.5} \tag{98}$$

Relation (97) and (98) yield

$$n_c = n_d^{0.25} \, n_w^{-0.5} = (n_d/n_w^2)^{0.25} \tag{99}$$

Relation (99) indicates that the scale factor for sediment concentration is equal to the distortion of the model. So for undistorted models, $n_d = n_w^2$, the scale factor for sediment concentration $n_c = 1$. This means that the sediment concentration in the model is equal to the sediment concentration in prototype.

The elaborations described above show that the first order description of the sediment transport process leads to interesting scale relations for model distortion, fall velocity and sediment concentrations. However, it should be stated that the dimensional analysis of the sediment concentration is more or less speculative (only a very small portion of the energy dissipation in the surfzone is used for maintaining the potential energy of the suspended particles). Therefore, the resulting scale relations should be verified by experiments.

## 4. Small scale model investigations

### 4.1 Experimental arrangement and test results

The major aim of the research project is to define the minimum dimensions of the dunes required to withstand a design storm surge. Small scale model tests will only provide useful results when the following conditions are satisfied:

1) The experimental arrangement of the tests is such that the results enable the determination of scale relations.
2) The test conditions are such that conversion to prototype provides a set of data representative for the coastal dunes of The Netherlands.

The first condition is satisfied by the reproduction of the process applying a range of different scale factors. The second condition is satisfied by the testing of representative beach profiles and representative storm surge conditions.

A total of 24 tests were carried out in the wind wave flume of the Delft Hydraulics Laboratory, de Voorst laboratory. Tests with four grain sizes were run simultaneously in four parallel flumes with a length of 100 m and a width of 0.90 m each. (see Figure 16). The grain sizes are characterized by $D_{50}$ = 225 µm, 150 µm, 130 µm and 95 µm. The beach and dune profiles tested are derived from the schematized average profile along the Dutch coast, see Figure 17. This average field profile, called the reference profile, has a dune height of 15 m above MSL, the slope of the dune front is 1:3 down to a level of MSL + 3.0 m. From MSL + 3.0 m down to MSL the slope of the beach is 1:20. From MSL down to MSL - 3.0 m the slope is 1:70. Further seaward the slope is 1:180. This profile was reproduced applying three different depth scale factors: $n_d$ = 84, $n_d$ = 47 and $n_d$ = 26. Random waves were applied with a Pierson and Moskowitz spectrum representing prototype conditions with $H_{Os}$ = 7.6 m and $\hat{T}$ = 12 s. In order to investigate the time scale relation the water level in the model was kept constant at the level equivalent of the design storm surge level MSL + 5.0 m. For each depth scale factor two tests were run with different steepness of the initial profile, to investigate the required distortion.

To define the steepness of the initial profile the term "steepness factor" is introduced. The steepness factor of the initial profile indicates the ratio of steepness of the model profile over the steepness of the (prototype) reference profile. As such, a steepness factor Sf = 2 refers to an initial profile in the model that is a factor 2 steeper than the reference profile.
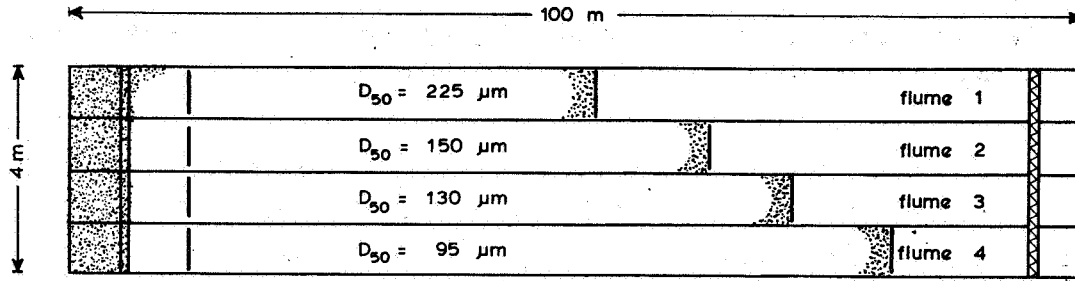
LAYOUT, FOUR PARALLEL FLUMES
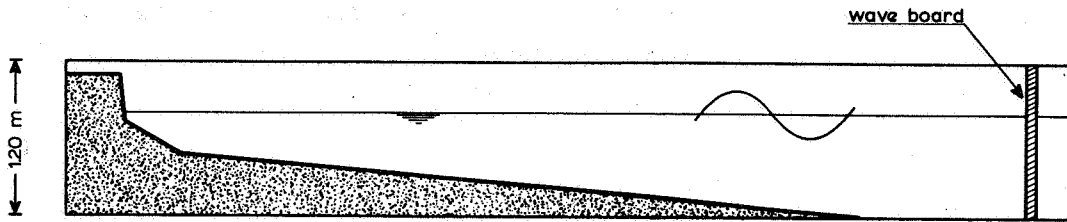


CROSS-SECTION WIND-WAVE FLUMES

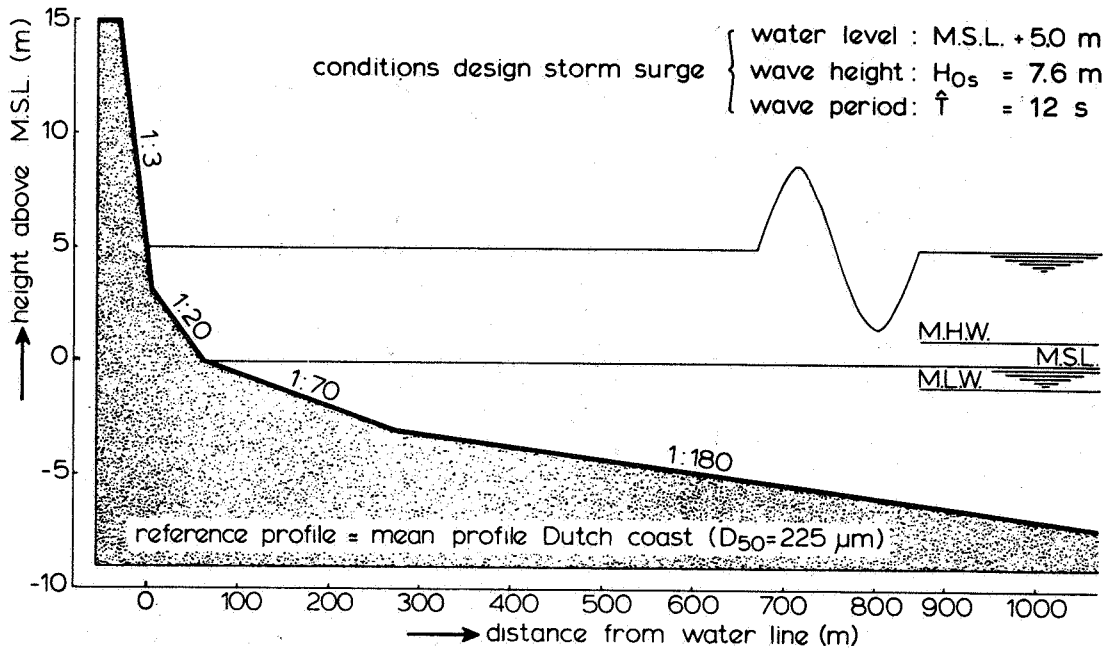**Figure 16** Experimental arrangement for two-dimensional tests



conditions design storm surge
$\left\{\begin{array}{l} \text{water level}: \text{M.S.L.} + 5.0 \text{ m} \\ \text{wave height}: H_{os} = 7.6 \text{ m} \\ \text{wave period}: \hat{T} = 12 \text{ s} \end{array}\right.$

reference profile = mean profile Dutch coast ($D_{50}$=225 µm)

**Figure 17** Prototype reference profile

The beach profiles tested in the model are considerably steeper than the prototype reference profile as a model distortion is anticipated. The initial and boundary conditions of the model tests are shown in Table 4. The actual steepness factor of the initial profile was computed on the basis of the measurements of the profile after moulding. The fall velocities that were

applied for the analysis of the test results are graphically shown in Figures 18 and 19. The fall velocities were determined by means of the Delft University Settling Tube (DUST), see Geldof and Slot (1979).

The duration of the tests was 40 hours (model time). The tests were stopped for profile recording at t = 0, 0.1, 0.3, 1.0, 3.0, 6.0, 10.5, 16.5, 25.5 and 40.0 hrs after start. The results during the first period of 6 hours are shown in Figures 20 through 43. From these figures it can be observed that the eroded sand is deposited over a rather limited distance. The profile changes beyond the settling region are negligible during the first 6 hours of the tests. Bars and troughs are developing at a later stage. The erosion quantity above storm surge level has been computed from the recordings. The cumulative result is shown in Table 5.

| test number | sand size $D_{50}$ in $\mu m$ | water temp °C | fall velocity m/s | depth scale factor $n_d$ | steepness factor initial profile $s_f$ | water depth at toe of profile (m) | wave characteristics $H_{0s}$ (m) | $\hat{T}$(sec) | H/Tw (-) |
|---|---|---|---|---|---|---|---|---|---|
| 111 | 225 | 12.5 | 0.0276 | 84 | 3.90 | 0.461 | 0.091 | 1.31 | 2.52 |
| 115 | 225 | 13.0 | 0.0278 | 84 | 2.71 | 0.461 | 0.091 | 1.31 | 2.50 |
| 112 | 150 | 12.5 | 0.0160 | 84 | 2.93 | 0.461 | 0.091 | 1.31 | 4.34 |
| 116 | 150 | 13.0 | 0.0161 | 84 | 1.89 | 0.461 | 0.091 | 1.31 | 4.31 |
| 113 | 130 | 12.5 | 0.0130 | 84 | 2.09 | 0.461 | 0.091 | 1.31 | 5.34 |
| 117 | 130 | 13.0 | 0.0132 | 84 | 1.44 | 0.461 | 0.091 | 1.31 | 5.26 |
| 114 | 95 | 12.5 | 0.0082 | 84 | 2.00 | 0.461 | 0.091 | 1.31 | 8.47 |
| 118 | 95 | 13.0 | 0.0083 | 84 | 1.18 | 0.461 | 0.091 | 1.31 | 8.34 |
| 101 | 225 | 15.5 | 0.0287 | 47 | 3.50 | 0.585 | 0.163 | 1.76 | 3.23 |
| 105 | 225 | 15.0 | 0.0285 | 47 | 2.45 | 0.585 | 0.163 | 1.76 | 3.25 |
| 102 | 150 | 15.5 | 0.0168 | 47 | 2.44 | 0.585 | 0.163 | 1.76 | 5.51 |
| 106 | 150 | 15.0 | 0.0167 | 47 | 1.79 | 0.585 | 0.163 | 1.76 | 5.55 |
| 103 | 130 | 15.5 | 0.0138 | 47 | 2.02 | 0.585 | 0.163 | 1.76 | 6.71 |
| 107 | 130 | 15.0 | 0.0137 | 47 | 1.62 | 0.585 | 0.163 | 1.76 | 6.76 |
| 104 | 95 | 15.5 | 0.0087 | 47 | 1.73 | 0.585 | 0.163 | 1.76 | 10.65 |
| 108 | 95 | 15.0 | 0.0086 | 47 | 1.40 | 0.585 | 0.163 | 1.76 | 10.77 |
| 121 | 225 | 10.5 | 0.0269 | 26 | 3.08 | 0.806 | 0.292 | 2.35 | 4.62 |
| 125 | 225 | 9.5 | 0.0265 | 26 | 1.95 | 0.806 | 0.292 | 2.35 | 4.69 |
| 122 | 150 | 10.5 | 0.0154 | 26 | 2.30 | 0.806 | 0.292 | 2.35 | 8.07 |
| 126 | 150 | 9.5 | 0.0152 | 26 | 1.48 | 0.806 | 0.292 | 2.35 | 8.17 |
| 123 | 130 | 10.5 | 0.0125 | 26 | 1.62 | 0.806 | 0.292 | 2.35 | 9.94 |
| 127 | 130 | 9.5 | 0.0123 | 26 | 1.10 | 0.806 | 0.292 | 2.35 | 10.10 |
| 124 | 95 | 10.5 | 0.0079 | 26 | 1.32 | 0.806 | 0.292 | 2.35 | 15.73 |
| 128 | 95 | 9.5 | 0.0078 | 26 | 1.04 | 0.806 | 0.292 | 2.35 | 15.93 |

**Table 4** Test conditions
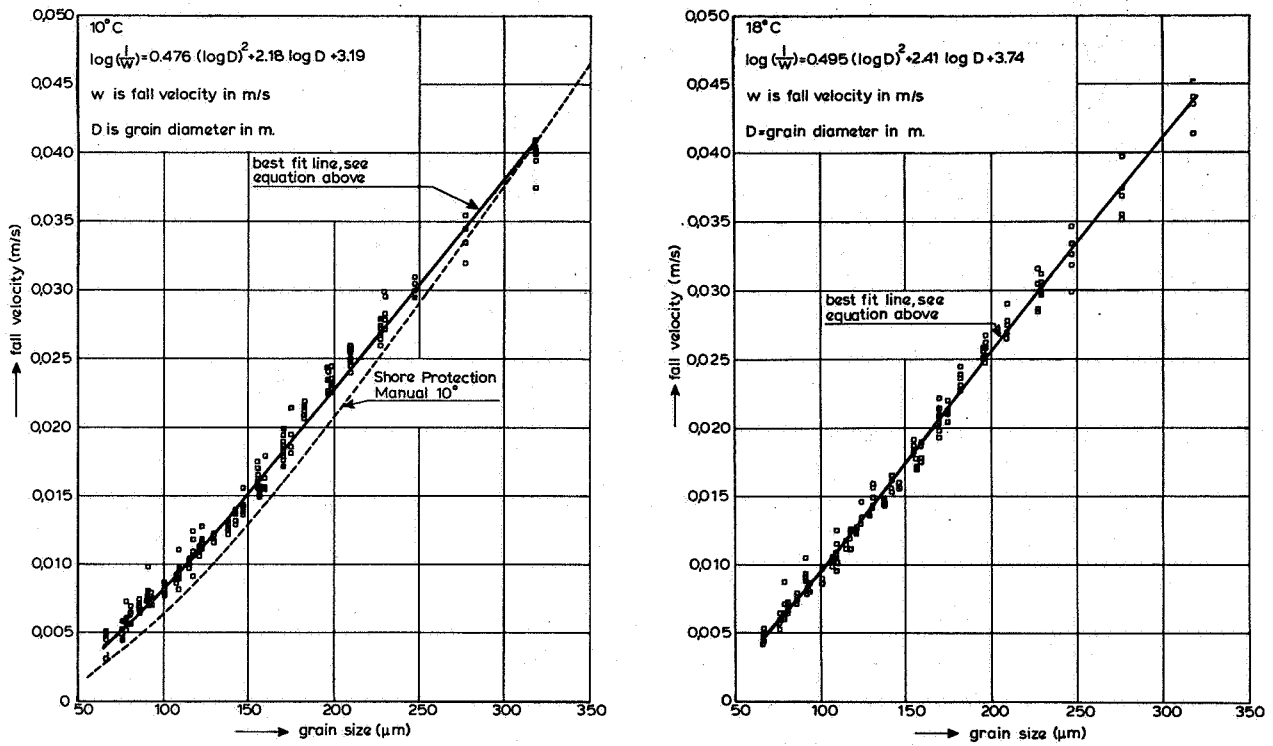
Figure 18/19 Fall velocity of sediment particles in stagnant water of 10 °C and 18 °C

| test number | cumulative erosion ($10^{-4}$ m³/m¹) hours after start of test | | | | | | | | |
|---|---|---|---|---|---|---|---|---|---|
| | 0.1 | 0.3 | 1.0 | 3.0 | 6.0 | 10.5 | 16.5 | 25.5 | 40.0 |
| 111 | 124 | 132 | 148 | 158 | 150 | 174 | 206 | 248 | 334 |
| 115 | 51 | 82 | 59 | 51 | 37 | 32 | 36 | 49 | 87 |
| 112 | 77 | 104 | 162 | 176 | 176 | 249 | 313 | 411 | 542 |
| 116 | 37 | 56 | 66 | 72 | 95 | 117 | 145 | 199 | 282 |
| 113 | 44 | 56 | 91 | 95 | 116 | 170 | 193 | 229 | 306 |
| 117 | 46 | 47 | 55 | 76 | 101 | 145 | 191 | 256 | 310 |
| 114 | 21 | 49 | 85 | 148 | 191 | 320 | 389 | 484 | 584 |
| 118 | 21 | 25 | 58 | 95 | 165 | 242 | 312 | 443 | 496 |
| 101 | 383 | 449 | 510 | 600 | 651 | 760 | 872 | 1034 | 1303 |
| 105 | 308 | 331 | 366 | 395 | 419 | 468 | 523 | | 838 |
| 102 | 465 | 571 | 636 | 776 | 865 | 975 | 1153 | 1381 | 1843 |
| 106 | 253 | 320 | 415 | 478 | 529 | 603 | 753 | 936 | 1225 |
| 103 | 377 | 469 | 540 | 634 | 754 | 903 | 1093 | 1337 | 1682 |
| 107 | 216 | 261 | 336 | 396 | 448 | 547 | 703 | 910 | 1197 |
| 104 | 318 | 473 | 646 | 956 | 1300 | 1648 | 2151 | 2662 | 2979 |
| 108 | 244 | 266 | 411 | 552 | 739 | 995 | 1314 | 1774 | 2271 |
| 121 | 1425 | 1838 | 2250 | 2914 | 3230 | 3623 | 3916 | 4141 | 3832 |
| 125 | 870 | 1852 | 1107 | 1265 | 1230 | 1260 | 1328 | 1349 | 1611 |
| 122 | 1327 | 1751 | 2207 | 2670 | 2734 | 2688 | 2747 | 2743 | 3027 |
| 126 | 493 | 1015 | 1293 | 1634 | 1690 | 1677 | 1729 | 1813 | 1946 |
| 123 | 978 | 1543 | 2345 | 3129 | 3463 | 3624 | 3836 | 4079 | 4077 |
| 127 | 520 | 779 | 1435 | 1964 | 2253 | 2300 | 2470 | 2606 | 3099 |
| 124 | 911 | 1610 | 2781 | 3891 | 4644 | 5183 | 5369 | 5323 | 5439 |
| 128 | 585 | 1175 | 1898 | 2673 | 3108 | 3943 | 4538 | 4729 | 4775 |

Table 5 Cumulative dune erosion quantities measured in the model
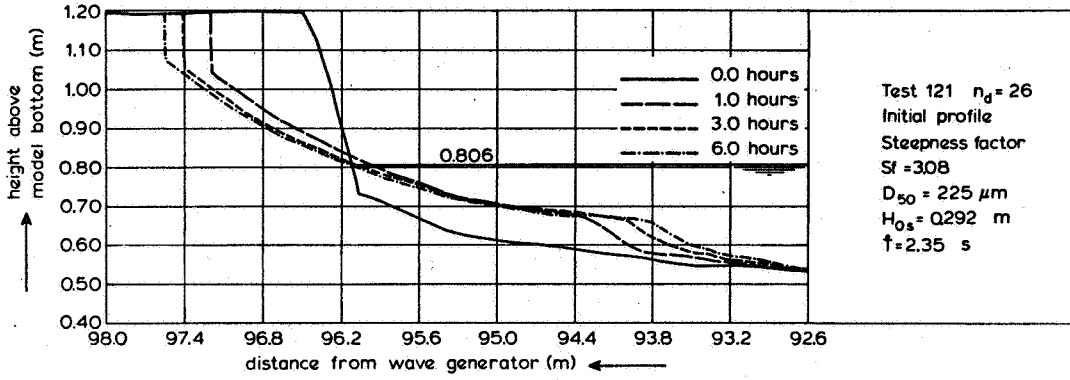
**Figure 20**  Erosion profile development, test 121
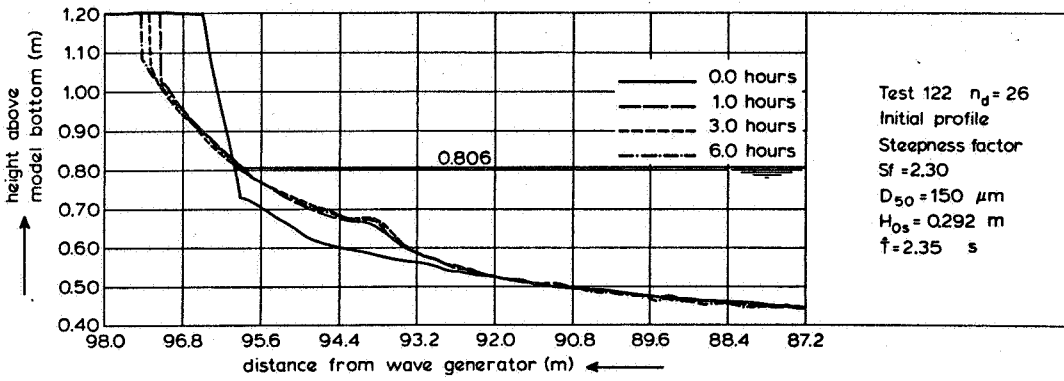


**Figure 21**  Erosion profile development, test 122
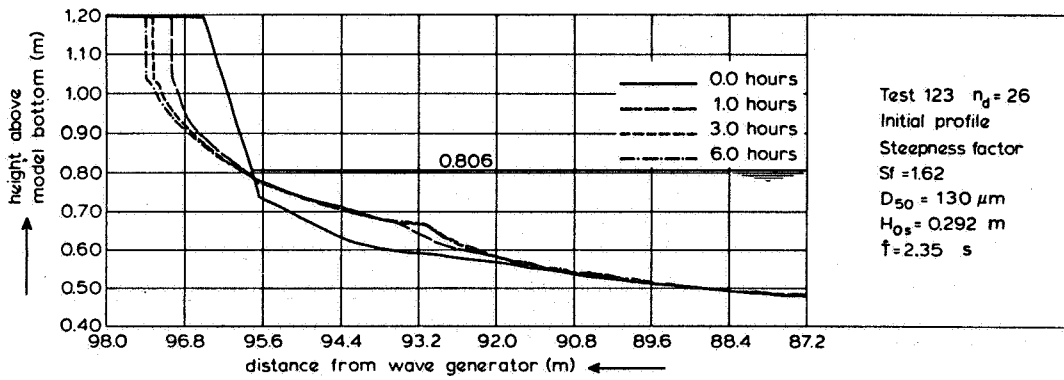


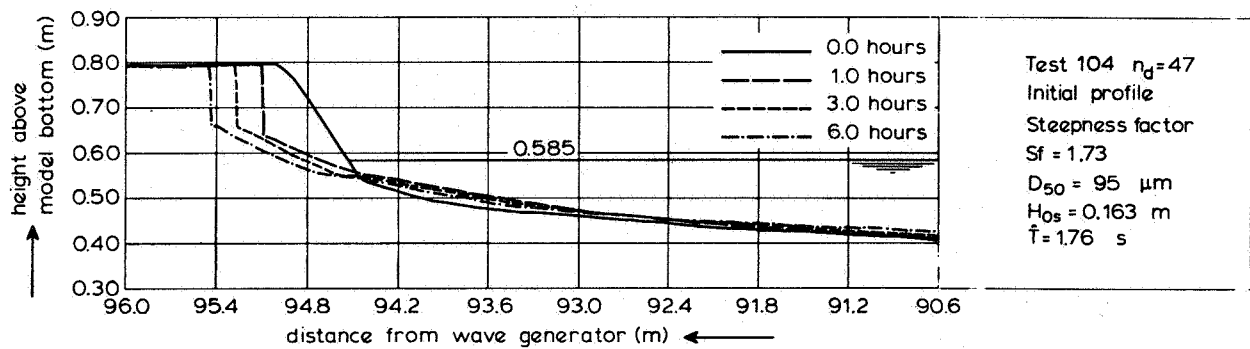**Figure 22**  Erosion profile development, test 123
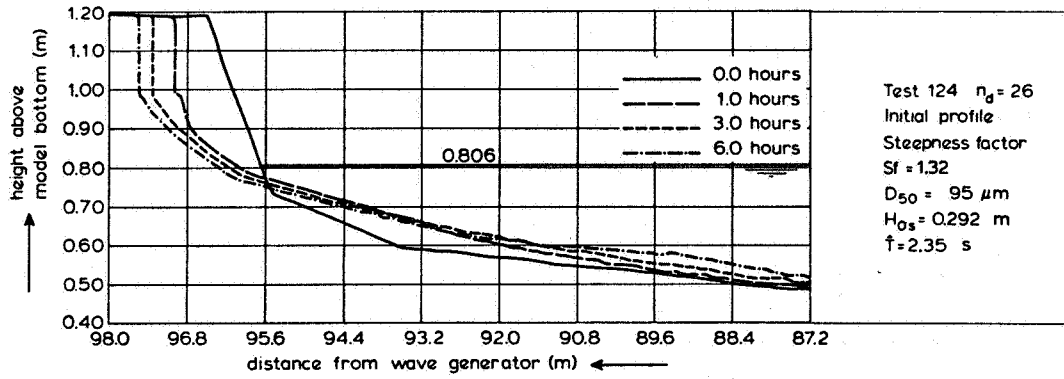


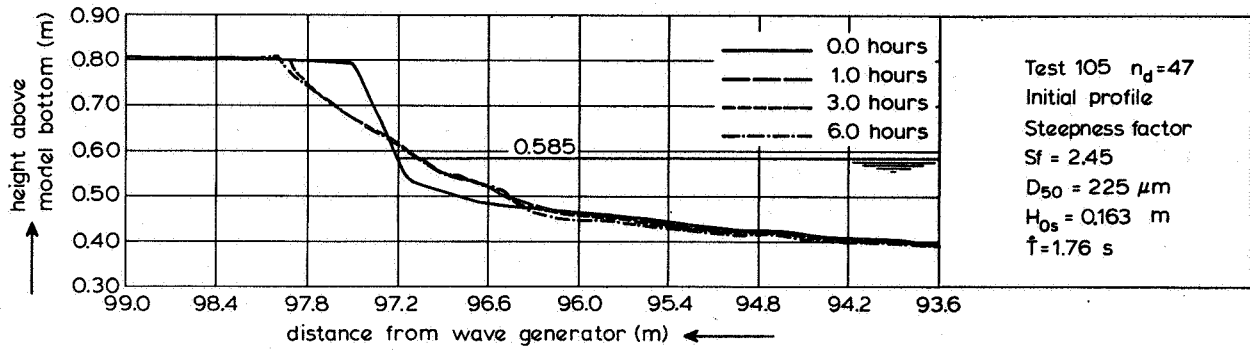**Figure 23**  Erosion profile development, test 124
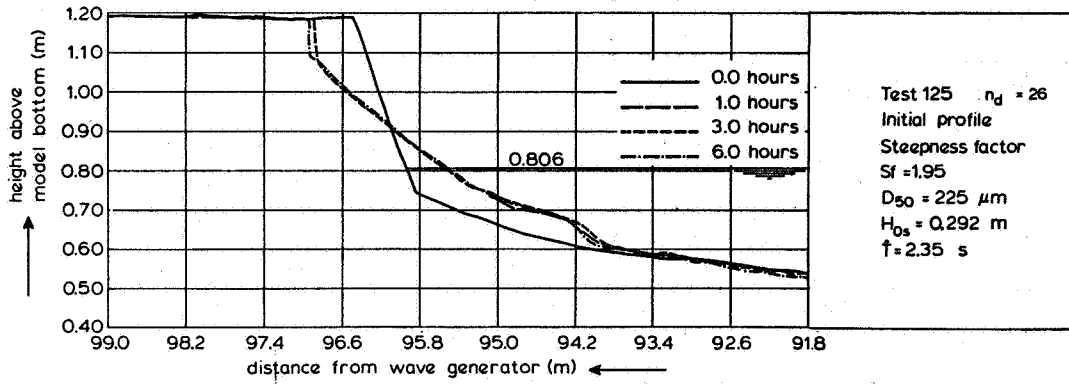
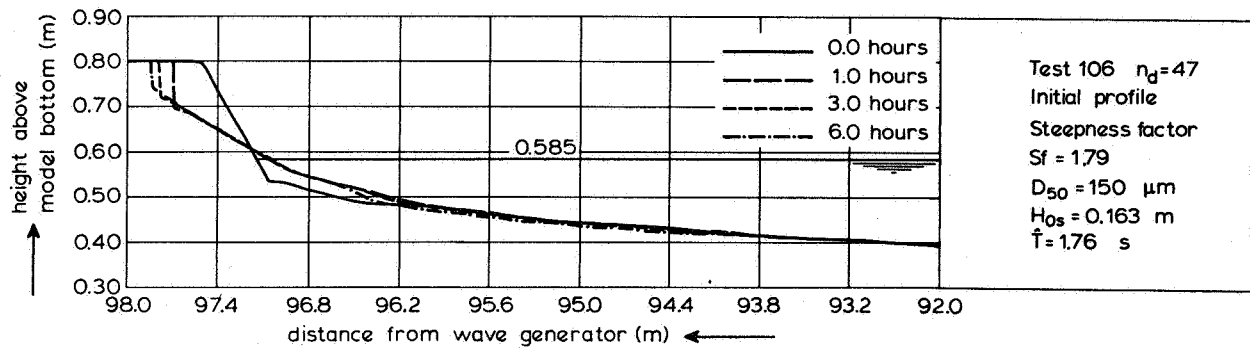**Figure 24** Erosion profile development, test 125
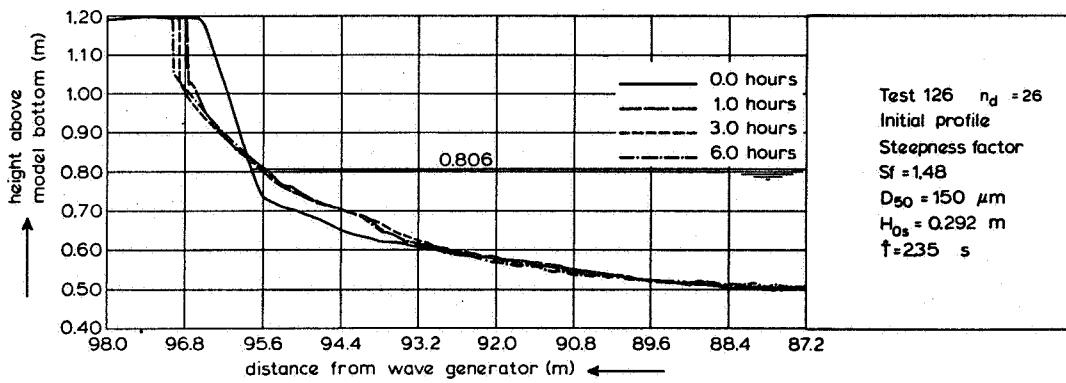


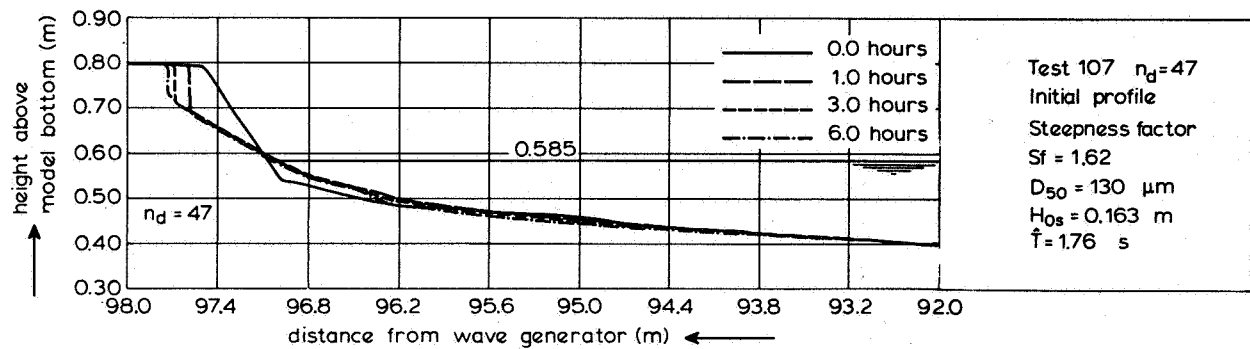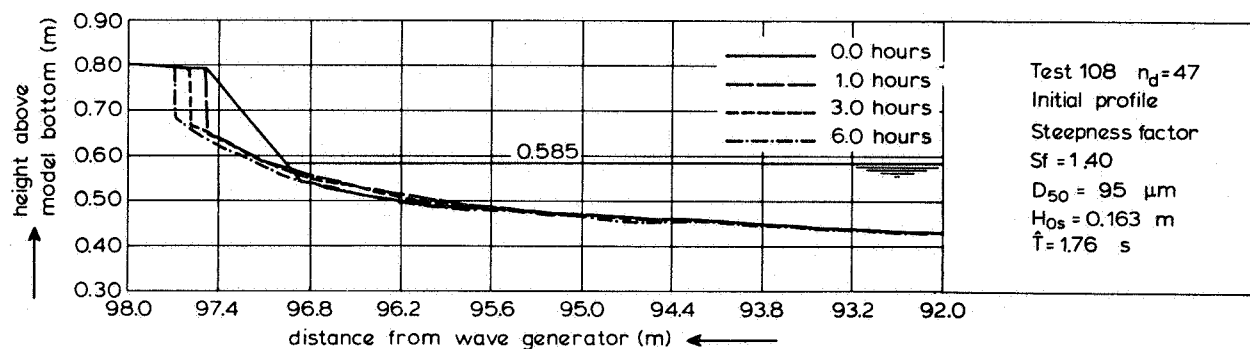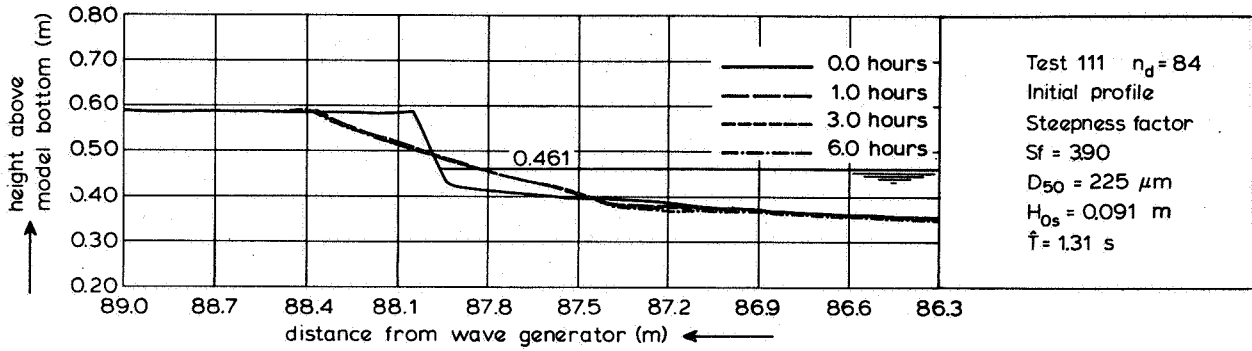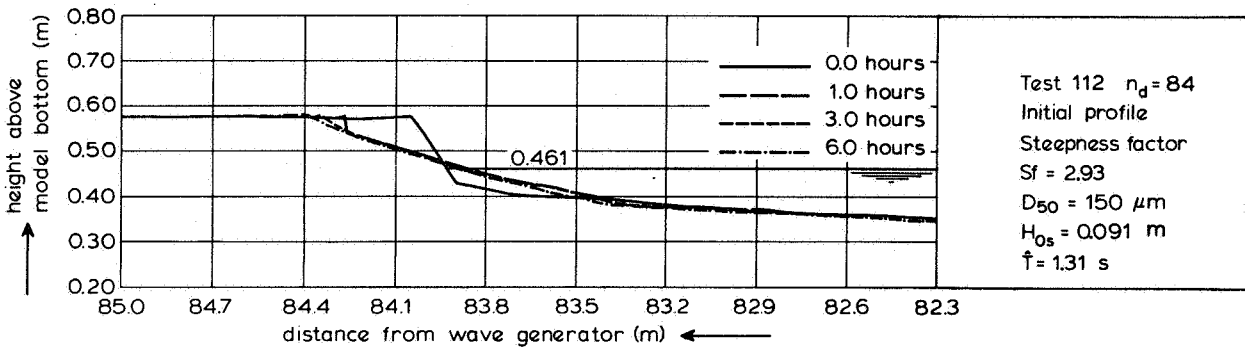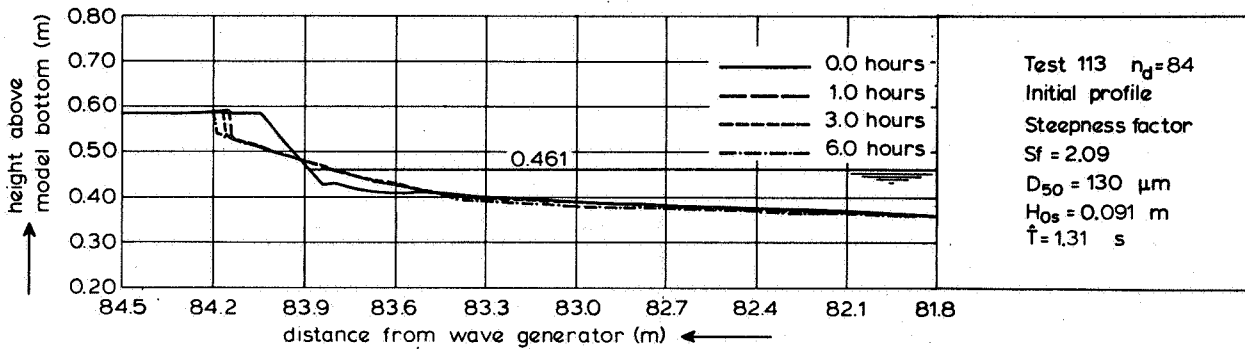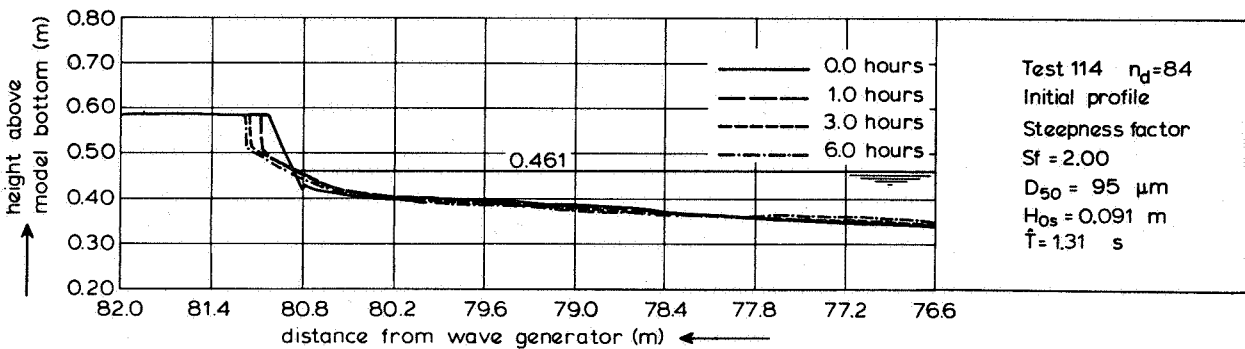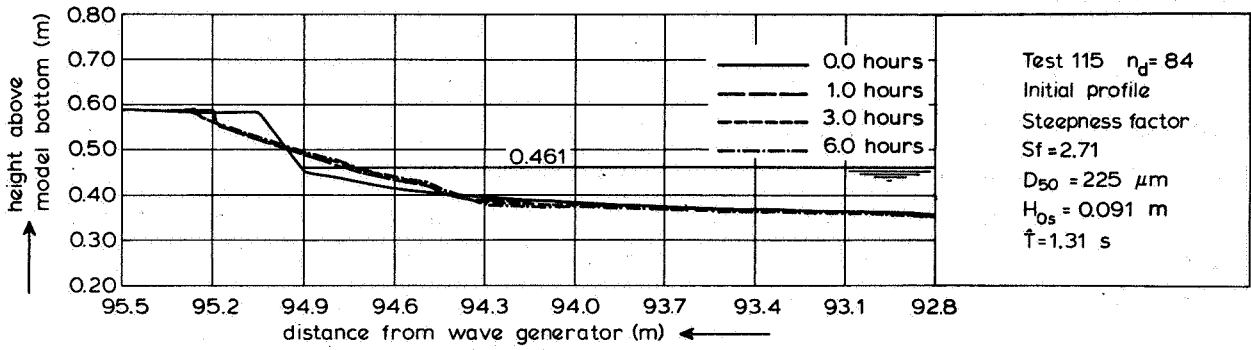**Figure 25** Erosion profile development, test 126
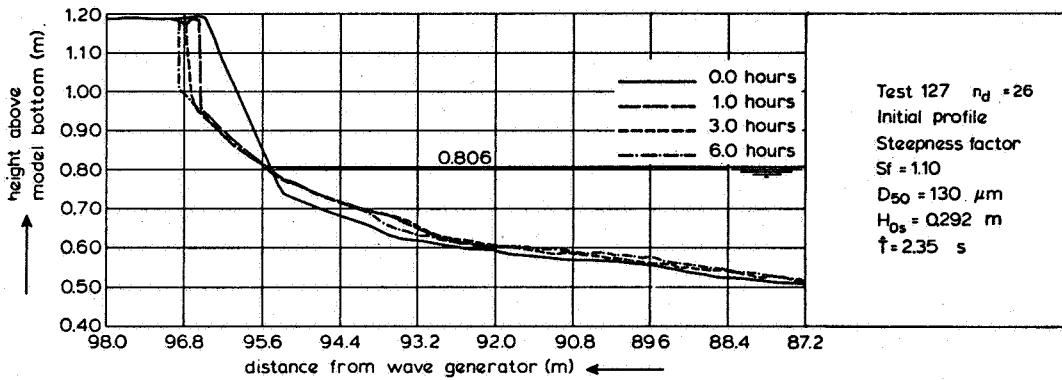


**Figure 26** Erosion profile development, test 127
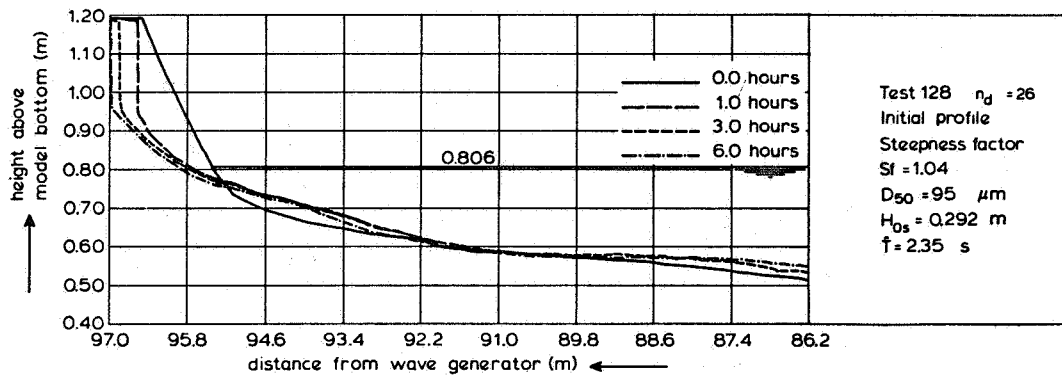


**Figure 27** Erosion profile development, test 128
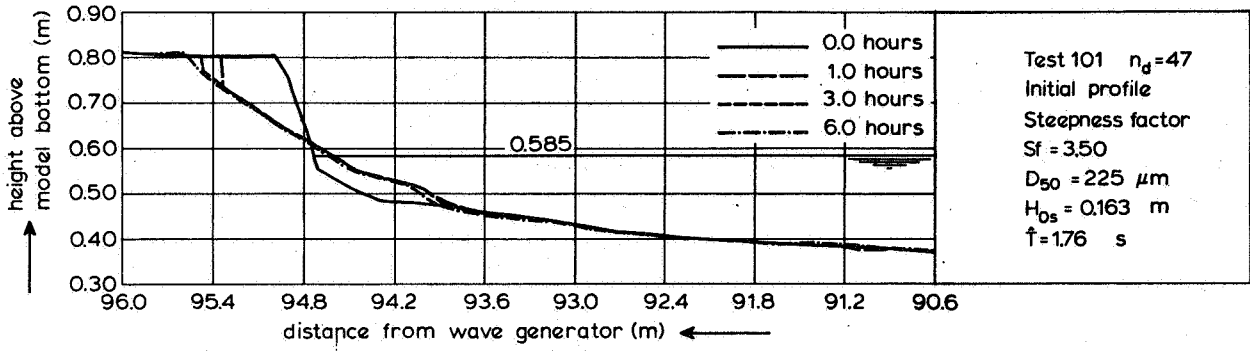
**Figure 28** Erosion profile development, test 101
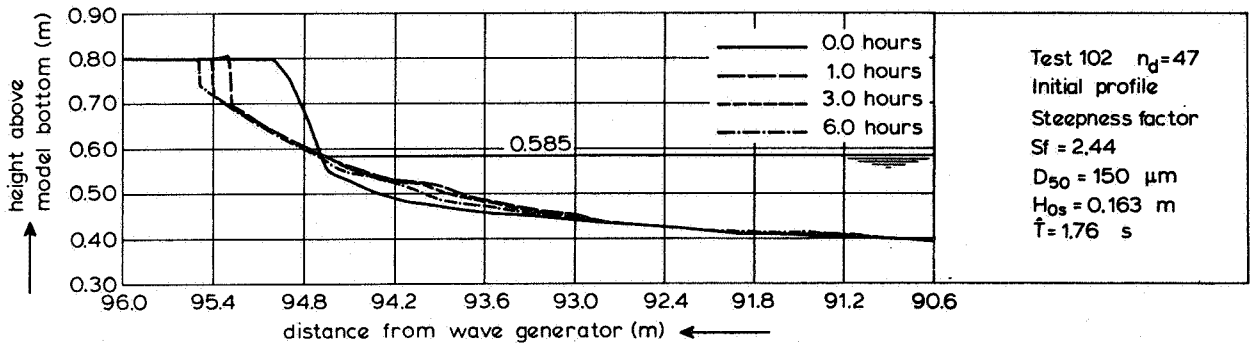


**Figure 29** Erosion profile development, test 102
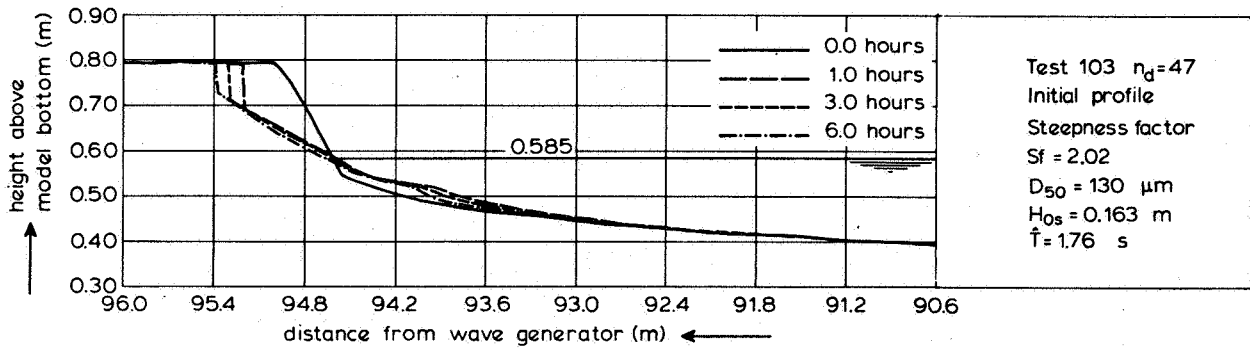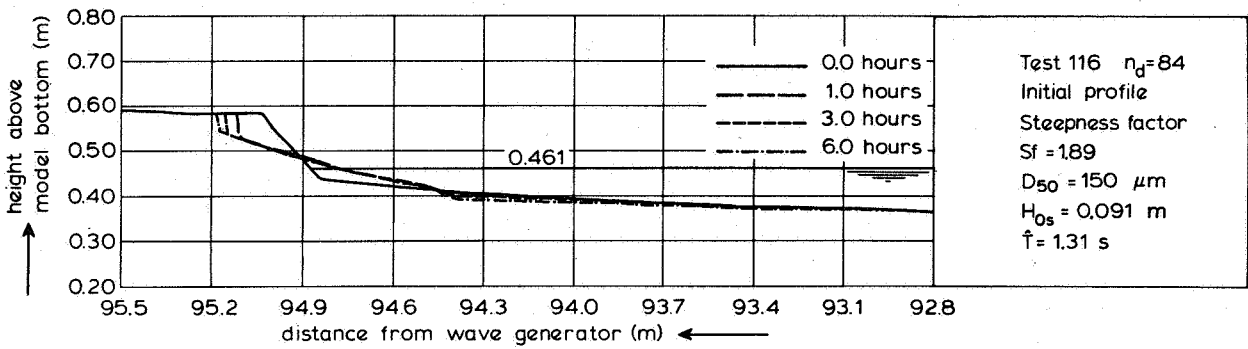


**Figure 30** Erosion profile development, test 103



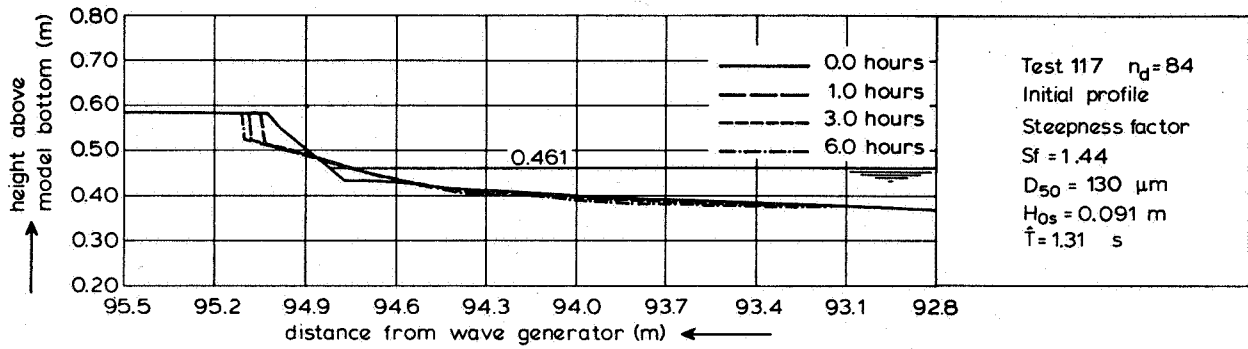**Figure 31** Erosion profile development, test 104

**Figure 32** Erosion profile development, test 105



**Figure 33** Erosion profile development, test 106



**Figure 34** Erosion profile development, test 107



**Figure 35** Erosion profile development, test 108

**Figure 36** Erosion profile development, test 111



**Figure 37** Erosion profile development, test 112



**Figure 38** Erosion profile development, test 113



**Figure 39** Erosion profile development, test 114

**Figure 40** Erosion profile development, test 115



**Figure 41** Erosion profile development, test 116



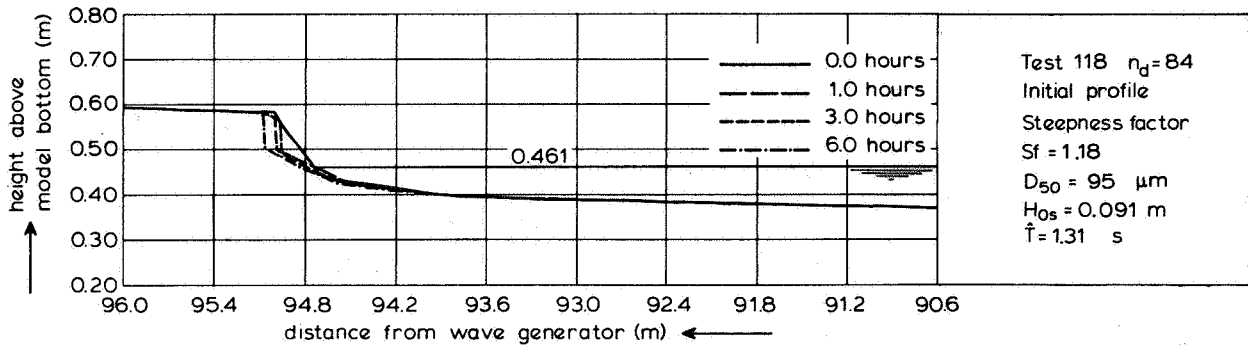**Figure 42** Erosion profile development, test 117



**Figure 43** Erosion profile development, test 118

## 4.2 Method for scale relation determination

A dimensional analysis of the sediment transport process has provided a basic form for the scale relations: $n_1/n_d = (n_d/n_w^2)^\alpha$, $n_t = (n_d)^\beta$. These relations are relatively simple and it may not be expected that all processes are covered. Therefore the basic form of the scale relations has been verified and the values of $\alpha$ and $\beta$ have been determined in a systematic way. The method is based on theoretical principles but also allows for choices based on empirical results. The method involves 4 specific steps, as shown in Table 6.

| step 1 | Verification of the basic form of the distortion relation by verification of the validity of the H/Tw parameter through analysis of the erosion profiles as a function of H/Tw. |
|---|---|
| step 2 | Conversion of tests with finer sand into tests with prototype size sand on the basis of the H/Tw parameter, generating a set of tests with depth scale factors ranging from $n_d = 2.28$ up to $n_d = 84$, all with $D_{50} = 225$ μm |
| step 3a | Verification of the basic form of the distortion relation and investigation of $\alpha$-value by analysing the erosion profiles |
| step 3b | Investigation of $\alpha$ and $\beta$ combinations by analysing the dune erosion quantities |
| step 3c | Verification of the basic form of the time scale relation and investigation of $\beta$-value by analysing the rate of erosion |
| step 4 | Determination of best fit values for $\alpha$ and $\beta$ in the relations $n_1/n_d = (n_d/n_w^2)^\alpha$ and $n_t = n_d^\beta$ |

Table 6  Method for scale relation determination

## 4.3  Verification of H/Tw parameter (step 1)

According to the H/Tw concept there should be a direct relation between the form of the beach profile and the value of the H/Tw parameter. Tests with equal H/Tw value should have a geometrically similar erosion profile, i.e. such profiles should correspond when compared on the basis of $n_1 = n_d$.

In the present study the dimensionless fall velocity parameter, H/Tw is only tested for wave conditions with constant wave steepness (the Froude scale

relations have been applied $n_H = n_L = n_T^2 = n_u^2$). This implies that the H/Tw parameter is only partially verified.

The H/Tw values of the model tests are indicated in Table 4. H is the significant deep water wave height $H_{0s}$, T is the wave period corresponding with the peak of the spectrum $\hat{T}$, w = $w_{50}$ is the fall velocity that is exceeded by 50% of the grains by weight ($w_{50}$ corresponds with $D_{50}$, disregarding minor shape effects).

The test results show that the erosion profile is independent of the initial profile. As an example the erosion profiles of test 124 and 128 are shown in Figure 44. It also appears from Figures 20 through 43 that the shape of the profile remains fairly constant. Through time it is extended in seaward direction. The constant shape makes it fairly easy to verify the H/Tw parameter. The profiles recorded in the model after 1 hr have been chosen for a comparison. The waterline has been taken as a horizontal reference. The profiles of the 24 tests have been converted to prototype with $n_1 = n_d$ (the shape does not change this way). Next the distance between the water line and the depth contours of 1 m, 2 m and 3 m respectively have been determined. The results for all 24 tests have been plotted as a function of the H/Tw parameter in Figures 45, 46 and 47. For a validation of the H/Tw parameter the test results should be found on a single (not necessarily straight) line. The figures show indeed that the scatter from a single straight line is relatively small.
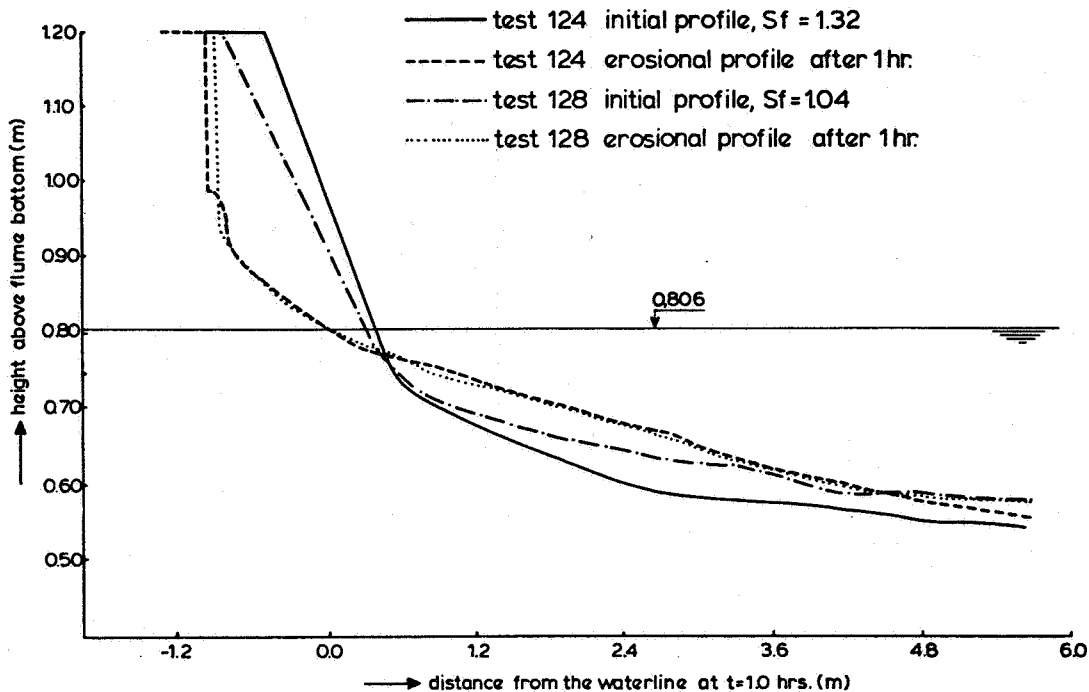


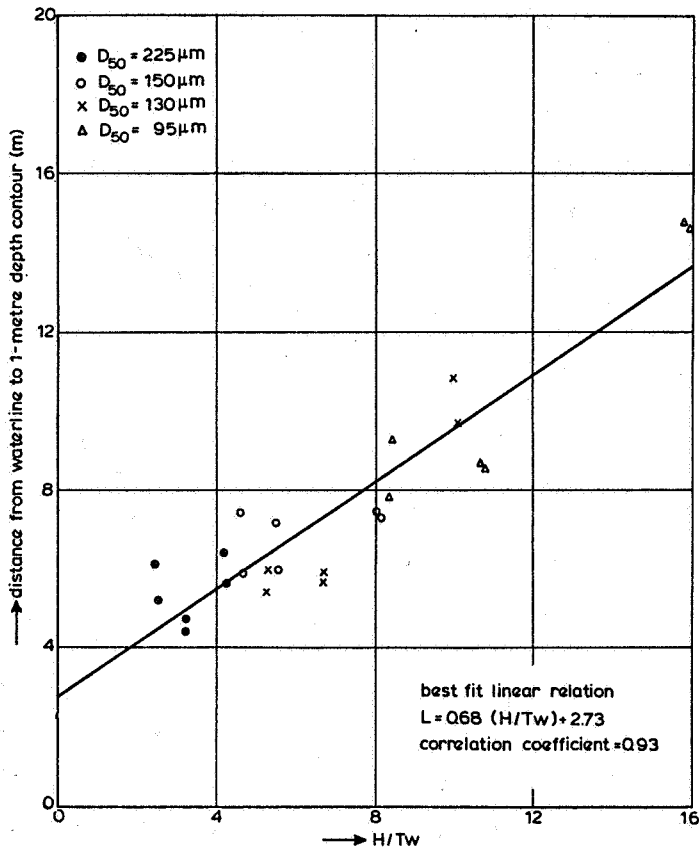Figure 44 Erosion profiles for different initial profiles

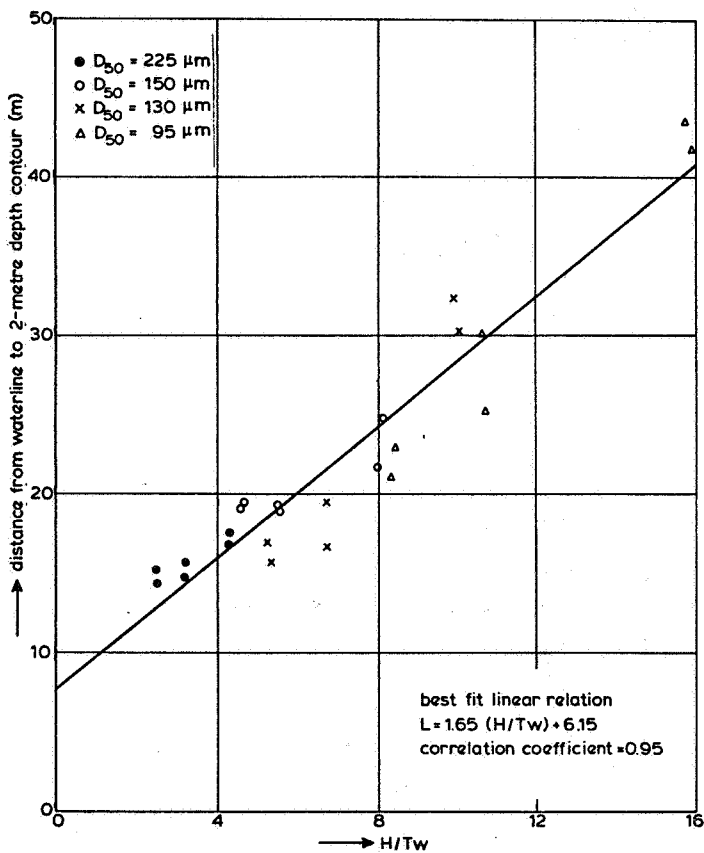**Figure 45**  Distance from waterline to 1-m depth contour as a function of H/Tw



**Figure 46**  Distance from waterline to 2-m depth contour as a function of H/Tw
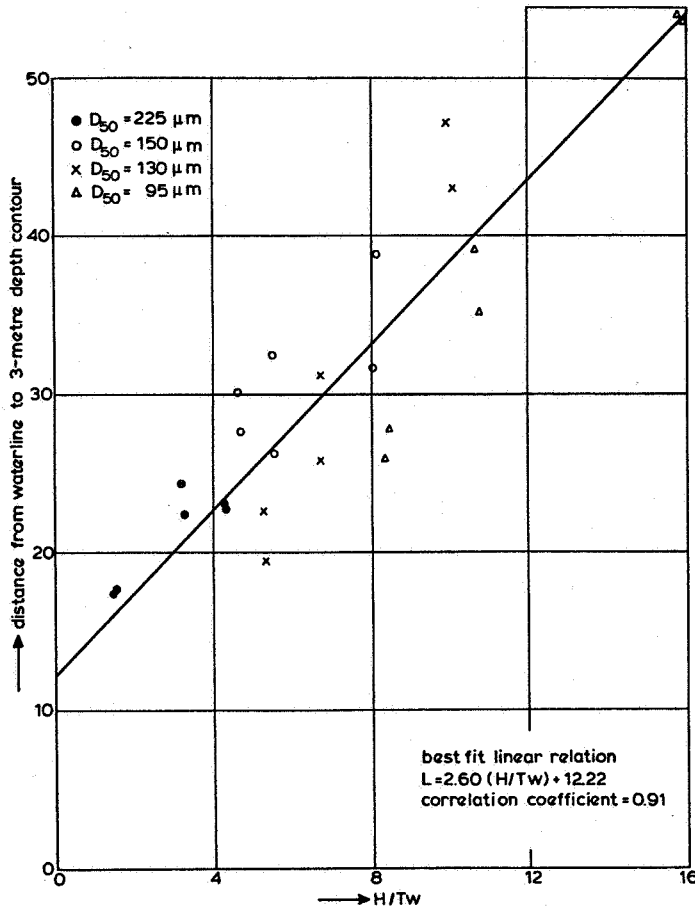
**Figure 47** Distance from waterline to 3-m depth contour as a function of H/Tw

## 4.4 Conversion of test results (step 2)

The validation of the H/Tw concept enables the conversion of tests with finer sand to tests with prototype sand on a larger scale. This way the scale series is extended and the scale relations can be investigated over a larger range of depth scale factors. The conversion method is illustrated below.

The result of a test with H/Tw = $H_1/T_1$ $w_1$, with depth scale factor $n_{d1}$, length scale factor $n_{l1}$, fall velocity $w_1$, steepness factor $Sf_1$ and erosion quantity $A_1$ at time $t_1$ is converted to the result of a test with fall velocity $w_2$ as follows:

$$n_{d2} = n_{d1}/(w_2/w_1)^2 \qquad \text{(derived from } H_2/T_2 \ w_2 = H_1/T_1 \ w_1 \text{ )} \qquad (100)$$

$$n_{l2} = n_{l1} \ (w_2/w_1)^2 \qquad (n_{l1}/n_{l2} = n_{d1}/n_{d2} \text{ as n(H/Tw) = 1)} \qquad (101)$$

$$Sf_1 = Sf_2 \qquad \text{(geometrically similar profiles, as H/Tw = 1)} \qquad (102)$$

$$t_2 = t_1 \ (w_2/w_1) \qquad \text{(derived from } n_t = n_d^{0.5}) \qquad (103)$$

$$A_2 = A_1 \ (n_{d1}/n_{d2})^2 = A_1 \ (w_2/w_1)^4 \qquad (104)$$

An example in a quantitative sense is shown below. Test 124 has a depth scale factor $n_d$ = 26, a bottom material with $D_{50}$ = 95 µm a fall velocity w = 0.0079 m/s (for water with a temperature of 10.5° C) and an initial profile steepness Sf = 1.32. At t = 1.0 hrs after start the erosion above the water level is 2781 $10^{-4}$ $m^3/m'$ (see table 5). Conversion to prototype size sand with $D_{50}$ = 225 µm and w = 0.0268 (for water with a temperature of 10° C) yields a test with:

$$\text{Depth scale factor } n_d = 26/(0.0268/0.0079)^2 = 2.28 \tag{105}$$

$$\text{Steepness factor Sf} = 1.32 \text{ (geometrically similar profile)} \tag{106}$$

$$\text{Time } t = 1 \ (0.0268/0.0079) = 3.38 \text{ hrs.} \tag{107}$$

$$\text{Erosion quantity A} = 2781 * 10^{-4} \ (0.0268/0.0079)^4 = 36.3 \ m^3/m^1 \tag{108}$$

The present tests as well as preceding tests by Van de Graaff (1977) have been converted this way. The results are presented in Table 7a and 7b.

| test number | $n_{d2}$ | $w_2$ | $Sf_2$ | $t_2$ | $A_2$ | $t_2$ | $A_2$ | $t_2$ | $A_2$ | $t_2$ | $A_2$ | $t_2$ | $A_2$ | $t_2$ | $A_2$ | $t_2$ | $A_2$ | $t_2$ | $A_2$ | $t_2$ | $A_2$ |
|---|---|---|---|---|---|---|---|---|---|---|---|---|---|---|---|---|---|---|---|---|---|
| 111 | 89.758 | 0.0267 | 3.90 | 0.097 | 109 | 0.290 | 116 | 0.967 | 130 | 2.902 | 138 | 5.804 | 131 | 10.158 | 153 | 15.962 | 180 | 24.668 | 217 | 38.696 | 293 |
| 115 | 91.064 | 0.0267 | 2.71 | 0.096 | 43 | 0.288 | 44 | 0.960 | 50 | 2.881 | 43 | 5.763 | 31 | 10.085 | 27 | 15.847 | 31 | 24.491 | 42 | 38.417 | 74 |
| 112 | 30.165 | 0.0267 | 2.93 | 0.167 | 597 | 0.501 | 806 | 1.669 | 1256 | 5.006 | 1365 | 10.013 | 1365 | 17.522 | 1931 | 27.534 | 2427 | 42.553 | 3187 | 66.750 | 4203 |
| 116 | 30.543 | 0.0267 | 1.89 | 0.166 | 280 | 0.498 | 424 | 1.658 | 499 | 4.975 | 545 | 9.950 | 719 | 17.413 | 885 | 27.363 | 1097 | 42.289 | 1505 | 66.335 | 2133 |
| 113 | 19.913 | 0.0267 | 2.09 | 0.205 | 783 | 0.616 | 996 | 2.054 | 1619 | 6.162 | 1690 | 12.323 | 2064 | 21.565 | 3025 | 33.888 | 3434 | 52.373 | 4075 | 82.154 | 5445 |
| 117 | 20.531 | 0.0267 | 1.44 | 0.202 | 770 | 0.607 | 787 | 2.023 | 921 | 6.068 | 1272 | 12.136 | 1691 | 21.239 | 2427 | 33.375 | 3197 | 51.580 | 4285 | 80.909 | 5189 |
| 114 | 7.923 | 0.0267 | 2.00 | 0.326 | 2361 | 0.977 | 5508 | 3.256 | 9555 | 9.768 | 16299 | 19.537 | 21470 | 34.189 | 35970 | 53.726 | 43726 | 83.030 | 54405 | 130.244 | 65645 |
| 118 | 8.117 | 0.0267 | 1.18 | 0.322 | 2249 | 0.965 | 2677 | 3.217 | 6211 | 9.651 | 10173 | 19.301 | 17669 | 33.777 | 25915 | 53.078 | 33411 | 82.030 | 47439 | 128.675 | 53115 |
| 101 | 54.305 | 0.0267 | 3.50 | 0.093 | 287 | 0.279 | 336 | 0.930 | 382 | 2.791 | 449 | 5.582 | 488 | 9.768 | 569 | 15.350 | 653 | 23.723 | 775 | 37.213 | 976 |
| 105 | 53.551 | 0.0267 | 2.45 | 0.094 | 237 | 0.281 | 255 | 0.937 | 282 | 2.811 | 304 | 5.621 | 323 | 9.837 | 361 | 15.458 | 403 | 23.889 | 495 | 37.474 | 646 |
| 102 | 18.608 | 0.0267 | 2.44 | 0.159 | 2967 | 0.477 | 3643 | 1.589 | 4058 | 4.768 | 4951 | 9.536 | 5519 | 16.688 | 6220 | 26.223 | 7356 | 40.527 | 8811 | 63.571 | 11758 |
| 106 | 18.387 | 0.0267 | 1.79 | 0.160 | 1653 | 0.479 | 2091 | 1.599 | 2712 | 4.796 | 3123 | 9.593 | 3456 | 16.787 | 3940 | 26.380 | 4920 | 40.769 | 6116 | 63.952 | 8004 |
| 103 | 12.555 | 0.0267 | 2.02 | 0.193 | 5283 | 0.580 | 6572 | 1.935 | 7567 | 5.804 | 8842 | 11.609 | 10566 | 20.315 | 12654 | 31.924 | 15316 | 49.337 | 18735 | 77.391 | 23570 |
| 107 | 12.374 | 0.0267 | 1.62 | 0.195 | 3116 | 0.585 | 3765 | 1.949 | 4847 | 5.847 | 5713 | 11.693 | 6463 | 20.464 | 7890 | 32.157 | 10142 | 49.697 | 13128 | 77.956 | 17269 |
| 104 | 4.990 | 0.0267 | 1.73 | 0.307 | 28209 | 0.921 | 41959 | 3.069 | 57306 | 9.207 | 84806 | 18.414 | 115322 | 32.224 | 146193 | 50.638 | 190813 | 78.259 | 236144 | 122.759 | 264264 |
| 108 | 4.876 | 0.0267 | 1.40 | 0.310 | 22669 | 0.931 | 24713 | 3.105 | 38185 | 9.314 | 51285 | 18.628 | 68659 | 32.600 | 92443 | 51.227 | 122081 | 79.169 | 164818 | 124.186 | 210993 |
| 121 | 26.391 | 0.0267 | 3.08 | 0.099 | 1383 | 0.298 | 1784 | 0.993 | 2184 | 2.978 | 2828 | 5.955 | 3135 | 10.422 | 3516 | 16.377 | 3801 | 25.310 | 4019 | 39.703 | 3719 |
| 125 | 25.612 | 0.0267 | 1.95 | 0.101 | 897 | 0.302 | 1084 | 1.008 | 1141 | 3.023 | 1304 | 6.045 | 1268 | 10.579 | 1298 | 16.625 | 1399 | 25.692 | 1390 | 40.302 | 1660 |
| 122 | 8.650 | 0.0267 | 2.30 | 0.173 | 11990 | 0.520 | 15822 | 1.734 | 19942 | 5.201 | 24125 | 10.403 | 24678 | 18.205 | 24288 | 28.607 | 24821 | 44.211 | 24785 | 69.351 | 27351 |
| 126 | 8.426 | 0.0267 | 1.48 | 0.176 | 4694 | 0.527 | 9664 | 1.757 | 12310 | 5.269 | 15557 | 10.539 | 16090 | 18.444 | 15966 | 28.984 | 16461 | 44.793 | 17261 | 70.263 | 18527 |
| 123 | 5.699 | 0.0267 | 1.62 | 0.214 | 20358 | 0.641 | 32120 | 2.136 | 48814 | 6.408 | 65134 | 12.816 | 72108 | 22.428 | 75439 | 35.244 | 79852 | 54.468 | 84910 | 85.440 | 84868 |
| 127 | 5.518 | 0.0267 | 1.10 | 0.217 | 11546 | 0.651 | 17297 | 2.171 | 31862 | 6.512 | 43608 | 13.024 | 50025 | 22.793 | 51068 | 35.817 | 54843 | 55.354 | 57863 | 86.829 | 68809 |
| 124 | 2.276 | 0.0267 | 1.32 | 0.338 | 11865 | 1.014 | 210069 | 3.380 | 362859 | 10.139 | 507689 | 20.278 | 605939 | 35.487 | 676267 | 55.766 | 700535 | 86.184 | 694533 | 135.190 | 709669 |
| 128 | 2.219 | 0.0267 | 1.04 | 0.342 | 80320 | 1.027 | 161326 | 3.423 | 260593 | 10.269 | 367000 | 20.538 | 426725 | 35.942 | 541369 | 56.481 | 623062 | 87.288 | 649286 | 136.923 | 655602 |

$n_{d2}$ = depth scale factor, converted from tests via $n_{d2} = n_{d1}/(w_2/w_1)^2$

$w_2$ = fall velocity (m/s),

$Sf_2$ = steepness factor initial profile

$t_2$ = (model) time in hrs, converted from tests via $t_2 = t_1 \ (w_2/w_1)$

$A_2$ = cumulative erosion quantity at $t_2$ hrs in $10^{-4} \ m^3/m^1$

**Table 7a** Test results after conversion to prototype size sand, present series of tests

| test number | $n_{d2}$ | $w_2$ | $Sf_2$ | $t_2$ | $A_2$ | $t_2$ | $A_2$ | $t_2$ | $A_2$ | $t_2$ | $A_2$ | $t_2$ | $A_2$ | $t_2$ | $A_2$ | $t_2$ | $A_2$ | $t_2$ | $A_2$ |
|---|---|---|---|---|---|---|---|---|---|---|---|---|---|---|---|---|---|---|---|
| 13 | 34.053 | 0.0267 | 9.46 | 0.314 | 2239 | 0.942 | 2641 | 3.141 | 3231 | 9.424 | 3730 | 23.716 | 4272 | 58.112 | 5409 | 102.559 | 6395 | | |
| 14 | 98.413 | 0.0267 | 8.01 | 0.185 | 197 | 0.554 | 221 | 1.848 | 235 | 5.543 | 263 | 13.951 | 313 | 34.183 | 401 | 60.329 | 500 | | |
| 15 | 34.053 | 0.0267 | 6.60 | 0.314 | 1095 | 0.942 | 1199 | 1.885 | 2008 | 6.911 | 2623 | 17.119 | 3389 | 38.165 | 4503 | 79.158 | 6566 | | |
| 16 | 98.413 | 0.0267 | 5.82 | 0.185 | 127 | 0.554 | 128 | 1.109 | 156 | 4.065 | 165 | 10.070 | 202 | 22.450 | 256 | 46.563 | 381 | 84.350 | 568 |
| 17 | 34.053 | 0.0267 | 4.46 | 0.314 | 1193 | 1.256 | 1369 | 3.141 | 1673 | 6.911 | 2075 | 23.245 | 3109 | 54.499 | 4996 | | | | |
| 18 | 98.413 | 0.0267 | 4.10 | 0.185 | 120 | 0.739 | 124 | 1.848 | 122 | 5.358 | 116 | 13.673 | 150 | 32.058 | 233 | 58.481 | 417 | | |
| 23 | 19.053 | 0.0267 | 6.53 | 0.314 | 6900 | 0.942 | 8604 | 3.141 | 10533 | 9.424 | 12425 | 23.559 | 13381 | 65.179 | 17025 | | | | |
| 24 | 55.064 | 0.0267 | 6.83 | 0.185 | 627 | 0.554 | 759 | 1.848 | 930 | 5.543 | 1057 | 13.858 | 1265 | 38.341 | 1354 | | | | |
| 25 | 19.053 | 0.0267 | 4.69 | 0.314 | 4801 | 0.942 | 6584 | 3.455 | 7563 | 9.424 | 8677 | 25.129 | 10326 | 58.583 | 15017 | 102.088 | 21297 | | |
| 26 | 55.064 | 0.0267 | 4.55 | 0.185 | 393 | 0.554 | 459 | 2.033 | 539 | 5.543 | 583 | 14.782 | 732 | 34.461 | 1035 | 60.052 | 1691 | | |
| 27 | 19.053 | 0.0267 | 3.14 | 0.314 | 2653 | 0.942 | 3255 | 3.141 | 4199 | 9.424 | 5592 | 22.459 | 7186 | 95.178 | 15419 | | | | |
| 28 | 55.064 | 0.0267 | 2.94 | 0.185 | 201 | 0.554 | 218 | 1.848 | 231 | 5.543 | 282 | 13.396 | 348 | 55.987 | 857 | | | | |
| 33 | 10.540 | 0.0267 | 3.04 | 0.314 | 12206 | 0.942 | 16350 | 3.141 | 22690 | 22.302 | 37373 | 67.221 | 41486 | | | | | | |
| 34 | 30.461 | 0.0267 | 3.14 | 0.185 | 1210 | 0.554 | 1426 | 1.848 | 1726 | 5.543 | 2122 | 13.119 | 2374 | 39.542 | 2132 | | | | |
| 45 | 10.540 | 0.0267 | 1.48 | 0.314 | 5841 | 1.256 | 7898 | 3.141 | 9900 | 9.424 | 12809 | 23.402 | 11701 | 62.981 | 15127 | | | | |
| 46 | 30.461 | 0.0267 | 1.44 | 0.185 | 471 | 0.739 | 577 | 1.848 | 659 | 5.543 | 515 | 13.766 | 356 | 37.047 | 262 | | | | |
| 47 | 10.540 | 0.0267 | 5.32 | 0.314 | 20719 | 1.256 | 28556 | 3.141 | 35189 | 9.424 | 43464 | 23.402 | 51873 | 62.981 | 56742 | | | | |
| 48 | 30.461 | 0.0267 | 5.42 | 0.185 | 2018 | 0.739 | 2535 | 1.848 | 3118 | 5.543 | 3903 | 13.766 | 4750 | 37.047 | 4848 | | | | |
| 61 | 34.053 | 0.0267 | 6.09 | 0.157 | 1655 | 0.471 | 1850 | 1.571 | 2227 | 4.712 | 2434 | 9.424 | 2738 | 16.491 | 3365 | 25.915 | 4095 | 99.418 | 7253 |
| 63 | 98.413 | 0.0267 | 7.17 | 0.093 | 139 | 0.277 | 154 | 0.924 | 201 | 2.772 | 199 | 5.543 | 216 | 9.701 | 253 | 15.244 | 290 | | |
| 64 | 98.413 | 0.0267 | 6.26 | 0.093 | 132 | 0.277 | 136 | 0.924 | 172 | 2.772 | 189 | 5.543 | 200 | 9.701 | 222 | 15.244 | 280 | | |
| 71 | 10.540 | 0.0267 | 3.12 | 0.157 | 10448 | 0.471 | 15005 | 1.571 | 20427 | 4.712 | 26092 | 10.994 | 31276 | 22.459 | 37811 | | | | |
| 74 | 30.461 | 0.0267 | 3.04 | 0.093 | 1145 | 0.277 | 1392 | 0.924 | 1732 | 2.772 | 1982 | 6.467 | 2124 | 13.211 | 2199 | | | | |

$n_{d2}$ = depth scale factor, converted from tests via $n_{d2} = n_{d1}/(w_2/w_1)^2$

$w_2$ = fall velocity (m/s)

$Sf_2$ = steepness factor initial profile

$t_2$ = (model) time in hrs, converted from tests via $t_2 = t_1 (w_2/w_1)$

$A_2$ = cumulative erosion quantity at $t_2$ hrs in $10^{-4}$ m$^3$/m$^1$

**Table 7b**  Test results after conversion to prototype size sand, test series by Van de Graaff (1977)

## 4.5 Investigation of erosion profiles, α-value (step 3a)

The erosion profiles that develop in a small scale model with prototype size sediment are steeper than prototype profiles. This is caused by the fact that the grains are too large and too heavy relative to the water motion. The relation between the depth scale factor and the steepness exaggeration of the erosion profile can be described by a distortion relation:

$$n_1/n_d = n_d^{\alpha} \qquad\qquad (8)$$

The most direct way to determine the value of α is to convert all model profiles to prototype with $n_1 = n_d$ and to determine the relation between the steepness of the profile and the depth scale factor. The prototype profiles are shown in Figure 48. The steepness of the profiles can be expressed in terms of the distance between the waterline and a certain depth contour. The relation is shown in Figures 49, 50, 51, for the 1.0 m, 2.0 m and 3.0 m depth contour. The results show that this relation is well described by:

$$\ell = \ell_1 (n_d)^{-\alpha} \qquad\qquad (109)$$

in which

$\ell$ is the distance from the waterline to a certain depth contour for a model
profile that has been converted to prototype with $n_1 = n_d$

$n_d$ is the depth scale factor

$\ell_1$ is the distance from the waterline to the depth contour for prototype
$(n_d = 1)$

Relation (109) means that the length $\ell$ from a model with depth scale factor
$n_d$ should be multiplied by a factor $n_d^\alpha$ to obtain the prototype value $\ell_1$. So
the length scale factor of a model should be factor $n_d^\alpha$ larger than the depth
scale factor:

$$n_1 = n_d^\alpha \, n_d \tag{110}$$

Relation (110) can also be written as

$$n_1/n_d = n_d^\alpha \tag{8}$$



| $n_{d2}$ | sediment size | profile number | test number |
|---|---|---|---|
| 53,55 | 225 $\mu$m | 1 | 105 |
| 26,39 | 225 $\mu$m | 2 | 121 |
| 25,61 | 225 $\mu$m | 3 | 125 |
| 18,39 | 150 $\mu$m | 4 | 106 |
| 8,65 | 150 $\mu$m | 5 | 122 |
| 8,43 | 150 $\mu$m | 6 | 126 |
| 5,70 | 130 $\mu$m | 7 | 123 |
| 5,52 | 130 $\mu$m | 8 | 127 |
| 2,28 | 95 $\mu$m | 9 | 124 |
| 2,22 | 95 $\mu$m | 10 | 128 |

$$n_{d2} = n_{d1}/(w_2/w_1)^2$$
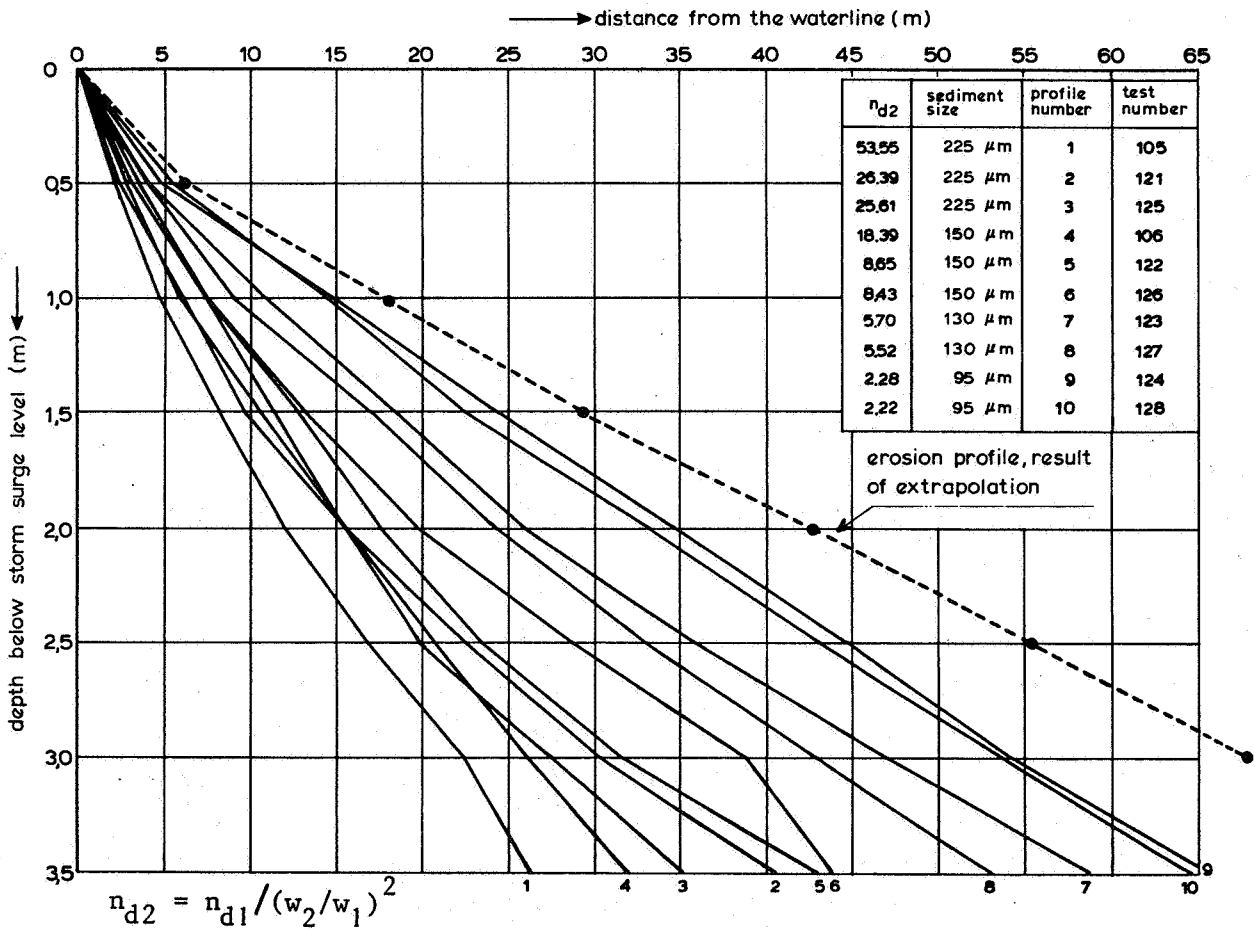
**Figure 48** Erosion profiles converted to prototype with $n_1 = n_d$
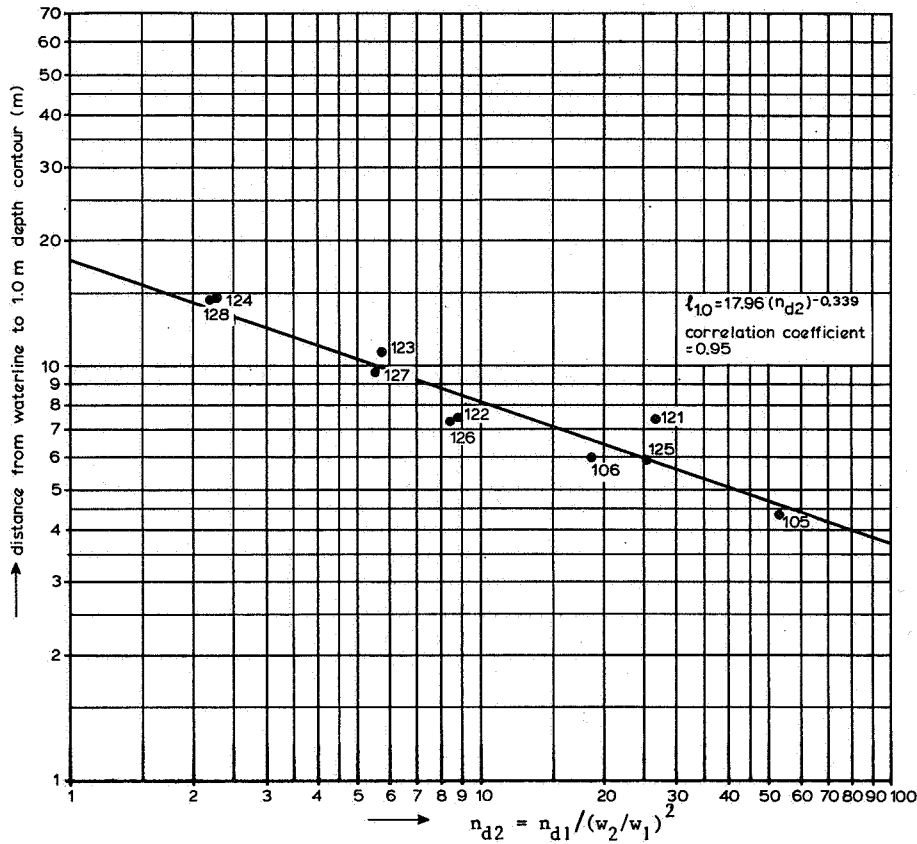
**Figure 49** Distance from waterline to 1-m depth contour as a function of $n_{d2}$
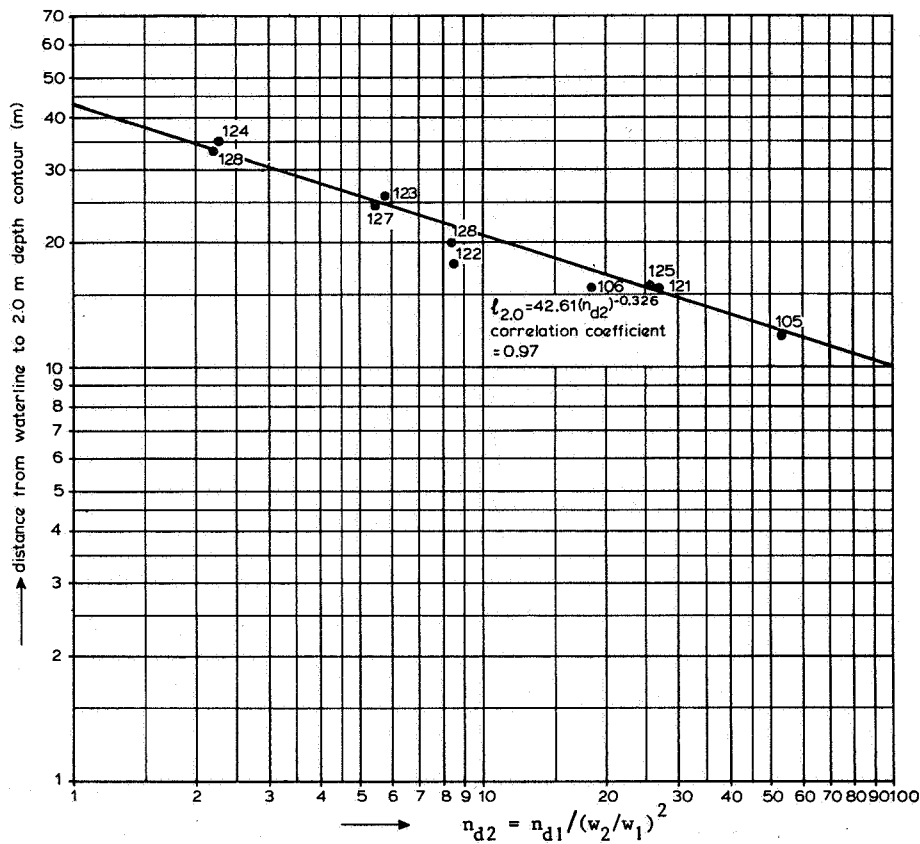


**Figure 50** Distance from waterline to 2-m depth contour as a function of $n_{d2}$
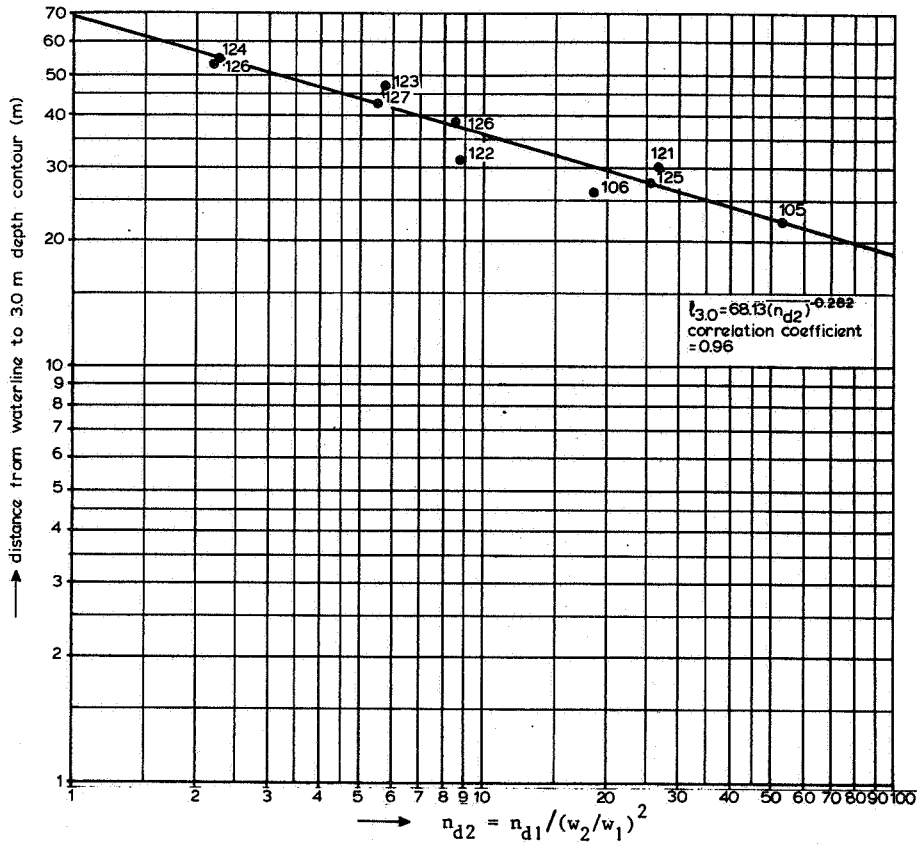
**Figure 51** Distance from waterline to 3-m depth contour as a function of $n_{d2}$

The results of Figures 49, 50 and 51 demonstrate that the basic form of relation (109) is confirmed by the model data. The best fit $\alpha$ values and the respective correlation coefficients are shown in Table 8.

| depth contour | $1_1$ | $\alpha$ | correlation coefficient |
|---|---|---|---|
| 1.0 m | 18.0 | 0.339 | 0.95 |
| 2.0 m | 42.6 | 0.326 | 0.97 |
| 3.0 m | 68.1 | 0.282 | 0.96 |
| | | average $\alpha$ = 0.316 | |

**Table 8** $\alpha$-values derived from erosion profiles

## 4.6 Investigation of erosion quantities ($\alpha$ - $\beta$ combination)(step 3b)

The most important aspect of the present investigations is the dune erosion quantity to be expected during extreme storm surge conditions. The cumulative erosion quantity above storm surge level as a function of time after start has

been recorded for all tests. The results of the tests, after conversion to prototype size sediment, are shown in Table 7a and 7b.

The prototype hydraulic conditions are identical for all tests. That leaves just two variables to describe the cumulative erosion quantity:

$$A = f(Sf, t) \tag{111}$$

in which

A  is the cumulative erosion quantity                                      $(m^3/m^1)$

Sf is the steepness factor of the initial profile                          $(-)$

t  is time                                                                  $(s)$

The relation between A and Sf for t = 1 hr for the tests with $n_d$ = 26 and $D_{50}$ = 225 µm is shown in Figure 52 as an illustration. It can be seen that there is a linear relationship between A and Sf. This also holds for the other tests.
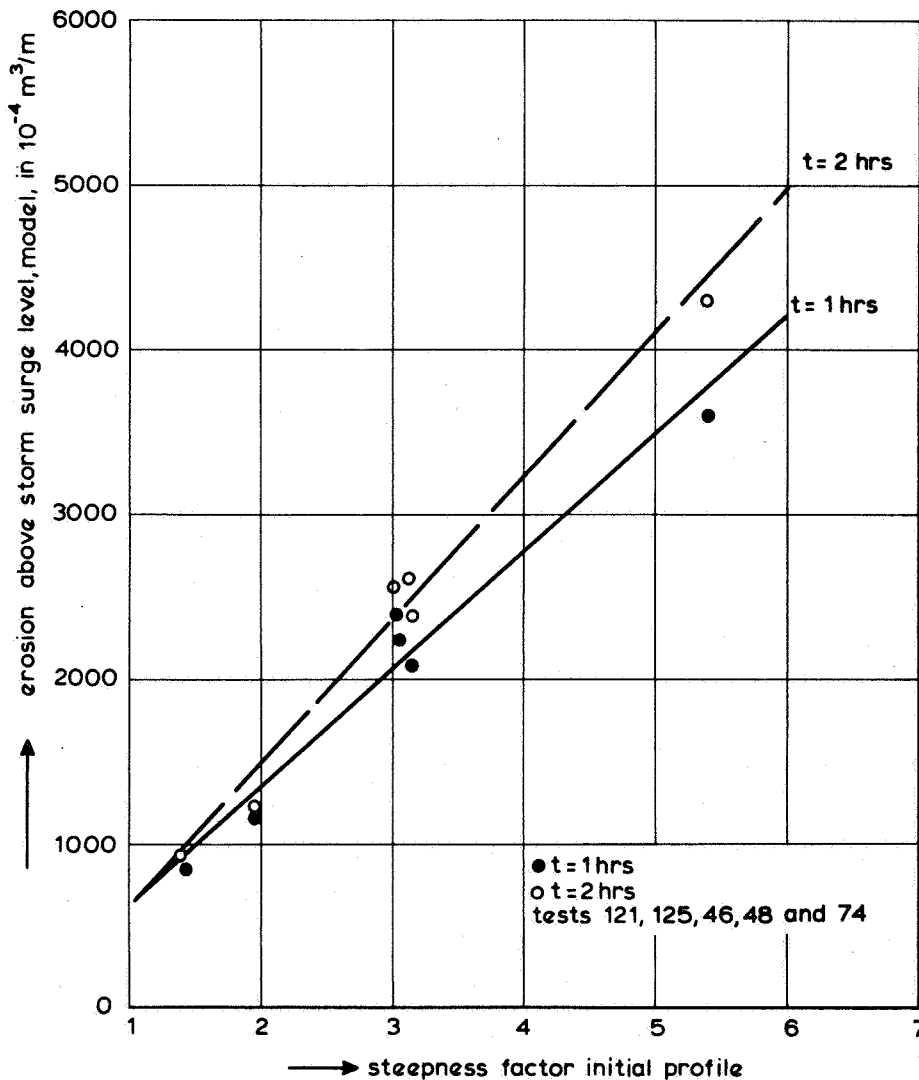


**Figure 52**  Relation between initial profile steepness and erosion quantity for tests with $n_d$ = 26 and $D_{50}$ = 225 µm for t = 1 hrs and t = 2 hrs.

The cumulative erosion quantities of all tests can be converted to prototype by conversion of A, Sf and t. The scale factors for these parameters are

$$n_A = n_1 * n_d = n_d^{2+\alpha} \tag{112}$$

$$n_{Sf} = n_d^{-\alpha} \tag{113}$$

$$n_t = n_d^{\beta} \tag{9}$$

The conversion is illustrated by the following example:
A test with depth scale factor $n_d$ = 2.28 and a model profile steepness Sf = 1.32 has yielded an erosion quantity A = 36.3 $m^3/m^1$ at t = 3.38 hrs after start. The respective values for Sf, A and t for prototype conditions are:

$$Sf_{prototype} = 1.32 (2.28)^{-\alpha} \tag{114}$$

$$A_{prototype} = 36.3 (2.28)^{2+\alpha} \tag{115}$$

$$t_{prototype} = 3.38 (2.28)^{\beta} \tag{116}$$

This conversion yields a set of prototype erosion data for every value of $\alpha$, $\beta$, Sf and t:

$$A_p = f(Sf, t, \alpha, \beta) \tag{117}$$

To enable an evaluation of the quality of the various $\alpha$ and $\beta$ combinations this relation was investigated for a range of values of t, $\alpha$ and $\beta$. For every combination of values a relation is found between A and Sf. As an example the test results as converted to prototype with $\alpha$ = 0.28, $\beta$ = 0.5 at t = 5 hrs after start (prototype) are shown in Figure 53. In case of perfect scale relations the results of Figure 53 should form a single line, not only for the time step t = 5 hrs, but for all time steps.

In practice a single line will not be found as there will always be some scatter in the measured test results. Moreover, it may not be expected that the scale relations cover all processes.
The scatter in the data points is a measure for the quality of the $\alpha$ and $\beta$ - combination. The scatter can be expressed in terms of a correlation coefficient. Investigation of the relation between A and Sf has shown that these variables are well described by a linear relation, see Figure 52 as an example.

$$A = Ao + a Sf \tag{118}$$
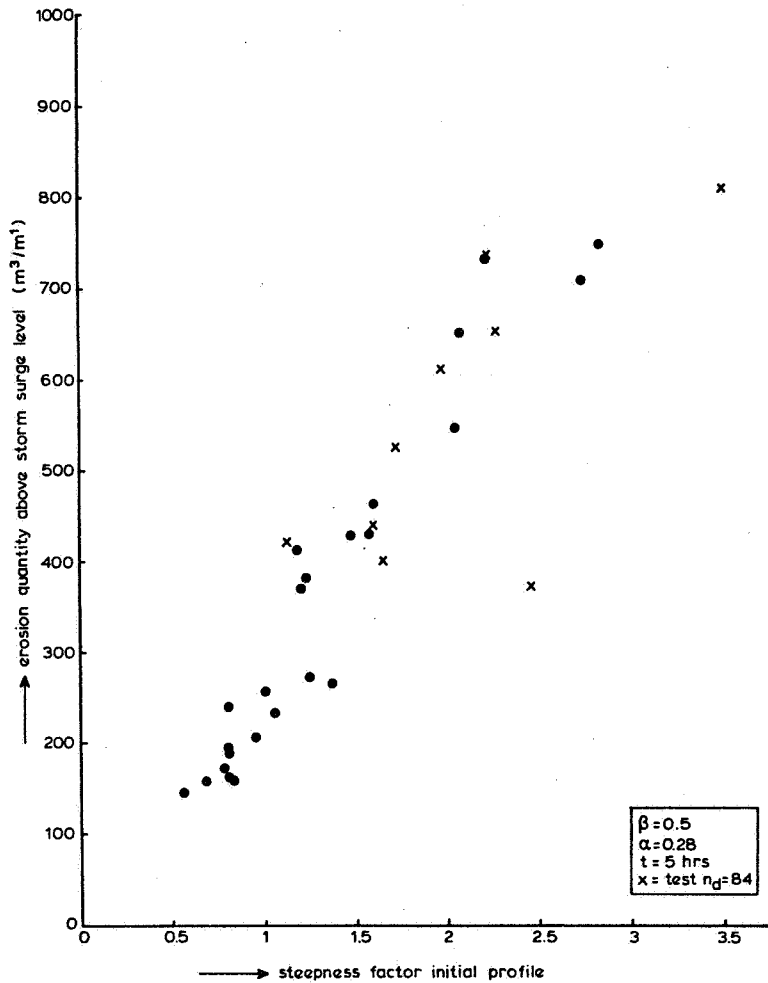
**Figure 53** Relation between initial profile steepness and erosion quantity for all tests, prototype, $\alpha = 0.28$, $\beta = 0.5$ and $t = 5$ hrs.

The correlation coefficients for linear regression are shown in Table 9 for four different $\alpha$-values and 7 different $\beta$-values. The correlation analysis has been carried out for 2 sets of tests. One set covering the tests with depth scale factors $n_d = 26$, 47 and 84 and another one consisting of tests with $n_d = 26$ and $n_d = 47$ only. Iso-correlation lines are indicated to detect the highest correlation coeffcient for the $\alpha - \beta$ combination. The results in Table 9 indicate that the correlation coefficients are relatively high over a large range of $\alpha$ and $\beta$ combinations. The results do not justify a specific choice of $\alpha$ and $\beta$ as the correlation coefficients are not sensitive to small changes in the $\alpha$ and $\beta$ values.

However, it is justified to conclude that an $\alpha$-value in the range of $\alpha = 0.20$ to $\alpha = 0.28$ in combination with a $\beta$-value in the range of $\beta = 0.0$ to $\beta = 0.50$ gives the best results for scaling of erosion quantities. The conclusion re-

garding the β-value would be more convincing if β-values greater than 0.5 had also been considered. Later on, in chapter 5, the results are shown of a correlation analyses of the present tests and the large scale tests for β-values ranging from β = - 0.50 up to β = 1.0.

| β \ α | 0.20 | 0.22 | 0.24 | 0.26 | 0.28 |
|---|---|---|---|---|---|
| -0.50 | 0.939 | 0.932 | 0.921 | 0.906 | 0.874 |
| -0.25 | 0.940 | 0.947 | 0.944 | 0.937 | 0.925 |
| 0.00 | 0.952 | 0.954 | 0.948 | 0.931 | 0.923 |
| 0.25 | 0.927 | 0.925 | 0.917 | 0.906 | 0.889 |
| 0.50 | 0.900 | 0.924 | 0.916 | 0.903 | 0.885 |

tests $n_d$=26, $n_d$=47 and $n_d$=84, t = 2 hrs

| β \ α | 0.20 | 0.22 | 0.24 | 0.26 | 0.28 |
|---|---|---|---|---|---|
| -0.50 | 0.952 | 0.944 | 0.932 | 0.917 | 0.899 |
| -0.25 | 0.956 | 0.951 | 0.941 | 0.928 | 0.914 |
| 0.00 | 0.971 | 0.965 | 0.955 | 0.943 | 0.926 |
| 0.25 | 0.971 | 0.964 | 0.954 | 0.941 | 0.925 |
| 0.50 | 0.983 | 0.972 | 0.962 | 0.950 | 0.933 |

tests $n_d$=26 and $n_d$=47, t = 2 hrs

| β \ α | 0.20 | 0.22 | 0.24 | 0.26 | 0.28 |
|---|---|---|---|---|---|
| -0.50 | 0.895 | 0.881 | 0.864 | 0.844 | 0.819 |
| -0.25 | 0.943 | 0.947 | 0.941 | 0.930 | 0.917 |
| 0.00 | 0.940 | 0.947 | 0.947 | 0.934 | 0.928 |
| 0.25 | 0.944 | 0.950 | 0.948 | 0.942 | 0.930 |
| 0.50 | 0.921 | 0.925 | 0.926 | 0.921 | 0.912 |

tests $n_d$=26, $n_d$=47 and $n_d$=84, t = 5 hrs

| β \ α | 0.20 | 0.22 | 0.24 | 0.26 | 0.28 |
|---|---|---|---|---|---|
| -0.50 | 0.931 | 0.927 | 0.912 | 0.897 | 0.877 |
| -0.25 | 0.958 | 0.954 | 0.946 | 0.936 | 0.921 |
| 0.00 | 0.961 | 0.960 | 0.954 | 0.946 | 0.936 |
| 0.25 | 0.962 | 0.960 | 0.955 | 0.947 | 0.933 |
| 0.50 | 0.973 | 0.974 | 0.974 | 0.970 | 0.961 |

tests $n_d$=26 and $n_d$=47, t = 5 hrs

| β \ α | 0.20 | 0.22 | 0.24 | 0.26 | 0.28 |
|---|---|---|---|---|---|
| -0.50 | 0.783 | 0.756 | 0.722 | 0.703 | 0.671 |
| -0.25 | 0.925 | 0.930 | 0.917 | 0.900 | 0.878 |
| 0.00 | 0.941 | 0.948 | 0.948 | 0.936 | 0.935 |
| 0.25 | 0.936 | 0.945 | 0.948 | 0.947 | 0.940 |
| 0.50 | 0.941 | 0.947 | 0.948 | 0.941 | 0.936 |

tests $n_d$=26, $n_d$=47 and $n_d$=84, t = 10 hrs

| β \ α | 0.20 | 0.22 | 0.24 | 0.26 | 0.28 |
|---|---|---|---|---|---|
| -0.50 | 0.829 | 0.812 | 0.793 | 0.771 | 0.746 |
| -0.25 | 0.949 | 0.945 | 0.937 | 0.926 | 0.911 |
| 0.00 | 0.958 | 0.959 | 0.954 | 0.947 | 0.935 |
| 0.25 | 0.954 | 0.956 | 0.954 | 0.949 | 0.940 |
| 0.50 | 0.964 | 0.971 | 0.970 | 0.967 | 0.958 |

tests $n_d$=26 and $n_d$=47, t = 10 hrs

**Table 9** Results of correlation analysis of erosion quantities to determine the best fit α/β combination

## 4.7 Investigation of erosion rates, $\beta$-value (step 3c)

The correlation analysis of erosion quantities gives best fit $\beta$-values in the range $\beta = 0$ up to $\beta = 0.50$. It is hardly possible to select a $\beta$-value as the differences indicated in Table 9 are not really significant.

The $\alpha$-values found so far range from $\alpha = 0.32$ as an average found by erosion profile analysis to $\alpha = 0.24$ as an average found by erosion quantity analysis. The range is not as large as with the $\beta$-values. Therefore it is judged acceptable to choose the average value, $\alpha = 0.28$ for a further investigation of the time scale relation.

A way to determine the time scale relation is to convert all model data to prototype with $\alpha = 0.28$, neglecting the time scale (thus applying $n_t = 1$). This provides a series of prototype erosion data with corresponding model time periods.

$$A_p = f (Sf_p, t_m) \tag{119}$$

As the scale dependency of the erosion rate has not been taken into account a relation between erosion rate and depth scale factor should be found. This can be investigated by considering the time required to produce a given erosion quantity as a function of the depth scale factor as shown in Figure 54. The results refer to an initial prototype profile with $Sf = 2$ and a cumulative erosion quantity of 200 $m^3/m^1$. The relation between the time needed to obtain this amount of erosion and the corresponding depth scale factor can be described by (analogous to the erosion profile analysis described in 4.5):

$$t = t_1 (n_d)^{-\beta} \tag{120}$$

in which:

t    is the time in the model (depth scale factor $n_d$) required to produce a certain amount of erosion

$t_1$   is the corresponding time in prototype ($n_d = 1$)

$n_d$   is the depth scale factor

$\beta$    is the exponent determined by correlation analysis

The results of this procedure for a range of initial profiles and erosion quantities are shown in Table 10. This way $\beta$-values are found ranging from $\beta = 0.5$ up to $\beta = 0.9$. It is evident that the result $\beta = 0$ as found by Van de Graaff (1977) on the basis of a correlation analysis of erosion quantities in the earlier tests falls beyond this range. For $\beta = 0$ the data points as shown in Figure 54 would form a horizontal line.

| Sf = 1 | | Sf = 2 | |
|---|---|---|---|
| erosion quantity | β-value | erosion quantity | β-value |
| $m^3/m^1$ | - | $m^3/m^1$ | - |
| 100 | 0.69 | 200 | 0.50 |
| 200 | 0.90 | 400 | 0.66 |
| 300 | 0.54 | 600 | 0.62 |

**Table 10** β-values determined by erosion rate analysis for α = 0.28



$$n_{d2} = n_{d1}/(w_2/w_1)^2$$
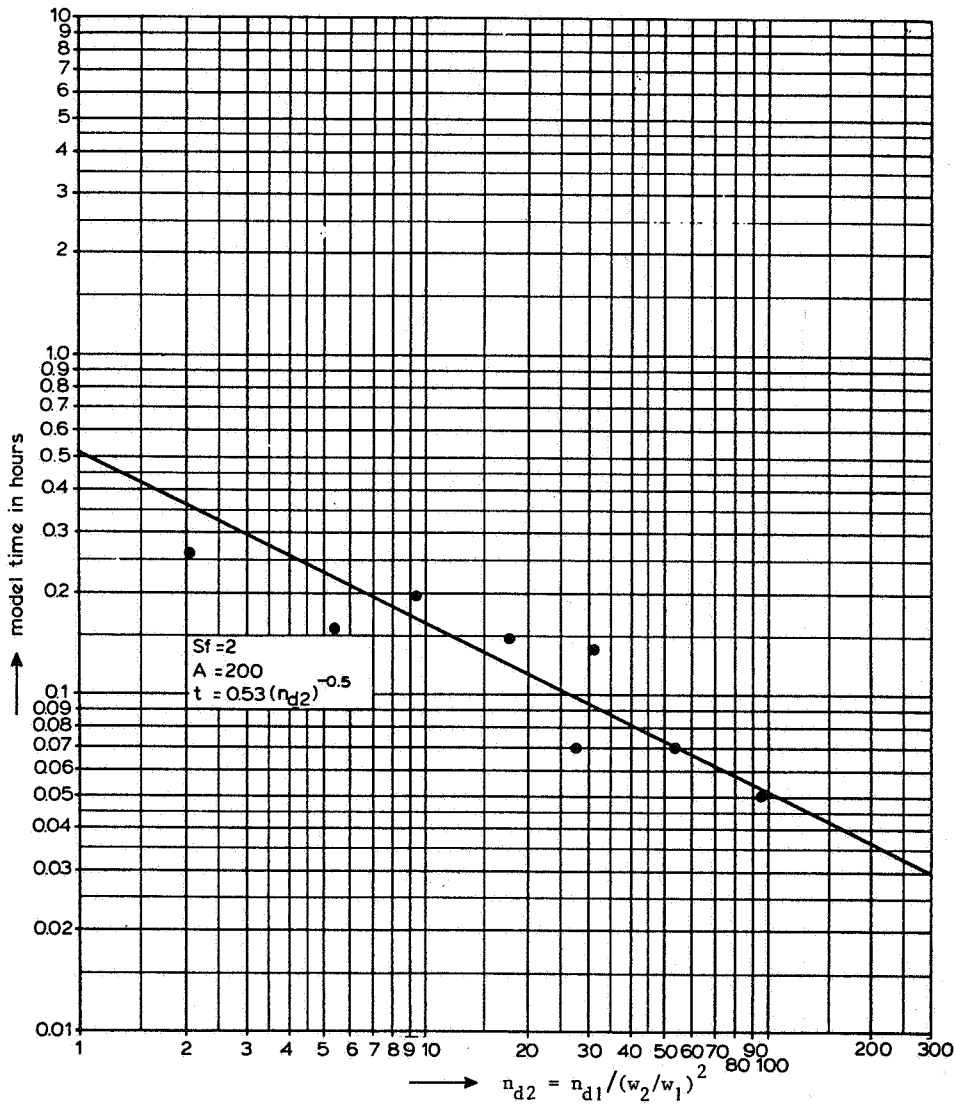
**Figure 54** Relation between depth scale factor and time required to produce a given erosion quantity

## 4.8 Determination of scale relations (step 4)

The previous elaborations have given an impression of the range of most promising values for $\alpha$ and $\beta$. The results are summarized in Table 11.

|  | prime interest | $\beta$ | $\alpha$ |
|---|---|---|---|
| analysis of erosion profiles | distortion relation, $\alpha$ | - | 0.28 - 0.34 |
| analysis of erosion quantities | combination of $\alpha$ and $\beta$ | 0.0 - 0.5 | 0.20 - 0.28 |
| analysis of erosion rates | time scale relation $\beta$ | 0.5 - 0.9 | - |
| overlapping values |  | 0.5 | 0.28 |

**Table 11** $\alpha$ and $\beta$ values, summary of results.

Considering the ranges of the $\alpha$ and $\beta$ values it is difficult to select a specific combination. The range of $\alpha$-values is relatively small and it is reasonable to select the overlapping value $\alpha = 0.28$. The range of $\beta$-values is relatively large. The various correlation coefficents as found by correlation analysis of the erosion quantities are relatively high over a large range of $\beta$ values. It is considered acceptable therefore to choose overlapping value which is also the most suitable time scale viz. $\beta = 0.5$. This value is the most suitable one in view of the hydraulic time scale. A morphological time scale different from the hydraulic time scale is possible in theory. However, as the basic form of the distortion relation, is based on the ratio of the fall velocity and orbital velocity, the corresponding time scale is most plausible:

$$n_T = n_t = n_d^{0.5} \tag{1}$$

Ultimately it is concluded that a combination with $\alpha = 0.28$ and $\beta = 0.5$ is the best result. So the scale relations finally determined are:

$$n_1 / n_d = (n_d / n_w^2)^{0.28} \qquad \text{(model distortion)} \tag{4}$$

$$n_t = (n_d)^{0.5} \qquad \text{(morphological and hydraulic time scale)} \tag{5}$$

These scale relations are virtually identical to the theoretically determined scale relations. The dimensional analysis of the sediment transport process yielded (see Chapter 3):

$$n_1/n_d = (n_t/n_w)^{0.5}, \tag{91}$$

$$\text{for } n_t = n_d^{0.5} \tag{92}$$

this can be written as

$$n_1/n_d = (n_d/n_w^2)^{0.25} \tag{94}$$

The theoretical relation (94) and the experimental result, relation (4), are identical except for the value of the exponent ($\alpha = 0.28$ in stead of 0.25). A value 0.25 for the exponent is more elegant when the dimensions are considered. However, the value 0.28 has been found from a thorough analysis of erosion quantities and erosion profiles. For practical use it is therefore recommended to apply the empirical value, $\alpha = 0.28$. For further theoretical analysis it may be better to apply the value $\alpha = 0.25$.

## 4.9  Results for prototype

At this stage of the investigations it is important to consider the dune erosion results for prototype conditions. The results of the series of model tests can be converted to prototype values with the scale relations presented in the previous section:

$$n_A = n_1 n_d = n_d^2 (n_d/ n_w^2)^{0.28} \tag{121}$$

$$n_{Sf} = (n_d/ n_w^2)^{-0.28} \tag{122}$$

$$n_t = (n_d)^{0.5} \tag{5}$$

### Erosion quantity

The test results as shown in Table 7 have been converted to prototype using (121) and (122). This conversion gives a relationship between the steepness factor of the initial profile and the cumulative erosion quantity for every selected period of time. The results after t = 2, 5 and 10 hrs are presented in Figure 55. It is assumed at this stage that the dune erosion quantity caused by a natural design storm surge is equivalent to the erosion quantity caused by a constant sea level at the top level of the hydrograph for a period

of 5 hrs, see Figure 56. This assumption will be verified in Chapter 5. On the basis of this assumption the prototype results can be compared to the dune erosion quantity as predicted by the provisional prediction model of Van de Graaff (1977). Figure 55 shows that the provisional prediction model results deviate systematically from the erosion quantities found in the scale models. The erosion quantity is overestimated by 25% - 50% depending on the steepness of the initial profile and the storm duration.

## Erosion profile

The erosion profile for prototype, as found from the model tests, can be compared with the erosion profile according to the provisional prediction model. The prototype erosion profile was determined by extrapolation of the model profiles. The method and the results are described in section 4.5.

The prototype erosion profile found this way is shown in Figure 57 together with the erosion profile from the provisional model. It can be seen, that the profile found from the model test agrees reasonably well with the profile according to the provisional prediction model, which was derived from field data (Van de Graaff, 1977).

A major point of difference between the model profile and the profile according to the provisional model is the extent of the profile in seaward direction. This aspect is further investigated by analysing the recovery distance of the sand eroded from the dunes.

## Recovery distance

The recovery distance is a measure of the spreading of the eroded sand in seaward direction. A recovery distance $L_{90\%}$ = 284 m means that 90% of the eroded sand has settled within a distance of 284 m from the water line.

The recovery distance can be determined in the same way as the prototype erosion profile. The results of the set of (converted) tests with $D_{50}$ = 225 have been taken as a basis. The profiles have been converted to prototype with $n_1 = n_d$. Thus the distortion is neglected and a clear depency between the recovery distance and the depth scale factor can be observed. This dependance can be described by a relation equivalent to the distortion relation $(n_1/n_d = n_d^\alpha)$ : $L = L_1 n_d^{-\alpha}$, in which L is the distance as found from a test with depth scale factor $n_d$, and $L_1$ is the distance for $n_d$ = 1. The distance $L_1$ is found by extrapolating the relation between $n_d$ and L.

As an example the 70% recovery distance as a function of the depth scale factor for t = 1.5 hours in prototype is shown in Figure 58. For $n_{d2}$ = 1 this distance is 106 m. The results for the 50% up to 90% recovery distance are
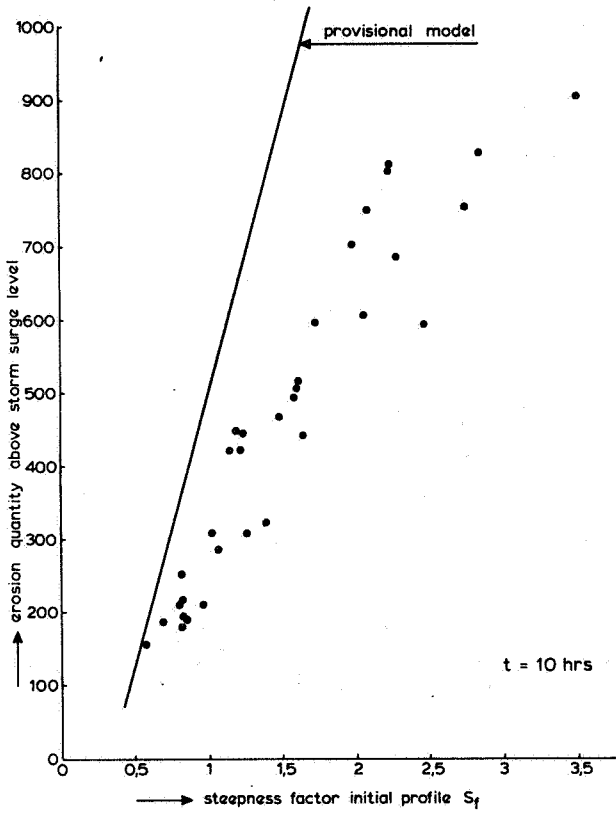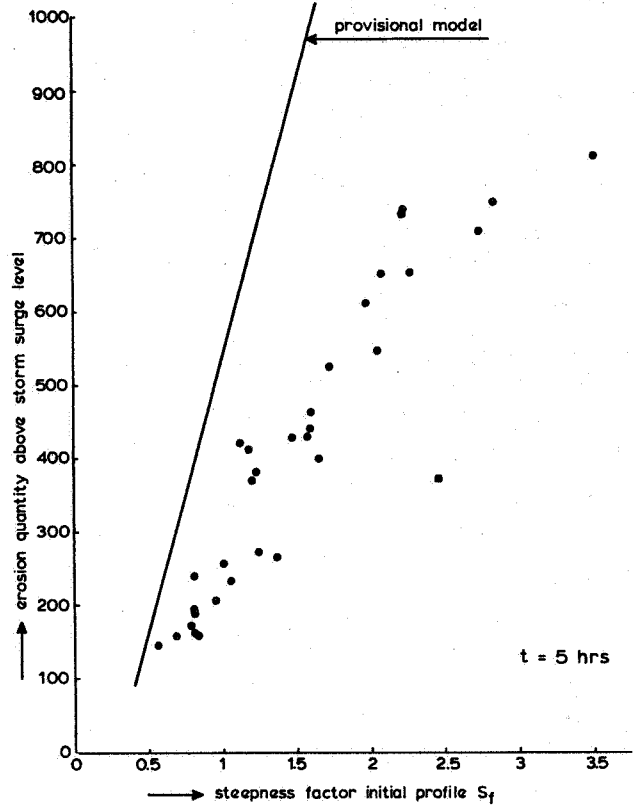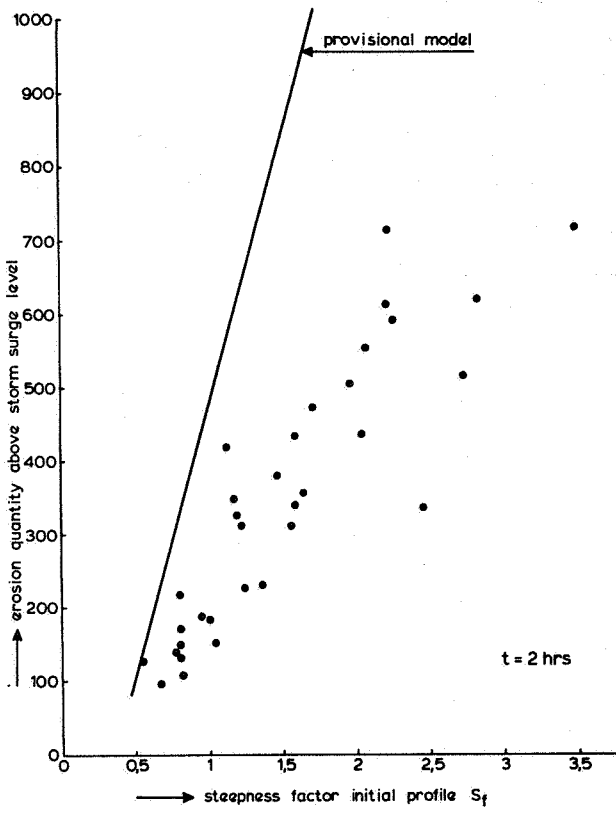
**Figure 55** Prototype erosion
quantity for t = 2 hrs,
t = 5 hrs and t = 10 hrs.
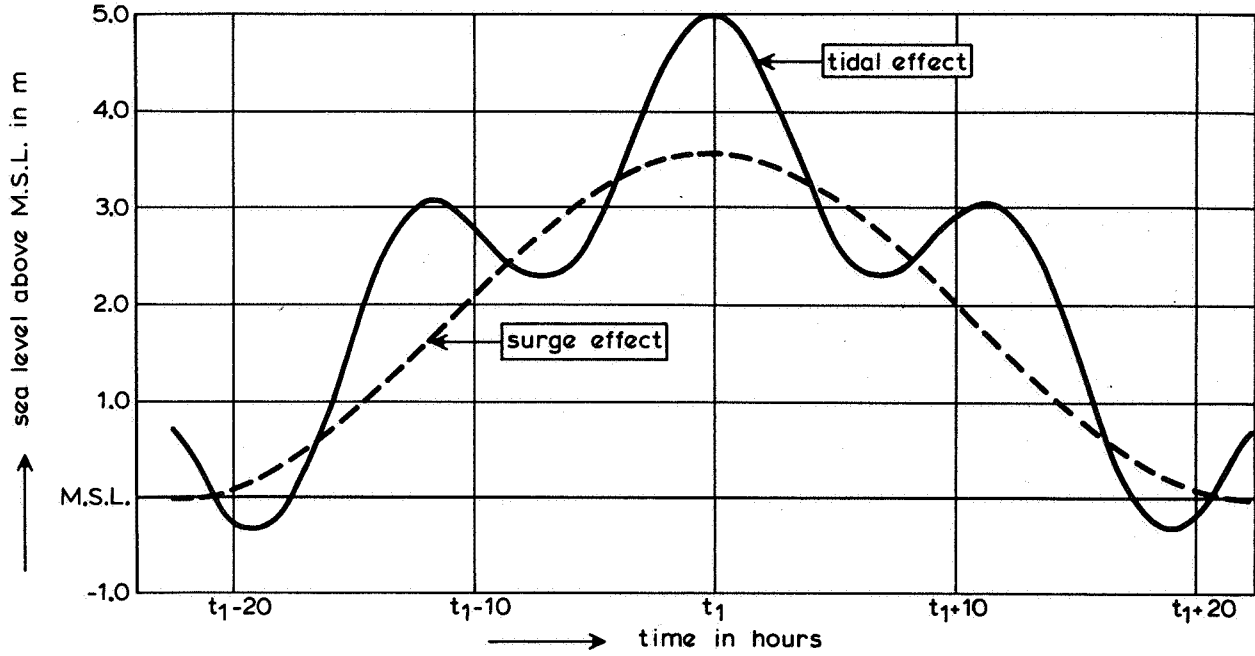
**Figure 56** North Sea storm surge hydrograph
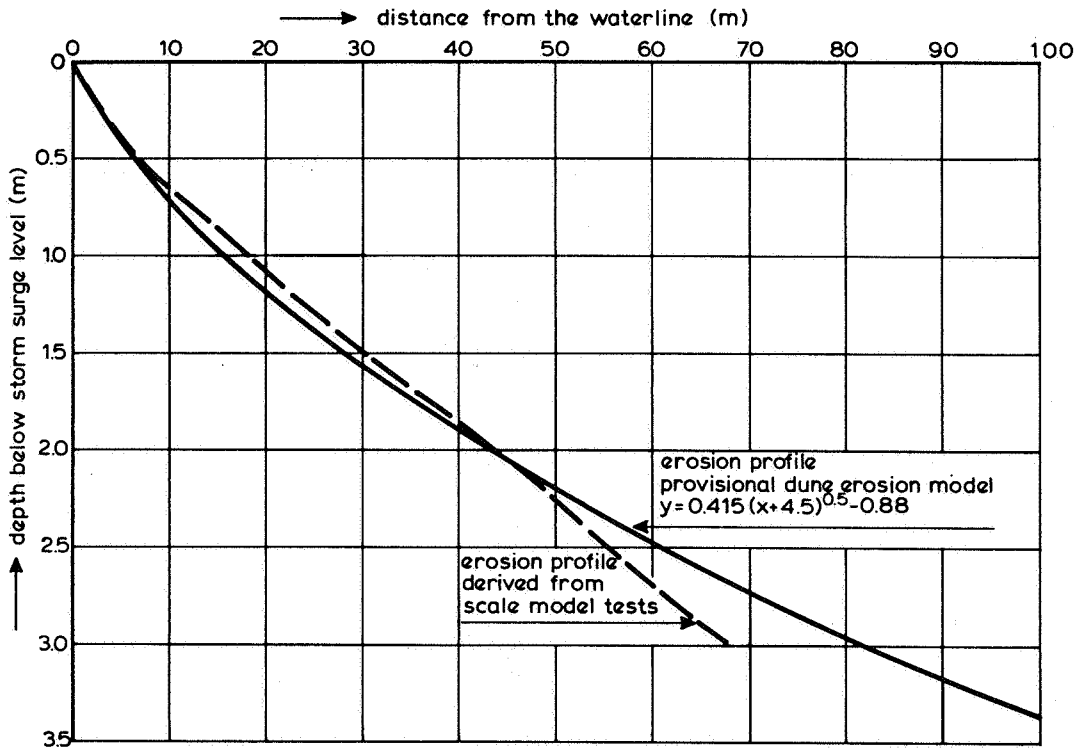


**Figure 57** Erosion profiles, model tests and provisional model

shown in Table 12. A 100% recovery distance could not be determined due to a marginal loss of sand-volume during the tests. The recovery distance has also been determined for the provisional dune erosion prediction model. In Table 13 the results are compared for identical initial profiles. It is concluded that

the provisional model over-predicts the distance over which the eroded sediment is transported by a factor 2.

| prototype hours | $L_{90\%}$ m | $L_{80\%}$ m | $L_{70\%}$ m | $L_{50\%}$ m |
|---|---|---|---|---|
| 1.5 | 284 | 164 | 106 | 82 |
| 5 | 280 | 187 | 135 | 116 |
| 15 | 785 | 773 | 277 | 242 |

**Table 12**  Recovery distance, model tests

| | prototype recovery distance | |
|---|---|---|
| | from model tests t=5 hrs, prototype | according to provisional model |
| | m | m |
| $L_{90\%}$ | 280 | 520 |
| $L_{80\%}$ | 187 | 460 |
| $L_{70\%}$ | 135 | 400 |
| $L_{50\%}$ | 116 | 320 |

**Table 13**  Recovery distance, model test and provisional prediction model



$$t = 1.5 \text{ hrs} \qquad L_{70\%} = 106 \, (n_{d2})^{-0.315}$$
$$\text{correlation coefficient} = 0.93$$

$$n_{d2} = n_{d1}/(w_2/w_1)^2$$
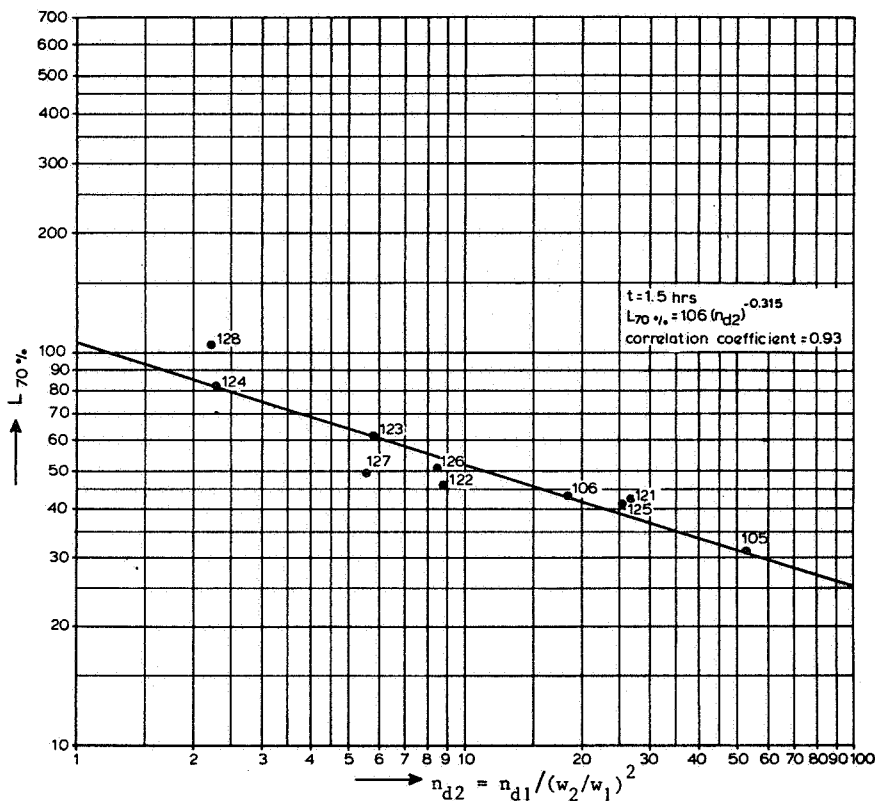
**Figure 58**  Recovery distance as a function of the depth scale factor

## Summary and evaluation of prototype results

A comparison of the test results with the provisional dune erosion prediction model of Van de Graaff (1977) has shown that the provisional model is conservative as it overestimates the distribution distance of the eroded sand. Clearly the assumption in the provisional model that the sand is transported over the entire width of the breaker zone, up to a depth of 1.28 $H_{bs}$, is not in agreement with the test results.

A new, less conservative dune erosion prediction model, however, requires a higher degree of reliability than the present tests can provide. Large scale testing of dune erosion to verify the scale relations and to further analyse the process can provide a more solid basis for the development of such a new prediction model.

An important aspect of the provisional model that has not been verified so far is the two-dimensional approach. Therefore the large scale reproduction of the dune erosion process has been preceded by a verification of this two-dimensional approach in a three-dimensional model (Delft Hydraulics Laboratory, 1981). A brief description of these three-dimensional verification tests is given in the next paragraph.

## 4.10 Three-dimensional model tests

It has been assumed so far that the erosion process during a storm surge can be considered as a two-dimensional process. This assumption is supported by observations in the field. After high storm surges, a straight dune front and uniform beach profiles are always found along the coast.

Also from a sediment balance point of view the assumption is plausible for situations without a longshore sand transport gradient. However, there exists no explicit proof of the hypothesis that the longshore currents and rip currents will not intensify the erosion rate or create an irregular erosion pattern. Therefore, three-dimensional model tests have been carried out to verify the two-dimensional approach (Delft Hydraulics Laboratory, 1981).

In a basin 30 m by 30 m with a 0.38 m water depth, the design storm surge conditions and the erosion process was reproduced with $n_d = 60$ and $n_w = 3$. The length scale of the model was determined on the basis of the earlier derived scale relations:

$$n_l/n_d = (n_d/n_w^2)^{0.28} \text{ for } n_d = 60 \text{ and } n_w = 3, \ n_l = 102 \tag{123}$$

Wave angles of $\theta_0 = 0^0$, $\theta_0 = 10^0$ and $\theta_0 = 20^0$ have been applied in the model, where $\theta_0$ stands for the angle between the shoreline and the wave crests at a waterdepth of 22.8 m prototype. The test conditions are summarized in Table 14.

During the tests no significant variations were observed in the erosion process along the 30 m model beach. As an example, the erosion quantities at various cross-sections as a function of time are shown in Figure 59 for $\theta_0 = 10^0$. It is concluded that a two-dimensional reproduction is fully acceptable.

| Test number | angle of wave incidence at wave board $\phi$ | wave period | water depth at wave board |
|---|---|---|---|
| | $(^\circ)$ | $T(s)$ | $(m)$ |
| P001 | 0 | 1.55 | -0.38 |
| P002 | 20 | 1.55 | 0.38 |
| P003 | 10 | 1.55 | 0.38 |
| P004 | 10 | 1.55 | 0.31-0.38 (var.) |

**Table 14** Summary of test conditions, 3-dimensional model
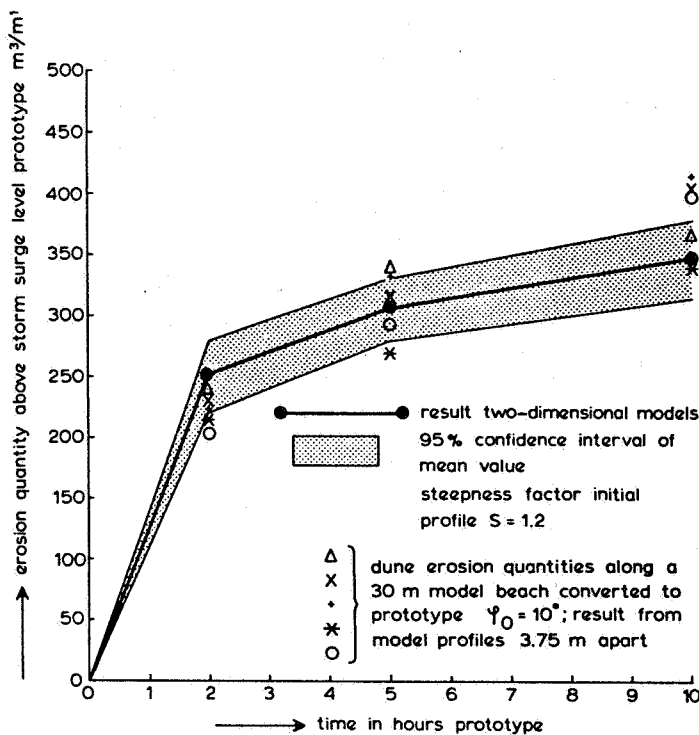


**Figure 59** Cumulative erosion quantity, two-dimensional and three-dimensional tests

## 5. Large-scale model verification

### 5.1 Experimental arrangement

The aim of the large-scale tests can be summarized to three points

1) verification of the scale relations,
2) verification of the reliability of the model results by reproduction of a well-documented case of dune erosion in nature,
3) increasing the knowledge about the dune erosion process by recording and analysing the velocity field and the sediment concentrations.

In total five tests were carried out. Two tests to verify the scale relations with a constant water level, with depth scale factor $n_d = 5$. A third test was done reproducing the naturally varying water level to find the equivalent of the tests with a constant water level. In test number four the reliability of the model results was verified by reproducing of the storm surge of 1953 with a scale factor $n_d = 3.27$. The fifth test can be considered as a full scale replica of a moderate storm surge in nature. The test programme is summarized in table 15 (Delft Hydraulics Laboratory, 1984).

| test number | hyraulic conditions | water depth d in front of wave generator (m) | wave height at depth d $H_s$(m) | wave period at depth d $\hat{T}$(s) | steepness factor initial profile Sf | depth scale $n_d$ | length scale $n_l$ |
|---|---|---|---|---|---|---|---|
| 1 | constant | 4.20 | 1.50 | 5.4 | Sf model = 3 *) | 5 | 7.85 |
| 2 | constant | 4.20 | 1.50 | 5.4 | Sf model = 2 *) | 5 | 7.85 |
| 3 | variable | 4.20 (max) | 1.50 (max) | 5.4 (max) | Sf model = 2 *) | 5 | 7.85 |
| 4 | variable | 4.20 (max) | 1.85 (max) | 5.0 (max) | Delfland-profile | 3.27 | 4.56 |
| 5 | constant | 5.00 | 2.00 | 7.6 | arbitrary profile | 1 | 1 |

*) Sf = 3 means that the initial profile in the model is a factor 3 steeper than the reference profile shown in Figure 17

**Table 15** Large scale test programme

The large scale facility is shown in Figure 60. The dimensions are as follows:

length 233 m
depth 7 m (locally 9 m)
width 5 m

The facility is equipped with a vertical wave board and a programmable wave generator.

The specifications are:

maximum wave height random waves   $H_s$ = 2 m
maximum wave height periodic waves  H  = 3 m
wave period range                   T  = 2 s to T = 10 s

During the tests the wave height, the velocity field and the sediment concentrations were recorded at various locations and during various phases of the process. Also water pressures and soil pressures were recorded. The results of these measurements will be discussed in Chapter 7.
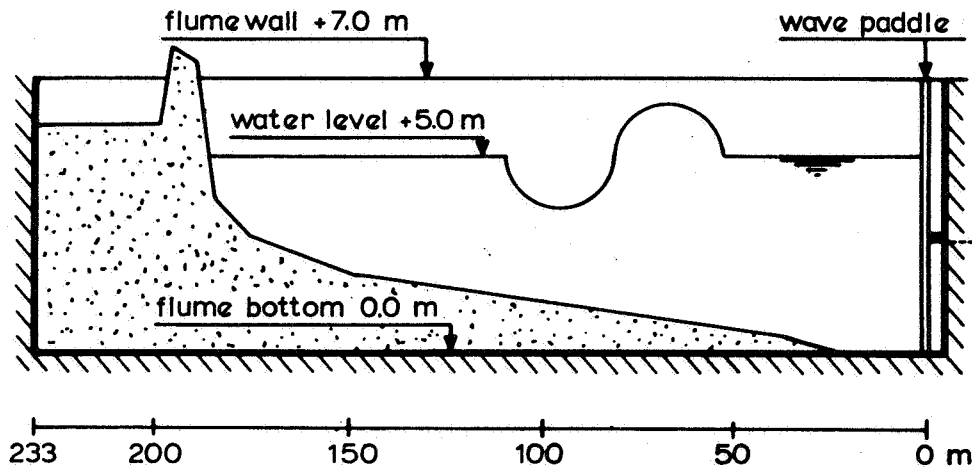


**Figure 60**  Section of large scale facility, the Delta flume

## 5.2  Verification of scale relations

The prototype conditions described in 4.1 were reproduced in tests 1 and 2. Relatively steep initial profiles with Sf = 3.0 and 2.0 respectively were applied as the length of the flume is the limiting factor. Sand from the field with $D_{50}$ = 225 μm was used as a bed material. The hydraulic conditions were reproduced with scale factors

$$n_H = n_L = n_T^2 = 5 \tag{127}$$

The water temperature during the tests varied between 6° and 9° Centigrade. The duration of the tests was 10 hrs at model scale. The waves were stopped for profile recording at t = 0.1 hrs, 0.3 hrs, 1.0 hrs, 3 hrs, 6 hrs and 10 hrs after start. The profiles were recorded by echo sounding in three parallel rays along the flume. The profile recordings are shown in Figures 61 and 62 for test 1 and in Figures 63 and 64 for test 2.
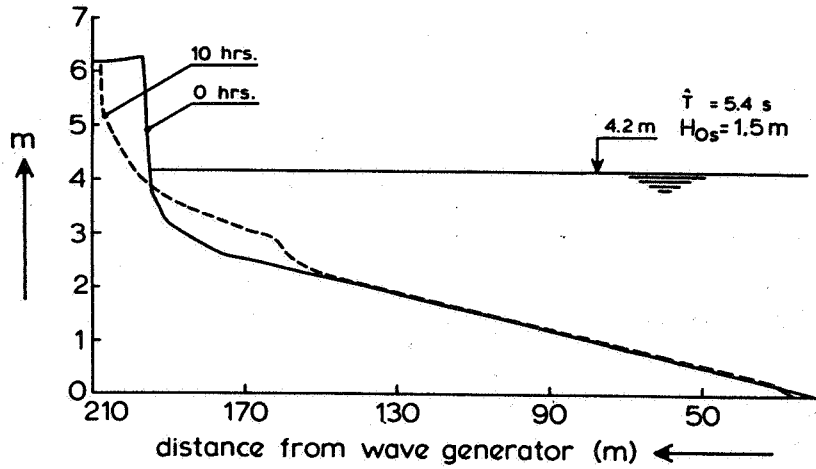
**Figure 61** Hydraulic conditions and profile development test 1
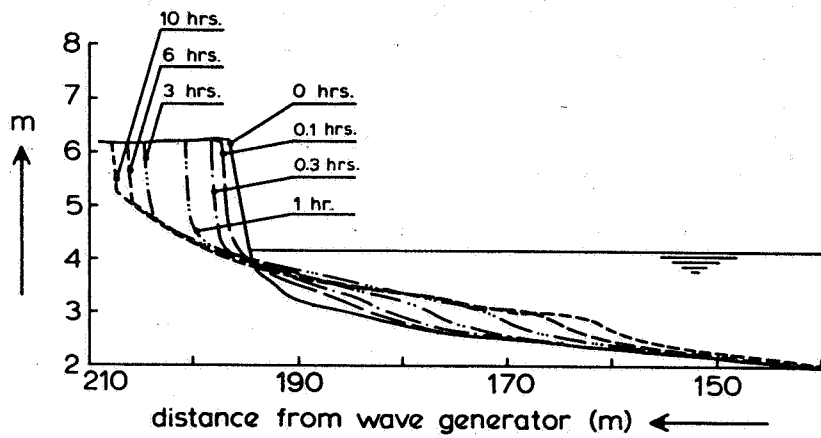


**Figure 62** Profile development test 1, detail
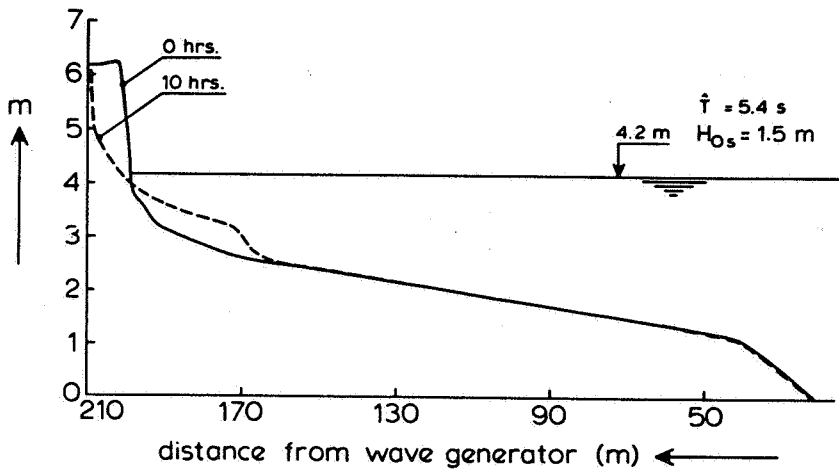


**Figure 63** Hydraulic conditions and profile development test 2
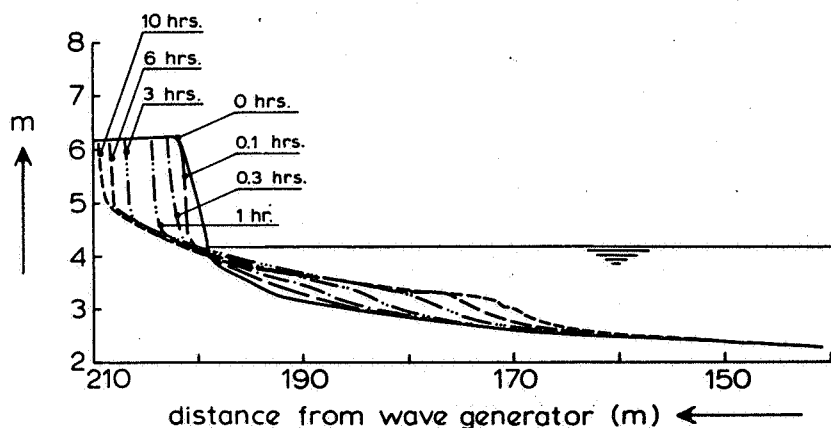
**Figure 64** Profile development test 2, detail

## Erosion quantities

The erosion quantity above storm surge level was derived from the profile recordings. The cumulative quantity is shown in table 16.

| time after start of test | erosion quantity above storm surge level, model | |
|---|---|---|
| | test 1, Sf = 3 (model) | test 2, Sf = 2 (model) |
| hours (model) | $m^3/m^1$ | $m^3/m^1$ |
| 0.1 | 2.64 | 1.76 |
| 0.3 | 4.71 | 3.92 |
| 1.0 | 9.42 | 7.08 |
| 3.0 | 15.76 | 11.07 |
| 6.0 | 17.77 | 13.25 |
| 10.0 | 19.22 | 14.77 |

**Table 16** Cumulative erosion quantity above storm surge level, large scale tests 1 and 2

The recorded profiles were converted to prototype using the scale relations:

$$n_d = 5$$

$$n_1 = n_d^{1.28} = 5^{1.28} = 7.85 \tag{124}$$

$$n_t = n_d^{0.5} = 5^{0.5} = 2.24 \tag{125}$$

$$n_A = n_1 \cdot n_d = n_d^{2.28} = 39.23 \tag{136}$$

The cumulative erosion quantity for prototype is shown in Table 17.

| time after start of test | erosion above storm surge level, prototype | |
|---|---|---|
| | test 1, Sf = 1.91 (prot.) | test 2, Sf = 1.27 (prot.) |
| hours (prototype) | $m^3/m^1$ | $m^3/m^1$ |
| 0.224 | 103.6 | 69.0 |
| 0.671 | 184.7 | 153.8 |
| 2.236 | 369.6 | 277.7 |
| 6.708 | 618.3 | 434.3 |
| 13.416 | 697.1 | 519.8 |
| 22.361 | 774.0 | 579.4 |

**Table 17** Cumulative erosion quantity above storm surge level after conversion to prototype, large-scale tests 1 and 2

As a first check of the scale relations, the prototype erosion results were plotted together with the small-scale test data in Figures 65, 66 and 67. for t = 2 hrs, 5 hrs and 10 hrs after start. The results of the large-scale tests agree very well with the results of the small scale tests. This does not automatically imply that no other combinations of α and β could give an equally good agreement. To check this, a correlation analysis of erosion quantities was carried out for a range of α and β combinations, as described in 4.6, but considering only the tests with sand having $D_{50}$ = 225 μm. This gives the most direct verification of α and β. The number of tests with scale factors $n_d$ = 84, $n_d$ = 47 and $n_d$ = 26 is much larger than the number of tests with $n_d$ = 5. Also the range of initial profiles that was tested is much larger. For this reason the small scale tests are represented by two tests per depth scale factor, with initial prototype profile steepness Sf = 1 and Sf = 2. The results of the correlation analysis are shown in Table 18.

The results illustrate that the optimal combination of α and β is slightly dependent on the phase of the process. At t = 2 hrs the highest correlation coefficients are found for β = 0.25 with α = 0.24 to 0.26. At t = 5 hrs the combination of β = 0.5 with α = 0.28 to 0.30 gives the highest score. At t = 10 hrs the combination of β = 0.75 with α = 0.32 to 0.34 gives the highest correlation coeficients. This dependency means that not all the scale effects are covered by the scale relations. However, the scale dependency is relatively small. Considering the overall result an average value can be found of α = 0.28 to 0.30 with β = 0.5. This agrees very well with the earlier results of the small-scale tests. So regarding the erosion quantities it can be concluded that the scale relations determined earlier are confirmed by the large scale tests.
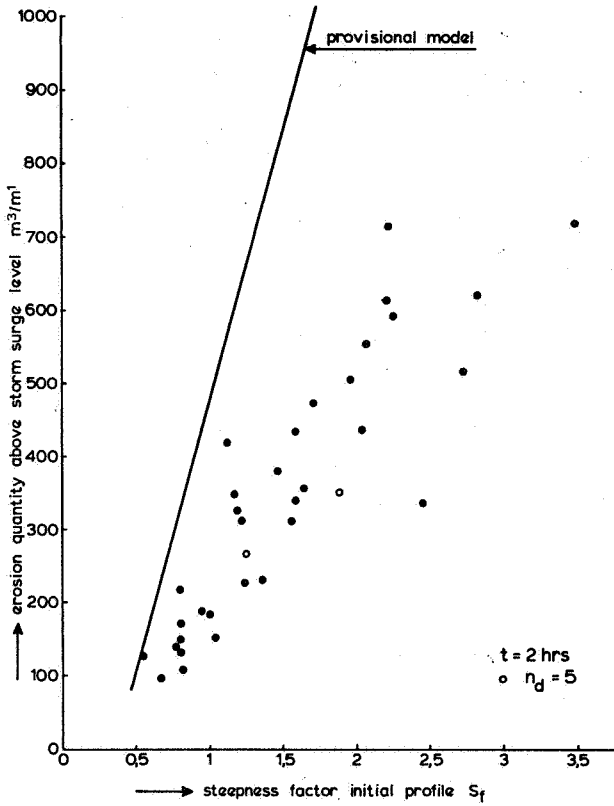
**Fig. 65** Erosion quantity as a function of initial profile, small scale and large scale test data, t = 2 hrs, prototype
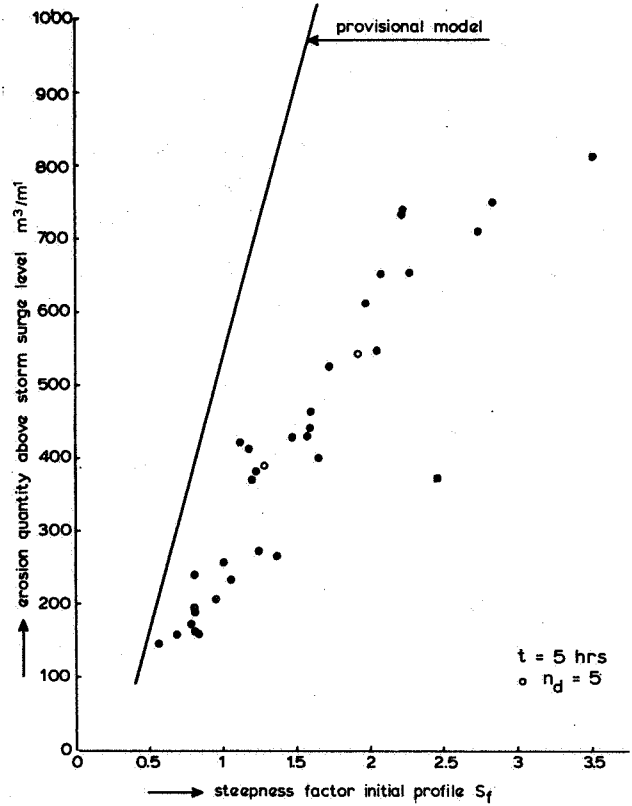


**Fig. 66** Erosion quantity as a function of initial profile, small scale and large scale test date, t = 5 hrs, prototype
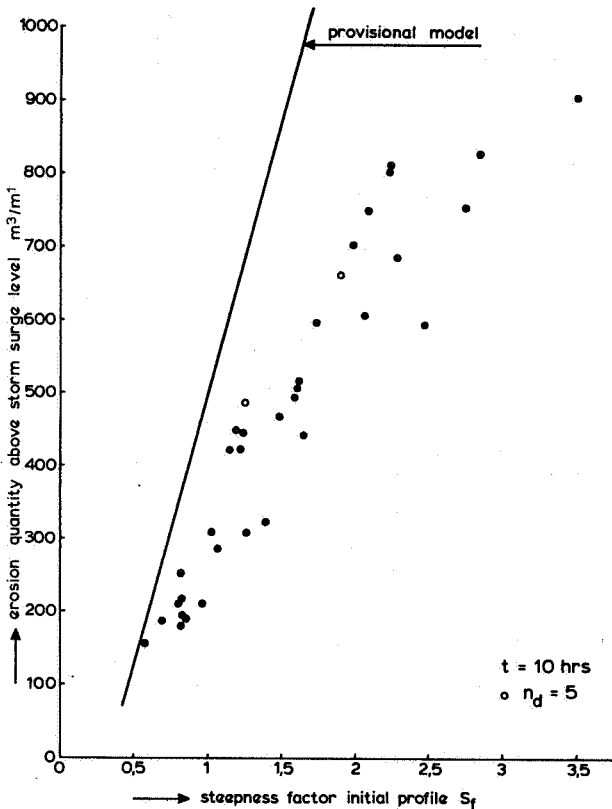


**Fig. 67** Erosion quantity as a function of initial profile, small scale and large scale test data, t = 10 hrs, prototype

| β \ α | .20 | .22 | .24 | .26 | .28 | .30 | .32 | .34 | .36 |
|---|---|---|---|---|---|---|---|---|---|
| **t = 2 hrs** | | | | | | | | | |
| -0.50 | 0.9078 | 0.9435 | 0.9538 | 0.9548 | 0.9391 | 0.9132 | 0.8629 | 0.8472 | 0.8123 |
| -0.25 | 0.8384 | 0.8837 | 0.9178 | 0.9388 | 0.9145 | 0.9372 | 0.9211 | 0.8907 | 0.8389 |
| 0.00 | 0.8810 | 0.9215 | 0.9471 | 0.9567 | 0.9508 | 0.9329 | 0.9053 | 0.8731 | 0.8283 |
| 0.25 | 0.9115 | 0.9438 | 0.9648 | 0.9631 | 0.9452 | 0.9166 | 0.8606 | 0.8414 | 0.7854 |
| 0.50 | 0.9261 | 0.9531 | 0.9595 | 0.9472 | 0.9222 | 0.8901 | 0.8526 | 0.8147 | 0.7766 |
| 0.75 | 0.9475 | 0.9509 | 0.9345 | 0.9040 | 0.8689 | 0.8303 | 0.7909 | 0.7542 | 0.7178 |
| 1.00 | 0.9388 | 0.9110 | 0.8697 | 0.8179 | 0.7693 | 0.7196 | 0.6775 | 0.6393 | 0.6043 |
| **t = 5 hrs** | | | | | | | | | |
| -0.50 | 0.8841 | 0.8968 | 0.8914 | 0.8706 | 0.8395 | 0.8058 | 0.7699 | 0.7363 | 0.7035 |
| -0.25 | 0.8397 | 0.8945 | 0.9365 | 0.9637 | 0.9692 | 0.9568 | 0.9300 | 0.8953 | 0.8569 |
| 0.00 | 0.7805 | 0.8357 | 0.8819 | 0.9167 | 0.9369 | 0.9413 | 0.9322 | 0.9119 | 0.8847 |
| 0.25 | 0.7630 | 0.8134 | 0.8576 | 0.8939 | 0.9191 | 0.9275 | 0.9264 | 0.9134 | 0.8927 |
| 0.50 | 0.8134 | 0.8733 | 0.9231 | 0.9599 | 0.9782 | 0.9786 | 0.9630 | 0.9353 | 0.9006 |
| 0.75 | 0.8378 | 0.8953 | 0.9390 | 0.9697 | 0.9778 | 0.9684 | 0.9450 | 0.9111 | 0.8714 |
| 1.00 | 0.8788 | 0.9276 | 0.9598 | 0.9688 | 0.9570 | 0.9313 | 0.8908 | 0.8379 | 0.8047 |
| **t = 10 hrs** | | | | | | | | | |
| -0.50 | 0.6007 | 0.6048 | 0.6045 | 0.5984 | 0.5902 | 0.5858 | 0.5652 | 0.5540 | 0.5415 |
| -0.25 | 0.8582 | 0.9062 | 0.9404 | 0.9501 | 0.9413 | 0.9180 | 0.8847 | 0.8473 | 0.8084 |
| 0.00 | 0.7584 | 0.8180 | 0.8660 | 0.9026 | 0.9306 | 0.9401 | 0.9176 | 0.8968 | 0.8691 |
| 0.25 | 0.7323 | 0.7945 | 0.8478 | 0.8935 | 0.9208 | 0.9415 | 0.9414 | 0.9270 | 0.9029 |
| 0.50 | 0.7456 | 0.8065 | 0.8638 | 0.9173 | 0.9531 | 0.9763 | 0.9731 | 0.9576 | 0.9301 |
| 0.75 | 0.7281 | 0.7872 | 0.8498 | 0.9071 | 0.9495 | 0.9782 | 0.9894 | 0.9819 | 0.9591 |
| 1.00 | 0.6202 | 0.6821 | 0.7459 | 0.8141 | 0.8733 | 0.9364 | 0.9612 | 0.9783 | 0.9744 |

**Table 18** Results of correlation analysis of erosion quantities of tests with $n_d = 84$, $n_d = 47$, $n_d = 26$ and $n_d = 5$ with sand having $D_{50} = 225$ µm, two tests per depth scale factor.

## Erosion profiles

Another way to verify the scale relations is to compare the erosion profiles. The erosion profiles of the tests with various scale factors are compared for t = 5 hrs prototype in Figure 68. Tests with $D_{50} = 225$ µm and equal or nearly equal initial profile steepness have been considered. The conversion was carried out with $\beta = 0.5$ and $\alpha = 0.28$.
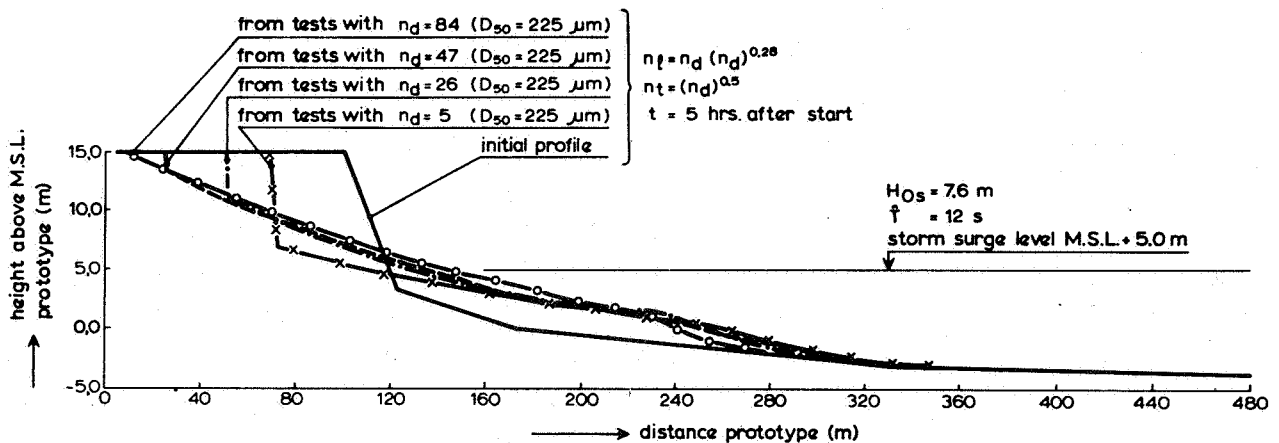


**Figure 68** Erosion profiles converted to prototype, $\alpha = 0.28$, $\beta = 0.5$, t = 5 hrs

The erosion quantities above storm surge level of the tests shown in Figure 68 are equal or nearly equal as was shown in the preceding pages. However, the shape of the erosion profile especially the part above the water level shows a systematic dependence on the scale factor. The systematic dependance above storm surge level must be due to the scale effects in wave run up. Now the effects of not properly scaling the surf similarity parameter are demonstrated. Battjes (1974) has shown that the wave run up can be described by

$$R_v = 0.7 \; \hat{T} \; \sqrt{g \; H_s} \; \tan \theta \qquad\qquad (127)$$

in which:

| | | |
|---|---|---|
| $R_v$ | is the wave run-up vertically measured in m above still water level, surpassed by 2% of the waves | (m) |
| $\hat{T}$ | is the peak wave period of the spectrum | (s) |
| $g$ | is the acceleration due to gravity | $(m/s^2)$ |
| $H_s$ | is the significant wave height | (m) |
| $\tan\theta$ | is the slope of the dike | (-) |

This formula is derived from small scale model tests with slopes ranging from 1:1.5 up to 1:8. The formula has not been tested for composite slopes or for beaches. Still the formula gives a basic indication of the parameters affecting the wave run-up. The scale factor for run-up can be derived from (127) as follows:

$$n_{R_v} = n \; (\hat{T}) \; n(H_s)^{\frac{1}{2}} \; n(\tan\theta) \qquad \text{yielding} \qquad (128)$$

$$n_{R_v} = n_d^{0.5} \; n_d^{0.5} \; n_d/n_1 \qquad \text{yielding} \qquad (129)$$

$$n_{R_v} = n_d^2/n_d^{1.28} = n_d^{0.72} \qquad\qquad (130)$$

Relation (130) indicates that the wave run-up in small scale models with prototype size sediment is a factor $n_d^{(1-0.72)} = n_d^{0.28}$ too large. The waves in the model reach a higher level than in prototype. This may well be the reason why the erosion profile above the still water level shows a strong scale dependency. For a proper reproduction of the erosion profile including the run up zone, undistorted models should be preferend. The small scale tests described in Chapter 4 showed that undistorted beach profile modelling is possible when the value of the dimensionless fall velocity parameter (H/Tw) in the model is equal to the value in prototype. This can be verified by comparing small-scale and large-scale test results.

## Dimensionless fall velocity parameter H/Tw

After the large scale tests a series of small scale tests was carried out to investigate the effect of a number of parameters on dune erosion (see the research programme in Table 1). The small-scale tests have been carried out with depth scale factor $n_d$ = 30 using sand with a $D_{50}$ = 95 μm. The results of these tests were reported by the Delft Hydraulics Laboratory (1982). The prototype conditions of small-scale test number 14 correspond to the prototype conditions of large scale test 2. The H/Tw-values and the corresponding distortions of the two tests are virtually equal, see Table 19. The erosion profile development for the two tests after conversion to prototype is shown in Figure 69. The agreement is much better than the results of Figure 68, where tests with prototype size sand have been compared. On the basis of these results, it is concluded that dune erosion can be very well reproduced in undistorted small-scale models, when the hydraulic conditions are reproduced according to the Froude scale relations, and the sediment size is chosen such, that the fall velocity has the same scale factor as the orbital velocity.

| | depth scale factor | wave height | wave period | fall velocity | fall velocity parameter | length scale factor |
|---|---|---|---|---|---|---|
| | $n_d$ (-) | $H_{Os}$ (m) | $\hat{T}$ (s) | w m/s | H/Tw (-) | $n_l$ (-) |
| test 2 | 5 | 1.52 | 5.37 | 0.0268 | 10.56 | 7.52 |
| test 14 | 30 | 0.253 | 2.19 | 0.0083 | 13.92 | 40.33 |

**Table 19** Test conditions large scale test 2 and small scale test 14
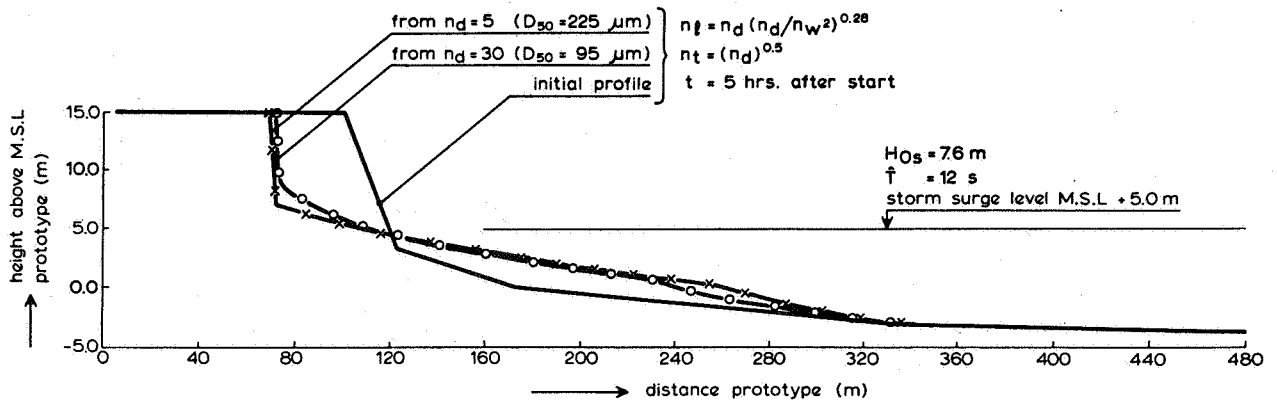


**Figure 69** Erosion profile development, large scale test 2 and small scale test 14

## 5.3 The effect of naturally varying water level and wave conditions

The model tests so far were carried out with a constant water level and with constant wave conditions. This idealization was necessary to determine the scale relations in an efficient way. At the present stage it is possible to investigate the effect of naturally varying water level and wave conditions. With this aim a third large scale test was carried out. The initial profile of test number 2 was tested again but now with a natural storm surge hydrograph and naturally varying wave height and wave period. The water level and the wave conditions are shown in Figure 70. Figure 71 gives the erosion profile development as recorded in the model. The cumulative erosion quantity above storm surge level is shown in Figure 72, together with the result of the test with constant hydraulic conditions. The erosion profile development of the two tests is shown in Figure 73.

On the basis of the results it is concluded that a period of about 5 hours with constant hydraulic conditions is equivalent to a naturally varying storm surge hydrograph. Naturally this result is only valid for the present North Sea storm surge hydrograph. Cyclone type storm surges with a different hydrograph may have a different equivalent period of time.
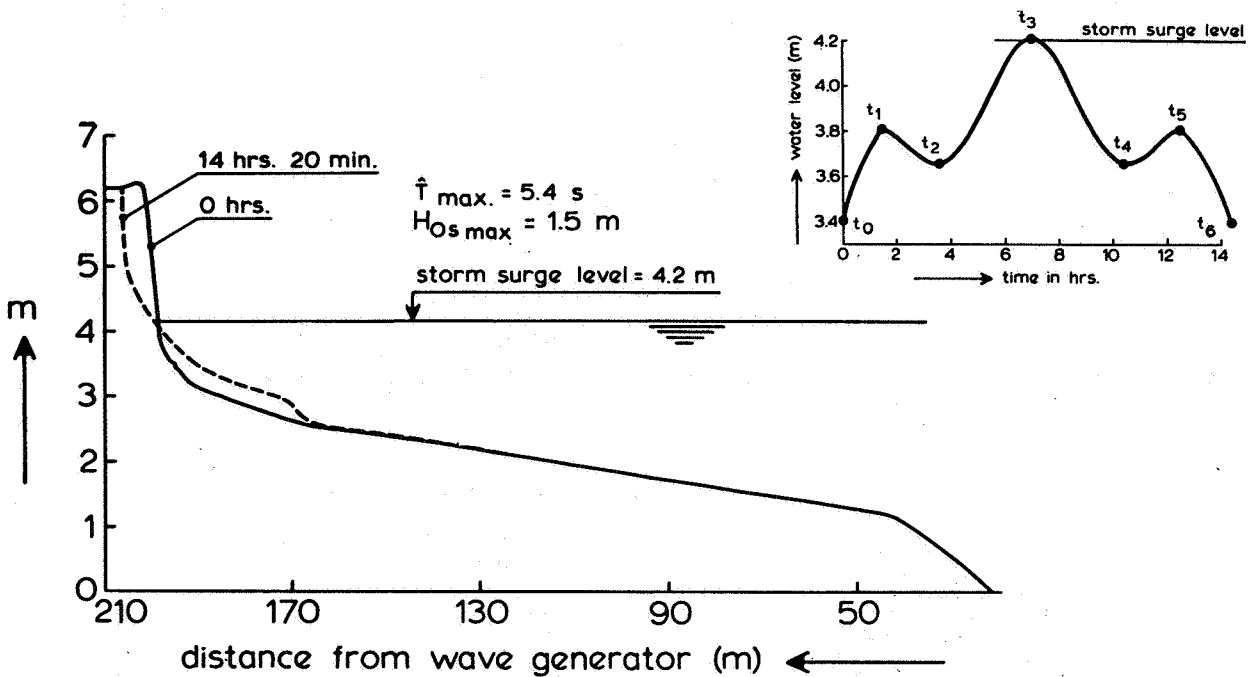


**Figure 70** Hydraulic conditions and profile development, test 3
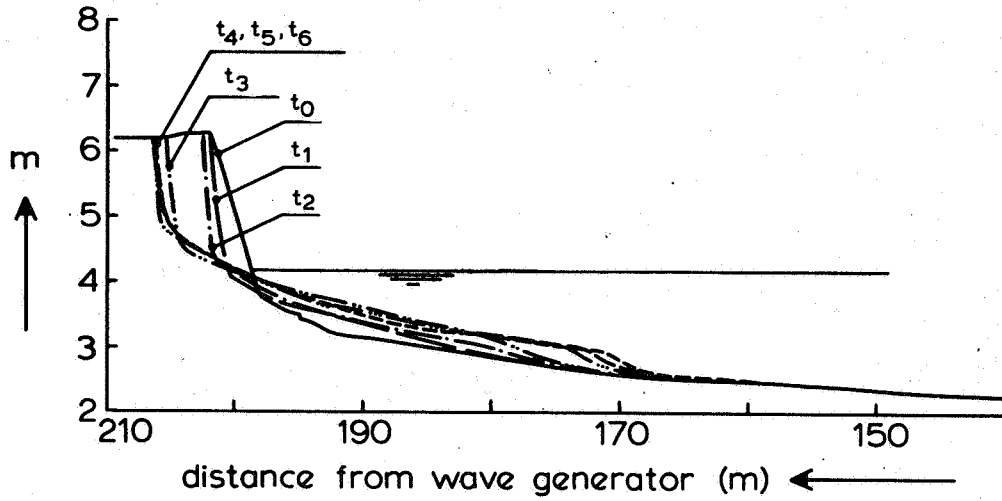
**Figure 71** Profile development test 3, detail



identical initial profiles (large scale tests 2 and 3)
——— constant water level M.S.L. +5.0 m, $H_{os}$ = 7.6 m
— — North Sea hydrograph maximum: M.S.L. +5.0 m, H = 7.6 m
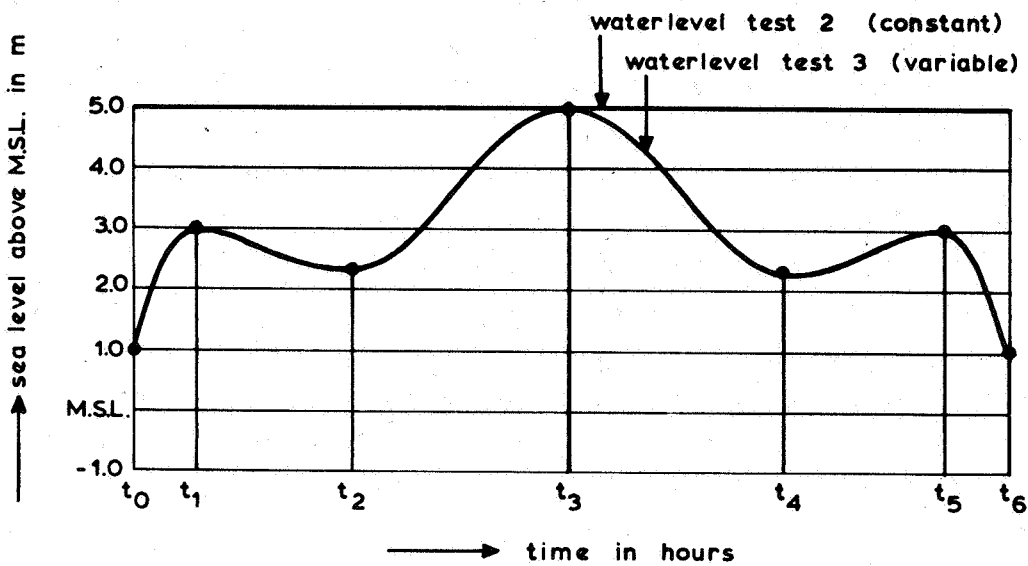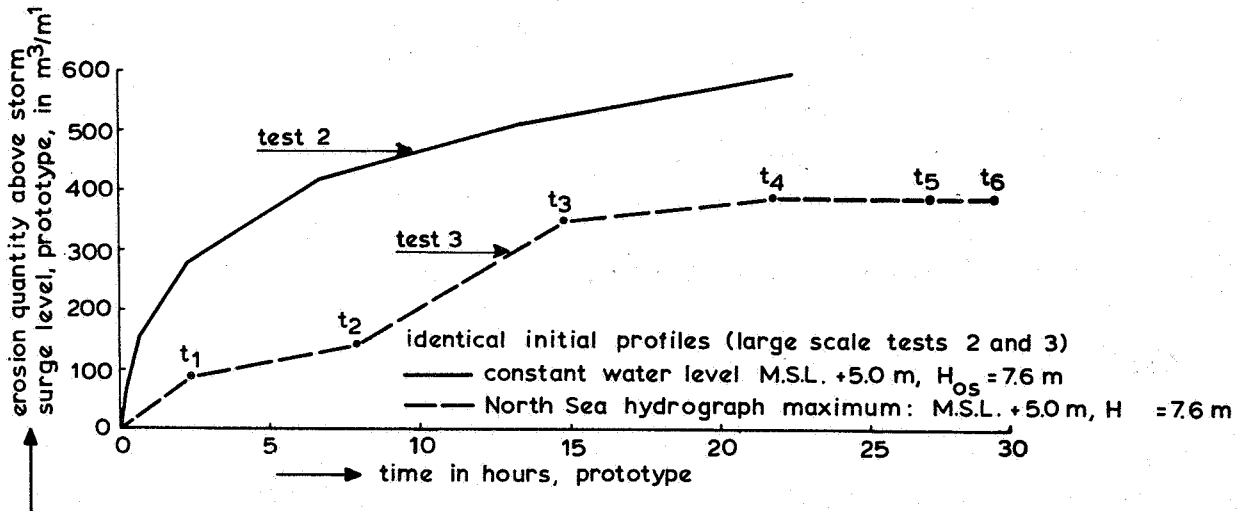


**Figure 72** Cumulative erosion quantity as of function of time, test 2 and 3
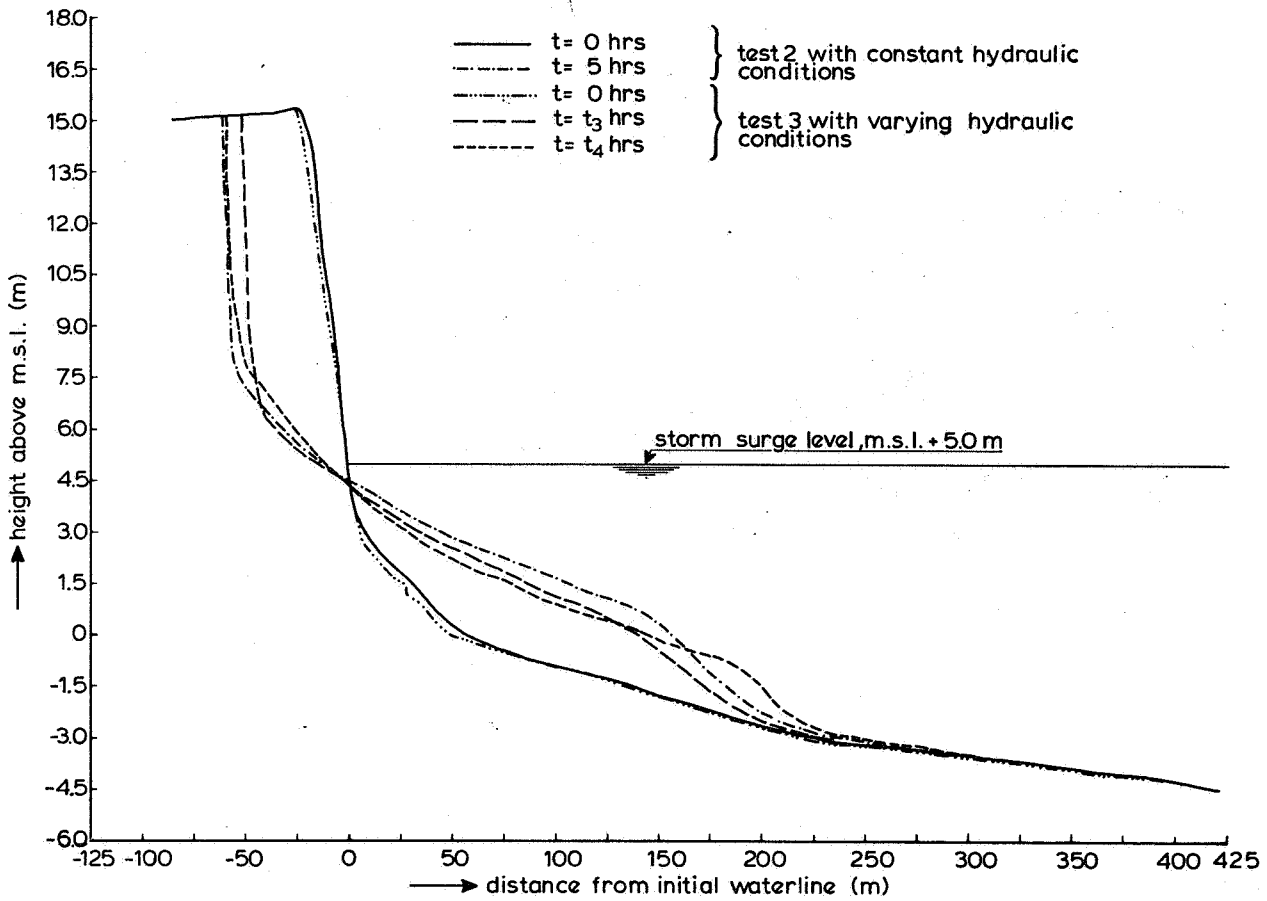
**Figure 73** Profile development, test 2 and test 3, prototype

## 5.4 Comparison with field data

The major aim of the large scale-tests is to verify the scale relations. Next to an internal verification (between tests with different scales), an external verification (comparison with field data) is also essential to asses the reliability of the model. External verification however, is difficult, as very few field data on dune erosion are available. The largest dune erosion quantity in recent history was recorded after the 1953 storm surge (see Figure 76). The erosion quantities were derived from the recordings of dune front recessions along a 17 km long reach between The Hague and Rotterdam, a few days after the storm. The time period between the pre-storm recording and the storm surge is 3 to 6 months. The scatter in the erosion quantities of Figure 76 is rather large. This is probably caused by the natural changes in the period between the profile recording and the storm surge and by the conversion of dune foot recessions to erosion quantities. As better data are not available it has been decided to reproduce the 1953 storm surge, accepting the uncertainties in the field data.

The water-level during the 1953 storm surge is well known from tide gauges in

nearby harbours. Wave height observations from the "light vessel" Goerree indicate a significant wave height $H_s$ = 4.5 m. (Delft Hydraulics Laboratory and Technical Committee on Water Retaining Structures, 1971). The wave observations, however, are not considered fully reliable. A wave hindcast study on the basis of meteorological data has led to a maximum height $H_s$ = 6.0 m (Sanders, de Voogt and Bruinsman). The latter result including the computed variation with time has been applied for the model test. Storm surge conditions and the reconstructed initial profile have been reproduced in the model with the following scale factors:

$$n_d = 3.27; \quad n_l = (n_d)^{1.28} = 4.56; \quad n_t = (n_d)^{0.5} = 1.81. \qquad (131)$$

The grain size is characterized by $D_{50}$ = 225 μm, as in the other large scale tests. The initial profile and the measured development of the erosion profile during the storm surge are shown in Figure 74 and Figure 75. The erosion quantity has been converted to prototype with $n_A = n_d \, n_l$ = 14.9. The final erosion quantity is shown in Figure 76 together with the field data. The agreement is rather good.

A small number of beach profiles were recorded a few weeks after the 1953 storm surge in the north of The Netherlands close to Den Helder. The field data together with the model profiles are shown in Figure 77. The model profiles have been converted to prototype with the scale relations mentioned above. The agreement between model and field is reasonably good.
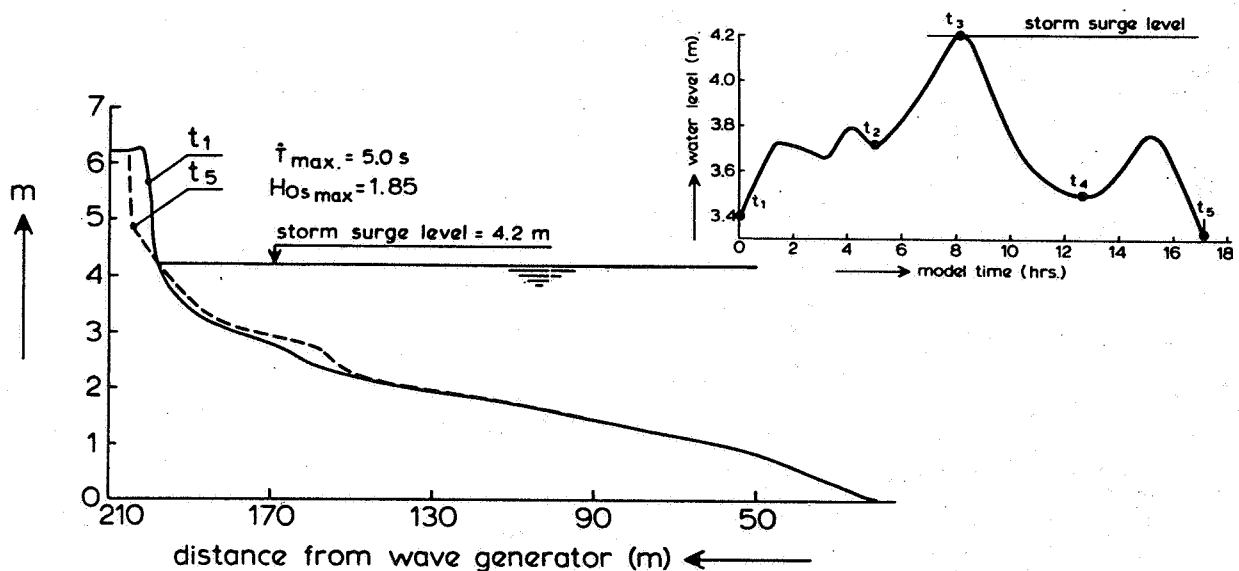


**Figure 74** Hydraulic conditions and erosion profile development, test 4
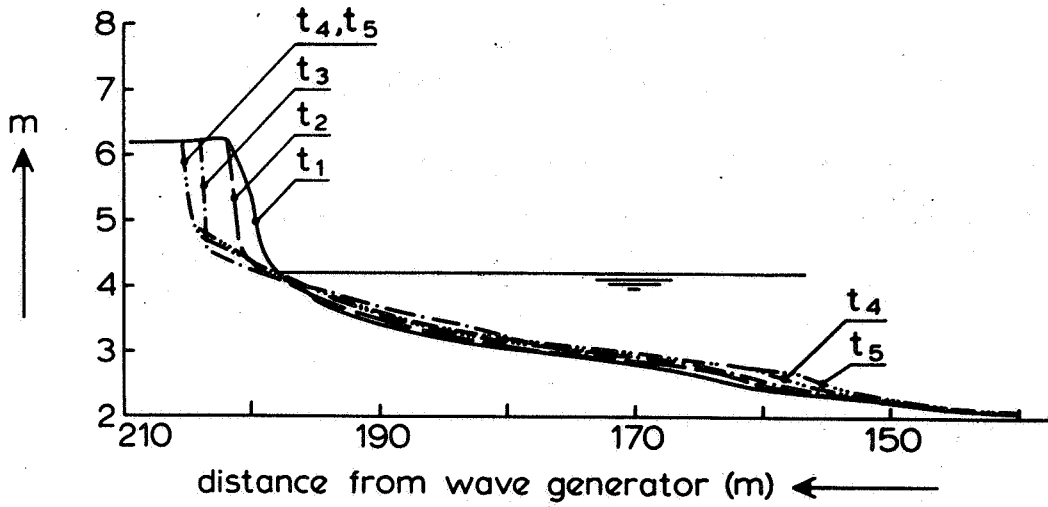
**Figure 75** Profile development test 4, detail
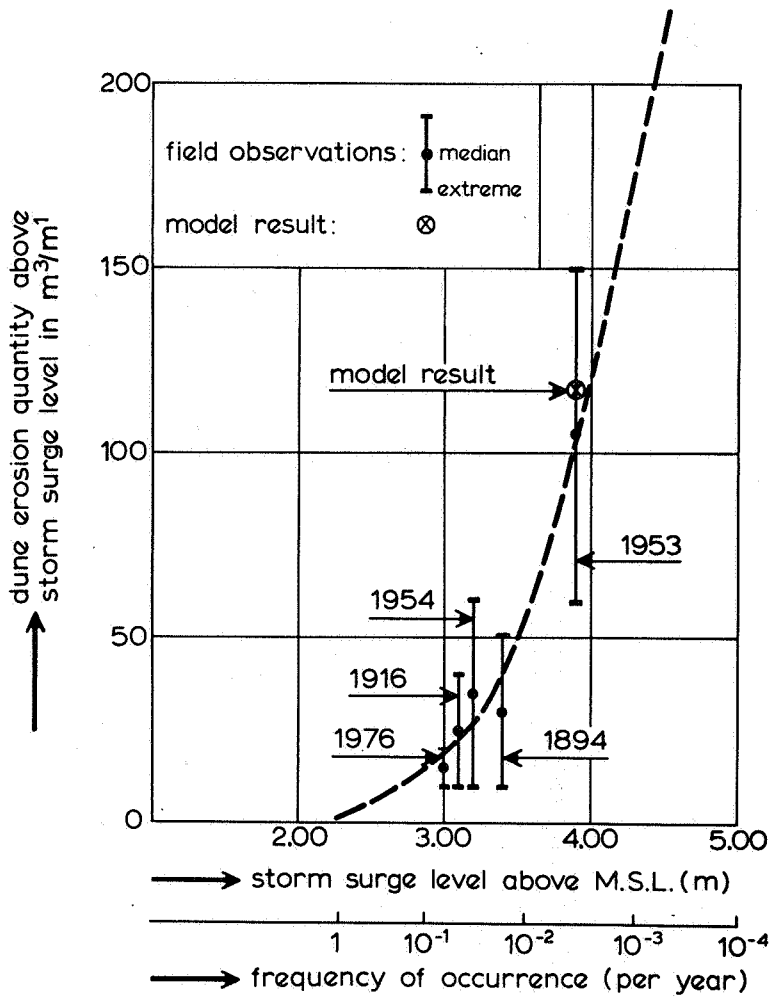


**Figure 76** Erosion quantity, model result and field data
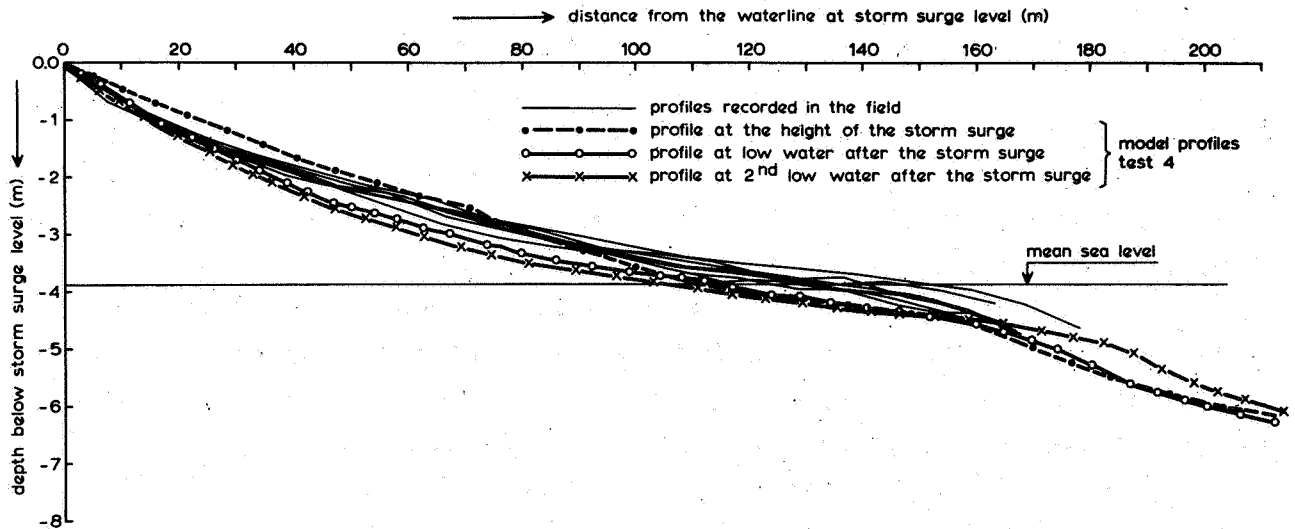
**Figure 77**  Erosion profiles model and field, 1953 storm surge

## 5.5  Full scale test

An additional test carried out in the large-scale testing facility aimed at a "full scale" reproduction of the conditions in situ. The wave height in the "model" $H_s$ = 2 m, the wave period $\hat{T}$ = 7.6 s, the dune height above storm surge level is 4 m, the water level is kept constant at 5.0 m above the bottom of the flume. The development of the erosion profile is shown in Figure 78. The erosion quantity above storm surge level measured in the model is 50 $m^3/m^1$ after 6 hours of testing.
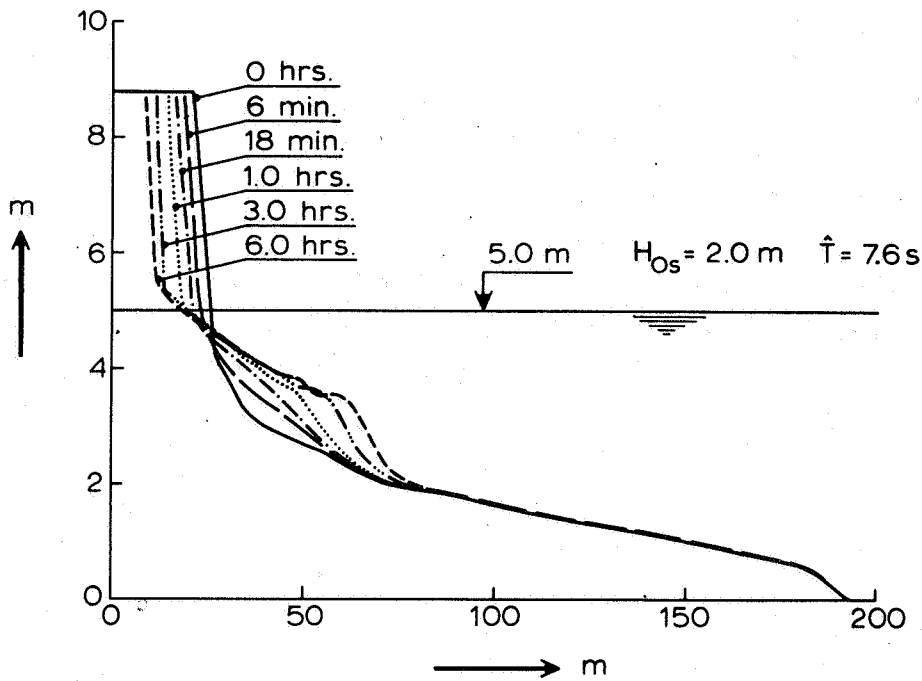


**Figure 78**  Hydraulic conditions and profile development, test 5

## 5.6 Illustration of the validity of the scale relations

An additional large-scale test was carried out with depth scale factor $n_d = 2$, to check the safety of a critical beach and dune profile at Schouwen in the south of The Netherlands (Delft Hydraulics Laboratory, 1982). This test was repeated in a small scale facility with depth scale factor $n_d = 15$. The value of the dimensionless fall velocity parameter is nearly equal for the two tests. A naturally varying water level and naturally varying wave conditions were applied for both tests. The relation between the two tests can be described by considering the large-scale tests as a prototype version of the small-scale test. In this case the scale relations are as follows:

$$n_d = n_H = n_T^2 = n_t^2 = 7.5 \tag{132}$$

$$n_w = 0.027/0.009 = 3.0 \tag{132}$$

$$n_1 = n_d \, (n_d/n_w^2)^{0.28} = 7.13 \tag{134}$$

$$n_1/n_d = 7.13/7.5 = 0.95 \tag{135}$$

The hydraulic conditions and the erosion profile development are shown in Figure 79. The results show that the large-scale and the small-scale profile development are very similar, for the peak of the storm surge, as well as for the lower water level conditions just before and after the surge. The most stringent verification of scale relations is the comparison of the time-dependent profile evolution for a small-scale and a large-scale test. The results of Figure 79 show the present scale relations have satisfied this verification test very well.

On the basis of the preceding results and the additional verification of the H/Tw parameter it is concluded that the scale relations and the related prototype data are a solid basis for the development of a dune erosion prediction model.
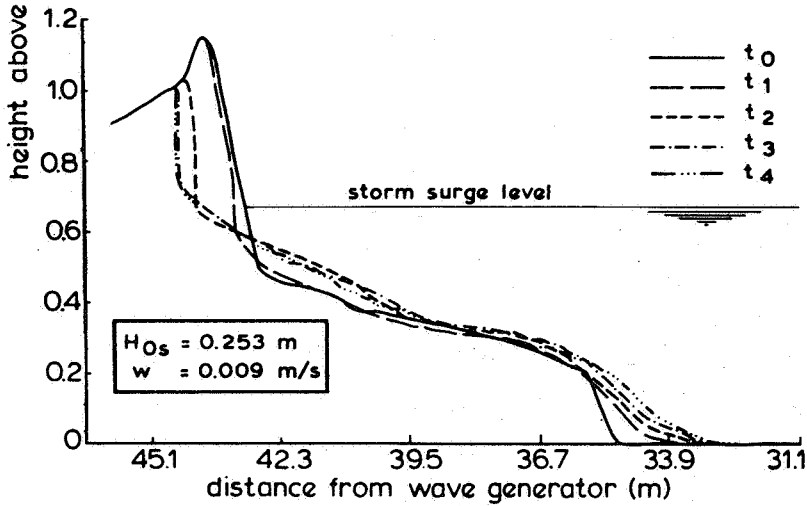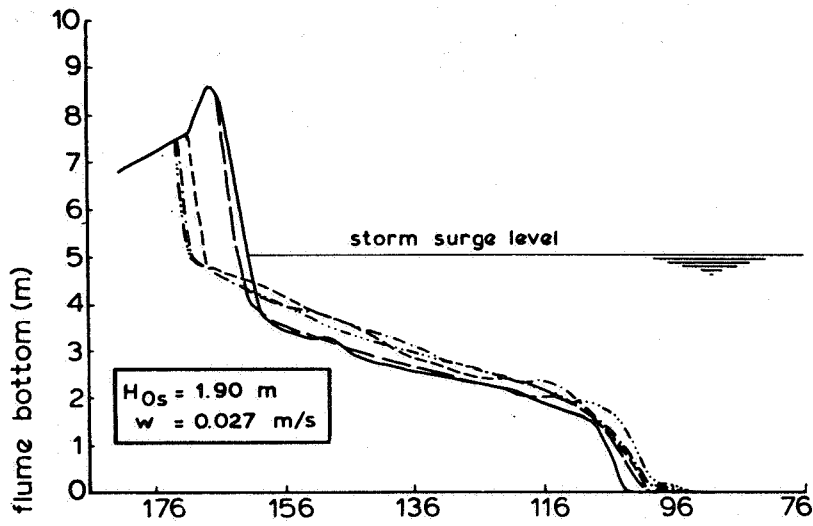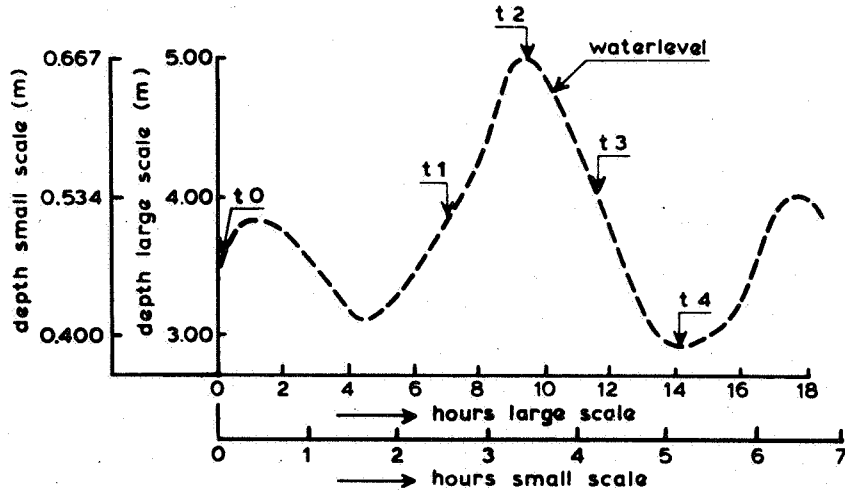
**Figure 79** Hydraulic conditions and profile development, large scale and small scale test

## 6. Development and verification of a dune erosion prediction model

### 6.1 Introduction

A provisional model for the prediction of dune erosion as developed by van de Graaff, was presented by the Technical Advisory Committee on Water Retaining Structures in 1971. The model was internationally published by Van de Graaff (1977). The prediction model was mainly based on field observations of the 1953 storm surge. A number of assumptions were made to obtain a well-defined computation method:

1) The beach profiles recorded after the 1953-storm surge are representative for beaches after storm surges with considerable dune erosion.

2) The eroded sand will be distributed over the zone of breaking waves and a typical erosion profile will develop up to a waterdepth $d = 1.28\ H_{sb}$ (in which d is the waterdepth below storm surge level and $H_{sb}$ is the wave height at breaking corresponding with $H_{0s}$, computed by linear wave theory and constant breaker index). Note that, the erosion profiles after the storm surge were measured over a length of about 90 m, whereas extrapolation up to nearly 700 m was required to cover the entire breaker zone for the design wave height $H_{0s} = 7.6$ m.

3) The level of the erosion profile is determined by the storm surge level.

4) The position of the erosion profile is defined by the conservation of sediment in a vertical plane perpendicular to the beach.

5) The form of the erosion profile is not affected by grain size, nor by wave height and wave period. The extent in seaward direction is only affected by wave height.

### Summary of results from laboratory and field investigations

The experimental investigations described in the previous chapters and additional field data indicate that the provisional model can be improved considerably. The points that are relevant for the development of a new model are summarized below.

1) A typical erosion profile will develop during a storm surge with dune erosion. The shape of the profile is independent of the initial profile. However, it is strongly dependent on the grain size. The seaward extent of the profile is determined by wave height and grain size.

2) A fully developed equilibrium profile will not be attained during a typical North Sea storm surge. The shape of the profile remains rather constant but the extent increases with time (see Figure 80).

3) The basic assumption of the provisional method concerning the distribution of the eroded sand over the entire breaker zone is rejected. The model tests demonstrate that during the storm surge a typical erosion profile develops which extends to a waterdepth of about 0.75 $H_{Os}$ below storm surge level (see Figure 80).

4) Three-dimensional model tests with a movable bed and random waves indicate that, given the wave height just outside the breaker zone, the angle of wave incidence has no significant effect on the erosion quantity.

5) The set-up of the model tests allows for the development of scale relations regarding length, depth and grain size. By means of these scale relations the erosion profile can be described in terms of wave height and fall velocity.

6) Considerable dune erosion was caused by the storm surge of January 3, 1976, when the sea level rose to 3.5 m above mean sea level. The field data from 58 coastal profiles, taken shortly after this storm surge have been analysed and the provisional prediction model has been evaluated. The principal conclusions are (Delft Hydraulics Laboratory, 1978)

   a) The provisional model over-estimates the erosion quantity by a factor 1.5 to 2 for average coastal profiles, and by a factor 2 to 10 for steep profiles.

   b) Examination of the 58 erosion profiles clearly shows a relation between grain size and profile steepness.
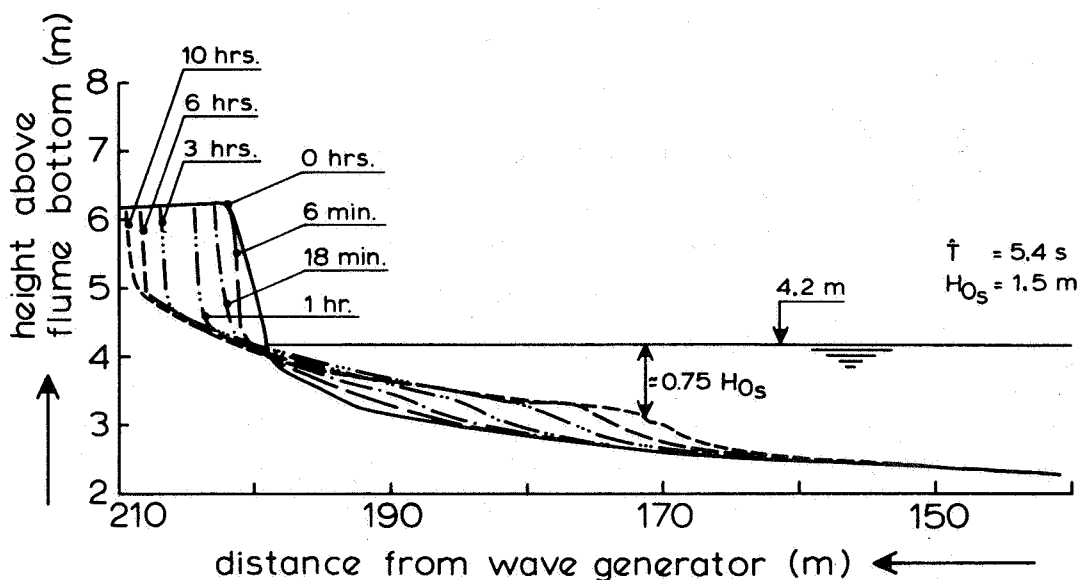


**Figure 80** Profile development, large scale test result

The results of the model and field investigations allow for the formulation of an improved dune erosion prediction model. In the development of such a model a number of successive steps can be distinguished, as indicated in Table 20. These steps will be described in the next sections.

| Development of a dune erosion prediction model | |
|---|---|
| step 1 | Assesment of a reference erosion profile on the basis of model tests with $H_{0s}$ = 7.6 m, $T$ = 12 s and $D_{50}$ = 225 µm . Determination of the seaward extent of the erosion profile. |
| step 2 | Introduction of grain size and wave height as independent parameters in the description of the erosion profile, on the basis of the scale relations. |
| step 3 | Verification of the prediction model by an additional series of small scale and large scale model tests. |
| step 4 | Verification of the prediction model by field observations of the 1953- and the 1976-storm surge. |
| step 5 | Assesment of the model accuracy. |
| step 6 | Applicability and limitations of the dune erosion prediction model. |

**Table 20** Scheme of development and verification of the dune erosion prediction model.

## 6.2 Reference erosion profile

The erosion profiles measured in the model were converted to prototype with the scale relations. The agreement is not fully satisfactory, as a distinct scale effect can be observed in the reproduction of the run up zone as shown in Figure 68. Since this scale effect is not described by the scale relations, a direct extrapolation of model profiles was carried out to determine the erosion profile for prototype. To avoid uncertainties with regard to the effect of the grain size only the tests with sand with $D_{50}$ = 225 µm were considered. First the position of the dune foot was determined, next the erosion profile was derived, as a best fit of model profiles.

Figure 68 shows that the position of the dune foot is clearly a function of the depth scale factor. For the dune foot positions shown in Fig. 68 various extrapolation methods have been applied to asses the level of the dune foot for prototype conditions. Values have been found ranging from 1.0 m below

storm surge level up to 1.0 m above storm surge level for the situation in prototype, 5 hrs after start. Values ranging from 0.5 m below up to 0.5 m above storm surge level were found in the field so far. On the basis of a careful analysis of model and field data the position of the dune foot to be applied in the dune erosion prediction model has been fixed at storm surge level, viz. the peak water level during the storm surge, just outside the zone of (depth) breaking waves (Delft Hydraulics Laboratory, 1982).

To determine the erosion profile, the model profiles have been converted to prototype with the scale relation $n_1 = n_d$. The profiles vertically averaged for all tests with equal scale factor are shown in Figure 81 for t = 5 hrs after start prototype. A distinct scale effect can now be observed as the distortion relation has not been applied. Hence, the steepness of the profile is a function of the depth scale factor.
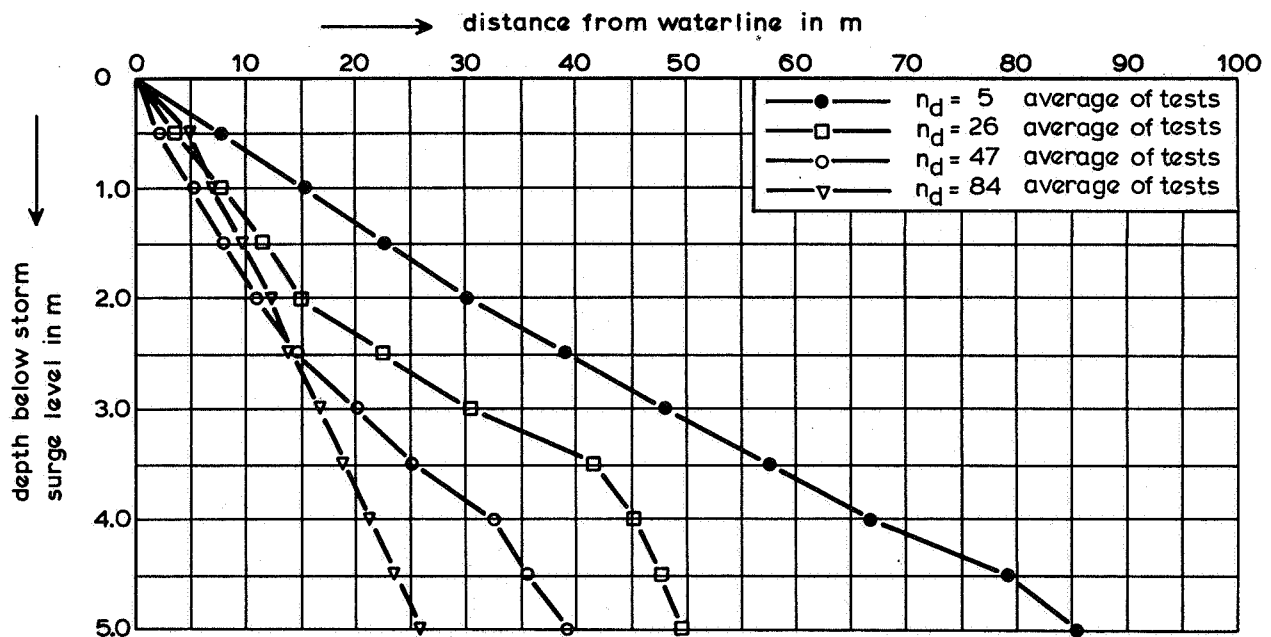


**Figure 81** Erosion profiles, prototype, $D_{50}$ = 225 μm via $n_1 = n_d$

The erosion profile for the 1:1 situation has been determined by extrapolation of the horizontal distance between the waterline and the various depth contours, see also 4.5. The extrapolation has been carried out along the "best fit" line: $\ell = \ell_1 n_d^{-\alpha}$ in which $\ell$ is the distance between the waterline and a certain depth contour for the profiles as shown in Figure 81, $n_d$ is the corresponding depth scale factor, $\ell_1$ is the distance between the waterline and this depth contour for prototype conditions (nd = 1) and α is the exponent in the distortion relation. The values for $\ell_1$ and α have been determined by curve-fitting. The results of the extrapolation for the various depth contours are shown in Figure 82. The profile below the 3.5 m depth contour deviates

slightly from the trend followed by the points above this level. Minor scale effects and random variations in the position and shape of the most seaward part of the erosion profiles are responsible for this. Finally, a regression analysis for the points from the waterline down to the 3.5 m depth contour leads to the following expression for the extrapolated profile:

$$y = 0.47 \ (x + 18)^{0.5} - 2.00 \qquad (\text{or: } x = 4.5 \ y^2 + 8 \ y) \qquad (136)$$

in which: $x = 0$, $y = 0$ represents the position of the dune foot; $x$ is the cross-shore horizontal co-ordinate (in m) and $y$ is the depth below storm surge level (in m). The profile is valid for storm surge conditions with $H_{Os} = 7.6$ m, $T = 12$ s and $D_{50} = 225$ µm, for $t = 5$ hrs after start with a constant water level at storm surge level.



— — — parabolic profile through curve fitting
x        result of extrapolation of profiles of figure 81
(x)      not taken into account with curve fitting
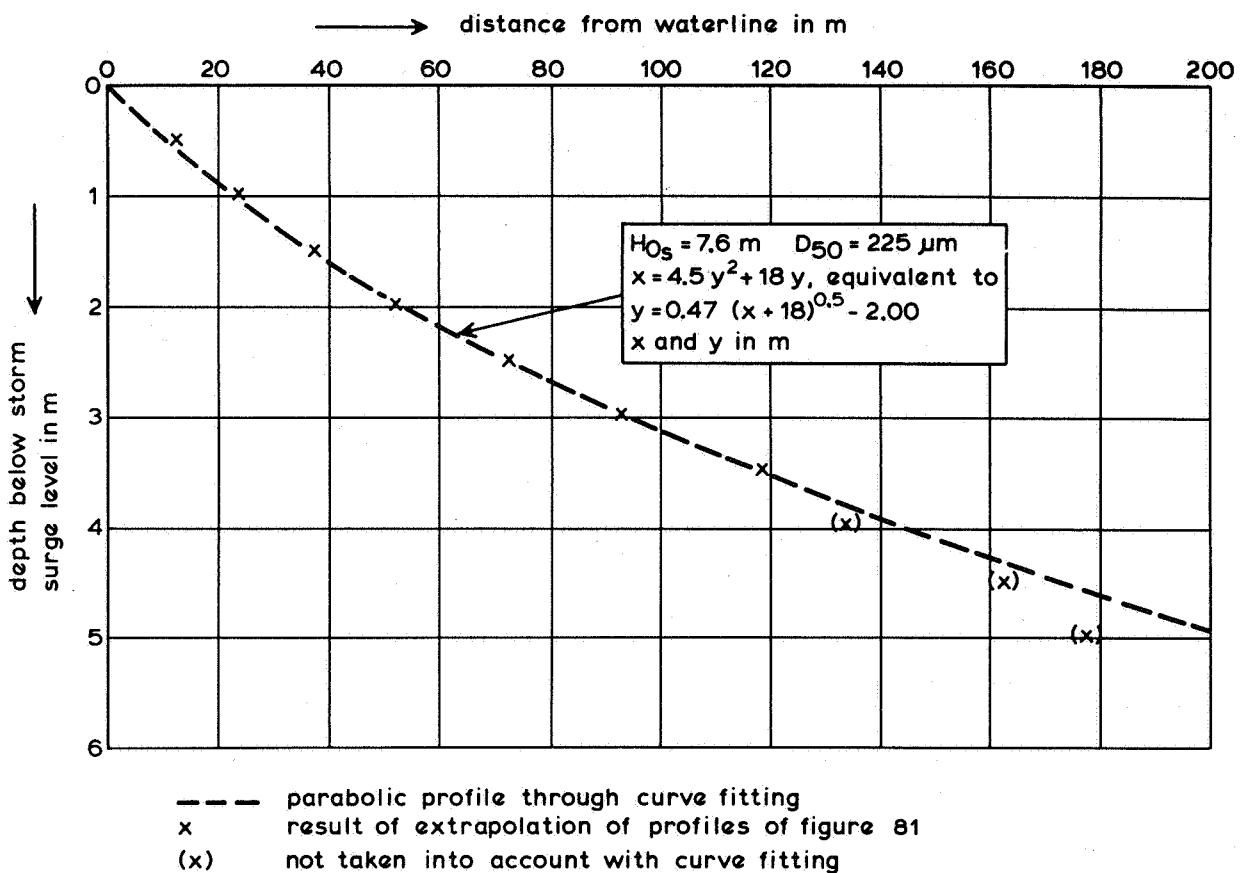
**Figure 82** Erosion profile prototype $D_{50} = 225$ µm, via extrapolation

## Recovery distance

The shape of the erosion profile, its extent in seaward direction and the recovery distance of the eroded sand are directly related.

A determination of the seaward extent of the erosion profile by extrapolation of the measured erosion profiles is rather inaccurate due to minor scale effects and random variations in the position and shape of the most seaward part of the erosion profile. The sediment balance is defined more accurately.

Therefore this parameter is used. The exact distance to be introduced in the prediction model has been determined by trial and error, aiming at an optimal agreement between measured an computed erosion quantities for the test series described in Chapter 4. The final erosion profile is shown in Figure 83. The parabola - shaped erosion profile extends from the dune front down to 5.72 m below storm surge level at a distance of 250 m from the dune front. The upward slope on the landward side is fixed at 1:1, based on field observations and the large-scale model tests. The downward slope on the seaward end is fixed at 1:12.5, based on an careful analysis and interpretation of small-scale and large-scale model data. The profile is valid for conditions with $H_{0s} = 7.6$ m, $\hat{T} = 12$ s and $D_{50} = 225$ µm
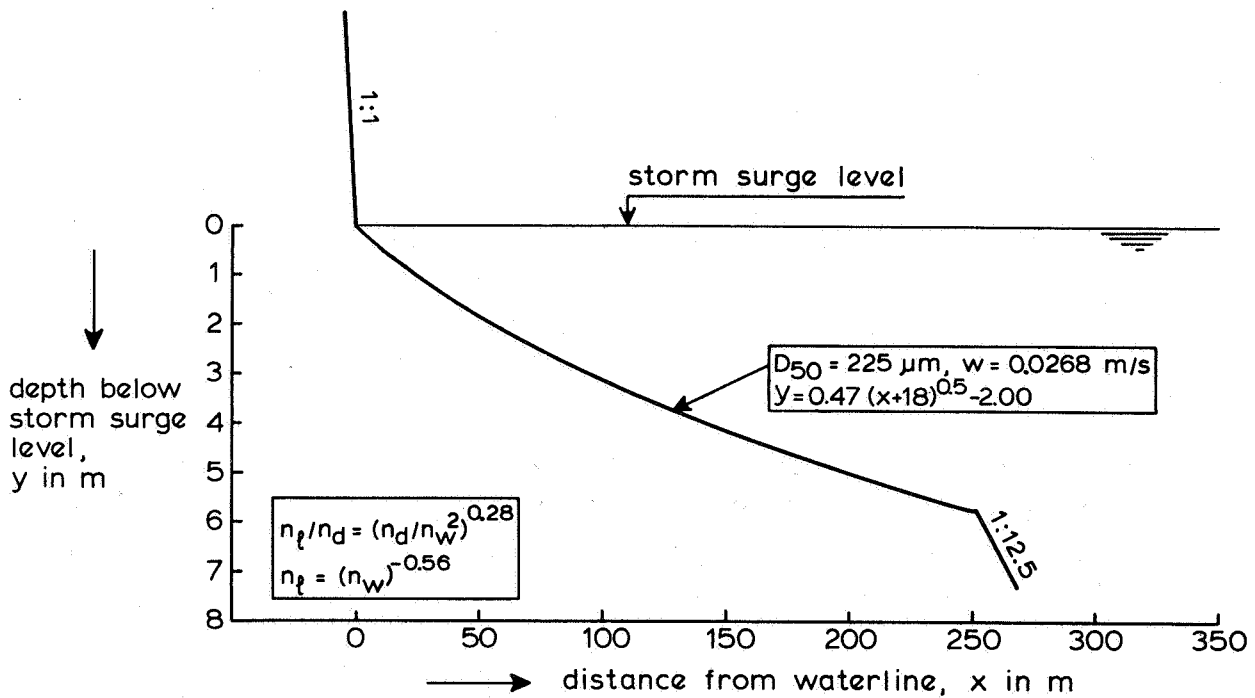


**Figure 83** Reference erosion profile

## 6.3 Effect of grain size and wave height

The reference erosion profile has been derived from tests with $D_{50} = 225$ µm. The effect of grain size is described by the fall velocity as indicated in the scale relation:

$$n_1/n_d = (n_d/n_w^2)^{0.28} \tag{4}$$

The reference profile holds for conditions with $H_{0s} = 7.6$ m. The relations between the wave height and the vertical and horizontal dimensions of the erosion profile are described by

$$n_d = n_H = n_L = n_T^2 \tag{1}$$

and by

$$n_1 = (n_d)^{1.28} \tag{137}$$

Scale relations are not just some formulae for small scale modelling. In essence scale relations describe the proces in dimensional terms, (see Chapter 3). The scale relations can be introduced in the formula for the erosion profile in such a way that this profile is described in terms of wave height and fall velocity.

**Grain size**

For situations with identical hydraulic conditions the relation between length and fall velocity can be derived from relation (4)

$$n_1/n_d = (n_d/n_w^{\,2})^{0.28} \tag{4}$$

If situations with identical hydraulic conditions are compared, the scale factor $n_d$ is equal to unity, so relation (4) yields:

$$n_1 = (n_w)^{-0.56} \tag{138}$$

Relation (138) implies that for conditions with identical hydraulic conditions an increase in the fall velocity by a factor 2 gives a decrease of the horizontal dimensions of the erosion profile by a factor

$$n_1 = (2)^{-0.56} = 0.68 \tag{139}$$

So coarser sand goes with steeper profiles. This agrees with the expectations. The effect of grain size is illustrated in Figure 84 (the relation between grain size and fall velocity as determined by settling tube test is indicated in Figures 18 and 19).
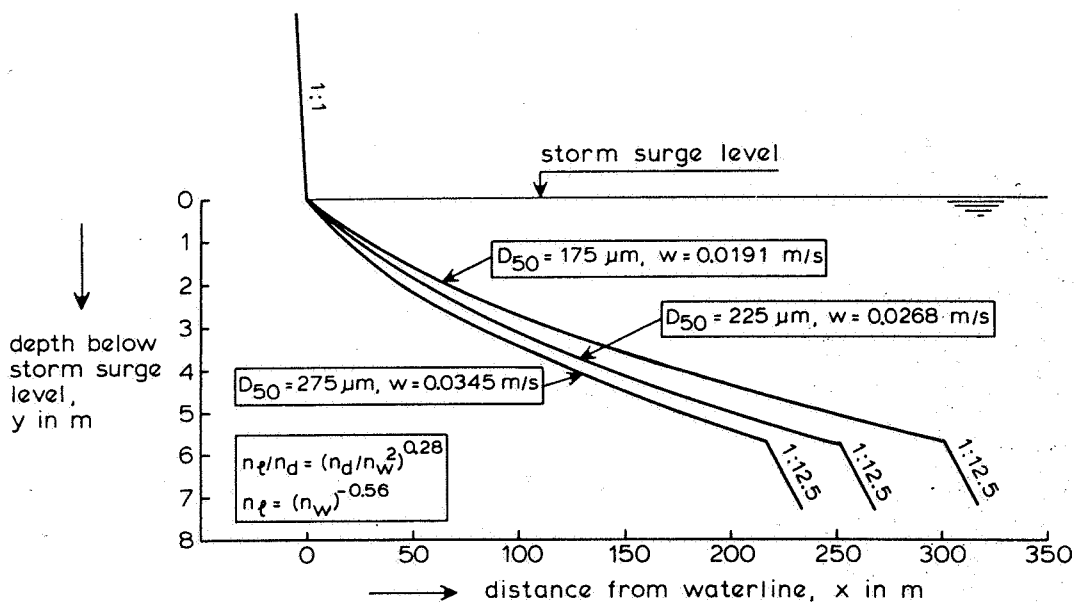


**Figure 84** Effect of grain size

The effect of the fall velocity can be described in the erosion profile by introducing the scale factor for the fall velocity in the parameter describing the length scale of the profile. Thus relation (136) becomes

$$y = 0.47 \ ((w/0.0268)^{0.56} \ x \ + \ 18)^{0.5} - 2.0 \tag{140}$$

**Wave height**

The effect of the wave height can be derived from scale relations (1) and (4)

$$n_d = n_H = n_L = n_T^2 \tag{1}$$

$$n_1/n_d = (n_d/n_w^2)^{0.28} \tag{4}$$

For conditions with a constant wave steepness and a constant fall velocity the effect of wave height is described by

$$n_d = n_H \qquad \text{and by} \tag{1}$$

$$n_1 = (n_d)^{1.28} \tag{137}$$

Substitution of (145) in (141) yields

$$n_1 = (n_H)^{1.28} \tag{141}$$

Relations (1) and (141) imply that when the waves are a factor 2 smaller, the vertical dimensions of the profile are a factor 2 smaller and the horizontal dimensions are a factor $(2)^{1.28} = 2.43$ smaller.

The effect of wave height is illustrated in Figure 85 for conditions with $D_{50}$ = 225 µm ($w$ = 0.0268 m/s) and a wave steepness $H_{0s}/L_0 = H_{0s}/(g \ T^2/2\pi) =$ 7.6/1.56 $(12)^2$ = 0.034.
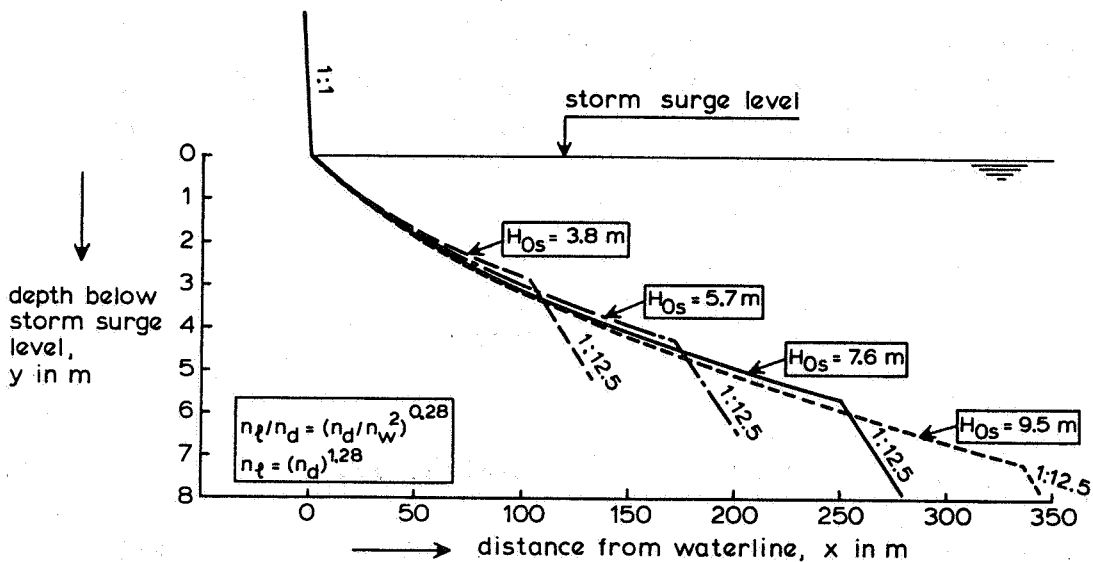


**Figure 85** Effect of wave height

Figure 85 shows that the shape of the erosion profile is hardly affected by the wave height. This means that the shape of the erosion profile may well be described by a power curve of the form:

$$y = px^{\gamma} \qquad (142)$$

This possibility is further discussed in section 6.8.

For conditions with $H_{0s} = 7.6$ m, $\hat{T} = 12$ s and $D_{50} = 225$ µm ($w = 0.0268$ m/s) the reference erosion profile is described by

$$y = 0.47 \ (x + 18)^{0.5} - 2.0 \qquad (136)$$

The effect of wave height can be described by introducing the relevant scale factors in the parameters describing the horizontal and the vertical dimensions of the profile:

$$(7.6/H_{0s}) \ y = 0.47 \left[ (7.6/H_{0s})^{1.28} \ x + 18 \right]^{0.5} - 2.0 \qquad (143)$$

**Effect of wave height and fall velocity combined**

The effect of grain size and wave height can be described in one formula by combining relation (140) and (143). Then the erosion profile for conditions with wave height $H_{0s}$ and fall velocity $w$ is described by:

$$(7.6/H_{0s}) \ y = 0.47 \left[ (7.6/H_{0s})^{1.28} \ (w/0.0268)^{0.56} \ x + 18 \right]^{0.5} - 2.00 \qquad (144)$$

in which

$H_{0s}$    is significant "deep water" wave height        (m)
$w$ is the fall velocity of the sediment in stagnant water      (m/s)
$x$ is the distance from the dune foot, in seaward direction     (m)
$y$ is the depth below storm surge level               (m)

The erosion extends from
$x = 0$ and $y = 0$ (dune foot at storm surge level)           (145)

down to

$$x = 250 \ (H_{0s}/7.6)^{1.28} \ (0.0268/w)^{0.56} \text{ and } y = 5.72 \ (H_{0s}/7.6) \qquad (146)$$

The principle of the dune erosion prediction model is shown in Figure 86. Formally speaking, the model is only valid for waves with $H_{0s}/L_0 = 0.034$ and

for conditions with a constant water level, 5 hrs after start. It will be illustrated in the next section that in practice the prediction model is valid for conditions with a wave steepness ranging from $H_{0s}/L_0 = 0.02$ up to 0.04 and for a realistic North Sea storm surge hydrograph as shown in Figure 87.
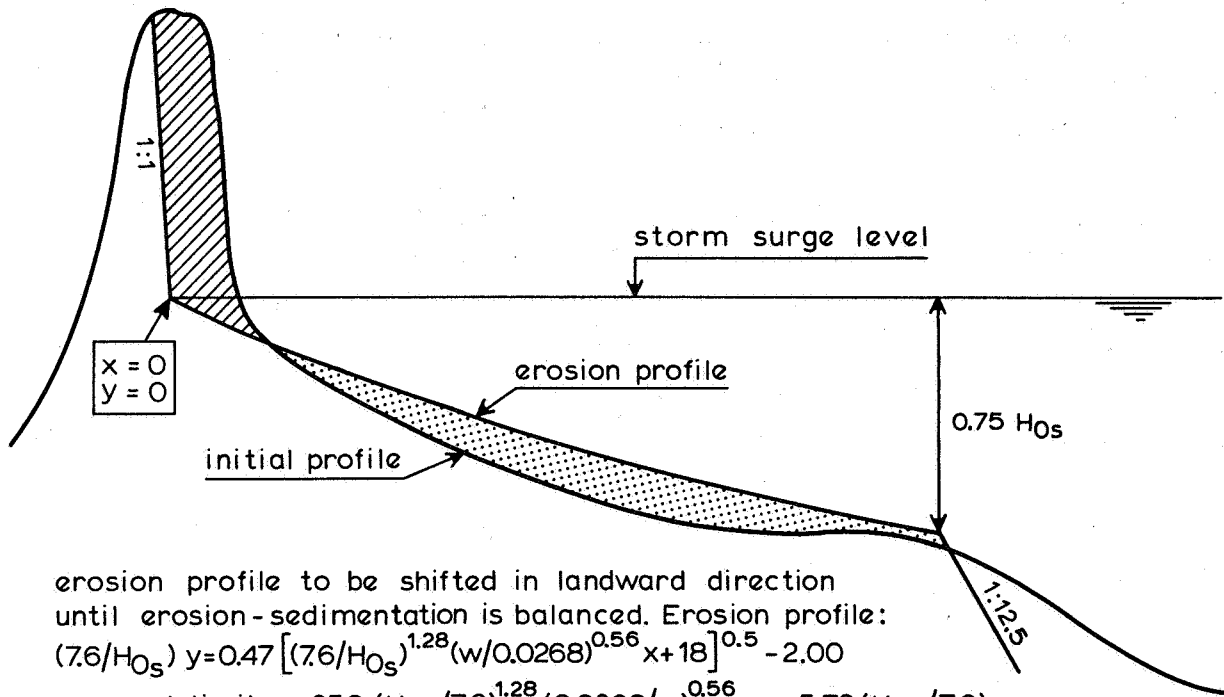


erosion profile to be shifted in landward direction until erosion-sedimentation is balanced. Erosion profile:

$(7.6/H_{0s})\ y=0.47\left[(7.6/H_{0s})^{1.28}(w/0.0268)^{0.56}x+18\right]^{0.5}-2.00$

seaward limit $x=250\ (H_{0s}/7.6)^{1.28}(0.0268/w)^{0.56}$ ; $y=5.72\,(H_{0s}/7.6)$

x, y and $H_{0s}$ in m; w in m/s

**Figure 86** Principle of dune erosion prediction model
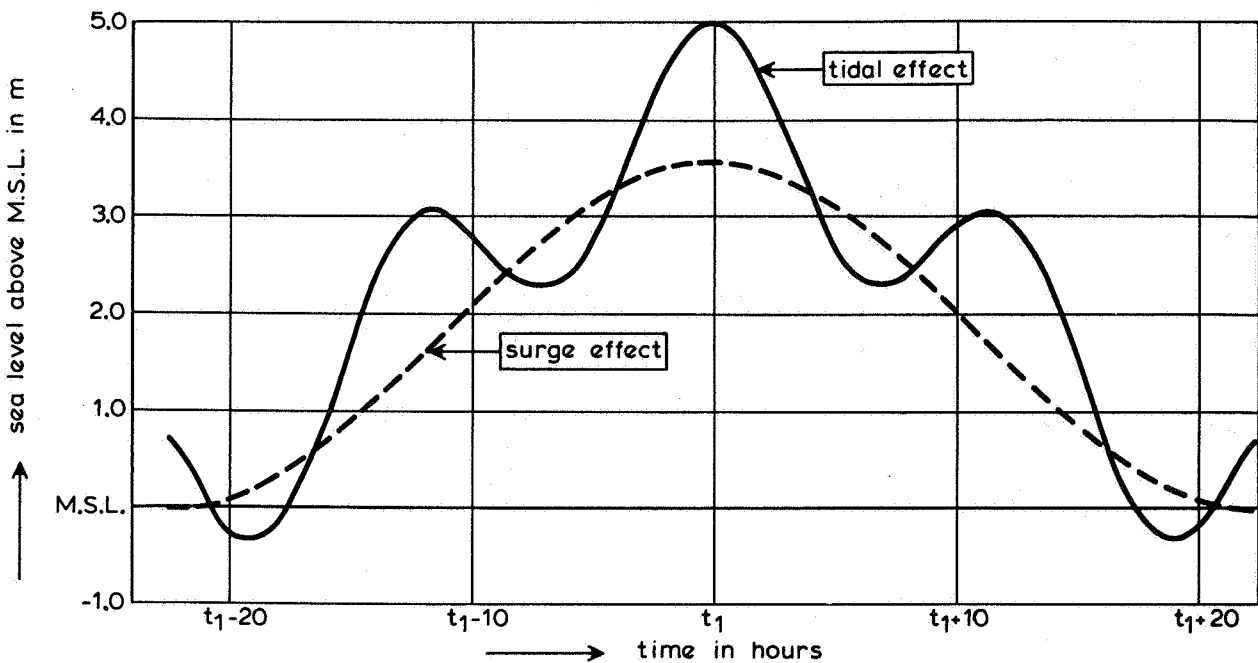


**Figure 87** North Sea storm surge hydrograph

## 6.4 Verification by additional large-scale and small-scale model tests

Five large-scale tests have been described in the previous chapter. Tests number 1 and 2 have been used for the development of the dune erosion prediction model. The remaining tests can be used to verify this model. Besides these tests, additional large scale model data are available from tests that have been carried out to check the safety of two critical coastal sections (Delft Hydraulics Laboratory, 1982).

The results of the verification for large-scale tests 3 and 4 are illustrated in Figures 88 and 89. The verification of the computed erosion quantities for all large-scale tests, including tests 1 and 2, is shown in Figure 90. On the basis of these results it is concluded that the prediction model is rather accurate in this respect. Besides these large scale tests an additional series of small scale tests has been carried out with a large range of hydraulic conditions and a large variety of initial profiles. The various parameters have been investigated in a systematic way, as is described hereafter.
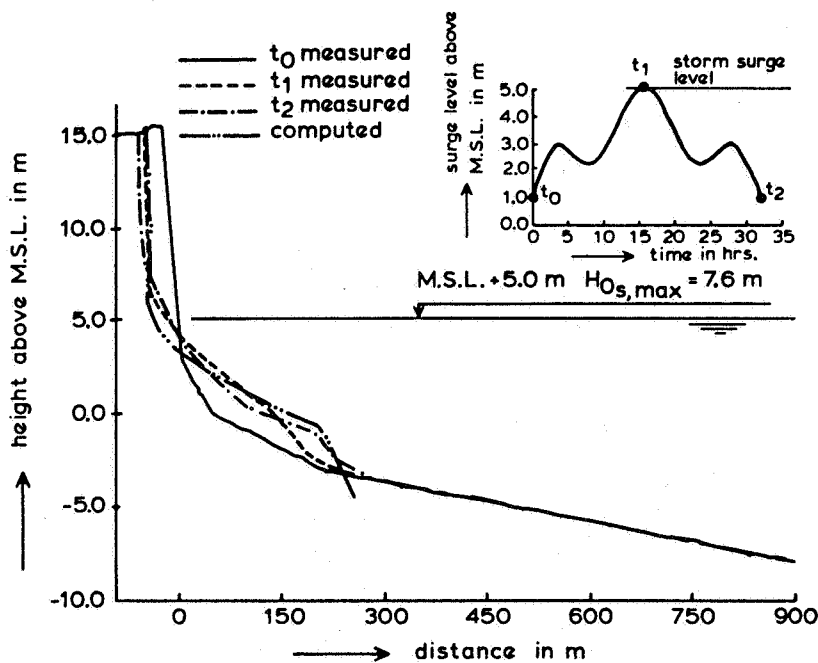


**Figure 88** Verification of dune erosion prediction model, large-scale test 3, prototype
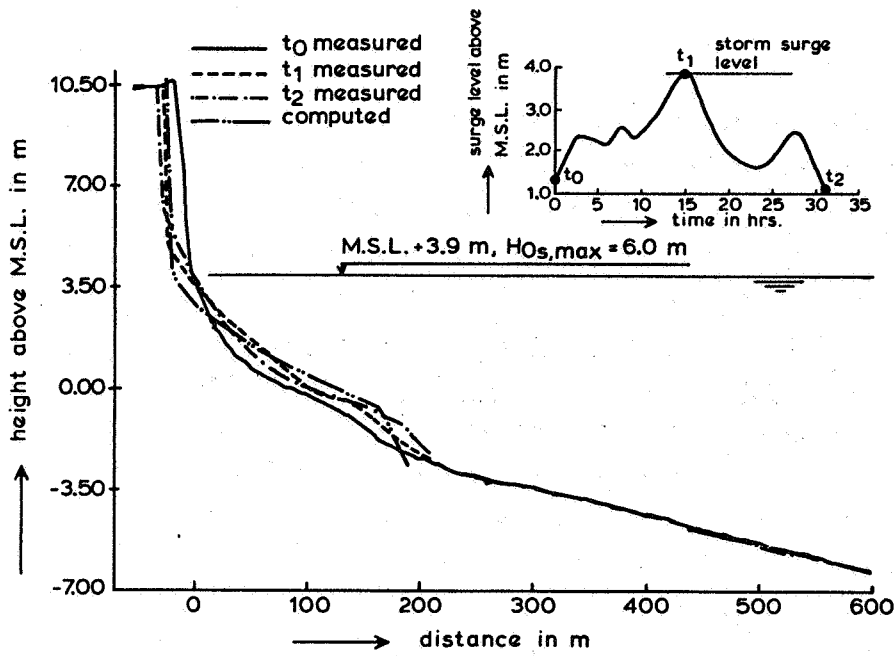
**Figure 89** Verification of dune erosion prediction model, large-scale test 4, prototype



o   large scale test 1, $Sf_m = 3.0$
x   large scale test 2, $Sf_m = 2.0$
▢   large scale test 3, $Sf_m = 2.0$, variable water level
✳   large scale test 4, 1953 - storm surge
▲   large scale test 5

▽
●} large scale tests for two critical coastal sections
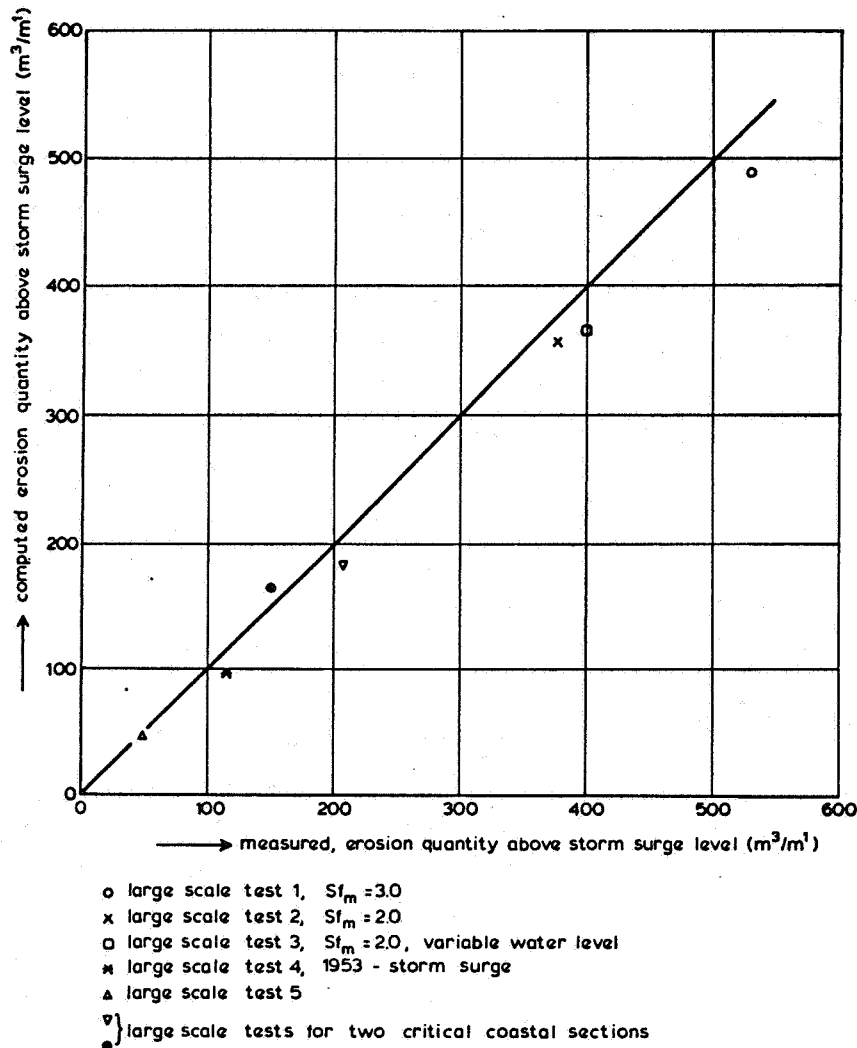
**Figure 90** Verification of dune erosion prediction model all large-scale tests, prototype

## Additional small-scale tests

The dune erosion prediction model was developed on the basis of model tests with rather idealized conditions. To verify the validity for a large range of conditions, additional small-scale model tests were carried out with a depth scale factor $n_d$ = 30. The sand applied for these model tests had a grain size characterized by $D_{50}$ = 95 μm. Fourteen tests were carried out with a, constant water level to investigate the effect of 1) storm surge level, 2) wave height, 3) wave steepness, 4) wave spectrum and 5) dune height. In addition six tests were carried out with identical hydraulic conditions and identical initial profiles to investigate the reproducibility of the tests. These six tests were also used to measure the sediment concentrations and the velocity field as will be discussed in Chapter 7. Finally another eight tests were done with a naturally varying water level for a range of initial profiles with bar and trough features. All tests are described extensively by Delft Hydraulics Laboratory (1982). A summary is presented hereafter.

## Effect of storm surge level

Four tests were carried out to asses the effect of the water level. The levels are: mean sea level + 4.0 m, + 4.5 m, + 5.0 m and + 5.5 m, respectively. The wave height is $H_{0s}$ = 7.6 m, the wave period T = 12 s. The initial profile of the tests has a steepness factor Sf = 1.2 (see Chapter 4). The profiles recorded in the model have been converted to prototype with the earlier developed scale relations. The dune erosion quantity was also computed with the dune erosion prediction model for the measured initial profiles. The results of the measurements at t = 5 hrs after start prototype and the computations are shown in Figure 91. The computed values agree reasonably well with the measured values. The trend is equal, and the computed erosion quantities are about 10% higher than the measured ones. The systematic difference in erosion quantities may be caused by a small error in the measured boundary conditions during the tests (viz. grain size or water level), or by an over-prediction of the computation model for the present test conditions.
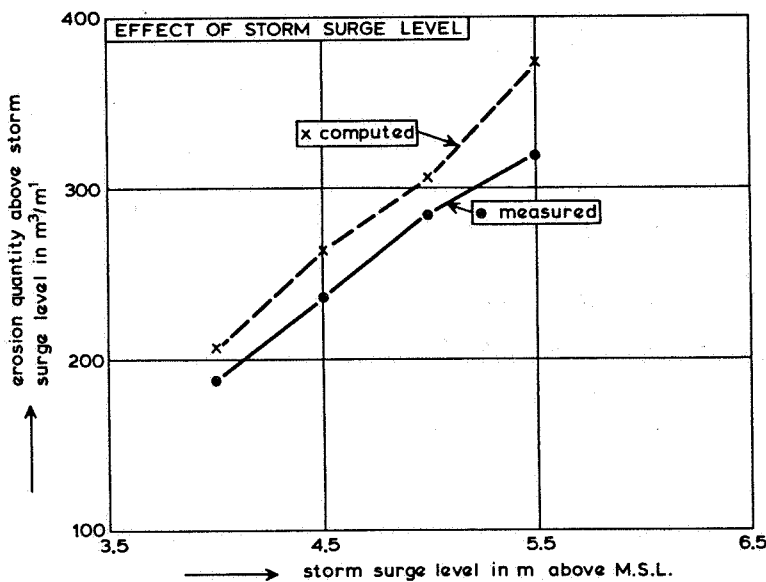


**Figure 91** Effect of storm surge level, measurements and computations

## Effect of wave height

To investigate the effect of wave height four other tests were carried out with a constant water level at 5 m above mean sea level. The wave conditions are $H_{0s} = 4.0$ m with $\hat{T} = 8.7$ s, $H_{0s} = 5.2$ m with $\hat{T} = 9.9$ s, $H_{0s} = 6.4$ m with $\hat{T} = 11.0$ s and $H_{0s} = 7.6$ m with $T = 12$ s, respectively. The wave steepness is $H_{0s}/L_0 = 0.034$ for all four tests. The initial profiles have a steepness factor $Sf = 1.2$. The profiles measured in the model have been converted to prototype. The erosion quanties have also been computed for measured initial profiles. The results of the measurements and computations are shown in Figure 92. The course of the lines is not smooth. This is due to small variations of the model profiles. The computed values agree reasonably well with the measured values. The trend is very similar. For waves higher than 4.5 m the computed values are slightly higher, for lower waves the one test shows that the computed value is slightly lower than the measured value. The reason for the differences is not known, see also the remarks for the previous case.
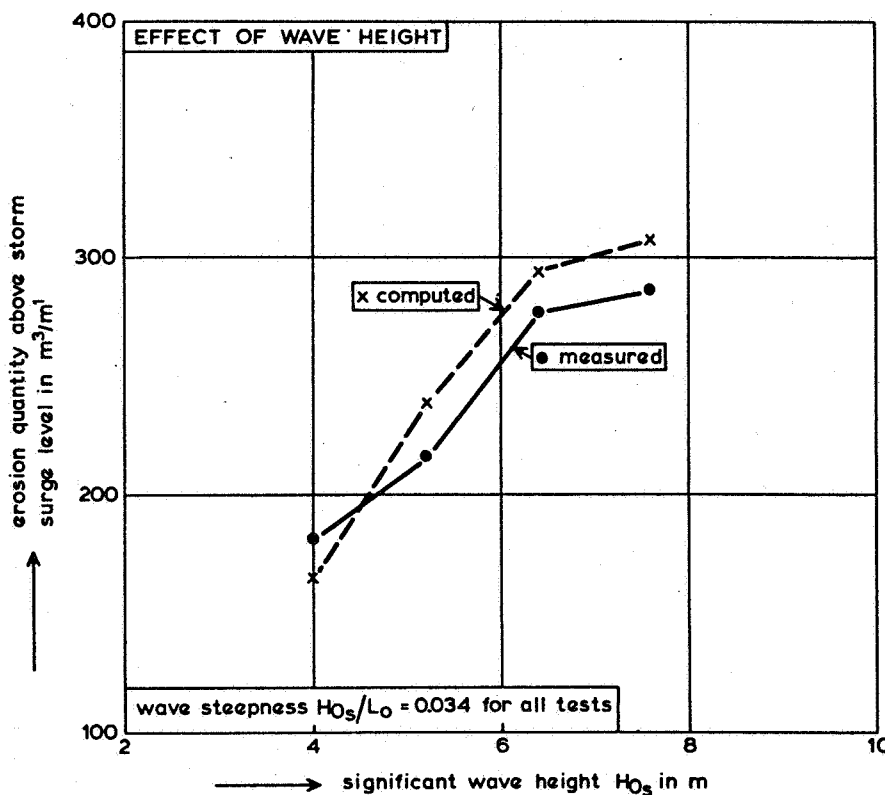


Figure 92 Effect of wave height, measurements and computations

## Effect of wave steepness

Five tests were done with a range of wave steepnesses. The initial profiles are characterized by $Sf = 1.2$. The water level was kept constant at 5 m above mean sea level. Three tests were carried out, with $H_{0s} = 7.6$ m and with a wave period $\hat{T} = 10$ s, $\hat{T} = 11$ s and $\hat{T} = 12$ s respectively. Two tests have been carried out with $H_{0s} = 4.0$ m and $\hat{T} = 8.7$ s and $\hat{T} = 12$ s, respectively. The results of the measurements and the computations are shown in Figure 93. The computed erosion quantity is not affected by the wave steepness as this para-

meter is not taken into consideration in the prediction model. The measured erosion quantities are reasonably well predicted for a wave steepness $H_{0s}/L_0$ = 0.034. For steeper waves the erosion quantity is over-estimated. For a smaller wave steepness the erosion quantity is under-estimated. The differences range from + 20% for $H_{0s}/L_0$ = 0.049 up to -20% for $H_{0s}/L_0$ = 0.018. The reason for the differences is not known. The number of tests is too small to derive solid conclusions.
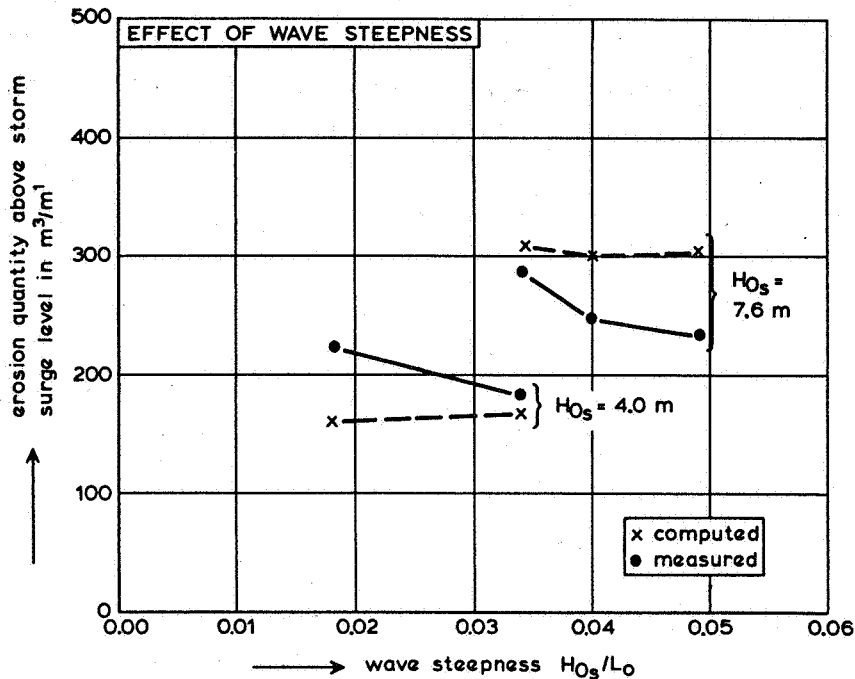


**Figure 93** Effect of wave steepness, measurements and computations

**Effect of wave spectrum**

The effect of the form of the energy spectrum of the waves is not taken into account by the dune erosion prediction model. To check this simplification two tests were done, one with a Pierson Moskowitz spectrum and the other with a Jonswap spectrum. The results of the measurements and the computations are shown in Figure 94. The differences in erosion between the two tests appear to be insignificant.

**Effect of dune height**

The effect of the initial profile is implicitly taken into account by the dune erosion prediction model. A certain shift of the fixed erosion profile in a situation with a relatively high dune produces more sand than the same shift in the case of a relatively low dune (geometry, balance of sediment). So for
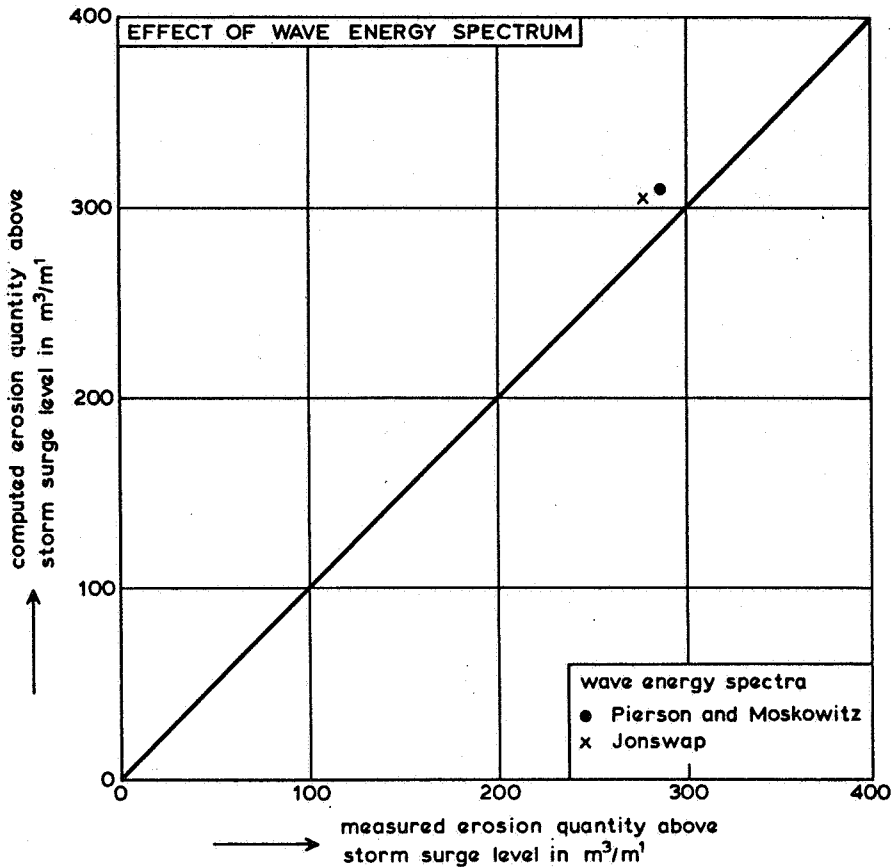
**Figure 94** Effect of wave energy spectrum, measurements and computations

geometrical reasons the dune front recession for a high dune will be smaller but the erosion quantity in $m^3/m^1$ will be larger than for a low dune. To check this implicit aspect of the prediction model, three tests were done with a dune height of 10 m, 15 m and 20 m above mean sea level. The water level was 5 m above mean sea level in these three tests, the wave height was $H_{0s} = 7.6$ m and the wave period $\hat{T} = 12.$s. The results of the measurements and the computations are shown in Figure 95. The trend of measured and computed values agrees very well, but the computed erosion quantities are consistantly about 10% larger than the measured quantities. Again, the reason for the differences may be a small difference between boundary conditions in the small-scale model and the boundary conditions applied for the computations. Another reason may be a small systematic overprediction of the computation model for the present test conditions.
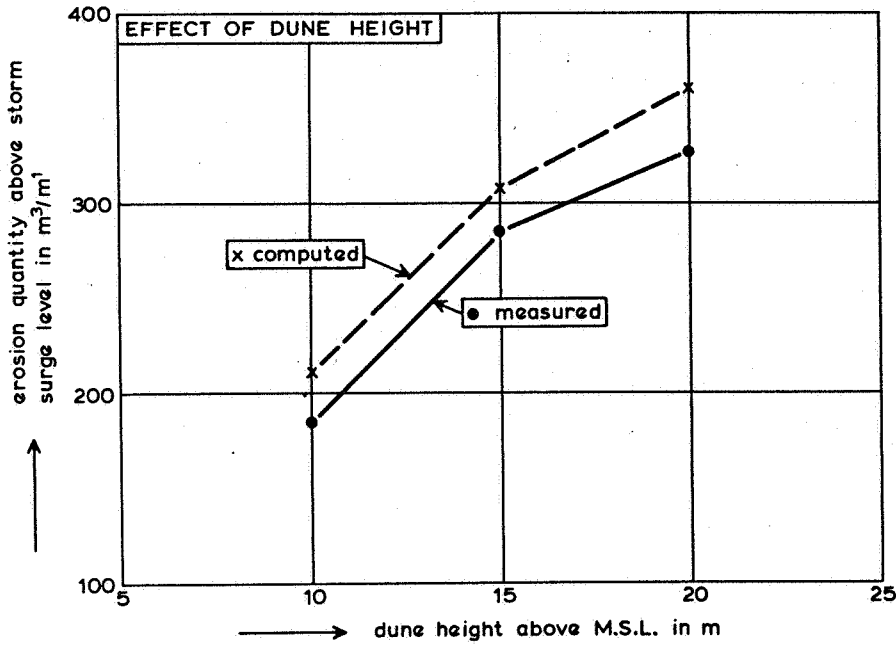
**Figure 95** Effect of dune height, measurements and computations

## Effect of bars and troughs

The effect of the initial profile is implicitly taken into account by the prediction model (geometry, balance of sediment). To check this effect, a series of eight tests was carried out reproducing a natural variation in the water level. The initial profiles that were tested are exaggerated versions of actual coastal profiles along the Dutch coast (Delft Hydraulics Laboratory, 1982) and a natural storm surge hydrograph as shown in Figure 87 was reproduced for the tests. The results of the measurements and the computations are shown in Figure 96. For all cases the computed erosion quantity is larger than the measured one. This implies that for coastal profiles with large bars and deep troughs the prediction model overestimates the dune erosion quantity.
This overestimation can be explained more or less tentatively as follows. The computation model is based on the difference between the initial profile and the erosion profile in terms of cross-sectional area. When two cases are considered, one with a relatively smooth initial profile and one with a very irregular profile with bars and troughs, and the relevant cross-sectional area and thus the average bottom slope of the two profiles is equal, then it is plausible that the wave energy reaching the dune front will be smaller for the irregular beach profile due to the irregular breaking of the waves. In that case the sediment transport capacity, and consequently the dune erosion quantity, will be less.
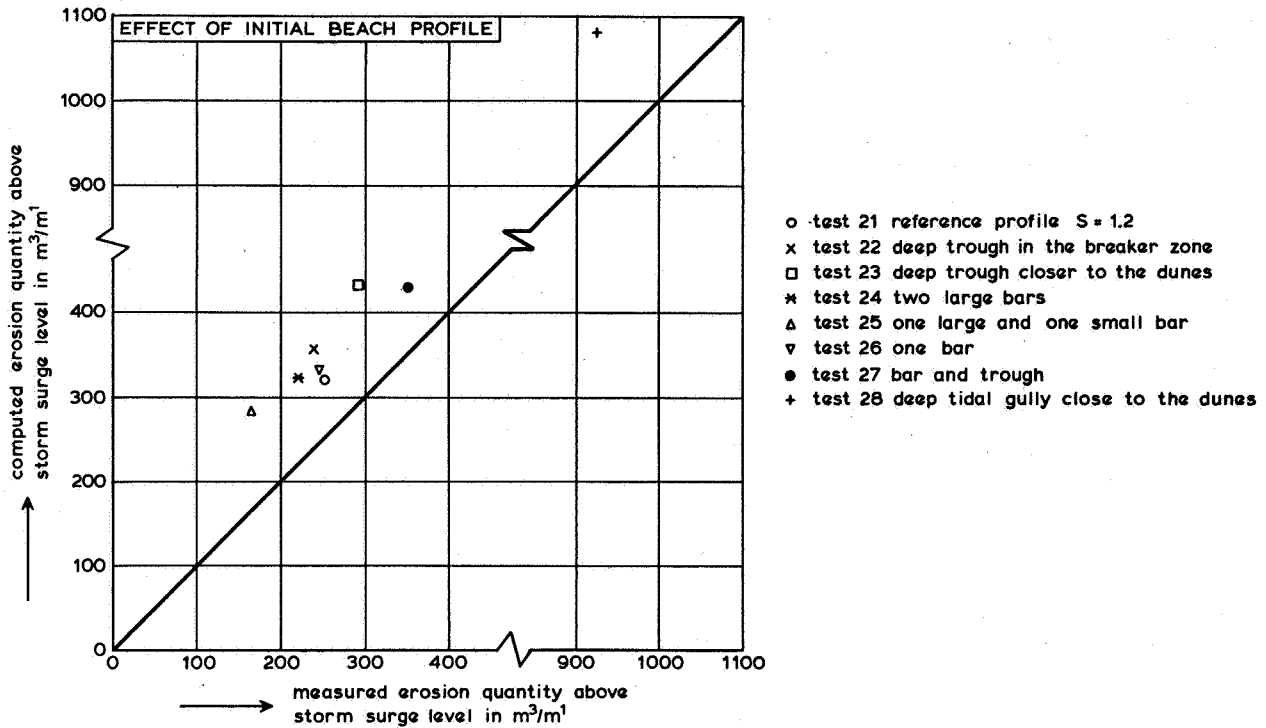
**Figure 96** Effect of large bars and deep throughs, measurements and computations

**Summary**

Considering the results of the parametric small-scale model investigations it is concluded that for this series of tests the newly developed dune erosion prediction model gives an overestimate of some 10% for the normal initial profiles and an over estimate of some 30% for the initial profiles with exaggerated bar and trough features. Thus although the prediction model is somewhat conservative for situations with large bars and troughs, it should be considered reasonably accurate for a large range of hydraulic conditions and initial profiles as are normally found in the field.

## 6.5 Verification by field data

Field data of dune erosion are scarce and generally not very accurate. The system of beach profile dynamics, dune formation and dune erosion as affected by wave motion, tidal motion and storm surges is such that substantial dune erosion has a frequency of occurrence in the order of once every 10 to 20 years. The major storm surges in Delfland (between Rotterdam and the Hague) since 1894 are shown in Figure 97. The 1953-storm surge is most interesting for a verification of the prediction model. However, the data are very limited. More data are available for the storm surge of 1976.Therefore the prediction model will be verified using the field data from both of these storm

surges together with the data on dune erosion caused by Hurricane Eloise in Florida in 1975.
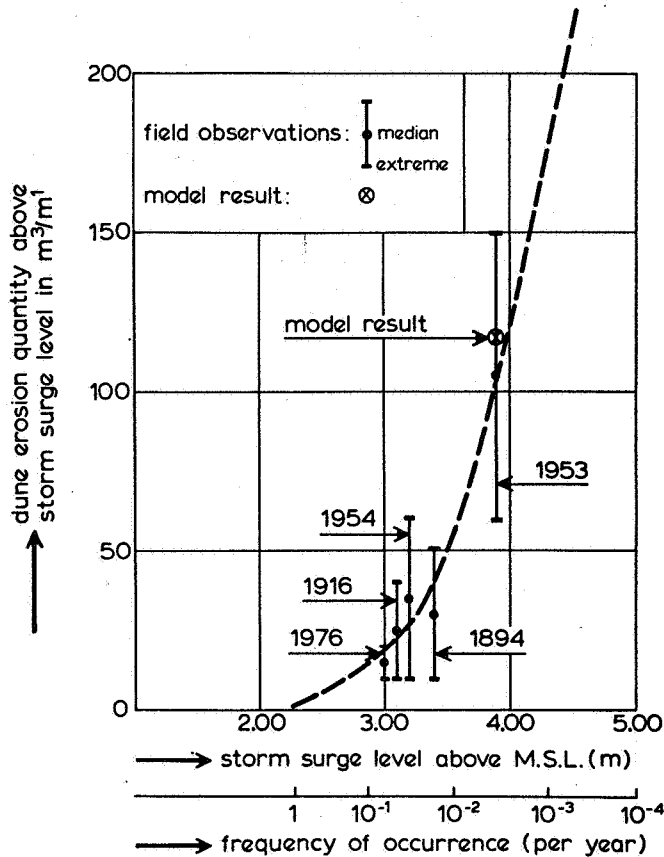


**Figure 97** Storm surge levels and erosion quantities at Delfland since 1894

**The 1953-storm surge**

The impact of the 1953 storm surge with regard to dune erosion was measured at Delfland. The "initial" beach and dune profile had been measured in October 1952. The position of the dune foot and the slope of the dune front was measured directly after the storm surge in February 1953. The dune erosion quantity was determined by reconstruction of the dune profile as it must have been just before the storm surge. The interpretation of the data is described by the Delft Hydraulics Laboratory and the Technical Advisory Committee on Water Retaining Structures (1971). The dune erosion quantity above storm surge level ranges from 55 $m^3/m^1$ up to 155 $m^3/m^1$. The average value for the 47 recorded profiles is 90 $m^3/m^1$. The standard deviation is 26 $m^3/m^1$.

The dune erosion data of the 1953-storm surge have been used as a verification of the scale relations as was described in Chapter 5. The dune erosion due to this storm was simulated in a model starting from the average coastal profile with a storm surge level of 3.9 m above mean sea level and a maximum wave height $H_{0s}$ = 6.0 m. The tests show an erosion quantity of 117 $m^3/m^1$.

The dune erosion prediction model gives an erosion quantity of 97 $m^3/m^1$ for the conditions given above. The results of the dune erosion prediction model agree rather well with the field data. The results are summarized in Table 21.

| 1953-storm surge | | | |
|---|---|---|---|
| erosion quantity recorded in the field | | erosion quantity found for the average initial profile with $H_{0s}$ = 6.0 m and $D_{50}$ = 225 µm | |
| average | standard deviation | large scale model test | dune erosion prediction model |
| 90 $m^3/m^1$ | 26 $m^3/m^1$ | 117 $m^3/m^1$ | 97 $m^3/m^1$ |

**Table 21** Erosion quantity above storm surge level 1953-storm surge

Another way to verify the prediction model is to compare the erosion profiles. Unfortunately, there are no profile data available for Delfland. Only in the northern part of North-Holland were beach profiles have been measured directly after the storm surge. These were the profiles that formed the basis of the provisional dune erosion prediction model. The measured profiles are shown in Figure 98 together with the profile computed with the present dune erosion prediction model. The profile is computed with $D_{50}$ = 250 µm and $H_{0s}$ = 6.0 m, being the most probable values of these parameters in this area during this storm. The computed profile agrees reasonably well with the measured profiles, although it should be noted that the computed profile lies about 0.15 m above the average of the measured profiles. This must be due to the fact that the computed erosion profile is derived from model profiles at the height of the storm surge, whereas the field profile may have lowered a little in the period between the storm surge and the survey. This phenomenon can also be observed in the profile development of the large scale test shown in Figure 99. Compare for example the profile for t = 30 hrs and 44 min. with the profile for t = 14 hrs and 46 min. However, this effect is not relevant for the dune erosion quantity, as it occurs after the height of the storm surge. When this is taken this into account, it is concluded that the computed erosion profile agrees rather well with the measured profiles.
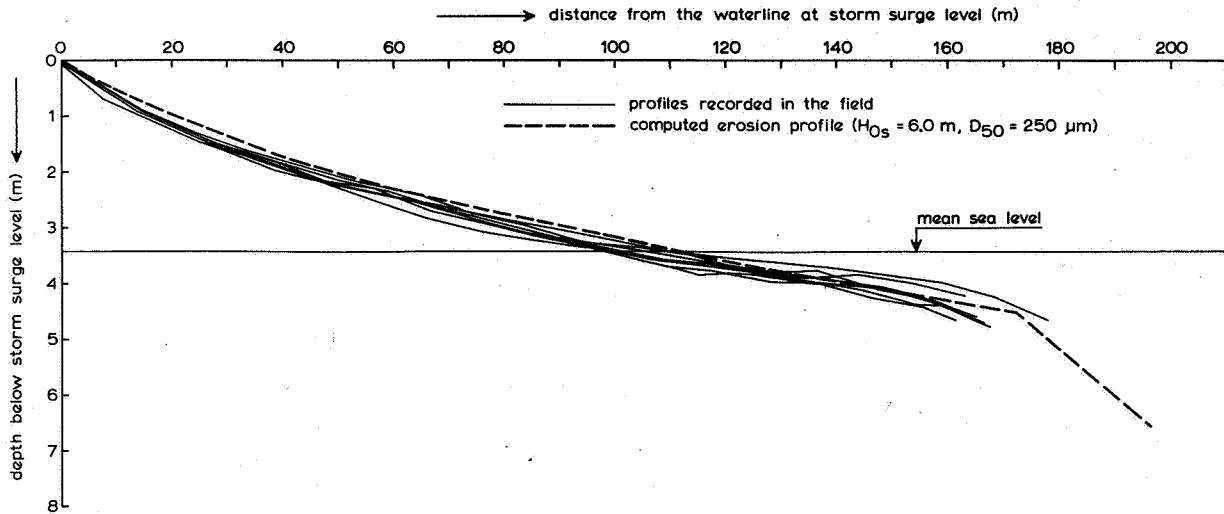
**Figure 98** Computed and measured erosion profiles, 1953-storm surge

## The 1976-storm surge

The storm surge of January 3rd, 1976 caused a dune erosion quantity of about 30 $m^3/m^1$ as an average along the Dutch coast. The sea rose to a level of 3.45 m above mean sea level at Ameland. Along the coast of North- and South-Holland the sea reached a level between 3.3 m and 3.0 m above mean sea level. In the southern delta area the maximum water level was 3.6 m above mean sea level. The dune erosion quantity above storm surge level, measured in 58 profiles, ranged from 5 $m^3/m^1$ up to an extreme value of 80 $m^3/m^1$. The recession of the dune front averaged at about 10 m.

Dune erosion hindcast computations have been carried out for the beach profiles as measured before the storm surge. The measured and the computed results are shown in Table 22. The computations were done for the grain sizes measured in the dunes after the storm surge. Computations have also been carried out for grain sizes as measured on the upper beach just in front of the dunes. The grain size on the upper beach is about 10% coarser than the grain size of the dune sand. In all computations this 10% increase was applied. The measured and computed data are shown in Figures 100 and 101. The results show a large scatter in measured and computed quantities.
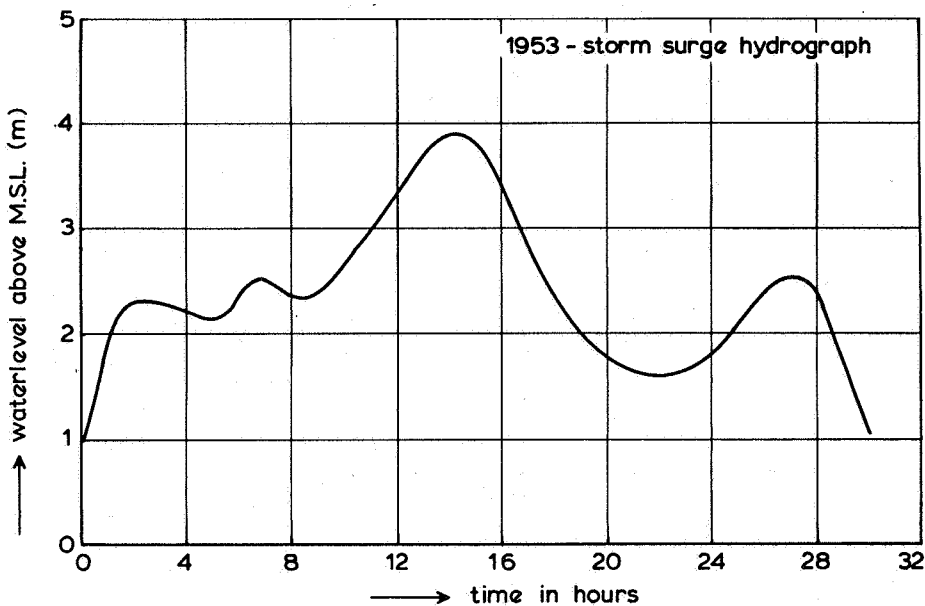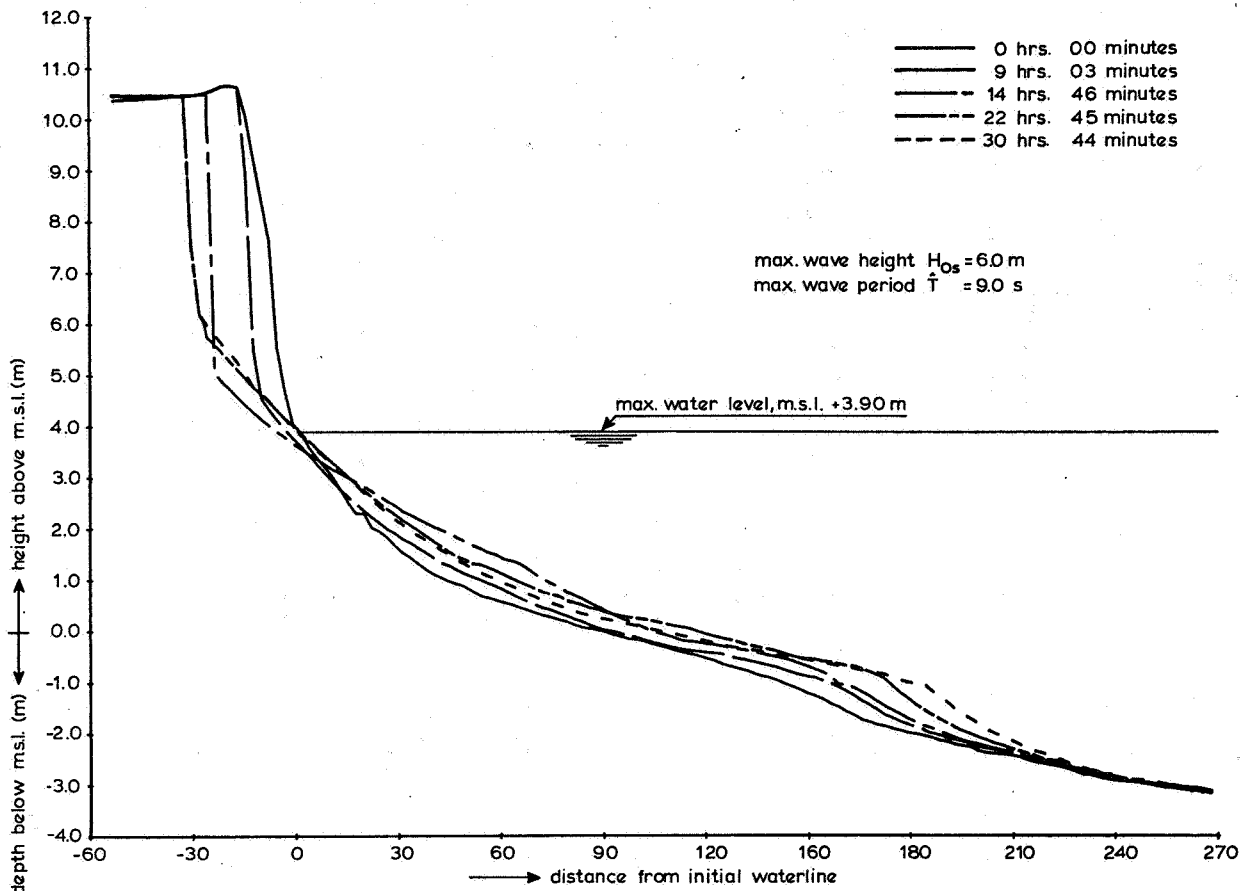
**Figure 99** Erosion profile development 1953-storm surge, large scale test 4; hydraulic conditions, measured erosion profiles and time, converted to prototype.

| location | position of coastal section | conditions | | | dune erosion | | |
|---|---|---|---|---|---|---|---|
| | | storm surge level above m.s.l. | wave height $H_{Os}$ | $D_{50}$ | measured | computed $(D_{50} = D_{50})$ | computed $(1.1D_{50})$ |
| | (km) | (m) | (m) | (μm) | $m^3/m^1$ | $m^3/m^1$ | $m^3/m^1$ |
| Ameland | 13.60 | 3.45 | 7.6 | 175 | 37 | 13.21 | 4.99 |
| | 13.80 | 3.45 | 7.6 | 175 | 33 | 21.39 | 11.28 |
| | 14.00 | 3.45 | 7.6 | 175 | 37 | 14.72 | 0 |
| | 14.20 | 3.45 | 7.6 | 175 | 30 | 9.0 | 0 |
| | 14.30 | 3.45 | 7.6 | 175 | 36 | 4.10 | 0.5 |
| average | | | | | 34.60 | 12.48 | 3.36 |
| Terschelling | 16.60 | 3.30 | 7.6 | 189 | 18 | 0 | 0 |
| | 6.80 | 3.30 | 7.6 | 189 | 28 | 11.21 | 5.47 |
| | 17.00 | 3.30 | 7.6 | 189 | 30 | 3.92 | 2.35 |
| | 17.20 | 3.30 | 7.6 | 189 | 22 | 0 | 0 |
| | 17.40 | 3.30 | 7.6 | 189 | 24 | 0 | 0 |
| average | | | | | 24.40 | 3.03 | 1.56 |
| Vlieland | 43.065 | 3.20 | 7.6 | 189 | 22 | 5.0 | 2.17 |
| | 43.400 | 3.20 | 7.6 | 189 | 42 | 27.86 | 14.99 |
| | 43.580 | 3.20 | 7.6 | 189 | 31 | 31.69 | 9.54 |
| | 43.950 | 3.20 | 7.6 | 189 | 26 | 37.73 | 11.10 |
| | 43.215 | 3.20 | 7.6 | 189 | 34 | 15.33 | 10.42 |
| | 43.765 | 3.20 | 7.6 | 189 | 28 | 38.63 | 15.04 |
| average | | | | | 30.50 | 26.04 | 10.54 |
| Texel | 19.12 | 3.10 | 7.6 | 205 | 27 | 45.41 | 28.75 |
| | 19.32 | 3.10 | 7.6 | 205 | 35 | 37.95 | 21.09 |
| | 19.52 | 3.10 | 7.6 | 205 | 36 | 62.91 | 43.64 |
| | 19.72 | 3.10 | 7.6 | 205 | 23 | 39.62 | 25.35 |
| | 19.92 | 3.10 | 7.6 | 205 | 28 | 35.48 | 19.58 |
| average | | | | | 29.80 | 44.21 | 27.68 |
| Noord-Holland | 5.68 | 3.03 | 6.0 | 237 | 58 | 75.14 | 47.50 |
| | 5.88 | 3.03 | 6.0 | 237 | 36 | 67.91 | 46.09 |
| | 6.08 | 3.03 | 6.0 | 237 | 38 | 63.19 | 38.84 |
| | 6.28 | 3.03 | 6.0 | 237 | 37 | 40.49 | 20.97 |
| | 10.54 | 3.06 | 6.0 | 267 | 23 | 44.46 | 33.34 |
| | 10.85 | 3.06 | 6.0 | 267 | 34 | 30.12 | 16.87 |
| | 11.15 | 3.06 | 6.0 | 267 | 40 | 49.14 | 31.47 |
| | 11.75 | 3.06 | 6.0 | 267 | 60 | 51.70 | 34.38 |
| | 34.0 | 3.18 | 6.0 | 235 | 26 | 10.83 | 4.03 |
| | 37.0 | 3.19 | 6.0 | 272 | 16 | 0 | 0 |
| | 41.0 | 3.22 | 6.0 | 237 | 35 | 70.55 | 55.54 |
| | 45.0 | 3.24 | 6.0 | 233 | 62 | 54.83 | 36.99 |
| | 49.0 | 3.26 | 6.0 | 220 | 68 | 118.99 | 94.99 |
| | 59.50 | 3.26 | 6.0 | 220 | 21 | 17.37 | 6.70 |
| | 50.0 | 3.26 | 6.0 | 220 | 60 | 114.08 | 89.56 |
| | 59.25 | 3.28 | 6.0 | 252 | 33 | 61.81 | 42.38 |
| | 59.50 | 3.28 | 6.0 | 252 | 54 | 105.29 | 78.88 |
| | 60.0 | 3.28 | 6.0 | 252 | 80 | 80.42 | 62.78 |
| | 61.0 | 3.28 | 6.0 | 252 | 47 | 111.48 | 84.80 |
| | 65.0 | 3.25 | 6.0 | 197 | 23 | 37.19 | 28.80 |
| | 70.5 | 3.22 | 6.0 | 226 | 29 | 60.12 | 43.40 |
| | 70.5 | 3.22 | 6.0 | 226 | 18 | 25.85 | 12.96 |
| | 71.0 | 3.22 | 6.0 | 226 | 20 | 69.99 | 52.82 |
| average | | | | | 40.11 | 75.69 | 38.12 |
| Zuid-Holland | 84.25 | 3.15 | 6.0 | 250 | 32 | 60.24 | 35.50 |
| | 84.50 | 3.15 | 6.0 | 250 | 30 | 55.27 | 32.45 |
| | 84.75 | 3.15 | 6.0 | 250 | 18 | 72.80 | 5.48 |
| | 108.07 | 3.0 | 6.0 | 250 | 18 | 39.52 | 17.59 |
| | 108.45 | 3.0 | 6.0 | 250 | 45 | 27.09 | 12.71 |
| average | | | | | 28.60 | 50.98 | 20.75 |
| Zeeland | 6.70 | 3.50 | 4.0 | 316 | 10 | 22.91 | 20.20 |
| | 7.03 | 3.50 | 4.0 | 316 | 5 | 7.47 | 6.30 |
| | 16.115 | 3.55 | 4.0 | 315 | 15 | 23.40 | 15.20 |
| | 16.532 | 3.55 | 4.0 | 315 | 15 | 31.98 | 24.85 |
| | 10.041 | 3.50 | 4.0 | 213 | 31 | 52.25 | 45.66 |
| | 10.441 | 3.50 | 4.0 | 213 | 32 | 85.22 | 66.91 |
| | 10.841 | 3.50 | 4.0 | 213 | 13 | 28.18 | 19.57 |
| | 27.315 | 3.75 | 4.0 | 247 | 21 | 0 | 9.61 |
| | 27.727 | 3.75 | 4.0 | 247 | 20 | 15.27 | 12.58 |
| average | | | | | 18.11 | 27.30 | 24.56 |
| total average | | | | | 32 | 40 | 26 |

**Table 22**  Measured and computed dune erosion quantities, 1976-storm surge
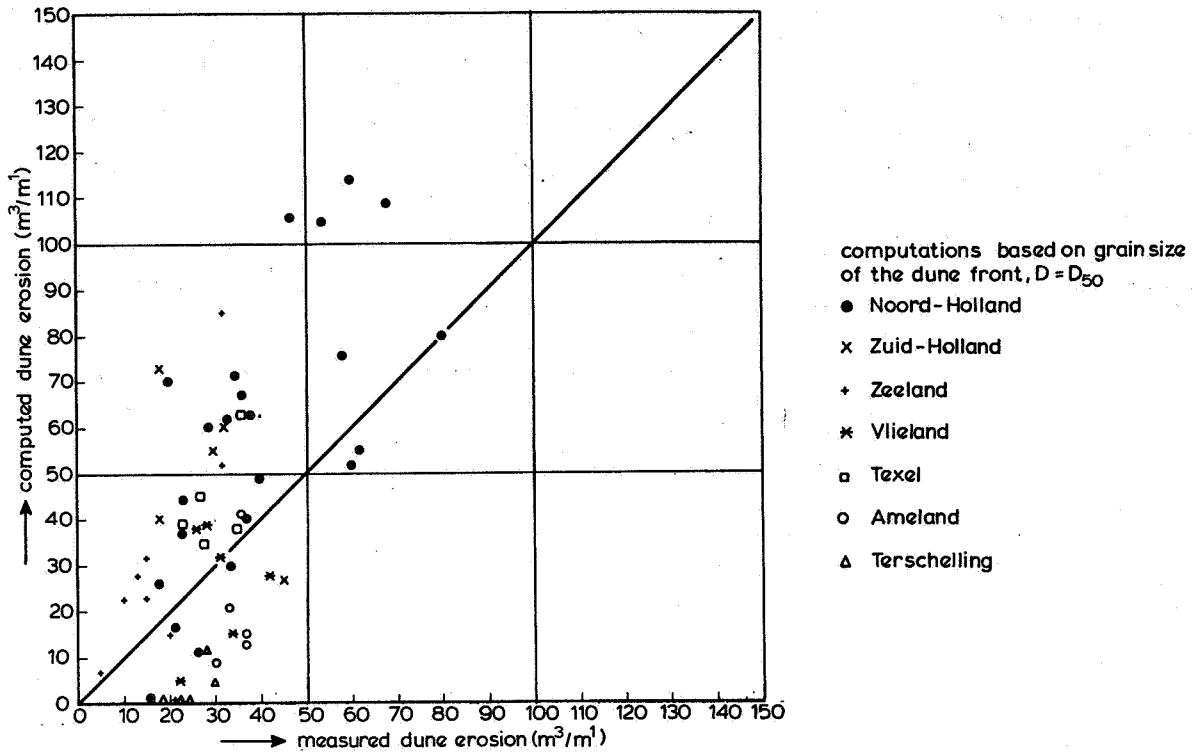
**Figure 100** Measured and computed erosion quantities, 1976-storm surge
($D_{50}$ of dune sand)
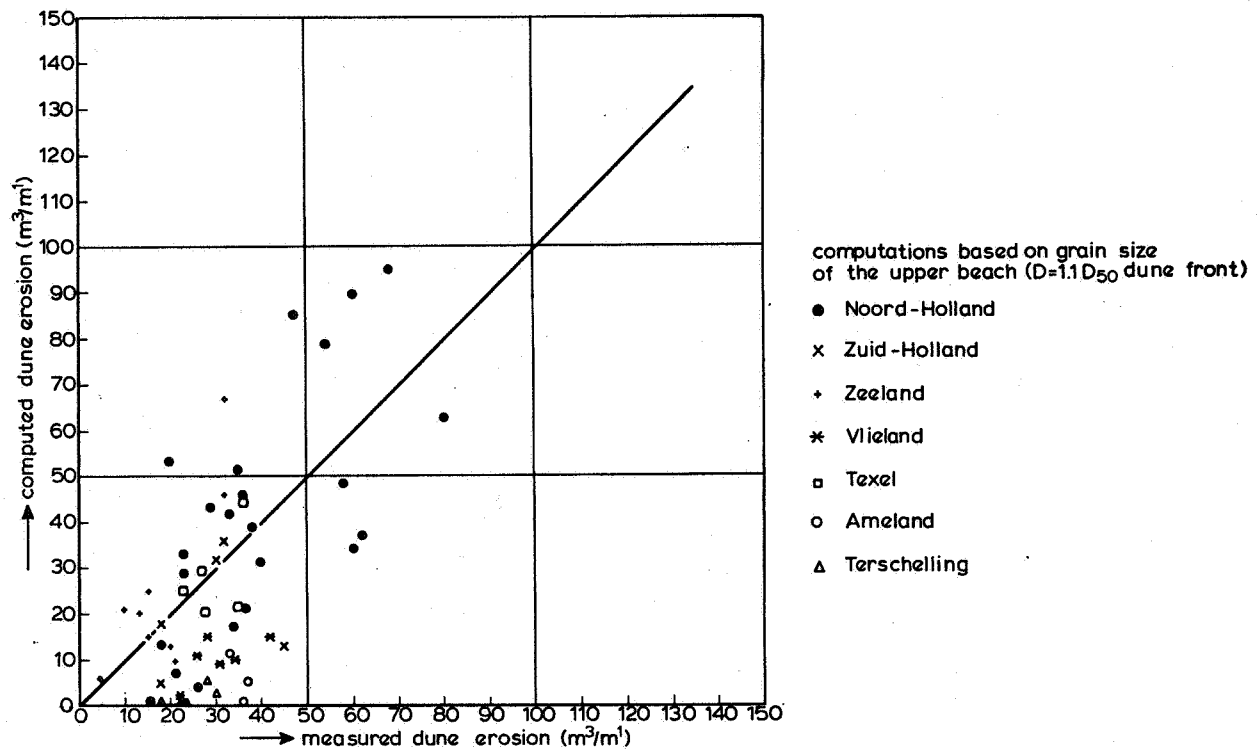


**Figure 101** Measured and computed erosion quantities, 1976-storm surge
($D_{50}$ of the upper beach sand)

The scatter in the data is expected to be mainly due to the inaccuracy of the input parameters: the profiles before the storm surge, the grain size, the storm surge level and the wave conditions, as explained below.

- Coastal profiles. The profiles had been measured several weeks up to several months before the storm surge. In this period the beach profile will probably have changed a little bit.

- Grain size. The grain size could not be determined accurately from the data available. Moreover it is not clear whether for these moderate dune erosion quantities the grain size of the beach or the grain size of the dune should be applied in the computations. The quantity of sand eroded from the dunes is in many cases so little that the "erosion profile" will mainly consist of beach sand.

- Storm surge level. The computed dune erosion quantity is very sensitive to small changes in storm surge level. An error of 0.1 m in the storm surge level gives rise to a difference in the dune erosion quantity of 10 to 15 $m^3/m^1$ (cf. Figure 91).

- Wave height. The sensitivity to the wave height in absolute terms is less than to the storm surge level. For values of $H_{0s}$ near 6.0 m an error in the wave height of 0.10 m gives rise to an error in the predicted dune erosion quantity of about 5 $m^3/m^1$ (cf. Figure 92).

The computed erosion quantities are relatively small compared with the erosion quantities to be expected during extreme storm surge conditions.
For such small quantities, small inaccuracies in the input parameters produce a relatively large scatter in the computed quantities. However, this scatter should be reduced when the average of a large number of profiles is considered. The average values for measured and computed erosion quantities are shown in Table 23. These results are in good agreement. Consequently it is concluded that the dune erosion prediction model gives results with a correct order of magnitude, also in cases with relatively small dune erosion. As an example some measured and computed profile changes are shown in Figures 102 and 103.

| 1976-storm surge | dune erosion quantities, average of 58 coastal profiles | | |
|---|---|---|---|
| | measured | computed | |
| | | $D_{50}$-dune | $D_{50}$-upper beach |
| average | 32 $m^3/m^1$ | 40 $m^3/m^1$ | 26 $m^3/m^1$ |
| standard deviation | 15 $m^3/m^1$ | 30 $m^3/m^1$ | 24 $m^3/m^1$ |

Table 23 Measured and computed dune erosion quantities, average values and standard deviation, 1976-storm surge
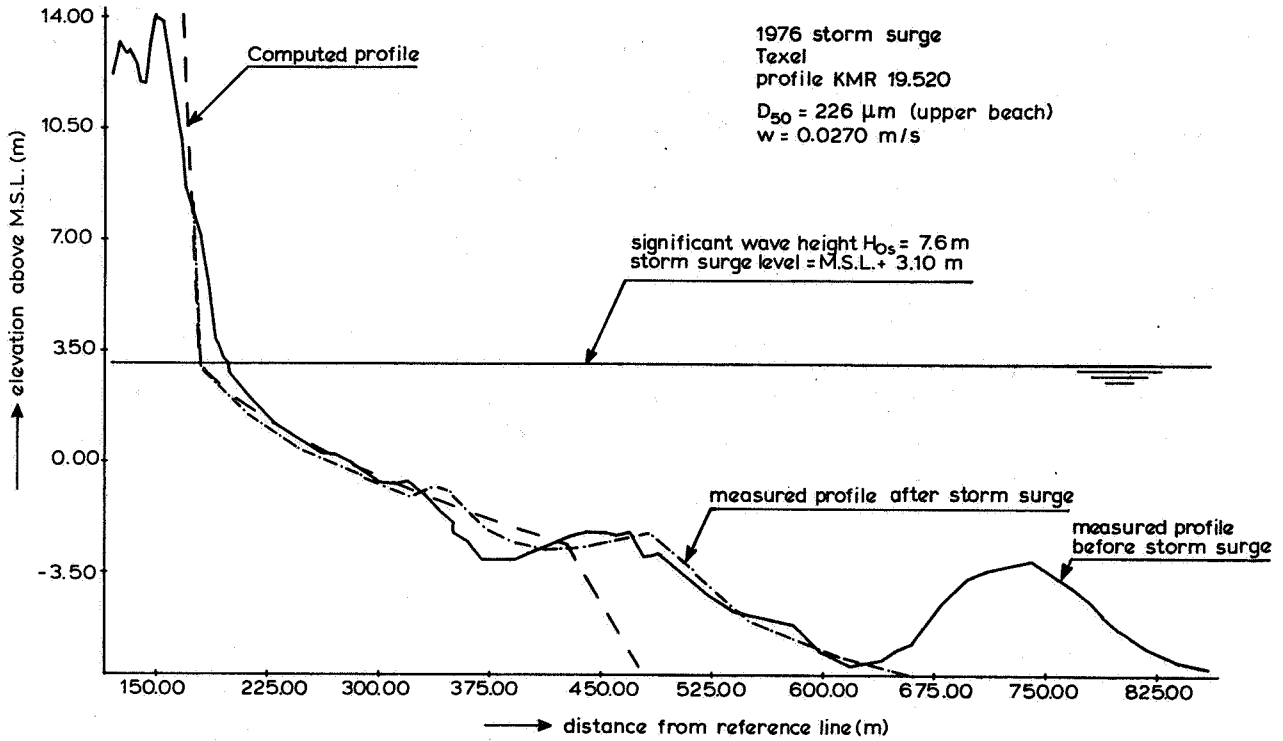
**Figure 102** Measured and computed profile changes 1976-storm surge KMR 19.520
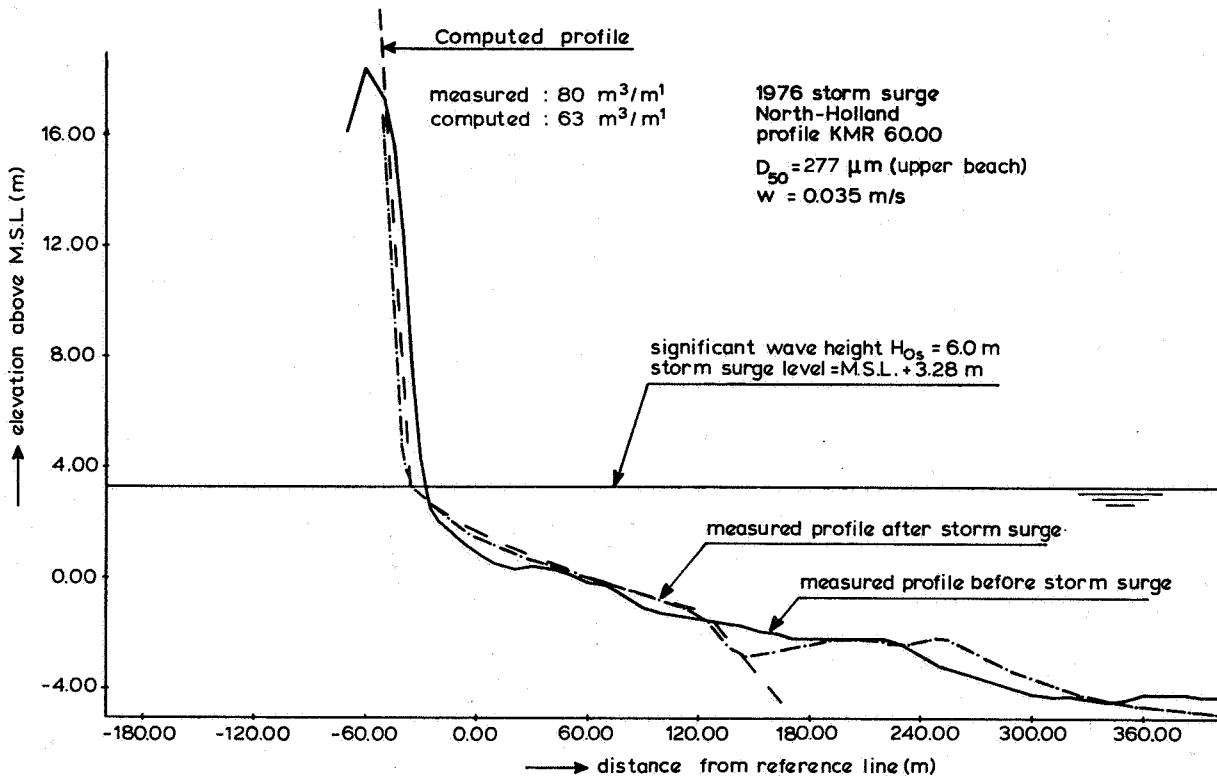


**Figure 103** Measured and computed profile changes 1976-storm surge KMR 60.000

## Hurricane Eloise

The Florida Panhandle was struck by Hurricane Eloise in September 1975. The storm surge and wave action eroded large sections of the natural beach-dune system of Walton County. The field conditions were reconstructed by Hughes and Chiu (1981). They applied this "case" for the calibration of dune erosion tests (Hughes, 1983). The field data are described below.

### profiles

In their report Hughes and Chiu (1981) present a small scale model version of the recorded pre-storm and post-storm profile. The depth scale factor $n_d$ = 25, the length scale factor $n_l$ = 51.56. The profiles have been converted to the field conditions using these scale factors, see Figure 104.

### storm surge hydrograph

Since no comprehensive data on storm surge levels during Hurricane Eloise were available, Hughes and Chiu estimated them on the basis of a "combination of prediction methods and logical arguments". They arrived at a final estimate of the peak level of "slightly over 8 feet" above mean sea level. The time history of the surge level rise was approximated as a linear increase from mean sea level to peak surge over a time span of 12 hours, a constant peak surge for one hour and a linear decrease over 6 hours. The reconstructed storm surge hydrograph and the typical North Sea storm surge hydrograph are shown in Figure 105.

### wave conditions

The significant wave height during the peak of the storm surge is approximated at 10 ft to 14 ft with $H_s$ = 12 ft as a best estimate. A "dominant" wave period of 11 seconds was recorded.

### grain size and fall velocity

Hughes and Chiu defined an "effective" grain size D = 262 μm as being representative for the coastal profile. This value is the average of "effective" grain sizes of samples taken from the dune, the mean high water contour and the mean low water contour. The input parameter for the dune erosion prediction model is the fall velocity corresponding to $D_{50}$ of the eroding sand from the dune. The sand of the dune was characterized as $D_{50}$ = 260 μm for the dune profile considered (R-42). Hughes and Chiu applied a representative fall velocity w = 0.040 m/s, determined from the curves of the Shore Protection Manual for D = 262 μm and a water temperature of 25°C. Settling tube tests carried out at Delft University of Technology indicate a slightly smaller fall velocity under such conditions. The results of these accurate tests for water temperatures of 10°C and 18°C are shown in Figures 18 and 19. Extrapolation to 25°C gives a fall velocity w = 0.036 m/s for $D_{50}$ = 260 μm.
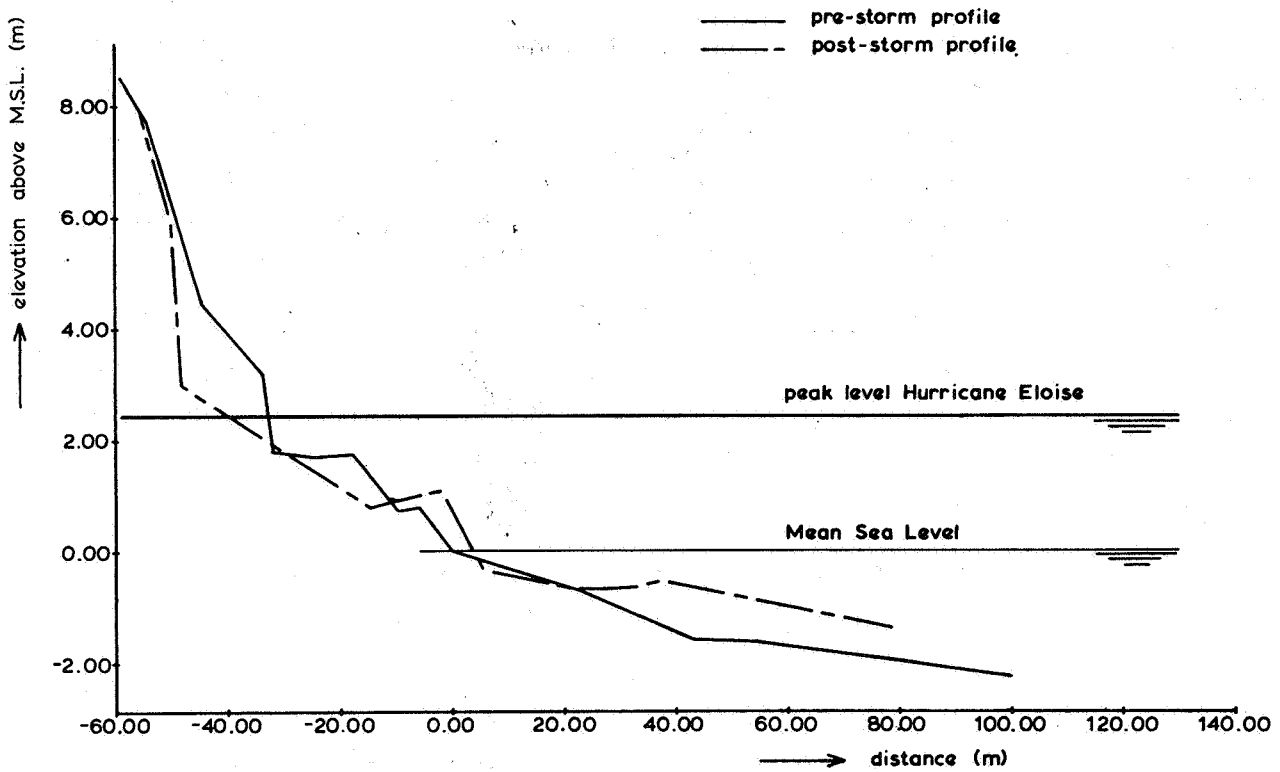
**Figure 104** Beach and dune profile Walton County before and after Hurricane Eloise (from Hughes and Chiu, 1981)
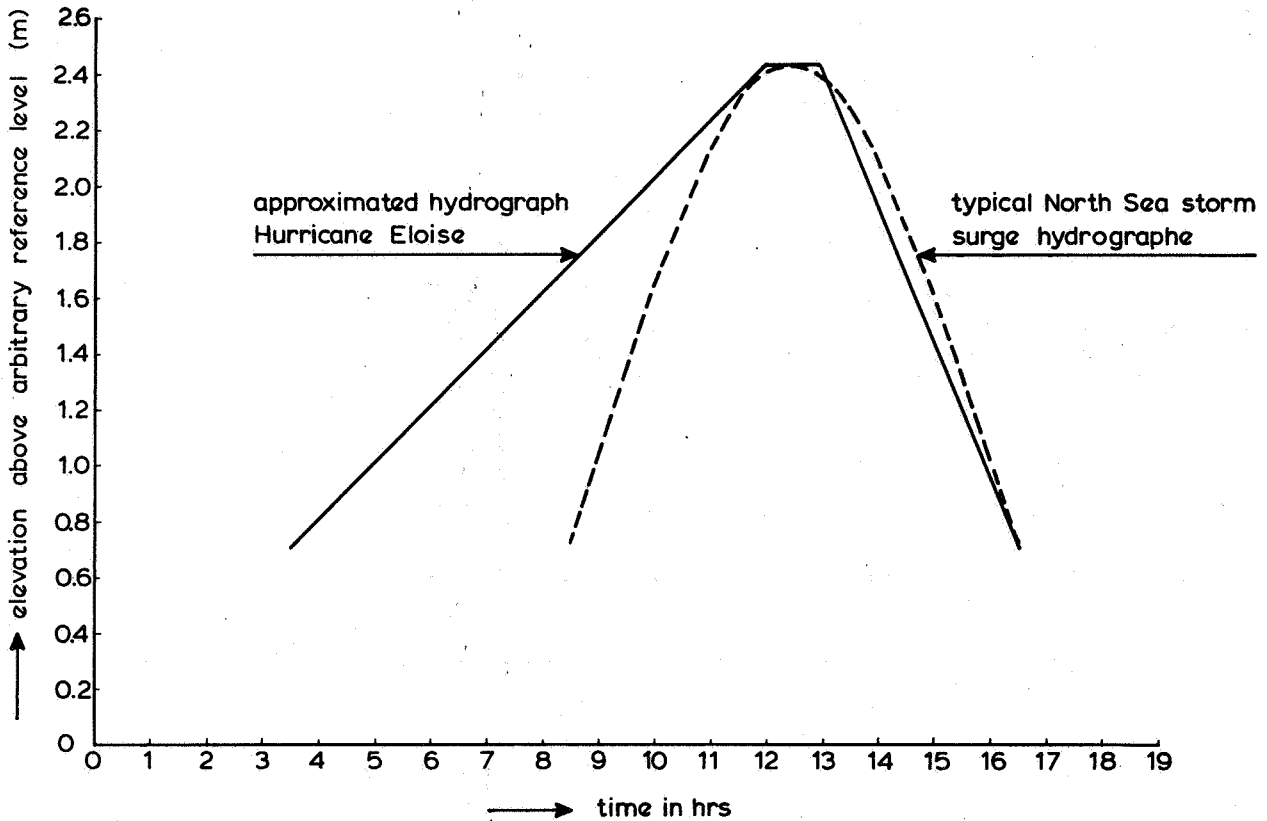


**Figure 105** Hurricane Eloise and North Sea storm surge hydrograph

## computations

The dune erosion prediction model was developed for a typical North Sea storm surge hydrograph. The reconstructed Eloise hydrograph is compared with the top of the North Sea storm surge hydrograph in Figure 105. The reconstructed hydrograph shows a considerably slower rise of water level. However, during the most important phase of dune erosion, around the peak, the two hydrographs are very similar. Due to the differences in shape it should be anticipated that the prediction model will slightly under-estimate the erosion quantity.

Computations were carried out for the initial profile shown in Figure 104. A range of values for maximum storm surge level, wave height and fall velocity was applied in a total of 6 computer runs. The conditions and the erosion quantities above storm surge level are shown in Table 24.

The input parameters of run no 1 are equal to the boundary conditions of the storm surge in nature as approximated by Hughes and Chiu. It can be seen from Table 24 that the computed erosion quantity above storm surge level is very close to the measured value: the computed quantity is only some 10% smaller. The additional runs show the sensitivity of the computed erosion quantity for minor changes in the input parameters.

| | Maximum storm surge level above m.s.1 (m) | Significant wave height during maximum storm surge level (m) | Grain size of dune sand $D_{50}(\mu m)$ | Fall velocity Shore Protection Manual 25°C (m/s) | Fall velocity settling tube tests 25° C(m/s) | Erosion quantity above storm surge level (m³/m') |
|---|---|---|---|---|---|---|
| Prototype conditions according to Hughes and Chiu | 2.438 (8 ft) | 3.66 (12 ft) | 260 | 0.040 | 0.036 | 27 |
| Run 1 | 2.438 | 3.66 | 260 | – | 0.036 | 24 |
| Run 2 | 2.591 | 3.66 | 260 | – | 0.036 | 29 |
| Run 3 | 2.286 | 3.66 | 260 | – | 0.036 | 19 |
| Run 4 | 2.438 | 4.27 | 260 | – | 0.036 | 29 |
| Run 5 | 2.438 | 3.05 | 260 | – | 0.036 | 17 |
| Run 6 | 2.438 | 3.66 | 260 | 0.040 | – | 18 ˙ |

**Table 24** Verification of dune erosion prediction model for Hurricane Eloise

The agreement between computed and measured erosion quantity is amazingly good, in view of the uncertainty of the input parameters:

1) The pre-storm profile was recorded in the field about two years before the Hurricane. It is very likely that in the meantime, the profile changed significantly.

2) The accuracy of the reconstructed maximum water level during the Hurricane is in the order of 0.1 m. The computational model shows an increase of 3 $m^3/m'$ for 0.10 increase in maximum storm surge level, for the present case.

3) The accuracy of the wave height is in the order of 0.6 m. The computational model shows an increase of 6 $m^3/m'$ for 0.6 m significant wave height increase, for the present case.

4) The accuracy of the grain size diameter of a single sample is generally in the order of 10% as compared with the local average. The dune erosion quantity is strongly dependent on the fall velocity and thus on the grain size. An 10% increase of $D_{50}$ gives a decrease in computed erosion quantity of about 15%.

The computed post-storm profile is shown in Figure 106 for computer run 1, together with the field data. It can be seen that the measured and computed profile agree reasonably well above mean sea level; below mean sea level the agreement is poor. This is not surprising as will be explained hereafter.

When the sea level falls, the process of dune erosion quickly comes to an end and the profile changes above the water level will be relatively small. At and below mean sea level however, the waves encounter an "overnourished" beach. Consequently this part of the beach profile will be reworked. It is thought that the bar is generated during this phase of the storm surge. A similar phenomenon was observed during the model investigations. The large scale test results show that during the process of dune erosion a gently sloping profile is generated without bars and troughs; only after a longer period or after a lowering of the water level, a tendency of bar and trough development can be noticed see Fig. 74 and 78.

**Summary and conclusions**

The dune erosion prediction model as developed for storm surges along the North Sea coast of The Netherlands has been successfully verified by field data of dune erosion during Hurricane Eloise in Walton County, Florida 1975, reported by Hughes and Chiu (1981). The difference between computed and measured erosion quantity is only 10% of the measured quantity. Actually a larger difference had been expected as the accuracy of the input parameters must be relatively small. Still this result gives additional support to the validity of the computational model. Moreover, it illustrates the general applicability of the model.

maximum storm surge level = 2.438 m above M.S.L.
significant wave height = 3.66 m
fall velocity = 0.036 m/s
erosion above storm surge level = 24 m³/m¹

_____ pre-storm profile
_____ post-storm profile, measured
_ _ _ post-storm profile, computed
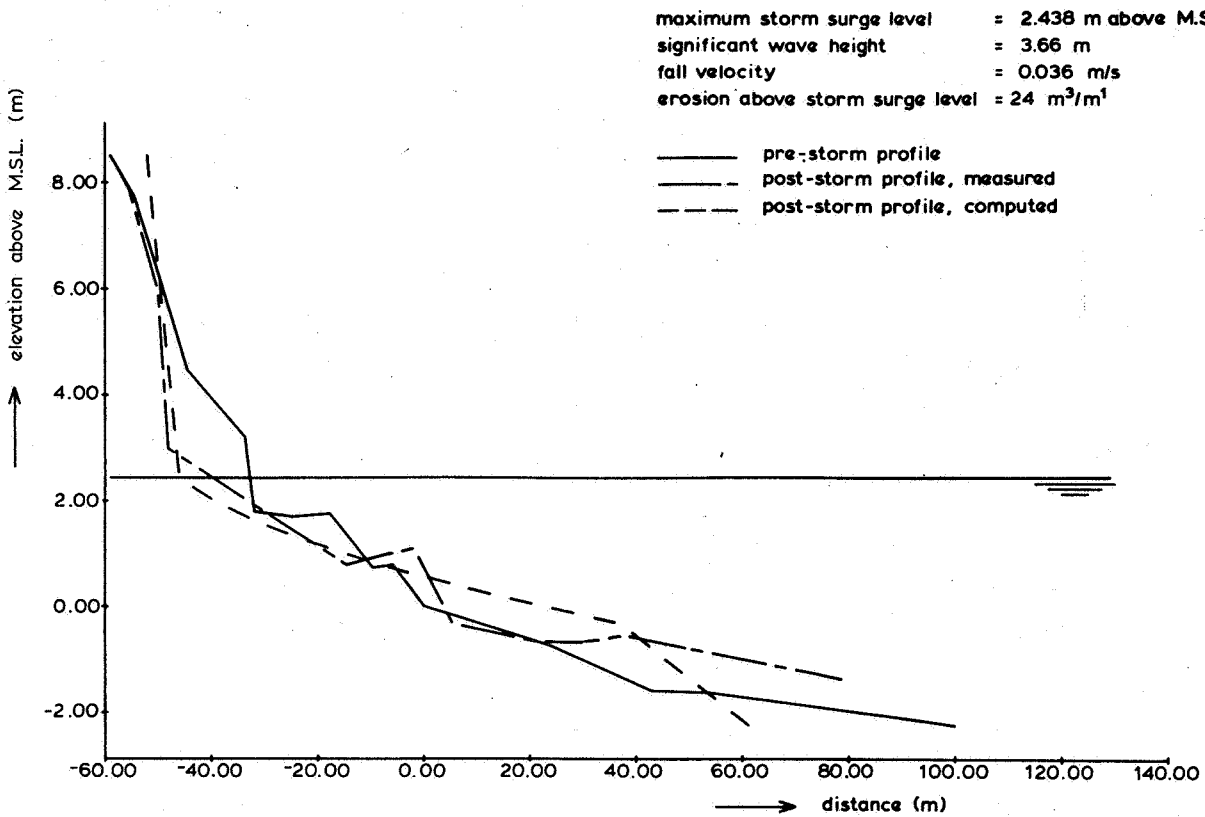
## 6.6 Accuracy of the prediction model

The prediction model was developed on the basis of model tests. The results of these tests have two sources of inaccuracy:

1) Inaccuracies of the measurements in the scale model (viz. initial profile, water level, wave height, grain size, and the resulting erosion quantity).

2) Inaccuracies in the scale relations for the conversion of model data to prototype

During the research relatively little attention was paid to an analysis of the accuracies. Too much was uncertain about the predominant parameters in the process to develop a realistic fault tree. Only as a part of the final series of small scale model tests certain test conditions were repeated six times to investigate repeatability.

The standard deviation of the measured erosion quantity for the repeatability tests appears to be only 3.3 % of the average of the measured values at t = 1 hr in the model as is shown in Table 25.

| Dune erosion quantity in repeatability tests, measured values and standard deviation | | | | | |
|---|---|---|---|---|---|
| test number | erosion quantity in $m^3/m^1$ | | | | |
| | time in hours after start of test | | | | |
| | 0.1 | 0.3 | 1.0 | 3.0 | 6.0 |
| T04 | 0.0834 | 0.1595 | 0.2348 | 0.3178 | 0.3687 |
| T15 | 0.0618 | 0.1375 | 0.2513 | 0.3178 | 0.3660 |
| T16 | 0.0763 | 0.1708 | 0.2483 | 0.3356 | 0.3650 |
| T17 | 0.0601 | 0.1215 | 0.2447 | 0.3215 | 0.3663 |
| T18 | 0.0510 | 0.1177 | .0.2315 | 0.3138 | 0.3481 |
| T19 | 0.0626 | 0.1369 | 0.2343 | 0.3252 | 0.3601 |
| T20 | 0.0564 | 0.1296 | 0.2346 | 0.3196 | 0.3605 |
| average | 0.0645 | 0.1391 | 0.2399 | 0.3216 | 0.3621 |
| standard dev. | 0.0114 | 0.0195 | 0.0080 | 0.0071 | 0.0069 |
| relative standard dev (%) | 17.7 | 14.0 | 3.3 | 2.2 | 1.9 |

**Table 25** Erosion quantities, standard deviation for a series of six tests in identical conditions

However, when the results of all tests are considered the scatter in the erosion quantities for a certain initial profile is much larger, see 5.2 and Figures 65, 66 and 67. Thus there must be other sources of inaccuracy. One source that has not been covered by the repetition tests is the inaccuracy of of the grain size. Another source is formed by the specific properties of a test facility and the measuring instruments. And, last but not least the inaccuracy of the scale relations should be mentioned. It has been shown in the previous chapters that, in spite of the theoretical and experimental basis of the scale relations, some scale effects are still present. This implies that the accuracy of the prediction model as well as the accuracy of the measured prototype results, is directly affected by the accuracy of the scale relations. This means that the various sources of inaccuracy are not independent. As the relationships between these sources of errors is difficult to establish, determining the accuracy of the prediction model in a theoretical way is a complicated task. Therefore, a practical approach was chosen to obtain a reliable estimate of the accuracy.

The measured dune erosion quantities in the small scale and large scale tests were considered as 100% accurate values. Next the prediction model has been applied to compute the erosion quantity for the various measured initial profiles. The differences between the measured and the predicted erosion

quantity has been expressed as a percentage of the predicted quantity. The standard deviation of these differences is 15% of the computed values. This means that the accuracy of the prediction model can be described by

$$\sigma_A = 0.15 \ A \tag{147}$$

in which A is the computed erosion quantity above storm surge level and $\sigma_A$ is the standard deviation of the differences between the predicted and the measured erosion quantities.

This definition of the accuracy applies rather well for conditions with a relatively large value for A, However, relation (147) indicates that when the computed erosion quantity is small, viz. for normal storm surges, the error in terms of $m^3/m^1$ would be very small. This does not agree with the results of the verification of the prediction model for the storm surge of 1976. In the initial stage of dune erosion the erosion quantity is strongly affected by a large number of satistically varying parameters, such as the initial steepness and soil mechanic stability of the dune front and the sequence of the waves. Thus with this combination of uncertainty a standard deviation of 1.5 $m^3/m^1$ is an unrealistically low estimate of the accuracy when an erosion quantity of 10 $m^3/m^1$ is computed. So relation (147) should be reconsidered.

A combination of an absolute quantity to cover the errors in the initial dune erosion phase, and a relative quantity to describe the errors for large erosion quantities is the most appropriate description of the overall inaccuracy of the prediction model. When the predicted results of the 1976-storm surge are considered together with the prototype data of the model tests the inaccuracy can very well be described as

$$\sigma_A = 0.10 \ A + 20 \ m^3/m^1 \tag{148}$$

The standard deviation is indicated in Figure 107 together with the model data and the field data.

Relation (148) describes the accuracy of the prediction model for given input parameters. The inaccuracy of these input parameters is an additional source of erros. The magnitude of the latter can be determined by simulation. Van de Graaff (1983) has described how the various uncertainties can be integrated into a probabilistic design of coastal dunes as a primairy sea defence system.

The application of the dune erosion prediction model and the limitations will be described in the following paragraph.
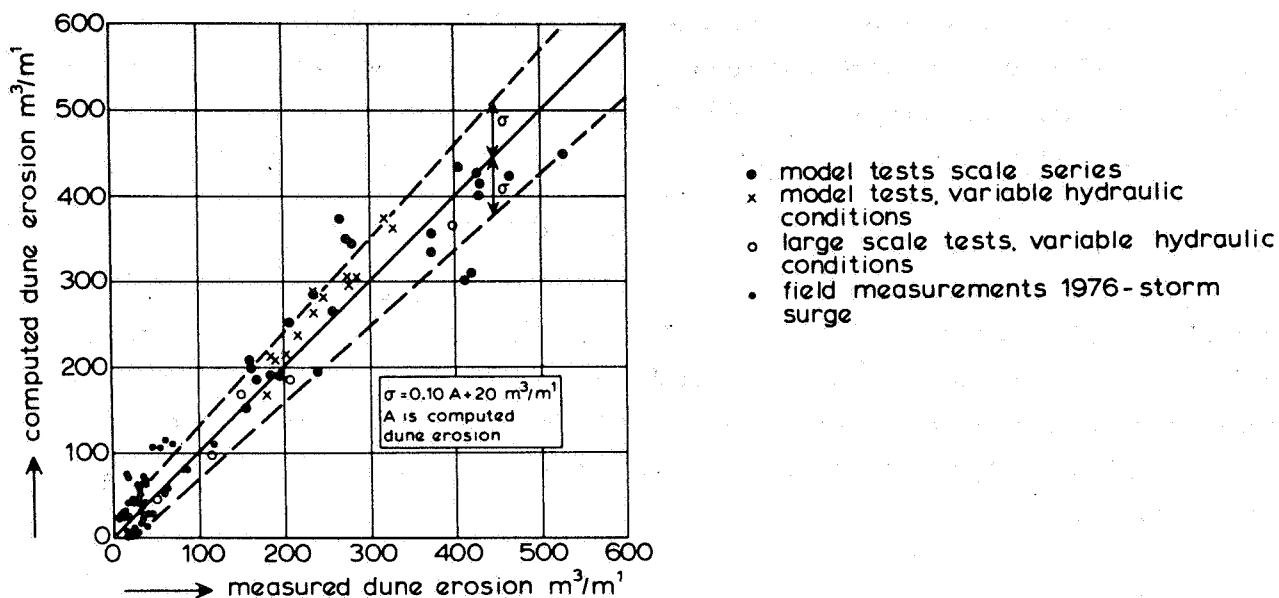
**Figure 107** Accuracy of computational model

## 6.7 Application and limitations

The dune erosion prediction model was developed on the basis of small-scale and large-scale tests with well-defined profiles and hydraulic conditions. The prediction model is based on a two-dimensional schematization of the erosion process. However, the situation in nature differs in two ways.

1) Three-dimensional effects. The sand that is eroded from the dunes will be redistributed in longshore direction as a result of longshore variations in wave conditions and beach and dune profile.

2) Inaccuracy of input parameters. The profiles and the hydraulic conditions in nature are never exactly known and will always be sources of uncertainty.

## Three-dimensional effects

The beach and dune profile may vary in longshore direction. As a result there will be a redistribution of sand during a storm surge. It has been observed in nature, that a storm surge cuts along the shore like a knife, leaving a very straight scarp of dune fronts. Apparently, in case of significant dune erosion an existing variability in longshore direction will more or less be straightened by the storm surge. This smoothening effect can be taken into account by application of a moving-average dune front recession along the shore.

The prediction model is based on a two-dimensional schematization. This means that the model is only valid for situations that are rather homogeneous in the longshore direction and thus for relatively straight beaches. An additional

amount of dune erosion should reckoned with in the case of a coastal section with a significant shoreline curvature or discontinuities in the erodibility of the beach and dune ridge. The additional amount of erosion compensates for the loss of sand in a coastal profile due to longshore transport gradients.

**Inaccuracy of input parameters**

Initial profile. The exact beach and dune profile just before a storm surge is hardly ever known. So the initial profile to be applied in the prediction model will always be a "best estimate". The sensitivity to variation in the initial profile can be determined by application of a series of initial profiles recorded at different times.

Storm surge level. A variation in storm surge level of 0.10 m gives a variation in dune erosion quantity in the order of 10 $m^3/m^1$ to 15 $m^3/m^1$ (see section 6.4). For practical situations the inaccuracy of the storm surge level can be expressed in terms of erosion quantities by simulation of a range of storm surge levels.

Wave height. A variation in wave height of 0.10 m gives a variation in dune erosion quantity in the order of 5 $m^3/m^1$ (see section 6.4). The actual inaccuracy of the wave height can be expressed in terms of erosion quantities by simulation.

Grain size. The rate of dune erosion is very sensitive to the grain size. A variation in grain size of 10% gives a variation in dune erosion quantity in the order of 15%. For actual situations the inaccuracy in the grain size can be expressed in terms of erosion quantities by simulation.

Duration of the storm surge. The dune erosion prediction model was developed for extreme storm surges occurring at the North Sea coast of The Netherlands. The prediction model is directly applicable for such storm surges. The effect of storm surges with a longer or a shorter duration can be described by analysis of the time history of dune erosion for tests with a constant water level and tests with a varying water level (see Figure 72) and introducing an adjustment to the present predictive model.

Gusts. The way the uncertainty of the storm surge level should be taken into account has been described above (an increase in storm surge level of 0.5 m gives an increase in dune erosion quantity of about 50 $m^3/m^1$ to 75 $m^3/m^1$.) The effect of a gust, being a water level rise of short duration, say 20 minutes, is smaller than this. The effect of a gust of 0.5 m on top of the peak level

of a normal storm surge hydrograph is estimated at an extra erosion quantity of 20 $m^3/m^1$ to 40 $m^3/m^1$ for the type of profiles tested.

## 6.8 General applicability of the erosion profile

The basic erosion profile has been derived for prototype conditions with $H_{Os}$ = 7.6 m, $\hat{T}$ = 12 s and $D_{50}$ = 225 μm. Profiles for other conditions have been derived by application of the scale relations. The general formula for erosion profiles for waves with steepness $H_{Os}/L_0$ = 0.034 is

$$(7.6/H_{Os})y = 0.47 \; [(7.6/H_{Os})^{1.28}(w/0.0268)^{0.56}x + 18]^{0.5}-2.00 \tag{144}$$

The profile is shown in Figure 85 for various wave heights. The shape of the profile appears to be almost independent of the wave height. This gives support to the idea that for a certain grain size the slope of the beach is uniquely related to the wave steepness. The basic erosion profile has been chosen arbitrarily as a parabola, see relation (144). For a wide range of wave heights these parabolae nearly coincide. In view of the scale relations applied this indicates that the erosion profiles can also be described by a single power curve as will be shown hereafter.

Let us assume that the dune erosion profile is described by a power curve:

$$y = p \; x^{\gamma} \tag{149}$$

in which y is the depth below still water level and x is the distance from the water line, p is a dimensional coefficient and $\gamma$ an unknown exponent.

Let $(x_p, y_p)$ and $(x_m, y_m)$ be points in this profile in which $(x_p, y_p)$ is the prototype image of $(x_m, y_m)$. So:

$$y_p/y_m = n_d \tag{150}$$

$$x_p/x_m = n_1 \tag{151}$$

$$y_p = p \; (x_p)^{\gamma} \tag{152}$$

$$y_m = p \; (x_m)^{\gamma} \tag{153}$$

The ratio of (152) and (153) and substitution of (150) and (151) yields:

$$n_d = (n_1)^{\gamma} \tag{154}$$

The earlier derived scale relation is:

$$n_1/n_d = (n_d)^{0.28}, \text{ which can be written as } n_d = (n_1)^{0.78} \tag{155}$$

Equating (154) and (155) yields $\gamma = 0.78$ and:

$$y = p \, x^{0.78} \tag{156}$$

The value of p can be derived from the original data of the basic erosion profile shown in Figure 82. Curve fitting gives $p = 0.080 \, m^{0.22}$ for sand with $D_{50} = 225 \, \mu m$ and $w = 0.0268 \, m/s$, so that:

$$y = 0.080 \, x^{0.78} \quad (x \text{ and } y \text{ in m}) \tag{157}$$

**comparison with 2/3 power curve**

It is very interesting to compare relation (157) with beach profile power curves developed by Bruun (1954), Dean (1977) and Hughes (1978). They find that beach profiles in the field can reasonably well be described by the power curve $y = p \, x^{2/3}$. Bruun (1954) finds theoretical support for this power curve by reasoning that the beach profile is formed by the onshore component of the shear stress due to wave action and that this shear stress should be constant both in time and along the onshore axis, and that the spatial gradient of the transported wave energy per unit area should also be constant in the onshore direction. Dean (1977) finds theoretical support for the same power curve by reasoning that nature aims at a uniform energy dissipation per unit volume of water. Bruun finds that $(y)^{3/2} = q \, x$ with $q = 0.09 \, (ft)^{1/3}$ gives the best correlation for North Sea beaches in the Thyboron area in Denmark. In the metric system this power curve can be written as:

$$y = 0.135 \, x^{2/3} \quad (x \text{ and } y \text{ in m}) \text{ (Bruun, 1954)} \tag{158}$$

Hughes and Chiu (1978) show that $p = 0.15 \, (ft)^{1/3}$ gives the best correlation for beaches along the coast of Florida. In the metric system this gives:

$$y = 0.10 \, x^{2/3} \quad (x \text{ and } y \text{ in m}) \text{ (Hughes, 1978)} \tag{159}$$

When a 2/3 power curve is fitted through the dune erosion profiles of Fig. 82 the best correlation is found for $p = 0.14$, so:

$$y = 0.14 \, x^{2/3} \quad (x \text{ and } y \text{ in m}) \text{ (present dune erosion tests)} \tag{160}$$

It should be noted that the erosion profile derived from dune erosion tests for North Sea storm surge conditions, relation (160), is practically identical to the field profiles of eroding beaches along the North Sea coast in Denmark, relation (158). This implies that relation (157), $y = 0.080 \ x^{0.78}$, will also give an accurate description of the Danish beach profiles analysed by Bruun (1954).

The power curves (157), (158), (159) and (160) are shown in Fig. 108 together with the erosion profiles of the predictive dune erosion model. There appears to be a substantial difference between the field data and related power curve of Hughes (1978) on the one hand, and the dune erosion profiles and Bruun's field profiles on the other. The Florida profile is much more gentle than the North Sea profiles. The reason may be the difference in wave conditions and tidal conditions and/or the difference in the grain size distribution across the coastal profile. Further data collection and data analysis may be able to explain the discrepancy.

Note: The theoretical derivation of the 2/3 power curve by Dean (1977) is very elegant. The 2/3 power curve fits so well with the data of Hughes and Chiu (1978) as well as with the dune erosion profiles and the data of Bruun (1954) that one would readily accept the underlying hypothesis of a uniform energy dissipation per unit volume of water. However, this hypothesis only leads to a 2/3 power curve in case of monochromatic waves, linear wave theory, a constant breaker index, and only if the beach profile landward of the point of initiation of breaking is considered. If the hypothesis is elaborated for a complete wave climate, which consists of a wide range of wave spectra, a 2/3 power curve will not necessarily be found. For further research it will be interesting to check the physical background of this hypothesis under such conditions.
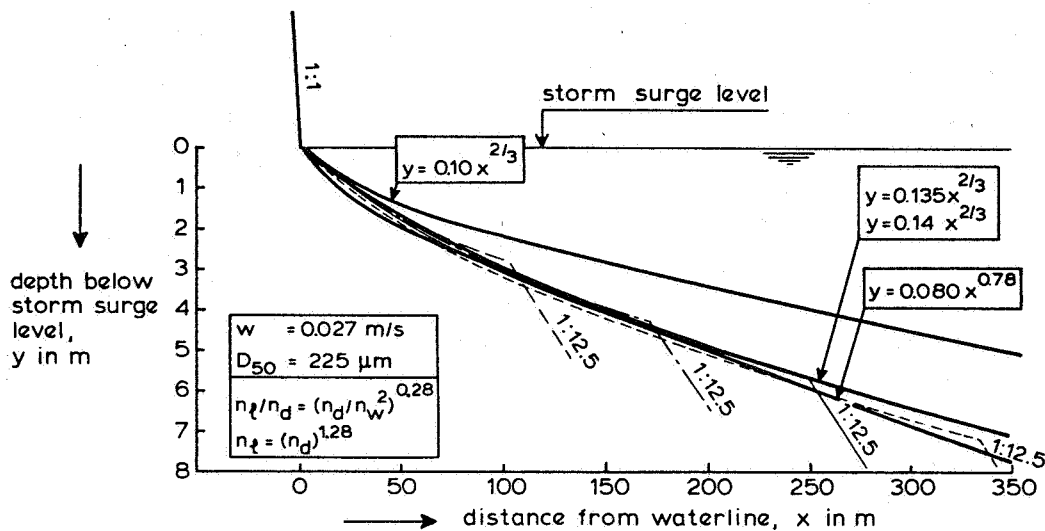


**Figure 108** Dune erosion profiles and various power curves

**Tentative description of a universal erosion profile for sandy beaches, gravel and rock beaches**

It has been shown that the effect of the grain size on the erosion profile can be described by the scale relation:

$$n_1/n_d = (n_d/n^2_w)^{0.28} \tag{4}$$

in which w is the fall velocity of a sand particle with $D = D_{50}$ in stagnant water.

Relation (4) can also be written as:

$$n_1/n_d = (n_d)^{0.28} (n_w)^{-0.56} \tag{161}$$

The fall velocity can be introduced in the power curve that describes the erosion profile. This yields:

$$y = p_1 [(w)^{0.56} x]^{0.78} = p_1 w^{0.44} x^{0.78} \tag{162}$$

Elaboration of the results of the model investigation of dune erosion has shown that erosion profiles that develop during storm conditions are described rather well by the power curve, $y = 0.08 x^{0.78}$. After introducing the fall velocity according to the scale relations, a general erosion profile is found:

$$y = 0.39 w^{0.44} x^{0.78} \tag{163}$$

in which y is the depth below still water-level in m, x is the distance from the water line in m and w is the fall velocity for $D = D_{50}$ in m/s.

Relation (163) describes erosion profiles from the water line down to a depth of approximately 0.7 up to 1.0 times the significant wave height. It gives an accurate description of the erosion profile under model conditions with random waves with $H_{0s}/L_0 = 0.025$ up to $H_{0s}/L_0 = 0.034$, for $H_{0s} = 0.04$ up to $H_{0s} = 2.1$ m, and for sediments with $D_{50} = 90$ µm up to $D_{50} = 225$ µm. Relation (163) has been verified with reasonable success in the field for conditions with $H_{0s} = 3.0$ m up to $H_{0s} = 8.0$ m, with $H_{0s}/L_0 = 0.025$ up to $H_{0s}/L_0 = 0.04$, and for beach sand with $D_{50} = 160$ µm up to $D_{50} = 400$ µm. It is also supported by the field data of eroding beaches in Denmark presented by Bruun (1954).

Bruun (1984) illustrates that the distortion relation $n_1/n_d = (n_d/n^2_w)^{0.28}$ is valid when tests with rocky material are compared to tests with sand. This result and a preliminary verification by results from model tests with gravel by van Hijum and Pilarczyk (1982) and by field data provided by Dean (1983) indicate that relation (163) also gives a reasonably accurate description of rock beaches.

Relation (163) can be simplified by introducing:

$$p = 0.39 \ w^{0.44} \qquad\qquad (164)$$

and tabulating p in terms of the grain diameter.
This yields:

$$y = p \ x^{0.78} \qquad (\text{x and y in m and p in } (\text{m})^{0.22}) \qquad (165)$$

The value of p is shown in Fig. 109 as a function of the grain size. As can be seen, relation (165) agrees reasonably well with the field data provided by Dean (1983).

The relation between the grain diameter D, and the fall velocity w, for grains larger than 0.004 m can be described by:

$$w = 1.1(\Delta gD)^{0.5} = 4.36 \ D^{0.5} \qquad (\text{Newton range for fall velocities}) \qquad (166)$$

For such grain sizes the coefficient in the power curve describing the profile is dimensionless:

$$y = 0.75 \ D^{0.22} \ x^{0.78} \qquad (\text{coefficient 0.75 is dimensionless}) \qquad (167)$$

This is not surprising as for $w \sim D^{0.5}$ the basic scale relation (4) can be written as:

$$n_l/n_d = (n_d/n_D)^{0.28} \qquad\qquad (168)$$
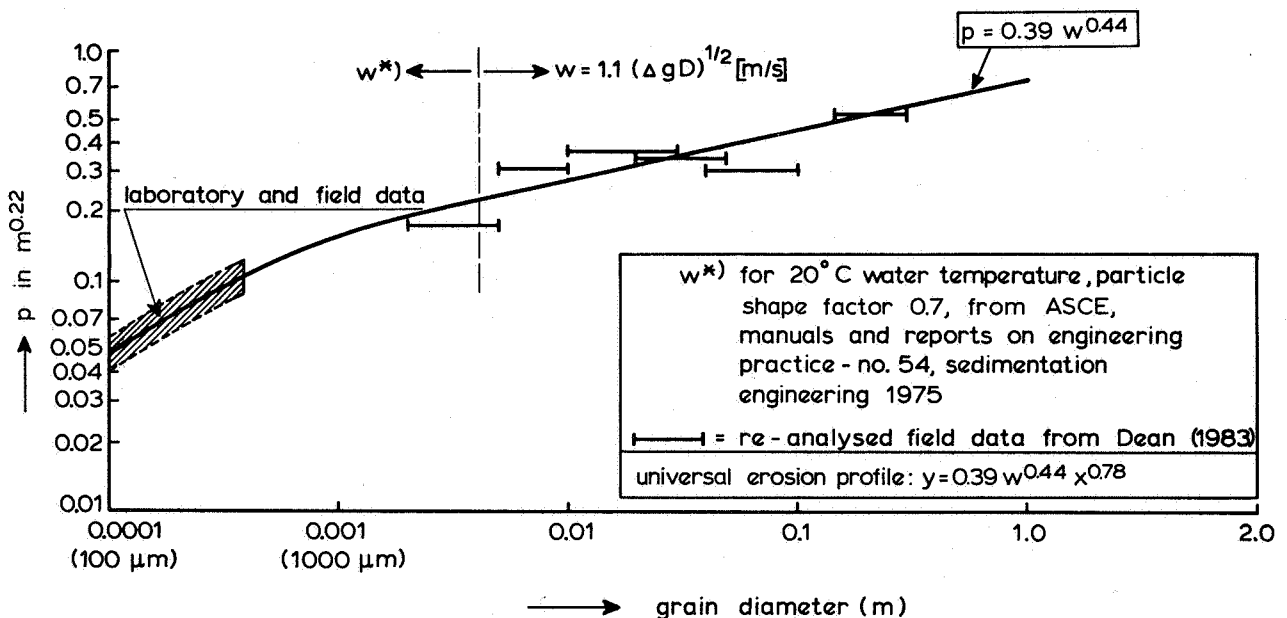


**Fig. 109** Universal erosion profile, relation between grain diameter and erosion profile.

Relation (168) shows that geometrically similar (so undistorted) profiles will be generated if $n_D = n_d$ and D is larger than 0.004 m. This is in agreement with the results obtained by Van Hijum and Pilarczyk (1982). They conclude that scale effects (viz. distorted profiles) in small-scale modelling of gravel beaches are avoided if the grain diameter in the model $D_{90}$ is larger than 0.006 m.

The results presented above give support to the idea of a universal, grain-size dependent S-shaped erosion profile for sand beaches, gravel beaches and rock beaches. In this context relation (163) should be regarded as the description of the main part of the profile. For practical use the profile should be completed for the area above still water and below the water depth $d \simeq H_{0s}$. With respect to its use in engineering practice it should be stressed that relation (163) has been checked for sandy beaches with $H_{0s}/L_0$ in the order of 0.034. For rock beaches a further verification is definitely required.

**Fall velocity and profile development**

The results of the dune erosion model tests with four different grain sizes have shown that the fall velocity is a major parameter for beach profile development. A verification of relation (163) has indicated that this may also hold for rock beaches. In view of the physical processes this seems logical. Equilibrium profiles are generally defined as profiles that maintain their form with time. However, this does not imply that the individual elements of such a profile are in static equilibrium. In every point of an equilibrium profile the time-mean up-slope transport balances the time-mean down-slope transport. The gross transports will vary along the profile. They will be zero at the upper end (outside the reach of the water) and at the lower end (beyond the depth of incipient motion). It is reasonable to suppose that the horizontal distance between these ends and hence the steepness of the profile is determined by a property of the transport system which may be called the diffusivity of the transport process.
Such a "diffusivity" can be defined as the degree of correlation between the transports at different places along the profile. It will mainly be determined by the speed at which the transport can adjust itself to the local hydraulic conditions by settling down and picking up of bed material (retarded adaptation). During storms the area of the active profile is increasing. It is plausible that for such conditions the adaptation of the sediment load, and hence the development of the profile is mainly determined by the spatial gradient in the "suspension" transport and thus by the settling velocity of the grains.

# 7. The process of dune erosion

## 7.1 Introduction

The scale relations and hence the dune erosion prediction model, are based on a theoretical description of the offshore sediment transport process in terms of sediment concentration and return flow velocity, see 3.5.

In the model tests the wave height, the velocity field and the sediment concentrations were measured at various positions along the profile. These data will be described and analysed in this chapter. Moreover, the theoretical description of the offshore sediment transport process will be verified and a tentative numerical model for sediment transport and time dependent beach and dune profile changes will be developed.

Simultaneously with the present dune erosion studies a number of other researchers has investigated the experimental and numerical simulation of dune erosion and cross-shore sediment transport. With respect to this the results of Hughes (1983), Hallermeier (1985), Kriebel and Dean (1985) and Stive and Battjes (1984) will be discussed in this chapter.

Finally the results of the present investigations will be evaluated, the future possibilities and problems regarding the modelling of coastal erosion during storm surges will be discussed and recommendations for further research will be given.

## 7.2 Wave height, velocity field and sediment concentration measurements

The measurements during the tests were focussed on the control of the hydraulic conditions and the recording of the profile changes. Measuring the wave height along the profile, the velocity field and the sediment concentrations had second priority. However, as the research programme evolved more and more attention was paid to measurements related to the sediment transport process. A large amount of data has become available, from the large-scale tests as well as from the small-scale tests. All measurements have been reported by Delft Hydraulics Laboratory (1984 and 1985). The most relevant results with respect to the analysis of the process are described hereafter.

### wave height

The wave height along the profile was measured during the large-scale tests with a water surface follower and with an acoustical device. The significant wave height measured during test 1 is shown in Figure 110. The most landward positions have been recorded by means of pressure gauges, installed in the wall of the flume. With these instruments the wave set up and the wave run-up was also measured (see Figures 111 and 112).

The detailed run-up and wave-overtopping results are reported in Delft Hydraulics Laboratory (1983) and (1984).

The most important conclusion from the wave measurements is that the ratio of the wave height over the waterdepth is in the order of 1 and even higher in the zone of the rapid profile changes. This means that the waves are mainly plunging breakers, which was confirmed by visual observations. The breaking waves have a strong impact on the entrainment of sediment. A considerable volume of air is enclosed by the overturning wave. Directly after the wave has overturned the compressed air "explodes" creating a fountain and "boiling water". It was observed that large quantities of sediment are stirred up by these plunging waves and kept in suspension by the "boiling" water thereafter.

In the initial phase of the process the beach slope is in the order of 1:10 to 1:20 depending on the position. In the final phase as the equilibrium profile is approached, the beach slope is in the order of 1:20 to 1:50. This suggests that in the course of the dune erosion process the breaking wave type changes from predominantly plunging to predominantly spilling.

The wave height attenuation along the profile is shown for large scale test 2 in Figure 113. The wave height measured during the series of small scale repetition tests is shown in Figure 114. The present investigations as well as those of Stive (1985) show that the wave conditions are reproduced very well if the Froude scale relations are satisfied.
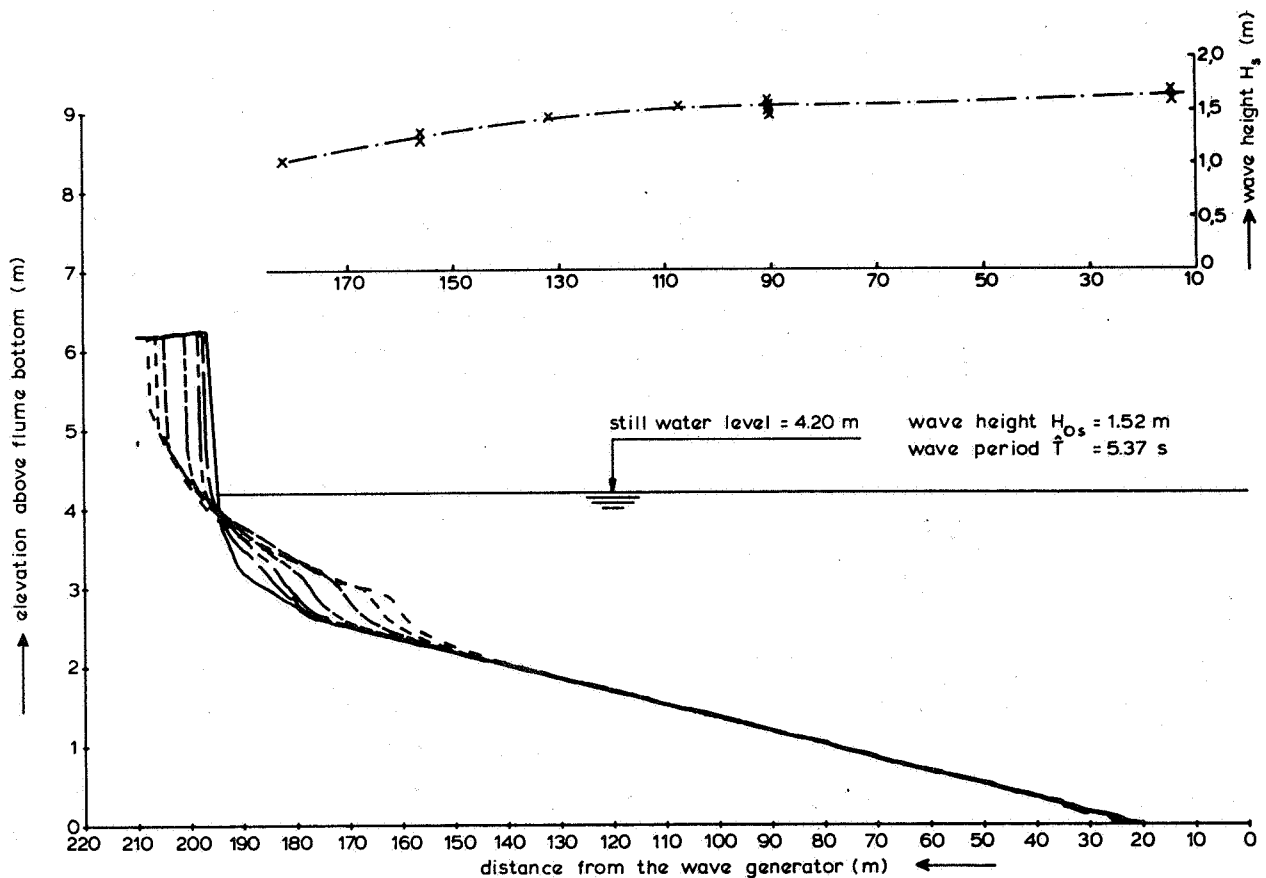


**Figure 110** Wave height attenuation along the profile, large-scale test 1
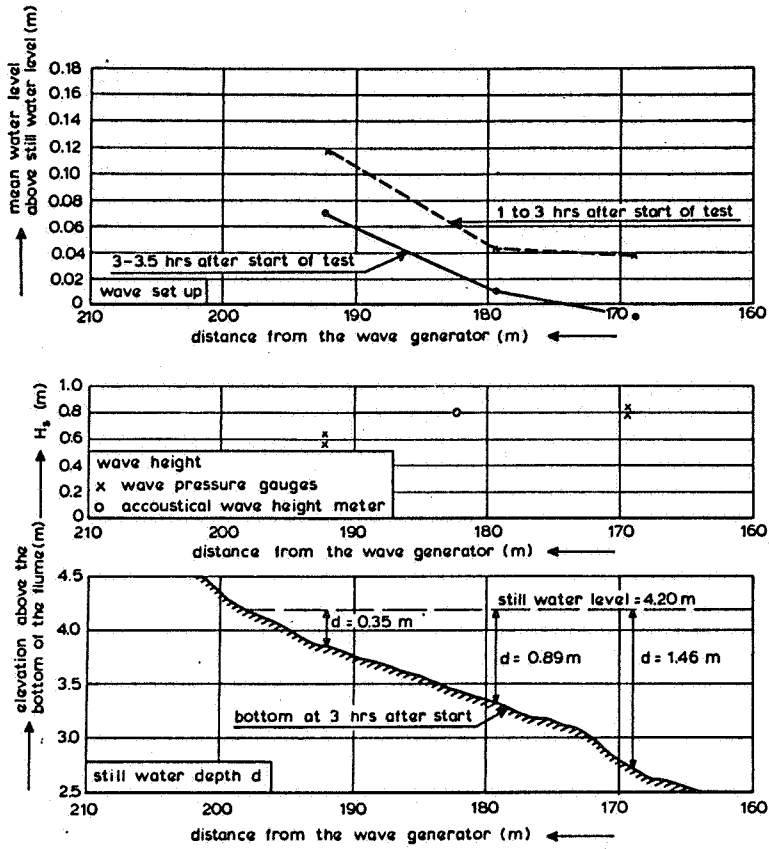
**Figure 111** Wave set-up and wave height, measured during large-scale test 1.
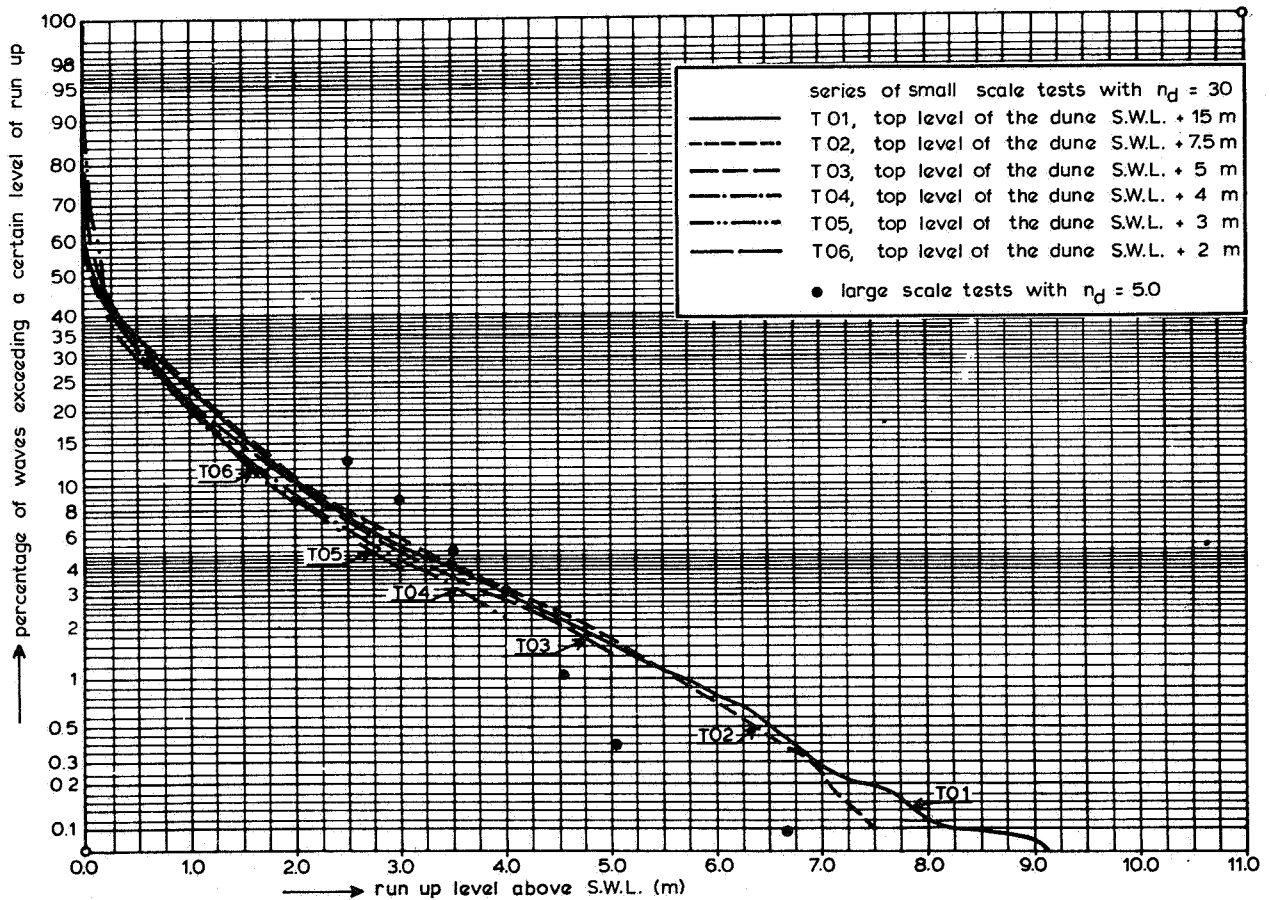


**Figure 112** Wave run-up small-scale tests and large-scale test 1
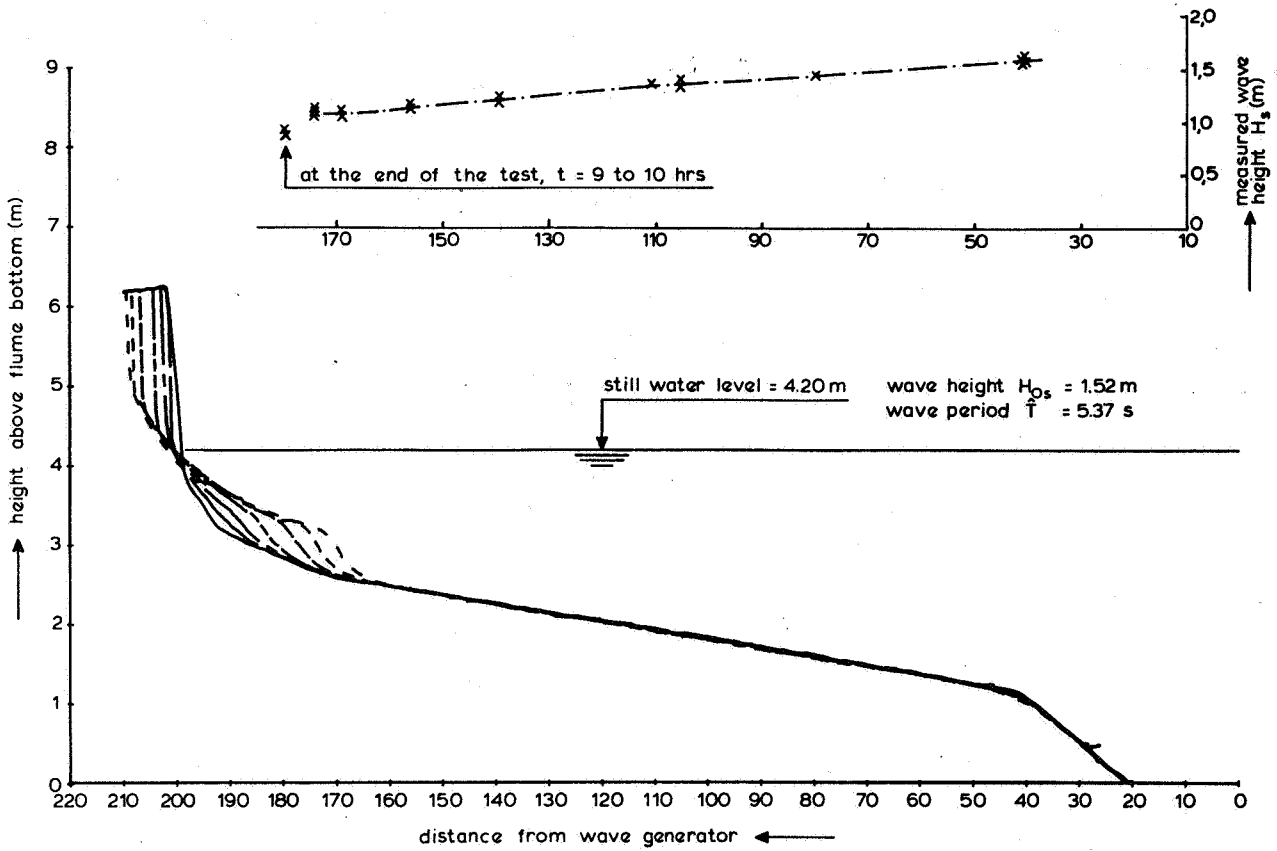
**Figure 113** Wave height attenuation along the profile, large-scale test 2
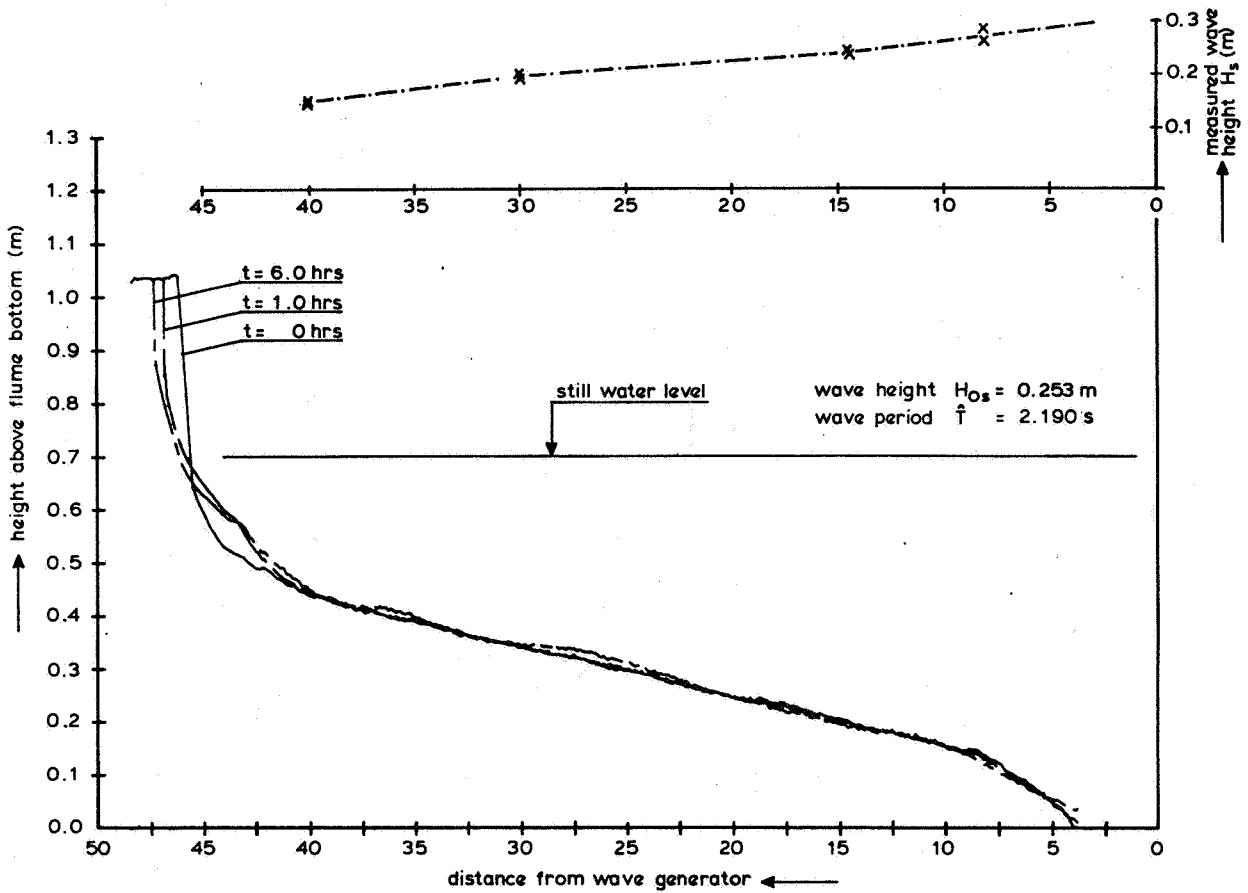


**Figure 114** Wave height attenuation along the profile, small-scale repetition tests

## velocity field

The velocity field was measured using an acoustic (doppler) current meter, as described by Janssen (1978). Measurements were taken during the large-scale tests and during the series of small-scale repetition tests. The detailed results are reported in Delft Hydraulics Laboratory (1984 and 1985). A selection of the results, relevant for the investigation of the sediment transport process, is presented below.

The results of the velocity measurements are expressed in terms of the time-averaged velocity $\bar{u}$ and the "significant" orbital velocity $u_{15}$.
The velocity was measured at various positions between the bottom and the level of the wave troughs. The results indicate that the vertical gradient of the measured velocities is practically zero. Therefore, the results presented below were averaged over the water column (from the bottom to the level of the wave troughs).

The time-averaged velocities measured in large-scale test 1 and 2 and in small-scale tests T15-T20 are shown in Figures 115, 116 and 117, respectively. The time-averaged flow below the troughs has a seaward direction in all positions. This current, called untertow, is part of the wave induced vertical circulation in the surf zone.

The time-averaged velocity measured in the large-scale tests in the zone of rapid profile changes has a value of 0.20 to 0.30 m/s. The corresponding velocity measured in the small-scale tests is 0.08 to 0.12 m/s. According to the Froude scale relations the ratio of the velocities of the large-scale and the small-scale tests should be

$$n_u = (n_d \text{ large-scale}/n_d \text{ small-scale})^{0.5} = (30/5)^{0.5} = 2.4 \tag{169}$$

The ratio of the measured velocities is about 0.25/0.10 = 2.5, which illustrates the validity of the Froude scale relations.

For a further analysis the orbital velocity is also expressed in terms of $u_{15shw}$, $u_{15sew}$, $u_{15}$ and $\Delta u_{15}$, in which $u_{15shw}$ is the orbital peak velocity in the shoreward direction that is exceeded by 15% of the number of waves. This parameter can be considered as a "significant" orbital velocity. The $u_{15sew}$ is the orbital peak velocity in the seaward direction that is exceeded by 15% of the number of waves; $u_{15}$ is the average of $u_{15shw}$ and $u_{15sew}$; $\Delta u_{15}$ is $u_{15shw} - u_{15sew}$. The measured values for $u_{15}$ and $\Delta u_{15}$ are also shown in Figures 115, 116 and 117. Some interesting aspects of the measurements are mentioned below.

The orbital velocity $u_{15}$ increases with decreasing water depth. The velocities at the waterline are 30% to 50% higher than just outside the breaker zone. The value for $u_{15}$ measured during the large scale tests is about 1.5 m/s. This means that the value for $u_{15}$ in prototype is about 1.5 $(5)^{0.5}$ = 3.5 m/s. The maximum orbital velocity will even be considerably higher. The measurements converted to prototype indicate a maximum peak velocity of 5 m/s.

The value for $\Delta u_{15}$ is positive in the seaward part of the breaker zone. This means that the shoreward component of the orbital peak velocity is larger than the seaward component, which implies a net shoreward sediment transport component. The value for $\Delta u_{15}$ is negative in the most landward part of the surf zone which indicates a net seaward sediment transport component.

For a further analysis of the velocity field the attention is focussed on the various phases of the dune erosion process.

The most detailed measurements of the velocity field are available from the small-scale tests. The velocity field has been measured in three different cross-sections within the zone of rapid profile changes, see Figure 117. The vertical distribution and the time average velocity $\bar{u}$ at various stages of the erosion process are shown in Figure 118 for the most relevant section, section 2. The results are shown relative to the (changing) bottom as well as relative to the still water surface. It can be seen that the magnitude of the time averaged return current remains fairly constant although the shape of the profile and the water depth are changing considerably. The constancy is even more striking when the water circulation is considered in terms of volume, see Figure 119.

ū (m/s) is time and vertical
average velocity between
bottom and wave troughs
in a seaward direction
(x = measurements)

u₁₅ (m/s) is 'significant' peak
velocity of orbital motion,
average over the vertical,
average of seaward
and shoreward component
(x= measurements)

Δu (m/s) is the difference
between shoreward and
seaward component of
orbital velocity
(x = measurements)

4.20 m still water level

distance from the wave generator (m)

**Figure 115**  Velocity field along the profile, large-scale test 1

ū (m/s) is time and vertical
average velocity between
bottom and wave troughs
in a seaward direction
(x = measurements)

0,40
0,30  ū (m/s)
0,20
0,10
0

190    170    150    130    110    90    70    50    30    10

u₁₅ (m/s) is 'significant' peak
velocity of orbital motion,
average over the vertical,
average of seaward
and shoreward component
(x = measurements)

2,00  u₁₅ (m/s)
1,50
1,00
0,50
0

190    170    150    130    110    90    70    50    30    10

0,40
0,20  Δu (m/s)
0

Δu (m/s) is the difference
between shoreward and
seaward component of
orbital velocity
(x = measurements)

0,20
0,40

190    170    150    130    110    90    70    50    30    10

height above flume bottom (m)

9
8
7
6
5
4
3
2
1
0

4.20 m still water level

220 210 200 190 180 170 160 150 140 130 120 110 100 90 80 70 60 50 40 30 20 10 0

distance from the wave generator ←——

**Figure 116**  Velocity field along the profile, large-scale test 2
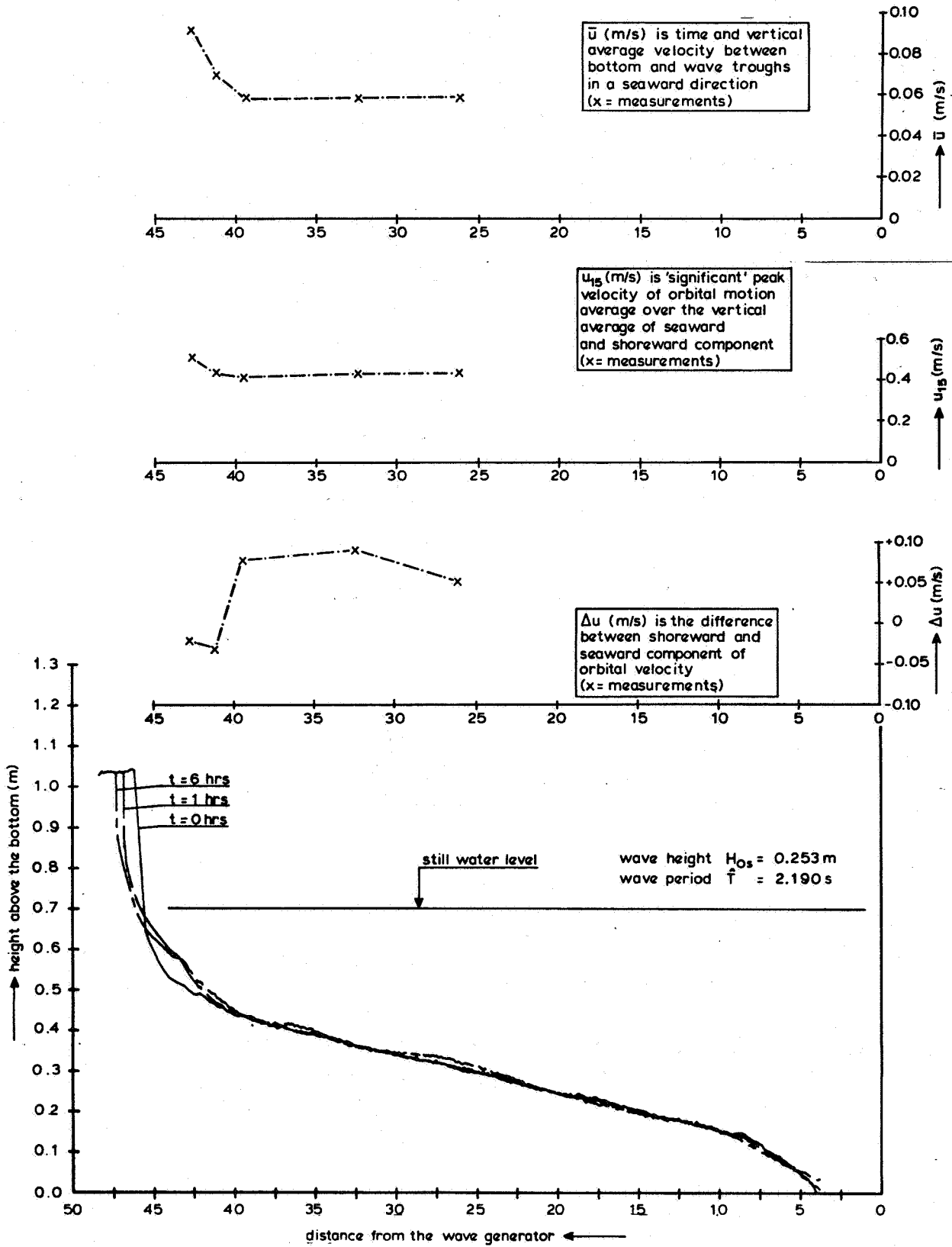
**Figure 117** Velocity field along the profile, small-scale test series
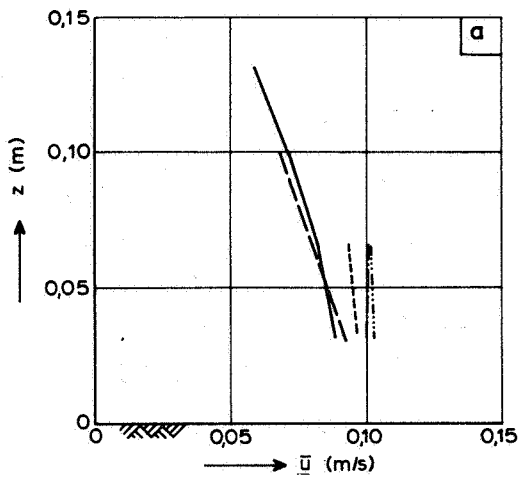
z (m) is height above the bottom
ū (m/s) is measured return flow
        velocity
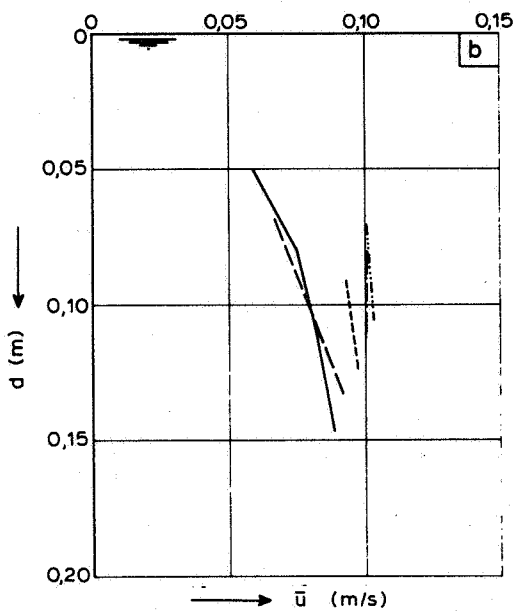
d (m) is waterdepth below still
        water level
ū (m/s) is measured return flow
        velocity

section 2
(42.87 m from
wave generator,
see Fig. 123)

t = 0 - 30 min.
t = 30 - 60 min.
t = 60 - 90 min.  after start of test
t = 90 - 120 min.
t = 5 - 6 hrs.

**Figure 118**  Velocity field at various positions and stages of the dune erosion
process; series of small-scale repetition tests, $n_d$=30
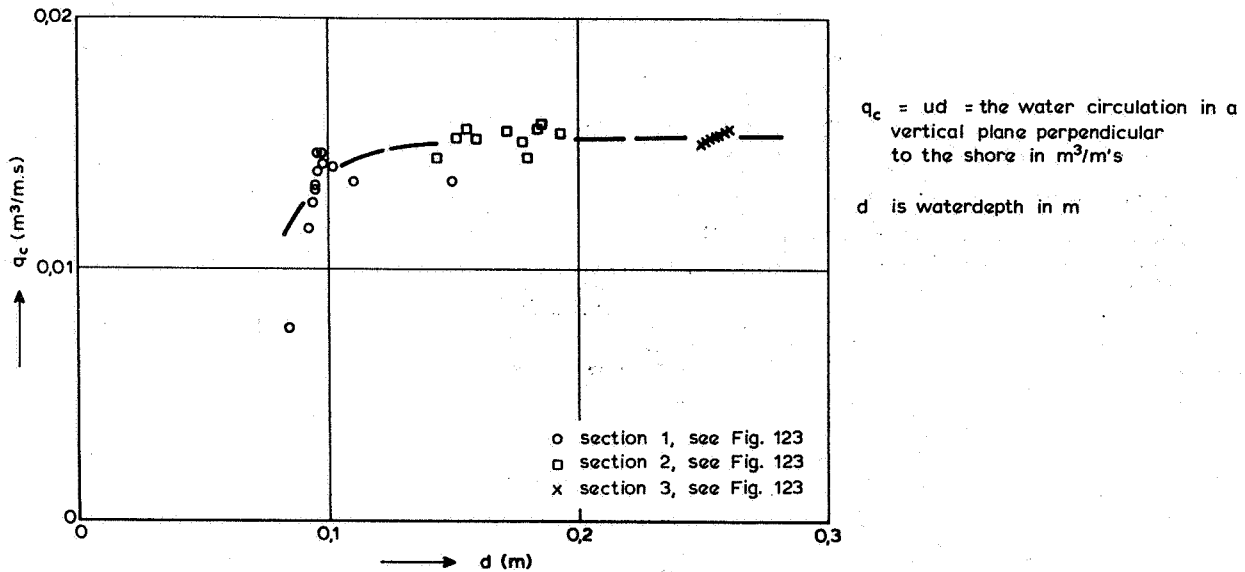
**Figure 119** Water circulation in terms of $m^3/m's$, series of small-scale repetition tests $n_d=30$

## sediment concentrations

Sediment concentrations were measured both in the large scale and in the small-scale tests by means of sampling the water-sediment mixture. The suction apparatus applied in the large-scale tests is shown in Figure 120. A similar set up has been applied during the small scale tests. The direction of suction is perpendicular to the orbital velocity direction. The intake velocity is more than four times the orbital velocity. For such conditions the efficiency is about 75% as shown by Bosman and Hulsbergen (1985). The detailed results of the measurements are reported by Delft Hydraulics Laboratory (1984 and 1985).

Some relevant examples of sediment concentrations measured in large-scale tests at various stages of the dune erosion process are shown in Figure 121. Corresponding results are given in Figure 122 for the small-scale tests.

In the large-scale tests the sediment concentrations in the zone of rapid profile changes are of the order of 10,000 mg/l, in the initial phase of the dune erosion process (see Fig. 121 a and c), and of the order of 3,500 mg/l at the same position in the final phase of the process (see Fig. 121 b and d). The corresponding concentrations during the small-scale tests are 12,000 mg/l and 5,000 mg/l (see Fig. 122 a and c and b en d, respectively).
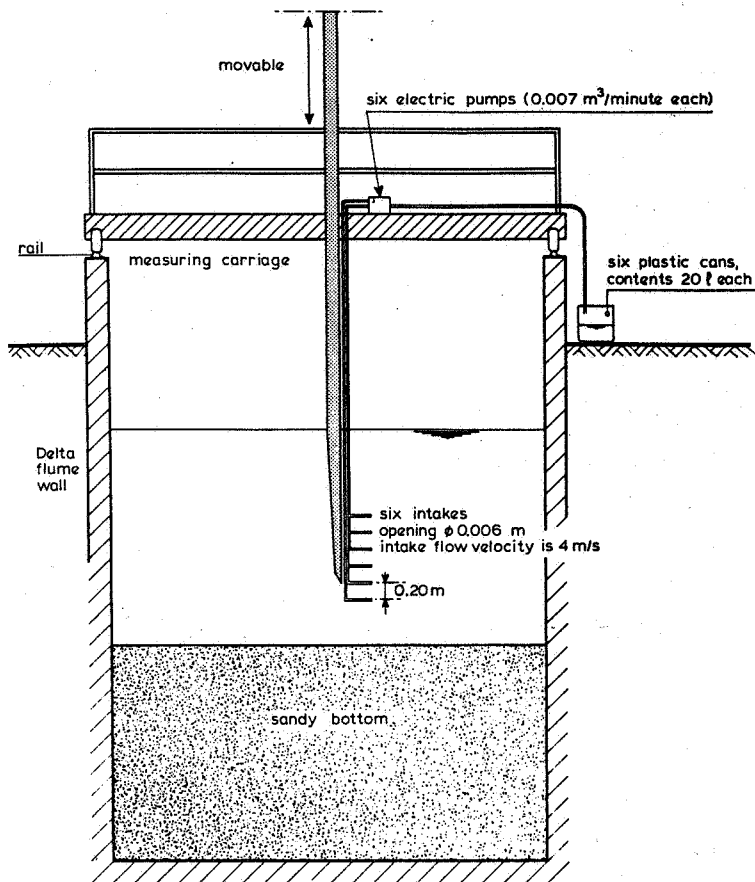
**Figure 120** Suction apparatus large scale tests

According to the theoretically derived scale relations, the scale factor for sediment concentration is (Chapter 3):

$$n_c = (n_d/n_w^2)^{0.25}$$

$$= (6/(0.0268/0.008)^2)^{0.25} = (6/11.2)^{0.25} = (0.53)^{0.25}$$

$$= 0.85. \tag{170}$$

This means that the sediment concentration in the small-scale model (with very fine sand) should be a factor $1/0.85 = 1.18$ larger than the sediment concentration in the large-scale tests. The measured results qualitatively support the theory as the measured ratios are of the order of $12,000/10,000 = 1.2$ and $5,000/3,500 = 1.4$ respectively.

In the next paragraph the results of the measurements will serve as a basis for the verification of the sediment transport process as described in Chapter 3.
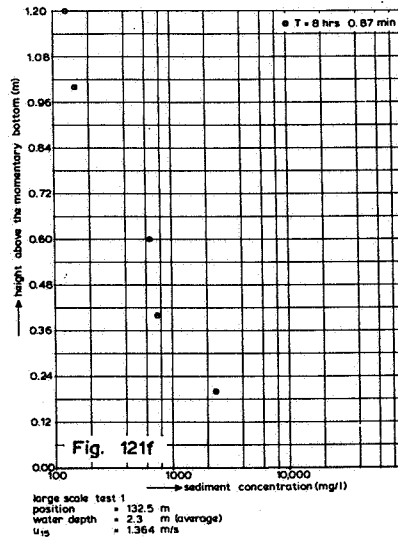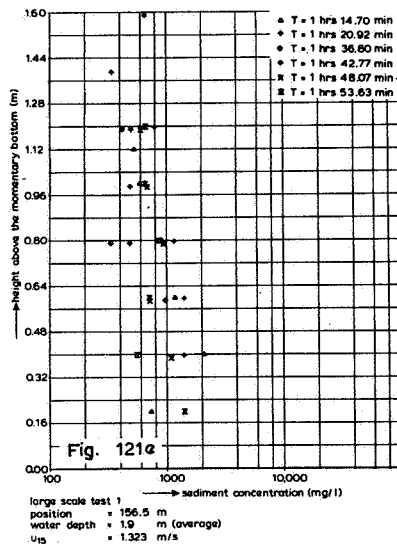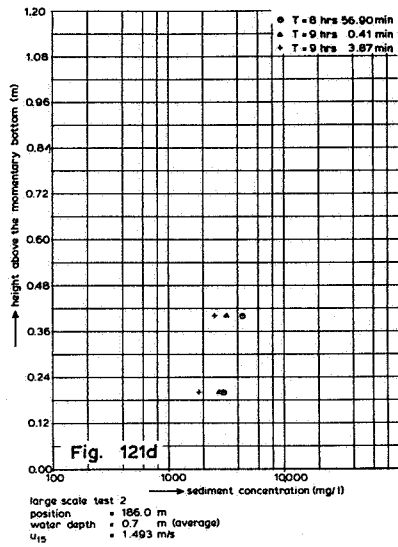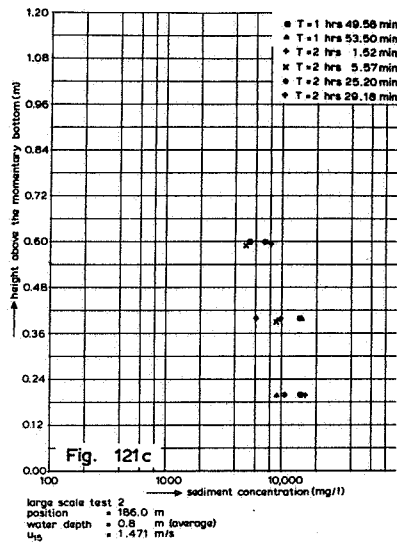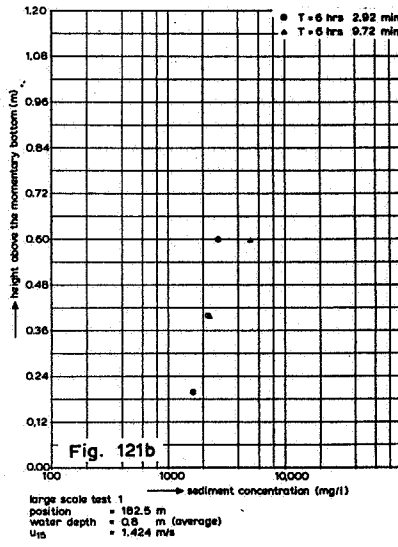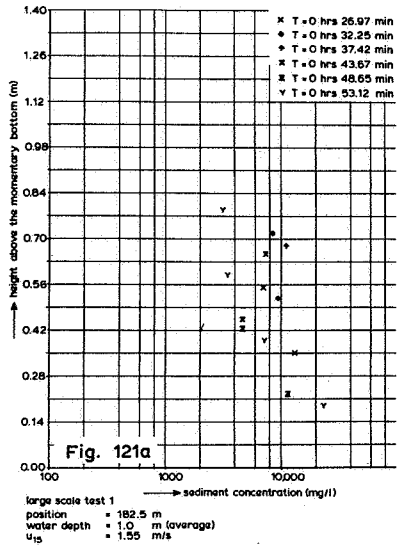
**Figure 121** Sediment concentrations large-scale test 1 and 2, various positions and stages
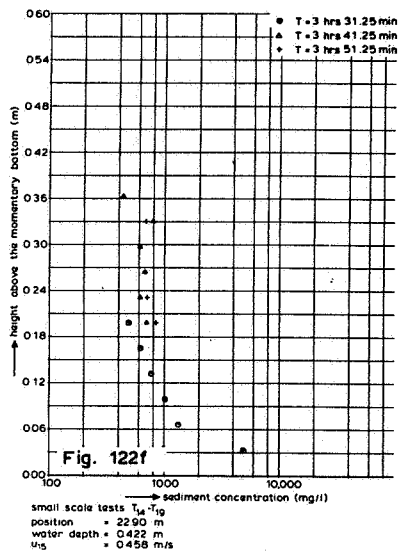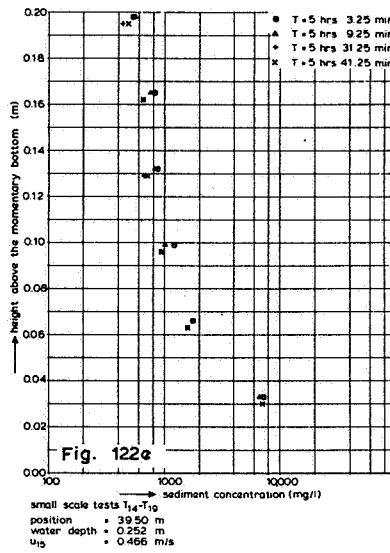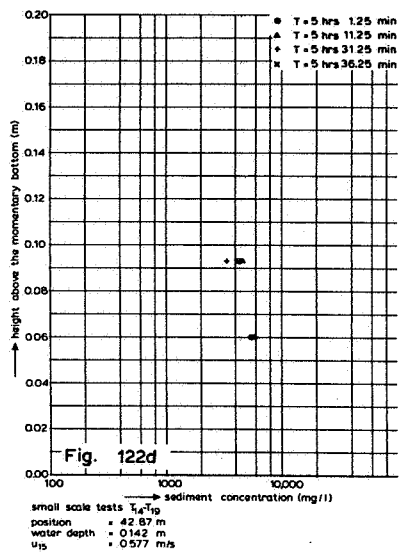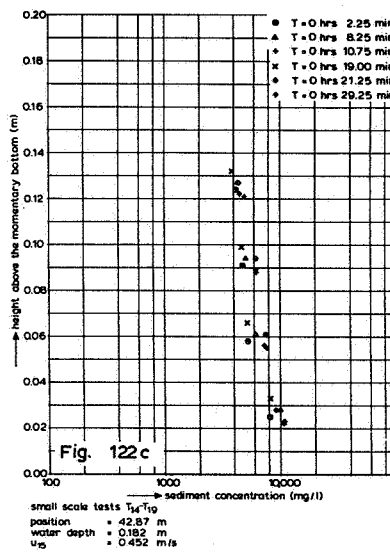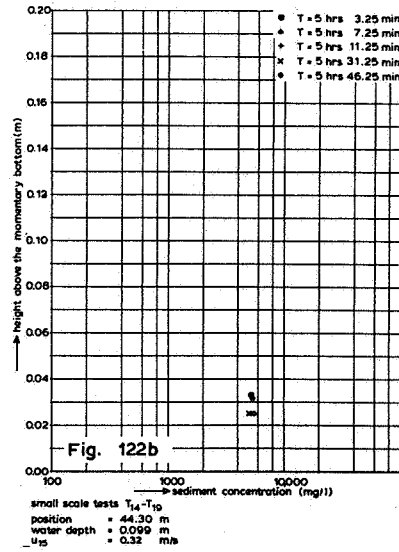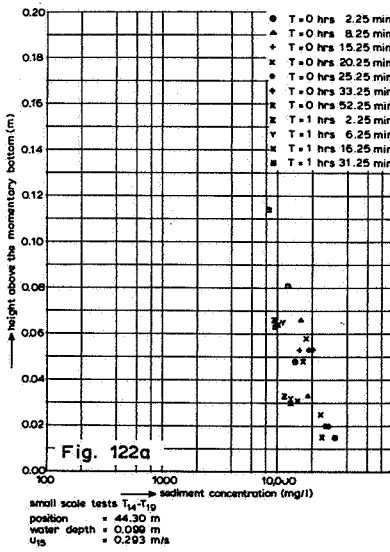
Figure 122 Sediment concentrations small-scale tests, various positions and stages

## 7.3 Offshore transport mechanism

The basic form of the scale relations was derived on the basis of a description of the offshore sediment transport in terms of dimensions.

In 3.5 it has been assumed that the sediment transport can be described by the product of the time-averaged flow velocity and the time-averaged sediment concentration. A brief verification of this hypothesis was presented by Vellinga (1982). A more detailed verification is described below.

Detailed measurements were carried out during the small-scale repitition tests. In 5 different sections the time-averaged velocity field and the time-averaged sediment concentration were measured, see Figure 123.
The product of these parameters should be compared with the measured profile changes to verify the above hypothesis.
The product of the time-averaged flow velocity and the time-averaged sediment concentration has been integrated over the water depth. For the zone below the level of the wave troughs the measured values have been taken. For the zone above this level the sediment concentration at the level of the wave troughs has been adopted. The landward flow in terms of $m^3/m$'s has been assumed to be equal to the seaward flow (continuity). The formulae are described in 3.5.

The sediment transport rate as the product of the measured water circulation and the measured sediment concentrations is compared with the sediment transport rate determined from measured profile changes in Figure 124. The results show a reasonable overall agreement in the order of magnitude. Hence it is concluded that the hypothesis underlying the theoretical description of the sediment transport process is confirmed. It should be pointed out, of course that this is a rather rough description of the process. In reality, the process of sediment entrainment, water circulation and sediment transport is much more complicated due to e.g. wave trains, surf beat, wave reflections, phase dependent sediment concentrations and phase-dependent exchange of water and sediment. Still the "first-order" description presented in 3.5 and verified in the present paragraph can be considered as a valuable basis for further research.

In 3.5 it was assumed that the sediment concentration in the zone of plunging breakers is related to the rate of wave energy dissipation. This assumption cannot be verified directly, as the wave energy dissipation has not been measured. Still the assumption can be verified by means of a transient sediment transport model. A tentative version of such a model has been developed on the basis of the sediment transport theory as described in 3.5. The computational procedure can be outlined as follows:
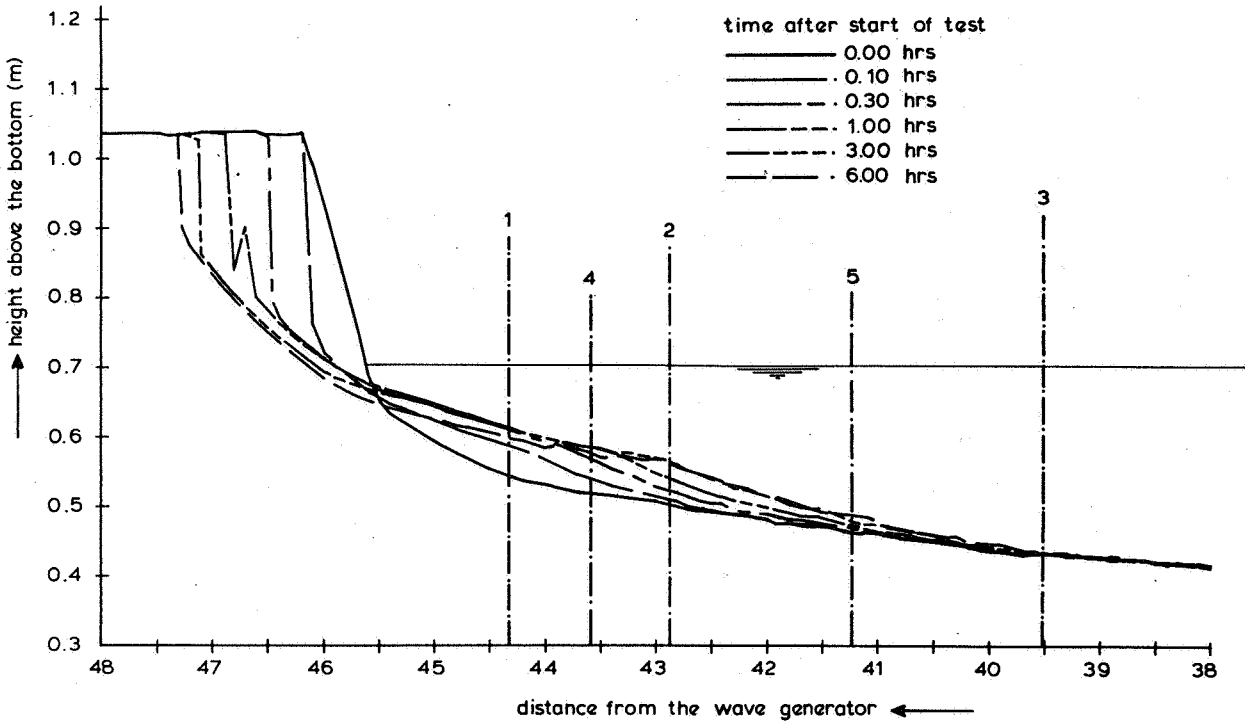
**Figure 123**  Detailed measurements small-scale repetition tests, position of the sections
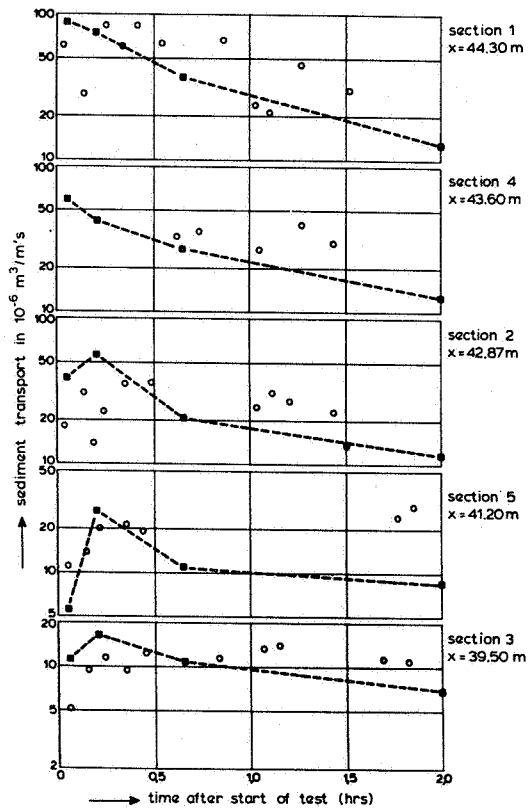


**Figure 124**  Measured profile changes versus product of time-averaged sediment concentration and time-averaged water circulation

1) wave energy decay model (Battjes and Janssen, 1978) yielding

$$H_{rms} (x), H_b (x), Q_b (x) \tag{171}$$

in which:

$H_{rms}$ is root mean square wave height

$H_b$ is breaking wave height, $H_b = \gamma d$

$Q_b$ is the fraction of breaking waves at a point

2) undertow flow velocity $\bar{u}$ (Stive and Battjes, 1984)

$$\bar{u} = 1/8 \ (g/d)^{\frac{1}{2}} \ H_b Q_b \tag{172}$$

in which:

d is still water depth

3) sediment concentration c (section 3.5 of this thesis)

$$c \sim \frac{\partial \ H_{rms}^{\ 2} \ d^{\frac{1}{2}}}{d \ \partial x} \tag{173}$$

4) sediment transport rate (see section 3.5 of this thesis)

$$S = \bar{u} \ d \ c_{eff} \tag{174}$$

in which: $c_{eff} = (c_2 - c_1) = c_3 \dfrac{\partial \ H_{rms}^{\ 2} \ d^{\frac{1}{2}}}{d \ \partial x}$ (section 3.5 of this thesis)

in which $c_2$ and $c_1$ are the time averaged sediment concentrations in the layer above and below the wave through and $c_3$ is a constant

5) bottom evolution

$$(1-p) \ \frac{\partial d}{\partial t} = \frac{\partial S}{\partial x} \tag{175}$$

in which p is the porosity of the bottom

The results of such a numerical model are shown together with the measured profile changes in Fig. 125 a and b. There is some agreement in the initial stage of the process, in that the shape of the computed profile agrees more or less with the measured profile. However, the numerical model overestimates the seaward extent of the profile and hence the rate of transport in the later stages of the process. This is explained by the fact that in the course of the process the breaking of the waves is changing from predominantly plunging to predominantly spilling. Under spilling wave conditions the suspended sediment

concentration is mainly determined by the orbital velocity and thus not so strongly related to the rate of wave energy dissipation. So for such conditions the basic assumptions are not valid.

The effect of the type of breaking of the waves has been introduced in the numerical model in a tentative way. A coefficient $c_c$, related to the ratio of the water depth and the root mean square wave height, was added to the description of the sediment concentration. The coefficient is defined as follows.

$$c_{eff} = c_c c_3 \frac{\partial}{d} \frac{H_{rms}^2 d^{\frac{1}{2}}}{\partial x} \quad \text{in which} \tag{176}$$

$$c_c = 0 \qquad \text{for } d/H_{rms} > 2$$

$$c_c = 2 - d/H_{rms} \quad \text{for } 2 > d/H_{rms} > 1$$

$$c_c = 1 \qquad \text{for } 1 > d/H_{rms}$$

The result of the numerical simulation is shown in Fig. 125c. The agreement with the measurements has considerably improved as compared with the results in Fig. 125b. but still various discrepancies between measurements and computations can be observed. The main conclusion from the "reconnaissance" computations is that the basic description of the sediment transport process as described in section 3.5, is valid for the phase of rapid profile changes. For near equilibrium conditions the assumptions with respect to the sediment concentrations and the sediment transport are not valid.

Finally it is concluded that the description of the offshore sediment transport process (section 3.5), and the scale relations that have been based on this description are valid only for conditions with plunging breakers and corresponding rapid profile changes, viz. for typically dune erosion conditions.

The results also show that the development of a numerical time dependent dune erosion model is within reach although still outside the scope of the present research project. At Delft Hydraulics Laboratory, promising developments are currently in progress (Stive, 1986; Steetzel, 1987)

FIG. 125 a



FIG. 125 b



FIG. 125 c
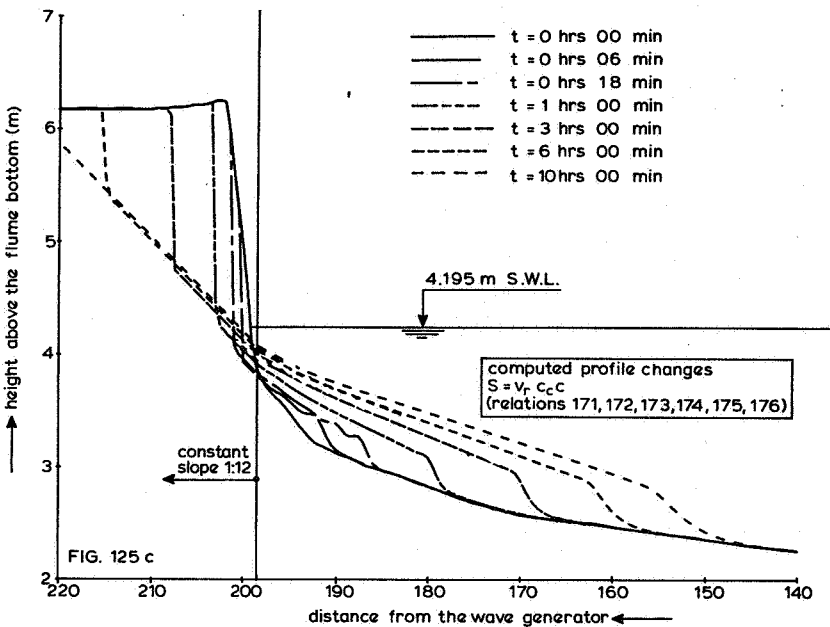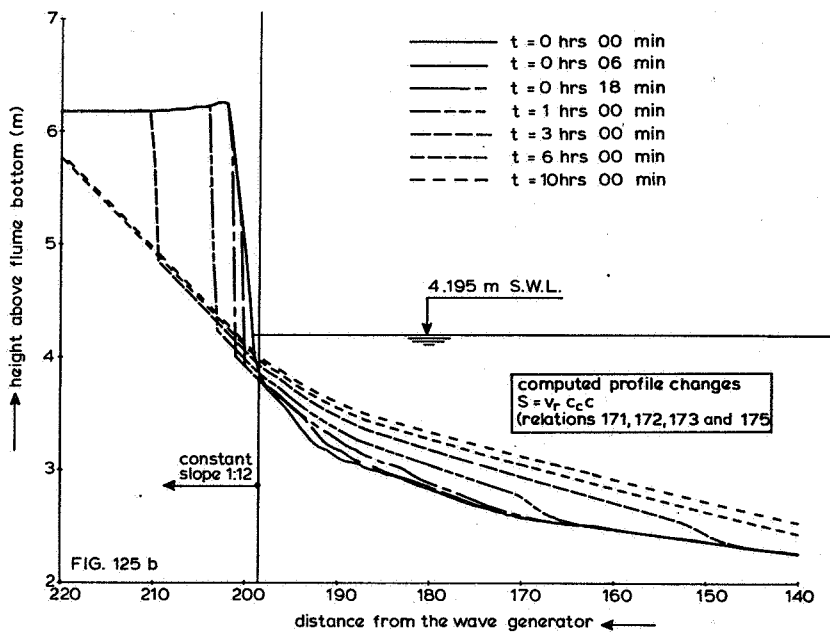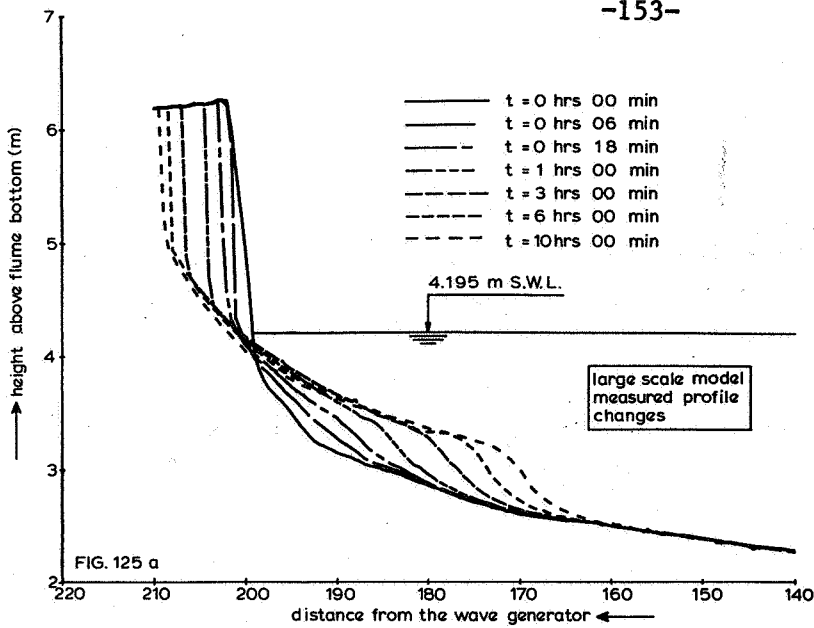
**Figure 125** Measured and computed profile changes

## 7.4 Results of simultaneous investigations

Simultaneously with the research activities described in this thesis, other investigators have been working on dune erosion and on the experimental and numerical modelling of cross-shore sediment transport. The various investigations sometimes had a major influence on each other.

Experimental research on dune erosion has been carried out at the University of Florida by Hughes and Chiu (1981) and by Hughes (1983). The set-up of the experiments and the scale relations were partly based on the findings reported by Van de Graaff (1977) and by Vellinga (1978). The resulting scale relations are somewhat different, as will be discussed below.

At CERC, Seelig (1982) and Hallermeier (1985) investigated cross-shore transport and the corresponding scale relations. They carried out experiments to verify the H/Tw concept as presented by the writer in 1982 (Vellinga, 1982). Hallermeier (1985) evaluated four sets of scale relations. He suggested a new set of scale relations on the basis of two expressions "ressembling those previously reported by Noda (1972) and Vellinga (1982)".

Also at CERC, Sargent and Birkemeier (1985) verified the dune erosion prediction model presented by Vellinga (1983) with reasonable succes for a number of storm surges and hurricanes along the U.S.A. East Coast and the Gulf coast.

At the University of Delaware, Kriebel and Dean (1985) developed a numerical model for dune erosion. The cross-shore transport in this model is based on the equilibrium profile philosophy described by Dean (1977). The rate of cross-shore transport is directly related to the rate of energy dissipation per unit volume of water. A similar approach was applied in the present development of scale relations (see 3.5).

At Delft University of Technology and Delft Hydraulics Laboratory Stive and Battjes (1984) have developed a numerical model for offshore sediment transport. The offshore transport is described as the product of the time averaged velocity field and the time averaged sediment concentration. This approach is consistent with Vellinga's (1982) conclusions regarding the sediment transport process under dune erosion conditions.

The principal results of the various investigations are discussed hereafter.

## Hughes (1983)

Hughes (1983) developed a set of scale relations for the small-scale reproduction of dune erosion. The scale relations were verified for a single case of dune erosion in nature, Hurricane Eloise, Walton County, September 1975. A series of tests were carried out to investigate a number of variables in a systematic way.

The scale relations developed by Hughes are slightly different from the present ones. Hughes' relations are based on the conservation of the surf similarity parameter ($n(\tan\theta/\sqrt{H_0/L_0}) = 1$) instead of dynamic similarity ($n_H = n_L = n_T^2 = n_d$). This leads to a distortion of the wave length in the model:

$$n_L = n_1 \, (n_1/n_d) \tag{177}$$

The basic form of the distortion relation for the beach profile is similar to the present one, except for the value of the exponent:

$$n_1/n_d = (n_d/n_w^2)^{0.5} \qquad \text{(Hughes)} \tag{178}$$

$$n_1/n_d = (n_d/n_w^2)^{0.25} \qquad \text{(present theoretical scale relation)} \tag{2}$$

The results of Hughes (1983) agree with the present scale relations when undistorted models are considered ($n(H/T_w) = 1$; $n_w^2 = n_d$).

Hughes (1983) reports that a model test with scale relations according to Vellinga (1982) resulted in shore accretion instead of the expected erosion. This is surprising considering the extensive series of tests of the present research programme. It is less puzzling however when Hughes' additional statements are taken into account. He states that accurate model results could not be obtained using irregular waves. In a discussion on Hughes' results, Vellinga (1984) disputes the theoretical background of the scale relations and the quality of the reproduction of the hydraulic conditions.

## Hallermeier (1985)

Hallermeier (1985) has evaluated four sets of scale relations. On the basis of this evaluation he has developed a new set of scale relations. His modelling guidance characterizes sediment excursions under wave action by means of a parameter that "includes the bed slope and the threshold of sediment movement".

The resulting condition for sedimentation similitude indicates that the appropriate sediment size and the horizontal scale depend on the selected vertical scale, along with the wave period and the prototype sand characteristics.

In the author's opinion this implies that the distortion of a model (horizontal scale over vertical scale) depends on the prototype wave period and on the prototype sediment size. For models with prototype size sediment Hallermeier suggests:

$$n_l/n_d = (n_d)^{0.25} * (F_{ss})^{-1} \qquad \text{in which} \qquad (179)$$

$$F_{ss} = 0.05 \ (\rho'g/D)^{0.25} \ T_p^{-0.25} \quad \text{(Hallermeier (1985))} \qquad (180)$$

Relation (179) agrees quite well with the present scale relations except for the factor $(F_{ss})^{-1}$. However, due to this $(F_{ss})^{-1}$ factor scale relation (179) would imply that it is <u>not</u> possible to reproduce beach profile changes in small-scale models. This is explained as follows.

Beach profile changes in nature are mainly caused by a change in the hydraulic conditions. Let us consider, as an example, the beach profile changes that occur when a period of normal wave conditions with say $H_s = 1.0$ m and $\hat{T} = 6$ s is followed by a storm with wave conditions of say $H_s = 4.0$ m and $\hat{T} = 10$ s.

When a small-scale model is built according to the "Unified modelling guidance for beach changes" presented by Hallermeier (1985), it is found that the model distortion is different for the two conditions. In fact the distortion for the storm conditions is a factor $(T_{p1}/T_{p2})^{0.25} = (6/10)^{-0.25} = 1.14$ larger. This means that the scale factor for volume $n_A = n_l * n_d$ is not constant throughout the test.

This contradiction in Hallermeier's modelling guidance does not necessarily mean that his approach to sedimentation similitude is fully wrong. The threshold of sediment movement is an important parameter in small scale modelling indeed, especially under conditions near the initiation of motion. However, when dune erosion is considered, the major part of the sediment is transported as suspended load which makes the threshold of sediment movement probably less relevant.

The principal conclusion to be drawn from Hallermeier's work is that dune erosion conditions and initiation of motion conditions can not be covered by a single set of scale relations.

Another aspect of Hallermeier's work is the dimensionless fall velocity parameter. On the basis of a series of small scale tests he disputes the validity of the H/Tw-concept for undistorted small scale modelling. A closer investigation of this series of tests, presented in Table 2 and Figures 1 through 7 (Hallermeier, 1985), shows that model waves are applied with a wave height in the range of 0.02 m up to 0.05 m. Such waves are affected by surface tension. This means that the surf zone processes are not properly reproduced. Additional evidence of this shortcoming is given in Hallermeier's paper as he explains a difference in profile development by reasoning that the very small wave height, H < 0.025 m, on the test slope did not result in an actual surf zone but rather in wave swashing on the shore, with no air entrainment.

In summary it is concluded that Hallermeier's review of the modelling laws is very valuable for a further discussion on scale relations. A further elaboration of Hallermeiers modelling guidance, however reveals an internal contradiction. The modelling would imply that beach profile changes as normally occur in the field cannot be reproduced in a small-scale model.
Finally, it has to be stated that Hallermeier's experimental "evidence" against the validity of the H/Tw-concept is based on tests with insufficient wave height. This explains the discrepancy between his conclusions and the present results.

**Kriebel and Dean (1985)**

Kriebel and Dean (1985) have developed a computational procedure for predicting the time-dependent, two-dimensional beach and dune erosion during storm surges. The rate of cross-shore transport is directly related to the deviation of the wave energy dissipation from its equilibrium level. Off-shore transport continues until the wave energy dissipation per unit volume of water is constant over the entire surf zone. According to Dean (1977) such a situation corresponds with a beach profile described by

$$y = p \, x^{2/3} \tag{180}$$

in which:
y   is the water depth                                    (m)
x   is the distance from the waterline                    (m)
p   is a constant                                         $(m)^{1/3}$

Based on equilibrium profile considerations, Kriebel and Dean have expressed the offshore transport at any point in the surf zone in terms of the difference between the actual and the equilibrium conditions of the wave energy dissipa-

tion in the surf zone:

$$Q_s = K(D_t - D^*) \qquad \text{(Kriebel and Dean, 1985)} \qquad (181)$$

in which

$Q_s$ is the rate of sediment transport $\qquad (m^3/m's)$

$D_t$ is the actual time-dependent energy dissipation

per unit volume of water $\qquad (W/m^3)$

$D^*$ is the energy dissipation per unit volume water

for equilibrium profile conditions $\qquad (W/m^3)$

$K$ is a parameter $\qquad (m^4/Ws)$

The results of the computations based on this transport formulation are impressive. Qualitatively the results make a sound impression. Still the theory behind it is hypothetical. Why would the rate of transport be related to levels of energy dissipation per unit volume of water?

In the author's opinion it is plausible that nature aims at equilibrium conditions. It is also plausible that the rate of change is related to the deviation of the actual situation from the equilibrium situation. There are many examples of such processes in physics. In a linear form this idea can be elaborated to:

$$\Delta S(t) = -a\, S(t)\, \Delta t \qquad (182)$$

in which $S(t)$ is the sediment transport rate, $\Delta S(t)$ is the change of the transport rate over time-step $\Delta t$ and $a$ is a constant.

Taking the limit of $\Delta t \to 0$, relation (182) yields

$$\frac{d\, S(t)}{S(t)} = -a\, dt \qquad (183)$$

Integration yields

$$S(t) = S(0)\, e^{-at} \qquad (184)$$

in which the initial condition

$$t = 0,\ S = S(0)$$

is used $\qquad (185)$

In the equilibrium situation ($t=\infty$) this leads to

$$S = S(\infty) = 0 \tag{186}$$

The cumulative erosion quantity as a fucntion of time A(t) can now be described as follows:

$$A(t) - A(0) = \int_0^t S(t) \, dt \tag{187}$$

As A(0) = 0, this yields $\tag{188}$

$$A(t) = ***** \tag{189}$$

The equilibrium erosion quantity follows from

$$A(\infty) = S(0)/a \tag{190}$$

Relation (189) is presented by Kriebel and Dean (1985). The author assumes that the background of this equation is as described above.
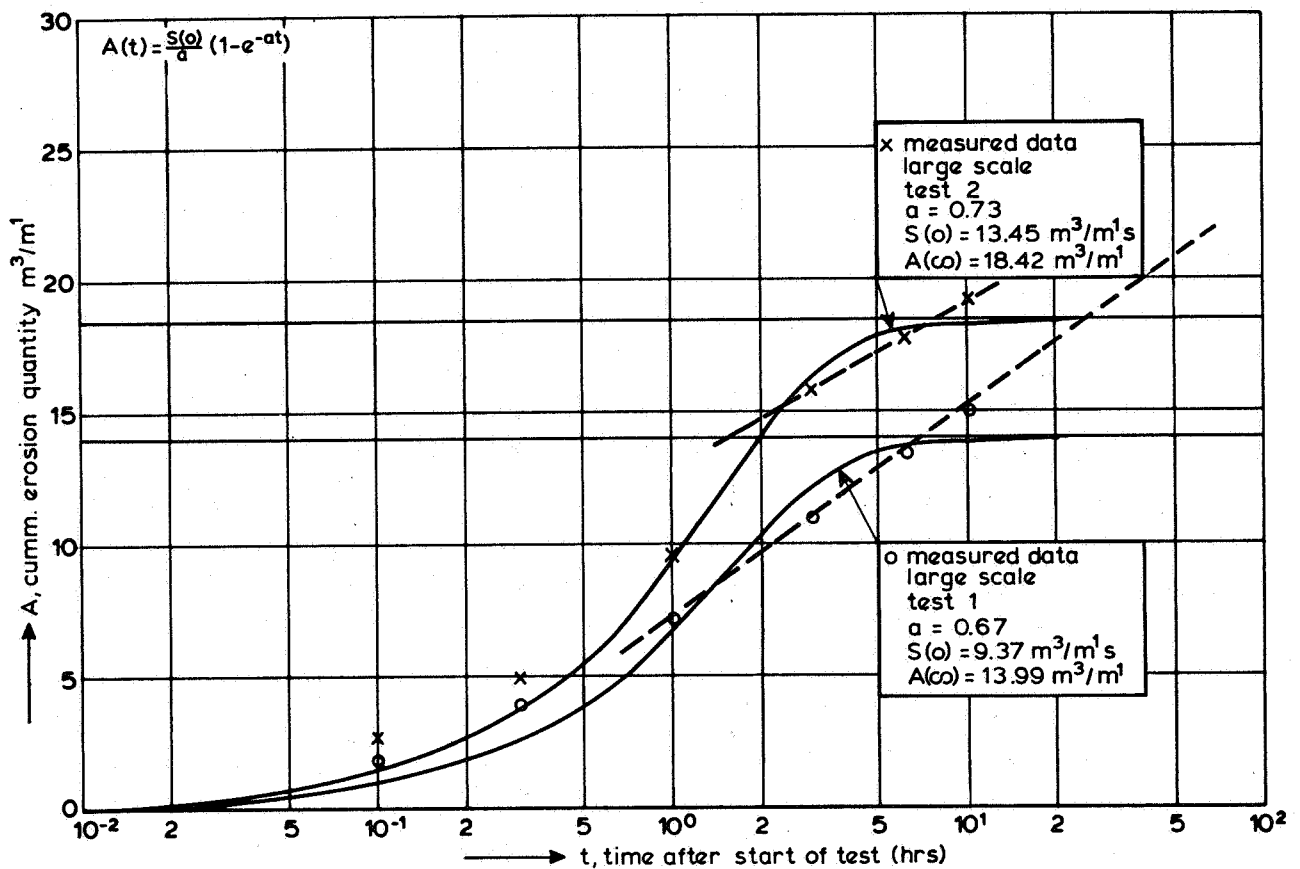


**Figure 126**  Cumulative erosion quantity, measurements and theory

The relation described by Kriebel and Dean (1985) had not been verified and the present data provided an opportunity for this. The cumulative erosion quantity as a function of time is presented in Table 16 for large scale tests

1 and 2. These tests were run with constant hydraulic conditions.
According to Kriebel and Dean's (1985) hypothesis the measured data should fit
with the theoretical relation (189). The measured data were compared with the
theoretical curve and the best fit values for S(0) and a were determined. The
results of this fit are shown in Figure 126. The results look reasonably good,
but a closer inspection reveals a significant descrepancy between the theore-
tical and the measured time history of dune erosion. The measured results
after 1 hr show a linear instead of an assymptotic development.Consequently it
is concluded that the theoretical basis of the Kriebel and Dean (1985) model
is not fully supported by the experimental data.

Another way to verify the hypothesis of Kriebel and Dean (1985) is to compare
the test results and the scale relations with the theory of the 2/3 power
curve. In section 3.4 it has been shown that the power curve as theoretically
derived by Dean (1977):

$$y = A(x)^{2/3} \tag{191}$$

yields a scale relation for the distortion of models with prototype size
sediment:

$$n_d = (n_l)^{2/3} \quad \text{which is identical to}$$

$$n_l/n_d = (n_d)^{0.5}. \tag{192}$$

The experimental data described in chapter 4 and 5 clearly show that the value
of the exponent in (192) is definitely not equal to 0.5. Consequently the 2/3
power curve is questioned.

Finally it should be mentioned that the Kriebel and Dean (1985) model has two
unknown coefficients:

p in the power curve $y = p(x)^{2/3}$ and
K in the transport formula $Q_s = K (D-D^*)$.

The values of these parameters have to be calibrated for the various (field
and laboratory) conditions. This means that, contrary to the present dune
erosion prediction model the computational model of Kriebel and Dean cannot be
applied without the availability of documented cases of dune erosion for the
various sites and conditions.

In summary:

- Kriebel and Dean's (1985) computational model gives results that agree qualitatively with what is expected and known from various sources, field observations and laboratory tests. However, from a quantative point of view the basic description of the rate of erosion does not fit too well with the large-scale test data.

- The computational model contains two unknown coefficients that may vary from site to site and from one condition to another. Kriebel and Dean (1985) do not give values of these coefficients in relation to sediment characteristics and hydraulic conditions. Such relations remain to be developed.

- The energy approach of Kriebel and Dean (1985) is very elegant, as it is based on a sort of least action principle. However, the resulting 2/3-power curve as derived by Dean (1977) does not fit with the scale relations derived herein. Maybe Dean's elaboration is too idealized (monochromatic waves and constant breaker index), but also the application of the least action principle may not be entirely sound.

### Stive and Battjes (1984)

The model developed by Stive and Battjes (1984) describes the sediment transport as a product of the time-averaged velocity field and the time-averaged sediment concentration in the surf zone. The velocity field is described in a "first-order" approach by the return flow. The return flow is computed on the basis of the energy decay model described by Battjes and Jansen (1978) and Stive and Battjes (1984). The description of the sediment concentration is based on theoretical considerations and measurements as presented by Nielsen (1979) and Bosman (1982).

The model has been verified by laboratory experiments. After calibration of a single coefficient the hindcast of profile changes is surprisingly good for the seaward half of the breaker zone. According to the formulation of Stive and Battjes (1984) the sediment transport is zero at the water line.

As to the situation without the possibility of calibration Stive and Battjes conclude that the modelling of sediment transport as a function of the wave conditions is insufficiently accurate to yield a universal value for the calibration coefficient and hence a fully predictive value. They state that

the value of this coefficient ranges from 0.25 up to 1.

The approach of Stive and Battjes (1984) with a description of the offshore transport process as the product of the time-averaged velocity and the time-averaged sediment concentration is consistent with the measurements under dune erosion conditions, the respective computations and the conclusions presented in section 6.5 and by Vellinga (1982).

The principal difference between the dune erosion conditions and the conditions described by Stive and Battjes is the sediment concentration.

The sediment concentration formulation applied by Stive and Battjes is based on Bosman's (1982) findings for sediment entrainment dominated by oscillatory shear. Bosman concludes that the total sediment load under wave action is hardly or not affected by the breaking of the waves. He reasons that the sediment entrainment is caused by shear at the bottom and that the major effect of the breaking of the waves is a further dispersion of the entrained sediment. It should be mentioned that Bosman's conclusions are based on measurements under conditions with mainly spilling breakers. However, Nielsen (1979), Nielsen (1984), and Kana (1979) have described that the breaking of waves strongly affects the sediment concentrations, depending on the type of breaking.

The results of Nadaoka and Kondoh (1982) may cast more light on this issue. They measured turbulence intensities under various types of breaking waves. As an illustration their results are shown in Figure 127. The Figures show that the turbulence intensity and the depth of penetration of breaking wave induced turbulence depends very much on the type of breaking.

The sediment concentration measurements in the dune erosion tests and the discussion in sections 7.2 and 7.3 indicate that the Bosman concept and thus the sediment load module of the Stive and Battjes (1984) model is not valid for the highly dissipative, dune erosion conditions. An illustration of sediment concentrations under breaking waves is also given by Dette (1985). In a large-scale flume sediment concentrations have been measured with a similar type of suction apparatus as described in section 7.2. The sediment concentration was measured down to a level of 0.02 m above the bottom, see Figure 128. The results show that the concentration is rather homogeneous over the water columm. For such conditions the Stive and Battjes (1984) approach of neglecting the effect of the breaking of the waves on the sediment concentrations may be disputed as follows.

The settling velocity of the sand grains in (stagnant) water is in the order of 0.03 m/s. Under the large-scale test conditions described in chapter 5 and under the test conditions described by Dette (1985) the still water depth is

about 1.0 m. Neglecting the effect of turbulence the settling of a grain during half a wave period is in the order of 0.10 m. Consequently the grains suspended at a level higher than 0.10 m above the bottom will not affect the sediment entrainment. In the Stive and Battjes (1984) approach this sediment load is neglected. This may lead to an underestimate of the offshore transport by a factor in the range from 1 to 10, depending on the breaker intensity. Considering these aspects it is amazing that the profile changes computed by Stive and Battjes (1984) agree so well with the measured profile changes. To the writer's opinion the agreement may well be explained by the fact that the wave breaking intensity is taken into account in the sediment transport formulation after all, though not in the sediment concentration but in the formula that describes the return flow velocity. Therefore, the conclusion is that the Stive and Battjes (1984) model gives promising results although the basic philosophy underlying the modelling of the sediment load in the zone of breaking waves is disputed.

A preliminary verification of the Stive and Battjes model for the dune erosion tests has shown that the model underestimates the sediment transport by a factor 5 to 10 in the initial and intermediate stage of the dune erosion process. The writer attempted to improve the model by relating the sediment concentrations to the wave breaking intensity. To describe this relation the rate of wave energy dissipation was introduced as a parameter describing the sediment concentration, see Section 7.3 and Figure 125. From this Figure it can be seen that the energy dissipation model gives reasonably good results for the initial and intermediate phase of the dune erosion process but that it gives deviating results for the final phase of the process.

In spite of the above shortcomings of the Stive and Battjes model, the various results do show that this type of offshore transport model leads the way to a new approach in cross-shore sediment transport modelling. However, a considerable effort is still required to describe the relevant dune erosion processes, such as breaking wave induced turbulence and sediment entrainment, wave reflection and surf beat, sediment settling and onshore transport.
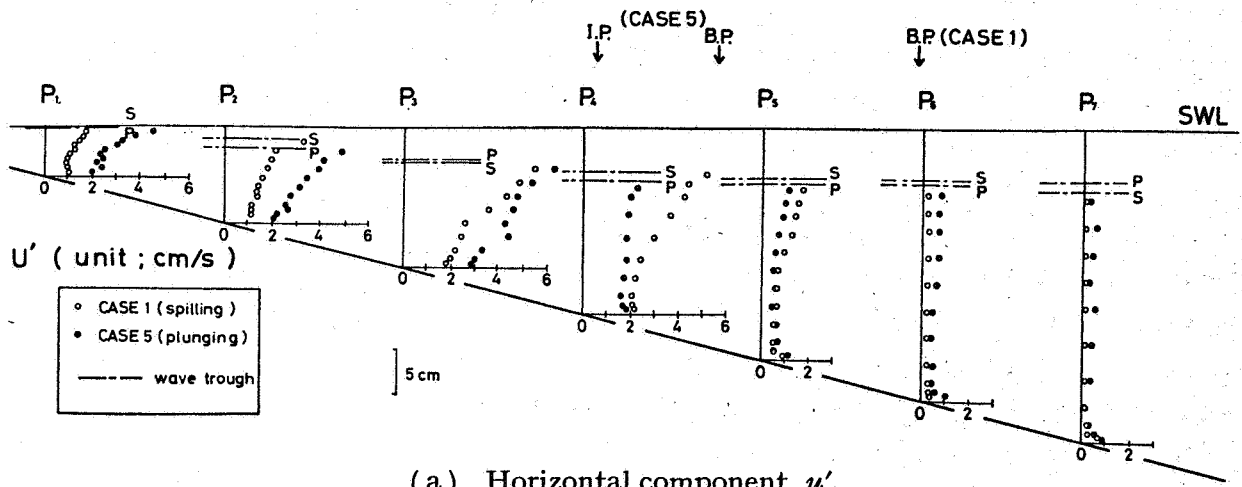
(a) Horizontal component, $u'$.
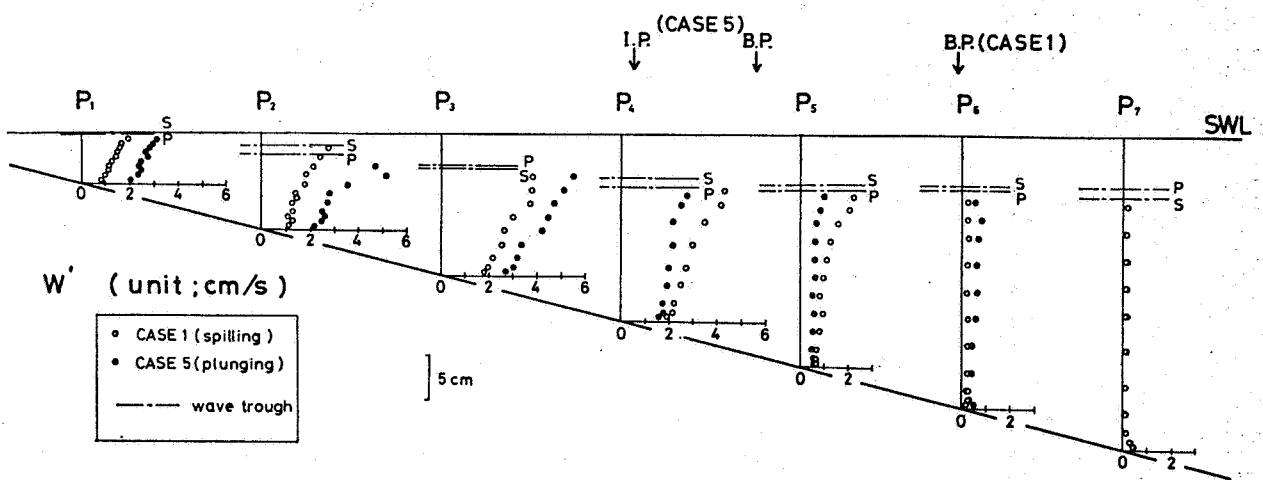


(b) Vertical component, $w'$.
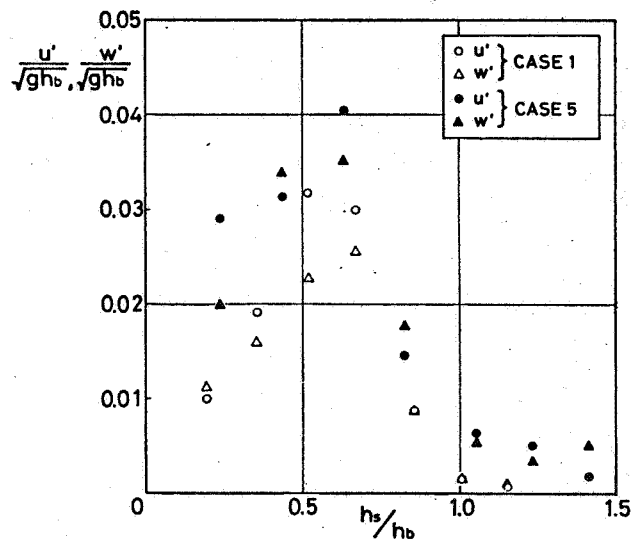


**Figure 127** Turbulence intensities under breaking waves from Nadaoka and Kondoh (1984)
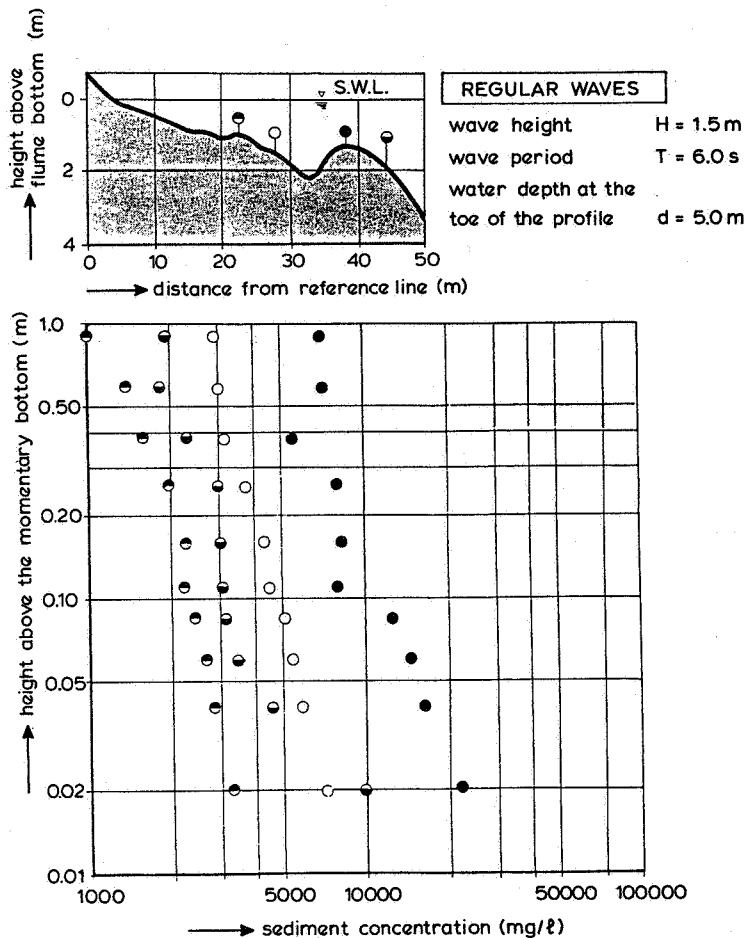
**Figure 128**  Sediment concentrations measured by Dette (1985)

## 7.5  Evaluation and recommendations for further research

The aim of the investigations was to increase the insight into the process of dune erosion and to develop a dune erosion prediction model by which the safety of the existing dunes as a primary sea defence system could be checked and the required reinforcements could be determined.

When evaluating the research programme, it is concluded that the approach of studying dune erosion by means of a series of tests with a range of scale factors has worked out well. The scale relations found by comparing tests agree rather well with the relations derived on a theoretical basis.

The demonstration that it is possible to reproduce the dune erosion process in an undistorted small scale model is particularly valuable.

Detailed measurements during the tests have shown that the offshore sediment transport derived from the profile changes agrees reasonably well with the product of the time-averaged velocity field and the time-averaged sediment concentrations.

A further analysis of the wave conditions, the velocity field, the sediment concentrations and the beach profile changes has shown that the very large offshore sediment transport under dune erosion conditions is mainly caused by the high sediment concentrations due to the plunging breakers as occur on the relatively steep upper beach just in front of the dunes. As the erosion process proceeds, the steep part becomes more gentle, due to a dune front retreat and due to sediment accretion on the beach. As a result, the breaking of the waves becomes less intensive and the sediment concentration decreases to normal surf zone conditions. By means of a provisional numerical model based on the physical processes described above, the profile changes measured during the tests could be reproduced reasonably well for the initial and intermediate stages of the dune erosion process (Fig. 125). However, considerable research is still required to develop an accurate numerical model for the time-dependent simulation of dune erosion.

On the basis of the present investigations, a relatively simple procedure was developed for the prediction of dune erosion during storm surges and for the assesment of the safety of the dunes as a primary sea defence system. An erosion profile was defined as a function of storm surge level, wave conditions and grain size characteristics. During a storm surge the existing beach and dune profile will be reworked until this erosion profile has formed. The model is based on the conservation of sediment volume in the direction perpendicular to the beach. The dune erosion prediction model has an accuracy in the order of 10% to 15% under a wide range of conditions. The model shows that the dune erosion to be expected during the design storm surge for the North Sea coast is 25% to 50% less than expected on the basis of previous prediction models. The model is presently applied to check the safety of the coastal dunes of The Netherlands as a primary sea defence system and to determine the reinforcements required. The model has been verified by Sargent and Birkemeier (1985) for a number of dune erosion cases along the U.S.-East Coast and the Gulf of Mexico. The prediction model can be considered as a reliable and practical tool for coastal managers. As such the investigations have met the expectations.

The results of the research programme have also wider implications. The experimental investigations have increased insight into the process of coastal erosion during storm surges and thus have increased confidence that the beach and dune system will protect coastal areas. The design of a dredged spoil storage basin presently built in the coastal waters south-west of Rotterdam may be considered as an example of the increased confidence. The basin will be protected from the sea by man-made sandy beaches and dunes without the traditional hard coastal protection elements.

Simultaneously with the author a number of other researchers have investigated the possibilities of numerical and experimental modelling of cross-shore sediment transport and dune erosion. In the experimental field Hughes (1983) and Hallermeier (1985) have defined scale relations that are to a certain extent different from the present ones. As discussed in 7.5 the differences can well be explained by the limited verification of the basic assumptions underlying the scale relations of Hughes (1983) and Hallermeier (1985). An evaluation of the various scale relations has shown that the chances of defining a universal set of scale relations for the small-scale reproduction of both short-term and long-term coastal profile changes should be considered very small. The short-term processes in which suspended load dominates require correct reproduction of the fall velocity of the sediment, whereas the reproduction of long term profile changes, in which near-bottom transport plays an important role requires correct reproduction of boundary shear stress and bottom layer thickness. Such requirements are conflicting (see 3.3 and 7.5). On the basis of these arguments the present scale relations should be considered reliable for the reproduction of (short term) dune erosion processes. Such small-scale model investigations should preferably be carried out in undistorted models (cf. Figure 68 and Figure 69). Moreover, the wave height in the model should be as large as possible to avoid scale effects in the wave breaking characteristics. The best results in the present studies have been found by comparing tests with $H_s$ = 0.25 m and very fine sand with tests with $H_s$ = 1.5 m and medium fine sand (see Figure 69 with Table 19 and Figure 79).

In the field of numerical modelling of offshore sediment transport Kriebel and Dean (1985) and Stive and Battjes (1984) have recently made considerable progress. The model of Kriebel and Dean (1985) qualitatively agrees with the present results. With respect to the theoretical background and the quantitative aspects the differences with the present studies are discussed in 7.5. The model of Stive and Battjes is a major step forward in the numerical modelling of cross-shore sediment transport. This model is not based on an energy-approach like the model of Kriebel and Dean (1985), but on a more detailed description of the physical processes. However, so far the model cannot be applied for the prediction of dune erosion as the transport at the waterline is fixed at zero and what is more important, the effect of breaking waves on the sediment entrainment is not taken into account. The first mentioned shortcoming of the Stive and Battjes model can easily be resolved by adopting a so called "geometric" model for the swash zone as used by Kriebel and Dean (1985) and by the author in the model described in 6.5. The second aspect will take a major effort in further theoretical and experimental research.

## Recommendations for further research

The present computational procedure gives a reliable prediction of the dune erosion for two-dimensional situations, viz. for coastal stretches that are relatively straight.
For situations with a strongly curved coastline and for situations with discontinuities in the line of dunes additional computations have to be carried out to predict the effect of longshore transport gradients. In view of the consequences, such computations are still rather unreliable due to the present state of the art. As a part of the present research activities, preliminary computations of longshore transport under dune erosion conditions have been carried out by the writer, Delft Hydraulics Laboratory (1983). The results show that the commonly applied longshore transport formulae such as Bijker's (1971) and the CERC-formula (Shore Protection Manual, 1983), underestimate the longshore transport and as such the longshore transport gradients under dune erosion conditions by a factor between 2 and 10. The application of these formulae in design procedures for the prediction of coastal erosion during storm surges and hurricanes may have dramatic consequences.

It is therefore recommended to develop a numerical model for coastal sediment transport that accurately describes the processes during storm surges. A first step towards such a model will be the development of a two-dimensional time-dependent cross-shore transport model that explicitly describes the sediment concentrations across the surf zone as a function of time. Such a model may be an improved version of the model described by the writer in 7.3 and/or the model described by Stive and Battjes (1984). A second step will be the integration of this two-dimensional cross-sectional model with a two-dimensional area model to yield a quasi three-dimensional model (see de Vriend and Stive, 1986). The final goal should be to develop a fully three-dimensional hydrodynamic and sediment transport model that simulates the seabottom and beach and dune profile changes.

The above mentioned first step model will also help to predict a number of phenomena that so far can only be estimated in a qualitative sense, such as the rate of erosion to be expected at the foot of a protected dune and the scouring at the toe of a sea wall. The foundation of the majority of the present dune front revetments and sea walls lies at a level of 1 m to 2 m below the surface of the upper beach. Large-scale experiments have shown that the scouring during extreme storm surges generally exceeds this foundation depth, Delft Hydraulics Laboratory (1985). Preliminary computations have already shown that such a scouring can be hindcasted reasonably well with a calibrated version of the offshore sediment transport model developed by Stive and Battjes (1984).

A time dependent dune erosion model will also provide a useful basis for the description of the process of dune wash-over and dune-breakthrough. There is an increasing need to describe these (terminal) dune erosion processes as the design procedures are changing from a deterministic approach to a probabilistic approach and probabilistic design procedures require a detailed knowledge of the failure mechanisms and the failure consequences.

The development of a coastal morphology model that describes the short term coastal profile changes (including dune erosion) for storm conditions will take a considerable effort in theoretical and experimental research. In the writer's opinion such investigations should start with carefully designed experiments in laboratory wave flumes and basins with realistic wave conditions not disturbed by reflection and other secondary effects. The velocity field and the sediment concentrations should be measured in the time domain with a high degree of accuracy. Simultaneously a numerical model should be developed step-wise. Such a model may be based on a number of assumptions regarding the process that is studied. It should be used to determine the relative importance of the various processes. Meanwhile the numerical model should be used as a steering device for further experiments and as a documentation and presentation of the state of the art.

# REFERENCES

Battjes, J.A., 1974. Computation of set-up, longshore currents, run-up and overtopping due to wind-generated waves. Comm. on Hydraulics, Dept. of Civil Eng., Delft Univ. of Technology, 74-2, 244 pp.

Battjes, J.A. and Janssen, J.P.F.M., 1978. Energy loss and set-up due to breaking of random waves. Proc. 16 th Conf. Coastal Eng. Am. Soc. Civ. Eng. Vol. 1, pp. 569-589.

Bosman, J.J., Van der Velden, T.J.M. and Hulsbergen, C.H., 1987. Sediment Concentration Measurement By Transverse Suction. To be published in Coastal Engineering Journal Elsevier, Amsterdam.

Bosman, L.J., 1982. Koncentratie-verdeling onder golven en stroom, de invloed van bodemhelling, waterdiepte, brekende golven, orbitaalsnelheid en stroomsnelheid (concentration distribution under wave and current action, the effect of bottom slope, water depth, breaking waves, orbital velocity and current velocity) internal report, M 1875, Delft Hydraulics Laboratory, in Dutch.

Bijker, E.W., 1971. Longshore transport computation. ASCE, J. Waterw. Harbours Coastal Eng. Div., 97 WW4: 687-701.

Bijker, E.W., Hyum, E. van and Vellinga, P., 1976. Sand transport by waves, Proc. 15th Conf. Coastal Eng. Honolulu, Am. Soc. Civ. Eng. p.p. 1149-1168.

Bruun, P., 1954. Coast erosion and the development of beach profiles, U.S. Army Corps of Engineers, Beach Erosion Board., Tech. Memo., No. 44.

Coastal Engineering Research Center, 1983. Shore Protection Manual, U.S. Army, Corps of Engineers.

Collins, J.I. and Chestnutt, C.B., 1975. Tests on the equilibrium profiles of model beaches and the effects of grain shape and size distribution. Proc. Symp. Modeling Techniques, San Fransisco, Cal., pp. 907-926.

Dalrymple, R.A. and Thompson, W.W., 1976. Study of equilibrium beach profiles. Proc. 15th Coastal Eng. Conf. Honolulu, pp. 1277-1299.

Dean. R.G., 1976. Beach erosion: causes, processes, and remedial measures. CRC Critical Review in Environmental Control, Vol. 6, ISSUE 3, pp. 259-296

Dean R.G., 1977. Equilibrium beach profiles: US Atlantic and Gulf Coasts. Newark (Delaware), University of Delaware, Department of Civil Engineering, Ocean Engineering Report No. 12.

Dean. R.G., 1983. Personal Communication

Delft Hydraulics Laboratory and Technical Advisory Committee on Water retaining structures, 1971. Interim-rapport, werkgroep 5 van de Technische Adviescommissie voor de Waterkeringen, Duinen als Waterkering, Report R 587, August 1971, in Dutch.

Delft Hydraulics Laboratory, 1976. Schaalserie duinafslag, verslag modelonderzoek M 1263 deel IA en IB (Scale Series en Dune Erosion, experimental research report M 1263 part IA and IB), in Dutch.

**REFERENCES** (continued)

**Delft Hydraulics Laboratory,** 1978. Duinafslag ten gevolge van de stormvloed op 3 januari 1976, toetsing van de Voorlopige Richtlijn (Dune erosion during the storm surge on Jan 3rd 1976, verification of the provisional dune erosion prediction model). Report R 587, in Dutch.

**Delft Hydraulics Laboratory,** 1979. Morfologie van de Waddenzee; Gevolgen van zand- en schelpenwinning (morphology of the Waddenzee; effects of sand and shell mining). report R 1336, in Dutch.

**Delft Hydraulics Laboratory,** 1981. Study on Wave Generation; Bed Deformations due to Secondary Waves in an Irregular Wave Field, R 702 part V.

**Delft Hydraulics Laboratory,** 1981. Schaalserie duinafslag, verslag modelonderzoek M 1263, deel IIA en IIB (Scale Series on Dune Erosion, experimental research report, M 1263 part IIA and IIB), in Dutch

**Delft Hydraulics Laboratory,** 1981. Onderzoek naar duinafslag tijdens stormvloed, toetsing van de resultaten van het twee-dimensionale onderzoek door middel van onderzoek in een drie dimensionaal model (Verification of dune erosion results from two-dimensional tests in a three dimensional model). Report M 1653, in Dutch.

**Delft Hydraulics Laboratory,** 1982. Rekenmodel voor de verwachting van duinafslag tijdens stormvloed, verslag modelonderzoek, M 1263 deel IV (Dune Erosion Prediction Model, research report M 1263 part IV), in Dutch.

**Delft Hydraulics Laboratory,** 1982. Duinafslag tijdens superstormvloed, Noorderstrand Schouwen, (Dune erosion during a super storm surge, Noorderstrand Schouwen, report M 1797), in Dutch.

**Delft Hydraulics Laboratory,** 1982. Systematisch Onderzoek naar Duinafslag bepalende Factoren (systematic investigation of parameters relevant for dune erosion, report M 1819 part I), in Dutch.

**Delft Hydraulics Laboratory,** 1983. Duinafslag bij gebogen kusten, orde-grootte bepaling van de gradiënt in het langstransport tijdens duinafslag aan een gebogen kust (dune erosion at curved beaches, determination of order of magnitude of the longshore sediment tranport gradient under dune erosion conditions, internal research report M 1263 part V), in Dutch.

**Delft Hydraulics Laboratory,** 1983. Golfoploop- en overslag bij duinen tijdens superstormvloed, verslag modelonderzoek M 1819, deel II (wave run-up and wave-overtopping for coastal dunes during storm surges, experimental research report M 1819 part II), in Dutch.

**Delft Hydraulics Laboratory,** 1984. Golfoploop en -overslag bij duinen tijdens superstormvloed, aanvullend onderzoek, verslag modelonderzoek M 1819 deel IV (wave run-up and wave-overtopping for coastal dunes during storm surges, additional investigations, report M 1819 part IV), in Dutch.

**Delft Hydraulics Laboratory,** 1984. Schaalserie duinafslag, Proeven op grote schaal in de Deltagoot (Scale Series on Dune Erosion, large Scale Tests in the Delta Flume, research report M 1263 part III), in Dutch.

REFERENCES (continued)

**Delft Hydraulics Laboratory,** 1985. Systematisch onderzoek naar de werking van duinvoetverdedigingen, een eerste analyse van de relevante processen op basis van reeds uitgevoerd modelonderzoek (systematic research on the effectiveness of dune toe revetments, a first analysis of the relevant processes based on results of earlier experiments, report M 2051, part I), in Dutch.

**Delft Hydraulics Laboratory,** 1985. Dwarstransport tijdens duinafslag, verslag onderzoek M 1263 deel V. (Crossshore Transport During Dune Erosion, rept. M 1263 part V), in Dutch.

**Delft Soil Mechanics Laboratory,** 1980. Grondmechanische aspecten bij duinafslag, voorstel onderzoek (soil mechanic aspects of dune erosion. proposal for investigations report CO-255580, 1980), in Dutch.

**Delft Soil Mechanics Laboratory,** 1982. Grondmechanische aspecten bij duinafslag (Soil mechanic aspects of dune erosion, results of investigations during large scale tests report CO-25580), in Dutch.

**Dette, H.,** 1985. Personal Communication.

**Edelman, T.,** 1961. Erosie en aanwas van het kustvak Den Helder-Hoek van Holland (erosion and accretion of the coastal reach between Den Helder and Hook of Holland). Report WWK 61-1, Ministry of Transport and Public Works Rijkswaterstaat, the Netherlands, in Dutch.

**Edelman, T.,** 1968. Dune erosion during storm conditions. Proceedings of the 11 th Conference on Coastal Engineering. London, chapter 46, pp. 719-722.

**Edelman, T.,** 1972. Dune erosion during storm conditions. Proceedings of the 13th Conference on Coastal Engineering. Vancouver, Vol. 2, pp. 1305-1311.

**Fairbridge, R.W.,** 1961. Eustatic changes in sea level, Physics and chemistry of the earth, Vol. 4, Pergamon Press, 1961, pp. 99-185.

**Fontanet, P.,** 1961. La Houille Blanche, no. 1,2.

**Geldof, H.J. and Slot, R.J.,** 1979. Settling Tube Analisis of Sand. Internal Report nr. 4-79 Laboratory of Fluid Mechanics, Civ. Eng. Dep., Delft University of Technology.

**Gourlay, M.R.,** 1980. Beaches: profiles, processes and permeability. Proc. 17th Coastal Eng. Conf. Sydney, pp. 1320-1339.

**Graaff, J. van de.,** 1977. Dune erosion during a storm surge; Coastal Eng., Volume 1, No. 2.

**Graaff, J. van de,** 1983. Probabilistic design of dunes. Proceedings Coastal Structures Conference American Society of Civil Engineers, pp 820-832.

**Hallermeier, R.J.,** 1985. Unified modelling guidance based on a sedimentation parameter for beach changes. Coastal Eng., 9:37-70.

**Hughes, S.A.,** 1978. The variation of beach profiles when approximated by a theoretical curve. M.S. Thesis, Univ. Florida, Gainesville, Florida.

REFERENCES (continued)

Hughes, S.A., and Chiu, T.Y., 1981. Beach and dune erosion during severe storms. Coastal and Oceanographic Engineering Department, University of Florida, Gainsville, Florida, UFL/COEL-TR/043, 288 pp.

Hughes. S.A., 1983. Movable bed modelling law for coastal dune erosion. Proc. ASCE, J. Waterway, Port, Coastal and Ocean Dvision, 109 (2): 164-179.

Hulsbergen, C.H., 1974. Effect and Suppression of Secondary Waves, Proc. 14th Coastal Eng. Conf. Copenhagen.

Hijum, E. van and Pylarczyk, K.W., 1982 Gravel Beaches; Equilibrium Profile and Longshore Transport of Coarse Material under Regular and Irregular Wave Attack. Delft Hydraulics Laboratory, Publication no. 274.

Iwagaki, Y and Noda, H., 1963. Laboratory study of scale effects in two-dimensional Beach Processes, Proc. 8 th Coastal Eng. Conf. pp. 194-210.

Jansen, R.H.J., 1978. The In Situ Measurement of Sediment Transport by means of Ultra Sound Scattering. Delft Hydraulics Laboratory Publication no. 203.

Jelgersma, S., 1961. Holocene Sea Level Changes in The Netherlands, E. v. Aalst, Maastricht.

Kamphuis, J.W., Davies, R.B., Nairn, R.B. and Sayao, O.J., 1986. Calculation of litoral sand transport rate, Coastal Eng., 10 pp 1-21.

Kana, T.W., 1979. Suspended Sediment in Breaking Waves. Techn. Rep. No. 18, Coastal Research Division, Dep. of Geology, University of South Carolina.

Kemp, P.H. and Plinston, D.T., 1968. Beaches produced by waves of low phase difference; Proceedings American Society of Civil Engineers, Journal of the Hydraulics Division, pp 1185-1194, September 1968.

Kohsiek, L., 1986. Personal Communication, to be published in 1987.

Kohsiek, L., 1987. Reworking of former eb-delta's into large longshore bars following the artificial closure of tidal inlets in the South-Western part of the Netherlands. Modern and ancient tidal clastic deposits. P. de Boer, Reidel.

Kolff, J. van der, 1985. Coastal Erosion at Delfland, Data available at the archives of Hoogheemraadschap Delfland, Delft, personal communication dec. 1985.

Komar, P.D. and Inman, D.L., 1970. Longshore transport of sand on beaches. J. Geophys. Res., 75(30): 5514-5527.

Kriebel, D.L. and Dean. R.G., 1985. Nummerical simulation of time-dependent beach and dune erosion. Coastal Eng., 9 pp. 221-245.

Leatherman. S.P., 1979. Beach and dune erosion interactions during storm surge conditions. Quarterly Journal of Engineering Geology, Vol. 12, pp. 281-290.

Méhauté, B. le, 1970. A comparison of fluvial and coastal similitude. Proc. 12th Coastal Eng. Conf., Washington D.C., Vol. 2, Chapter 69, pp. 1077-1096.

REFERENCES (continued)

Meulen, T. van der, and Gourlay, M.R., 1968. Beach and dune erosion tests.
Proceedings of the 11th Conference of Coastal Engineering, London, Vol. 1, pp.
701-707.

Miller, R..L., 1976. Role of vortices in Surf Zone Prediction: sedimentation
and wave forces. Beach and Nearshore Sedimentation, Society of Economic
Paleontologists and Mineralogists, special publication No. 24, Tulsa Oklahoma,
U.S.A.

Nadaoka, K. and Kondoh, T., 1982. Laboratory Measurements of Velocity Field
structure in the Surf Zone by LDV. Coastal Engineering in Japan, Vol. 25,
1982.

Nielsen, P., 1979. Some basic concepts of wave sediment transport. Series
Paper no. 20, Inst. of Hydr. and Hydr. Eng. (ISVA), Techn. Unviversity of
Denmark.

Nielsen, P., 1984. Field measurements of time averaged Suspended Sediment
Concentrations, Coastal Eng., 8 51-72.

Noda, E.K., 1972. Equilibrium beach profile scale-model relationship. Proc.
ASCE, J. Waterw., Port, Coast. Ocean Div., 98:511-528.

Reinalda, R., 1960. Scale Effects in Models with Litoral Sand Drift,
Proceedings of the 7th Conference on Coastal Engineering, The Hague.

Roelse, P., 1985. Artificial Nourishment as Coastal Defence Mechanism,
previous Fills, future Developments, report WWKZ-85. V 261 Ministry of
Transport and Public Works/Rijkswaterstaat, The Netherlands.

Sargent, F.E. and Birkemeier, W.A., 1985. Application of the Dutch Method for
Estimating Storm Induced Dune Erosion Instruction Report CERC-85, Coastal
Engineering Research Centre, US-Army Engineers.

Saville, T., 1957. Scale effects in two-dimensional beach studies. Trans. 7th
Meeting Int. Assoc. Hydraul. Res., Lisbon, pp. A3-1 - A3-10.

Seelig, W.N., 1982 a. Documentation of CERC profile development tests, Unpub.
Memo, Coastal Engineering Reserach Center.

Seelig, W.N., 1982 b. Prediction of Beach Erosion and Accretion. Unpub.
Manuscript, Coastal Eng. Research Center.

Schoorl, H., 1982. Petten en de Hondsbosse Zeewering in kaart en beeld en
reconstructie, 1466-1611 (Petten and the Hondsbosse Seawall a reconstruction
of shoreline developments). Published in "Vrienden van de Hondsbossche",
16 p., 23 figs., 19 refs., Alkmaar, 1982, in Dutch.

Steetzel, H.J., 1987. Cross-shore transport modelling for storm surge
conditions, Coastal Sediments 1987 A.S.C.E., in preparation.

Stive, M.J.F., 1980. Velocity and pressure field of spilling breakers, Proc.
17th Conf. Coastal Eng., Sydney.

Stive, M.J.F., and Battjes, J.A., 1984. A model for offshore sediment
transport. Proc. 19th Conf. Coastal Eng., Am. Soc. Civ. Eng. pp. 1420-1436.

**REFERENCES** (continued)

**Stive, M.J.F.,** 1985. A scale comparison of waves breaking on a beach. Coastal Eng., 9 pp. 151-158.

**Stive, M.J.F.,** 1986. Cross Shore Sediment Transport, Coastal Engineering, in preparation.

**Straaten, L.M.J.U. van,** 1975. De sedimenthuishouding in de Waddenzee (sediment balance in the Waddenzee), Amsterdam, Symp. Waddenonderz., april 1973, Werkgroep Waddengebied, meded. nr. 1, 1975, in Dutch.

**Valembois, J.,** 1960. Etude sur Modele du Transport Littoral, Conditions de Similitude, Proceedings of the 7th Conference on Coastal Enineering, The Hague.

**Veen, C.J. van der,** Ice sheets, atmospheric $CO_2$ and Sea Level. Utrecht, Rijksuniversiteit, Proefschrift Fac. Wiskunde en Natuurwetenschappen, 13 oktober 1986.

**Veenstra, H.J.,** 1968. De zeespiegelstijging in Noord-Nederland (sea level rise in the northern part of The Netherlands) Waddenbulletin, Jg. 3, nr. 1, 1968, in Dutch.

**Veenstra, H.J.,** 1976. Getijdenlandschap; struktuur en dynamiek, (tidal-landscape; structure and dynamics) Waddenzee, deel I: Waddenzee getijdenlandschap, Land. Ver. Behoud Waddenzee, Harlingen/Ver. Behoud Nat. Mon. Ned., '-s-Gravenhage, 1976, in Dutch.

**Vellinga, P.,** 1978., Movable Bed Model Tests on Dune Erosion, Proc. 16th Conf. Coastal Eng., Hamburg, pp. 2020-2039.

**Vellinga, P.,** 1982. Beach and dune erosion during storm surges. Coastal Engineering, 6 pp. 361-387.

**Vellinga, P.,** 1983. Predictive Computational Model for Beach and Dune Erosion during storm Surges, Proc. Coastal Structures Conference, American Society of Civil Engineers, pp. 806-819.

**Vellinga, P.,** 1984. A tentative description of a universal Erosion Profile for Sandy Beaches and Rock Beaches, Discussions. Coastal Engineering, 8 pp. 171-188.

**Vellinga, P.,** 1984. Proc. ASCE J. of Waterway Port Coastal and Ocean Division, 110. Discussion on Hughes' Movable Bed Modelling Law for Coastal Dune Erosion, Proc. ASCE 1983, 109 (2).

**Vriend, H.J. de and Stive, M.J.F.,** 1986. Modelling of nearshore currents and morphology. JONSMOD'86 Meeting Delft, The Netherlands, Proceedings to appear in a special issue of Coastal Engineering.

**Wiegel, R.L.,** 1964. Oceanographic Engineering, Prentice Hall, Englewood Cliffs N.Y. 1964.

**Yalin, M.S.,** 1971. Theory of Hydraulic Models. London, MacMillan Press Ltd, 266 pp.

## LIST OF SYMBOLS

| Symbol | Units | Description |
|---|---|---|
| $A_o$ | $m^3/m^1$ | (theoretical) dune erosion quantity for Sf = 0 |
| $A$ | $(m^3/m^1)$ | cumulative dune erosion quantity above storm surge level |
| $A(t)$ | $(m^3/m^1)$ | A as a function of time t |
| $A_{nd}*$ | $m^3/m^1$ | A, corresponding with a (fictive) test with $n_d = n_d*$ |
| $a$ | (-) | coefficient |
| $c$ | (-) | sediment concentration |
| $c(z,t)$ | (-) | sediment concentration as a function of the height above the bottom and time |
| $\bar{c}(z)$ | (-) | time averaged sediment concentration as a function of the height above the bottom |
| $c_1$ | (-) | time averaged and bottom layer averaged sediment concentration |
| $c_2$ | (-) | time averaged and top layer averaged sediment concentration |
| $c_c$ | (-) | coefficient describing the predominant type of wave breaking |
| $c_g$ | (m/s) | (wave) group velocity |
| $c_{ph}$ | (m/s) | (wave) phase velocity |
| $D$ | (m) | grain size diameter |
| $D_{50}$ | (m) | characteristic grain size diameter such that 50% of the grains by weight have a diameter larger than $D = D_{50}$ |
| $d$ | (m) | water depth |
| $D_t$ | $(W/m^3)$ | time dependent energy dissipation rate per unit volume of water, defined by Kriebel and Dean (1985) |
| $D*$ | $(W/m^3)$ | energy dissipation rate per unit volume of water under equilibrium profile conditions, defined by Kriebel and Dean (1985) |
| $E$ | $(J/m^2)$ | wave energy per unit area |
| $F_{ss}$ | (....) | factor related to sediment mobility similitude, defined by Hallermeier (1985) |
| $f(D)$ | $(W/m^3)$ | rate of wave energy dissipation per unit volume of water for equilibrium profile conditions, defined by Kriebel and Dean (1985) |

| | | |
|---|---|---|
| $Fr_*$ | (-) | densimetric Froude number |
| $g$ | $(m/s^2)$ | gravitational acceleration |
| $H$ | (m) | wave height |
| $H_{0s}$ | (m) | significant wave height $H_s$ in "deep water" (d > 0.5 L) |
| $H_s$ | (m) | significant wave height, equal to the average height of the highest 1/3 part of the waves |
| $H_{bs}$ | (m) | wave height at breaking corresponding to $H_{0s}$ (computed by linear wave theory and constant breaker index) |
| $H_0$ | (m) | "deep water" wave height (d > 0.5 L) |
| $H_{rms}$ | (m) | root mean square wave height |
| $K$ | $(m^5/Ws)$ | transport rate parameter, defined by Kriebel and Dean (1985) |
| $L$ | (m) | wave length |
| $L_0$ | (m) | "deep water" wave length (d > 0.5 L) |
| $L_i$ | (m) | horizontal distance from the water line to the i − m depth contour |
| $L_{i\%}$ | (m) | i % of the sand eroded from the dune has settled within a distance of $L_{i\%}$ from the water line |
| $l$ | (m) | length |
| m-index | (--) | referring to scale model dimensions |
| $n$ | (-) | $c_g/c_{ph}$ |
| $n_i$ | (-) | scale factor equal to the ratio of prototype value over model value of index-parameter |
| $n_d$ | (-) | depth scale factor |
| $n_l$ | (-) | length scale factor |
| $n_w$ | (-) | fall velocity scale factor |
| $n_u$ | (-) | orbital velocity scale factor |
| $n_{d2}$ | (-) | depth scale factor after conversion to a fictive test with fall velocity w = 0.0268 m/s |
| $n_T$ | (-) | scale factor for wave period |
| $n_D$ | (-) | scale factor for grain size |

| | | |
|---|---|---|
| p | $(m)^{--}$ | dimensional coefficient |
| q | $(m)^{--}$ | dimensional coefficient |
| p-index | (-) | index referring to prototype dimensions |
| $q_{ret}$ | $(m^2/s)$ | time average water flow rate in the breaker zone in a vertical plane perpendicular to the beach |
| $Q_s$ | $(m^3/m^1 s)$ | rate of sediment transport, defined by Kriebel and Dean (1985) |
| $R_v$ | (m) | wave run up, above still water level, vertically measured, that is exceeded by 2% of the number of waves |
| Re | (-) | Reynolds number |
| r | (-) | correlation coefficient |
| $S_x$ | $(m^3/ms)$ | sediment transport per unit width |
| S(t) | $(m^3/ms)$ | sediment transport per unit width as a function of time |
| T | (s) | wave period |
| $\hat{T}$ | (s) | wave period, peak of spectrum |
| t | (s) | time (after start of test) |
| t* | (s) | time (after start of test) after conversion to a fictive test with $n_d = n_d$* |
| u | (m/s) | horizontal component of orbital velocity |
| $\bar{u}$ | (m/s) | time average value of u |
| $u_{15shw}$ | (m/s) | orbital (peak) velocity in shoreward direction that is exceeded by 15% of the number of waves (roughly corresponding to the significant wave height) |
| $u_{15sew}$ | (m/s) | orbital (peak) velocity in seaward direction that is exceeded by 15% of the number of waves (roughly corresponding to the significant wave height) |
| $u_g(z,t)$ | (m/s) | horizontal velocity component of the sediment grains as a function of time and height above the bottom |
| u(z,t) | (m/s) | horizontal velocity component of the velocity field |
| $\bar{u}(z)$ | (m/s) | time average value of u(z,t) |
| v | (m/s) | vertical component of the orbital velocity |

| | | |
|---|---|---|
| v* | (m/s) | bottom shear stress velocity |
| w | (m/s) | fall velocity of sediment with grain size $D = D_{50}$, in stagnant water |
| x | (m) | horizontal coordinate |
| y | (m) | vertical coordinate only referred to for beach profile description |
| z | (m) | vertical coordinate to indicate the position with reference to the position of the bottom |
| α | (-) | exponent applied to describe the distortion of a model |
| β | (-) | exponent to describe the time scale relation |
| γ | (-) | exponent applied to describe a beach profile by a power curve |
| η (t) | (m) | elevation of the water surface above the bottom as a function of time |
| $\bar{\eta}$ | (m) | time averaged water surface elevation above the bottom |
| $\bar{\eta}_1$ | (m) | time averaged thickness of the layer with resulting seaward flow |
| μm | | micro-meter $= 10^{-6}$ m |
| ν | (m²/s) | viscosity |
| ξ | (-) | dimensionless surf zone similarity parameter, defined by Battjes (1974) |
| ρ | (kg/m³) | mass density |
| $\rho_s$ | (kg/m³) | mass density of sediment |
| $\rho_w$ | (kg/m³) | mass density of water |
| Δ | (-) | relative density of sediment with respect to water $\Delta = (\rho_s - \rho_w)/\rho_w$ |
| $\sigma_A$ | (m³/m¹) | standard deviation of the differences between the computed and the measured dune erosion quantities |
| tan θ | (-) | slope of beach profile |
| $\theta_o$ | (°) | angle between the shoreline and the wave crests at a waterdepth of 22.8 m prototype. |

# LIST OF TABLES

## LIST OF FIGURES